Annual Report

Leibniz-Institut für Kristallzüchtung

im Forschungsverbund Berlin e.V.

2015

Annual Report

Leibniz-Institut für Kristallzüchtung

im Forschungsverbund Berlin e.V.

2015

Preface

Liebe Leserinnen und Leser, liebe Kolleginnen und Kollegen,

Unsere heutige Gesellschaft steht vor vielfältigen Herausforderungen. Dazu zählen etwa eine saubere und effiziente Energieversorgung, Gesundheit und Wohlergehen, Mobilität, Nachhaltigkeit und Ressourceneffizienz, Kommunikation und die Digitalisierung der Gesellschaft. Die Erforschung neuer Materialien gilt für diese Bereiche als Schlüsseltechnologie und Innovationsmotor. Gerade kristalline Materialien, wie sie am Leibniz-Institut für Kristallzüchtung (IKZ) erforscht werden, liefern häufig die unverzichtbare Grundlage für die notwendigen technischen Lösungen. Das Spektrum reicht von Silizium und anderen Halbleitern für die Leistungselektronik oder zur Gewinnung erneuerbarer Energien über Aluminium- oder Galliumnitrid für die innovative Beleuchtung bis hin zu dünnen Oxidschichten.

Gerade die Oxidelektronik bietet ein großes Potential für die Entwicklung in den genannten Zukunftsbereichen. Applikationen finden sich besonders im Bereich der transparenten Elektronik, als Speichermedien, aber auch in der Medizintechnik oder der Energieerzeugung und -umwandlung. Das IKZ ist international führend in der Entwicklung von Materialien für dieses Forschungsfeld. Es verfügt über die weltweit einzigartige Möglichkeit, die Züchtung und Erforschung von Oxidkristallen als Substratmaterialien mit der Abscheidung halbleitender oder ferroelektrischer Oxidschichten zu verbinden. Einen weiteren wesentlichen Beitrag zu dieser Forschung leisten die Gruppen der Charakterisierung. Aufgrund seiner Kompetenzen ist das IKZ maßgeblich in den Leibniz WissenschaftsCampus GraFOx - Growth and Fundamentals of Oxides for Electronic Applications - eingebunden, der 2016 seine Arbeit aufgenommen hat. Dieses Netzwerk verbindet Akteure aus Hochschulen und Forschungseinrichtungen insbesondere im Berliner Raum, aber auch darüber hinaus.

Die Mitarbeit bei der Bestimmung der Avogadro-Konstante - und damit verbunden eine mögliche Neudefinition des Kilogramm-Maßstabs - bleibt ein weiteres Highlight unserer Forschung. Das IKZ züchtet die nahezu isotopenreinen Silizium-Einkristalle höchster Perfektion und Reinheit, die die Grundlage für dieses Vorhaben bilden. Ähnlich hohe Ansprüche stellt das Projekt GERDA - Germanium Detector Array - das grundlegende Aufschlüsse über die Natur von Neutrinos geben soll. Zu diesem Zweck werden isotopenangereicherte Germanium-Kristalle in einer Qualität benötigt, die sonst nicht verfügbar ist. Isotopenreine oder -angereicherte Einkristalle sind nicht nur in der Grundlagenforschung interessant. Sie gelten auch als vielversprechende Kandidaten für Anwendungen in der Quantentechnologie.

Die Verfügbarkeit von kristallinen Materialien in entsprechender Qualität und mit geeigneten Eigenschaften spielt für die Forschung, aber auch die Anwendung eine entscheidende Rolle. Dazu gehört auch die Entwicklung von Züchtungsmethoden, um diese mit annehmbaren Kosten herstellen zu können Das IKZ ist auf diesem Gebiet traditionell ein gefragter Partner. Seit 2015 ist das Institut eingebunden in das Konsortium Advanced UV for Life, das im Rahmen der BMBF-Initiative Unternehmen Region: Zwanzig20 – Partnerschaft für Innovation gefördert wird. Aufgabe des IKZ ist hierbei die Entwicklung einer industriell einsetzbaren Züchtungstechnologie für Aluminiumnitrid als Substratmaterial für sehr kurzwellige UV-Leuchtdioden.

Das IKZ bietet eine ein Europa einmalige Infrastruktur und gilt als das Kompetenzzentrum für die Züchtung und Erforschung kristalliner Materialien. Es ist eine weltweit einzigartige Einrichtung, die das ganze Spektrum in diesem Bereich abbildet, von der Herstellung der Substratkristalle und der Kristallbearbeitung über die Abscheidung von funktionalen Schichten bis hin zur Charakterisierung der physikalischen und strukturellen Eigenschaften. Das Institut lebt wesentlich von der Kompetenz und dem Engagement seiner Mitarbeiterinnen und Mitarbeiter, die das Institut stabil durch das dritte Jahr einer „Zwischenzeit" unter kommissarischer Leitung getragen haben. Ein besonderer Dank gilt unseren Zuwendungsgebern aus Land und Bund, die es ermöglicht haben, dass das IKZ auch im Jahr 2015 seine Aktivitäten in hoher Qualität weiterführen konnte.

Ich wünsche Ihnen eine unterhaltsame Lektüre,

Ihr

Günther Tränkle

Preface

Dear readers, dear colleagues,

Today, society faces multiple challenges, like clean and efficient energy supply, health and welfare, mobility, sustainability and resource efficiency and communication and the digitalization of society. In these fields, the research on new materials plays a crucial role as key technology and driver of innovation. Especially crystalline materials as explored at the Leibniz Institute for Crystal Growth often provide the indispensable basis for necessary technological solutions. This includes silicon and other semiconductors for power electronics or the production of renewable energies, aluminium and gallium nitride for innovative lightning, as well as thin oxide films.

Especially the field of oxide electronics harbors great potential for the mentioned future-oriented areas. Possible applications can be found in transparent electronics, storage devices, medical devices and power generation and conversation. In the development of materials for this research area, the IKZ has assumed a leading position. It possesses a unique combination of research and growth of oxide crystals as substrate materials with the deposition of semiconducting or ferroelectric oxide films, supported significantly by the characterization groups. Therefore, the IKZ contributes substantially to the Leibniz ScienceCampus GraFOx – Growth and Fundamentals of Oxides for Electronic Applications –, which has started in 2016. This network connects partners from university and research institutions in the Berlin region and beyond.

The contribution to the determination of the Avogadro constant – in combination with the possible redefinition of the kilogram measurement – is still one of our research highlights. With the growth of nearly isotopically pure silicon crystals of highest perfection and purity, the IKZ provides literally the basis for this project. Similar high demands have to be met in the frame of the project GERDA – Germanium Detector Array – that aims at a better understanding of the nature of neutrinos. Here again, isotopically enriched germanium crystals are required with highest quality available. Isotopically pure or enriched single crystals do not only play an important role in basic research, they are also considered as promising candidates for quantum technology applications.

For research and application, the availability of crystalline materials with appropriate quality and suitable characteristics plays a crucial role. This also includes the development of growth technologies for cost-effective manufacturing. Here, the IKZ is traditionally a requested partner. Since 2015, it is member of the consortium *Advanced UV for Life*, funded in the frame of the BMBF initiative *Twenty20 – Partnership for Innovation*. The main task of the IKZ is the development of an industrially applicable growth technology for aluminium nitride as substrate material for UV light emitting diodes in the very short wavelength region.

IKZ's infrastructure is unique in Europe and the institute is established as *the* competence center for growth and research on crystalline materials. It is the only institution worldwide covering the whole spectrum in this field. This ranges from the growth of substrate materials and their crystal machining to the deposition of functional layers and the characterization of their physical and structural properties. The institute lives substantially from the expertise and commitment of its employees, who kept the institute stable throughout the third year of the "interim period" under provisional leadership.
We wish to express our special thanks to our funding authorities from state and federal governments, who have enabled us to continue our research activities with high quality in 2015 again.

I wish you an enjoyable reading,

Yours sincerely,

Günther Tränkle

Content

2 Preface
6 The Institute
10 Events

Highlight

12 Understanding polarity control in group-III nitrides on sapphire

Classical Semiconductors

20 Silicon & Germanium
26 Multi-crystalline Silicon
30 Gallium Arsenide

Dielectric & Wide Bandgap Materials

38 Oxides/Fluorides
48 Gallium Nitride
54 Aluminium Nitride

Layers & Nanostructures

64 Semiconducting Oxide Layers
70 Si/Ge Nanocrystals
74 Ferroelectric Oxide Layers

Simulation & Characterization

84 Physical Characterization
90 Electron Microscopy
96 Chemical & Thermodynamic Analysis
100 Crystal Machining

102 Appendix

The Institute

Foto: Lothar M. Peter

Leibniz-Institut für Kristallzüchtung im Forschungsverbund Berlin e.V.

FOUNDED 1992
PART of Forschungsverbund Berlin e.V.
MEMBER of the Leibniz Association (WGL)

STAFF	104
Scientists	44 (external funding: 18)
Ph.D. students	14 (external funding: 4)
Technicians	42 (external funding: 9)
Trainees	4
BUDGET 2015	11.7 Mio €
Basic funding	9.1 Mio €
Third-party funding	2.6 Mio €

The Institute

Das Leibniz-Institut für Kristallzüchtung (IKZ)

ist eine staatliche Forschungs- und Service-Einrichtung, die sich experimentell und theoretisch mit den wissenschaftlich-technischen Grundlagen des Wachstums, der Züchtung, der Bearbeitung und der physikalisch-chemischen Charakterisierung von kristallinen Festkörpern beschäftigt. Dies reicht von der Grundlagenforschung bis hin zum Vorfeld industrieller Entwicklung. Die zurzeit entwickelten Materialien finden vorwiegend Verwendung in der Mikro-, Opto- und Leistungselektronik, der Photovoltaik, in Optik und Lasertechnik, in der Sensorik und Akustoelektronik.

Das Forschungsgebiet des IKZ umfasst Volumenkristalle, kristalline Schichten und Nanostrukturen sowie die Entwicklung von materialübergreifenden Kristallzüchtungstechnologien.

Arbeitsschwerpunkte des Institutes sind:

- *Entwicklung von Züchtungs-, Bearbeitungs- und Charakterisierungsverfahren für Massivkristalle sowie kristalline Gebilde mit Abmessungen im Mikro- und Nanometerbereich sowie von materialübergreifenden Kristallzüchtungstechnologien*
- *Bereitstellung von Kristallen mit speziellen Spezifikationen für Forschungs- und Entwicklungszwecke*
- *Modellierung und Erforschung der Kristallwachstums- und Kristallzüchtungsprozesse*
- *Experimentelle und theoretische Untersuchungen zum Einfluss von Prozessparametern auf Kristallzüchtungsvorgänge und Kristallqualität*
- *Erarbeitung von Verfahren zur Kristallbearbeitung und Erforschung der dabei ablaufenden Vorgänge*
- *Physikalisch-chemische Charakterisierung kristalliner Festkörper und damit verbunden die Entwicklung geeigneter Methoden; Untersuchung von Materialeigenschaften und den zugrundeliegenden Vorgängen*
- *Entwicklung und Bau von Anlagenkomponenten für die Züchtung, Bearbeitung und Charakterisierung von Kristallen*

Als Züchtungsverfahren werden Methoden der Züchtung aus der Schmelze, aus der Lösung, aus der Gasphase und davon abgeleitete Verfahren zur Herstellung kristalliner Schichten verwendet.

Durch die mögliche Synergie zwischen Volumenkristallzüchtung und der Abscheidung von Schichten verfügt das Institut über ideale Voraussetzung zur Herstellung von Substrat/Schicht-Kombinationen mit maßgeschneiderten Eigenschaften.

Materialien

- *Halbleiter mit großem Bandabstand (Aluminiumnitrid, Galliumnitrid und halbleitende Oxide) für die Hochtemperatur-, Leistungs- und Optoelektronik*
- *Oxidische und fluoridische Kristalle für Lasertechnik, Optik, Sensorik und Akustoelektronik*
- *Silizium-Kristalle für Leistungselektronik und Photovoltaik*
- *Silizium/Germanium Kristalle für Strahlungsdetektoren, thermoelektrische Komponenten und Beugungsgitter, SiGe-Nanodrähte und Beugungsgitter*
- *Silizium Schichten auf amorphen Unterlagen für die Photovoltaik*
- *Ferroelektrische und halbleitende Oxidschichten für Anwendungen in der Elektronik, Sensorik, MEMS oder als Speichermaterialien*

The Leibniz Institute for Crystal Growth

is a governmental research and service institute, which is theoretically and experimentally investigating the scientific-technical fundamentals of crystal growth, processing and physico-chemical characterisation of crystalline solids. This ranges from explorative fundamental research to pre-industrial development. The materials presently in development are of fundamental importance in micro-, opto- and power electronics, in photovoltaics, in opto- and laser technology, in acousto-electronics and sensor technology as well as for fundamental research.

The research activities of the institute include bulk single crystals as well as crystalline layers and nanostructures, but also the development of comprehensive crystal growth technologies, which are suitable for different materials.

The Institute

The research and service tasks of the institute include:

- Development of technologies for growth, processing and characterization of bulk crystals and of crystalline structures with dimensions in the micro- and nanometer range and of comprehensive growth technologies
- Supply of crystals with non-standard specifications for research and development purposes
- Modelling and investigation of crystal growth processes
- Experimental and theoretical investigations of the influence of process parameters on crystal growth processes and crystal quality
- Development of technologies for the chemo-mechanical processing of crystalline samples and scientific investigation of related processes
- Physico-chemical characterisation of crystalline solids and development of suitable methods; investigation of the correlation between physical properties and related physical processes
- Development and construction of components for growth, processing and characterization of crystals

Crystals are grown from the melt, from solutions and from the vapour phase and new techniques are developed and improved for the preparation of crystalline layers.

With the combination of bulk crystal growth and layer deposition, the institute possesses ideal conditions to produce customized substrate/layer-combinations.

Materials presently in development

- Wide band gap semiconductors (crystalline aluminium nitride and gallium nitride, semiconducting oxides) for high temperature, power- and optoelectronics
- Oxide and fluoride crystals for acousto-electronics, laser-, opto- and sensor technology
- Si-crystals for power electronics and photovoltaics
- Silicon and germanium crystals for radiation detectors, thermo-electric components and diffraction gratings, Si/Ge nanowires-crystals for radiation detectors and diffraction gratings
- Si layers on amorphous substrates for photovoltaics
- Ferroelectric and semiconducting oxide layers for use in electronic, sensoric and MEMS applications or as storage material

Organisation Chart/Organigramm

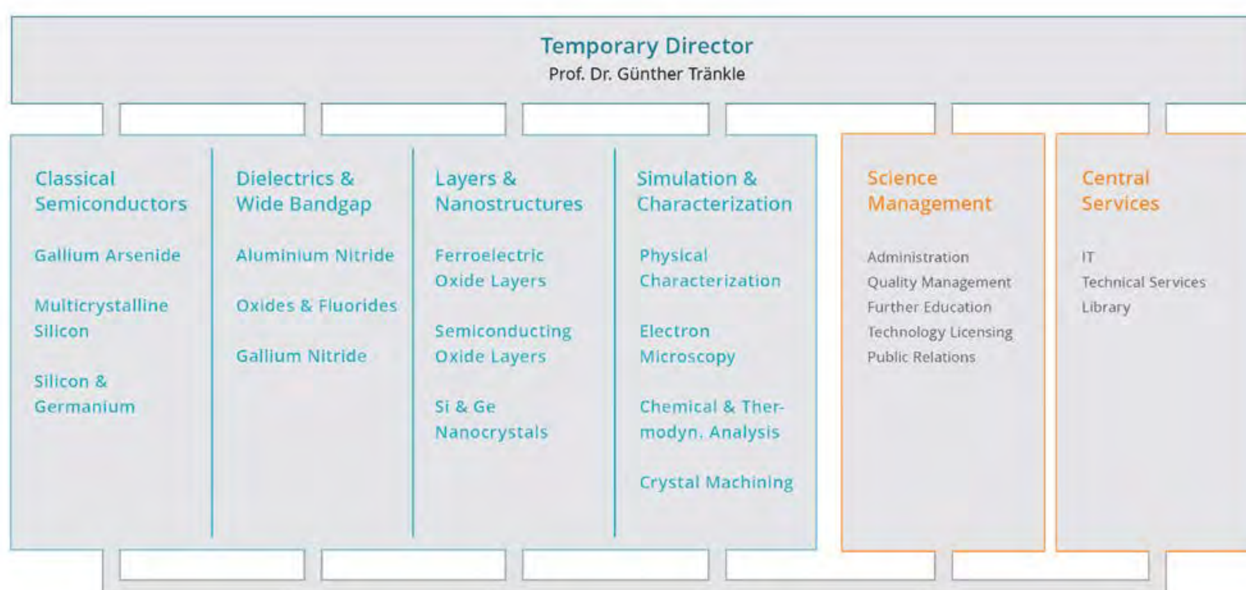

Scientific Advisory Board 2015
Wissenschaftlicher Beirat 2015

Dr. Stefan Eichler (Chairman)
Freiberger Compound Materials GmbH (FCM), Freiberg

Dr. Lothar Ackermann
Forschungsinstitut für mineralische und metallische Werkstoffe,
Edelsteine/Edelmetalle – FEE GmbH, Idar-Oberstein

Dr. Hubert Aulich
SC Sustainable Concepts GmbH, Erfurt

Prof. Dr. Silke Christiansen
Helmholtz-Zentrum Berlin, Institut für Nanoarchitekturen für die Energieumwandlung, Berlin

Prof. Dr. Knut Deppert
Department of Solid State Physics, Lund University, Sweden

Prof. Dr. Saskia Fischer
Department of Physics, Humboldt-Universität zu Berlin

apl. Prof. Dr.-Ing. Michael Heuken
Faculty of Electrical Engineering and Information Technology,
RWTH Aachen University & Vice President of Research and Development
AIXTRON AG, Aachen

Prof. Dr. Michael Kneissl
Institute of Solid State Physics, Technische Universität Berlin

Prof. Dr. Götz Seibold
Brandenburgische Technische Universität BTU, Cottbus-Senftenberg

Dr. Ulrich Steegmüller
Head of Research and Technology OSRAM Opto Semiconductors GmbH, Regensburg

Prof. Dr. Eicke Weber
Fraunhofer Institute for Solar-Energy-Systems ISE, Freiburg

Representative of the State of Berlin

Marie Trappiel
Senatsverwaltung für Wirtschaft, Technologie und Forschung, SenWTF Berlin

Representative of the Federal Republic

Dr. Fabian Kohler
Dr. Ulf Lange
Bundesministerium für Bildung und Forschung, BMBF Bonn / Berlin

Guests

Dr. Manuela Urban
Forschungsverbund Berlin e.V.

Events

IKZ Sommerschule Kristallzüchtung

Die IKZ-Sommerschule ist eine etablierte jährliche und vom IKZ organisierte Veranstaltung, bei der ein international ausgewiesener Experte einen tiefen Einblick in ein Thema aus dem Bereich der Kristallzüchtung gibt. Die 8. IKZ-Sommerschule zur Kristallzüchtung wurde am 13.–15. Juli 2015 abgehalten. Vortragender war Herr Prof. Dr. habil. Peter Rudolph, sein Thema die „Defektbildung bei der Kristallzüchtung aus der Schmelze und auserwählten Epitaxievorgängen“. In fünf Vorlesungen stellte Herr Prof. Rudolph Erkenntnisse aus der Theorie, der Modellierung und der praktischen Züchtungskontrolle vor, zumeist aus dem Bereich der Halbleiter-Kristallzüchtung.

Vielen Teihnehmenden war Prof. Rudolph noch in guter Erinnerung. Er hat zu vielen Themen der Kristallzüchtung beigetragen und damit auch den Ruf des IKZ weltweit mit begründet. Man kann die Sommerschule deshalb auch als Zusammenfassung seiner Arbeiten am IKZ sehen, in die nicht nur seine, sondern immer auch die Erkenntnisse von Fachkollegen eingeflossen sind.

In der Veranstaltung wurden wichtige Defektklassen in Kristallen sowie deren Herkunft und Interaktion während der Kristallzüchtung unter Betrachtung verschiedener Züchtungsverfahren angesprochen. Zuerst wurden Punktdefekte in Kristallen (Verunreinigungen und Eigendefekte) diskutiert. Dabei wurden sowohl die Generation und der Einbau von Punktdefekten als auch Segregationsphänomene angesprochen. Anschließend ging es um Versetzungen und deren räumliche Verteilung, um die Rolle der Versetzungsdynamik inklusive der Zellenbildung bei hohen Temperaturen und um die Kinetik sowie Techniken zur Verringerung von Versetzungen in der Epitaxie. Danach wurden Korngrenzen und deren Bildungsmechanismen, die Facettierung, der inhomogene Einbau von Verunreinigungen und die Zwillingsbildung sowie die Bildung von Einschlüssen und Ausscheidungen besprochen. Die Grundlagen der Gleichgewichts- und der Nichtgleichgewichts-Thermodynamik, der Kinetik und der Wechselwirkung zwischen den Defekten, die als treibende Kraft für die Defektbildung angesehen werden können, sowie Einbau und Strukturbildung von Defekten wurden jeweils mit berücksichtigt und an ausgewählten Beispielen gezeigt. Die Sommerschule von Herrn Prof. Rudolph war eine Expedition in das interdisziplinäre Feld der wissenschaftlich begründeten Kristallzüchtungstechnologie und enthielt sehr viel nützliche Informationen für Neulinge, Experten und experimentell arbeitende Personen in der Kristallzüchtung.

Herr Prof. Rudolph wurde dabei seinem Ruf als exzellenter Lehrer, der immer gut unterhält, Sachverhalte plastisch und lebhaft beschreibt und dabei eng auf seine Zuhörerschaft eingeht, absolut gerecht. Neben dem interessierten Publikum aus dem IKZ nahmen externe Zuhörer aus Universitäten und Forschungseinrichtungen an der Sommerschule teil.

IKZ Summer Course on Crystal Growth

The IKZ summer school is a well-established annual event where an internationally renowned expert provides an in-depth insight on a topic related to crystal growth. The 8th IKZ Summer Course on Crystal Growth took place on 13–15 July 2015. The lecture was held by Prof. Dr. habil. Peter Rudolph, entitled "Defect formation during crystal growth from melt and selected epitaxial processes". In five lectures, he presented results of theory, modeling, and practical in-situ control, with strong emphasis on semiconductor crystal growth.

As a former member of the IKZ, Prof. Rudolph was well known to many of the audience. He communicated the IKZ research worldwide and contributed to numerous fields of crystal growth. In this regard, the lectures were also a worthy summary of his work at the IKZ, while considering the work of other experts, too.

In his summer school course, Prof. Rudolph gave an overview of important defect types, their origins and interactions during the bulk crystal growth from various growth techniques. His lectures started with zero-dimensional defect types, i.e. native and extrinsic point defects. He discussed their generation and incorporation mechanisms as well as micro- and macro-segregation. Dislocations and their patterning, the role of high-temperature dislocation dynamics for cell structuring and bunching, and some features of epitaxial dislocation kinetics and engineering were covered.

Events

After that, he gave an insight into grain boundary formation mechanisms, interplay between facets, inhomogeneous dopant incorporations and twinning as well as second phase precipitation and inclusion trapping. The foundations such as equilibrium and nonequilibrium thermodynamics, kinetic and interaction principles, which are considered as driving forces of defect generation, incorporation, and clustering into structures, as well as selected examples, were presented for every topic.

Prof. Rudolph prepared a thorough expedition into the interdisciplinary field of crystal growth science and technology with lots of important information for scientists, practitioners, and newcomers. Furthermore, Prof. Rudolph met his reputation to be an excellent teacher, giving an entertaining and vivid lecture, and including the audience in a most perceptive way. The lecture was very well attended, and apart from the IKZ staff, scientists from universities and other research institutes participated.

Das IKZ als familienfreundlicher Arbeitgeber

Das IKZ möchte seinen Beschäftigten ein offenes, kooperatives und familienfreundliches Arbeitsumfeld bieten. Das Institut unterstützt daher seine Mitarbeiterinnen und Mitarbeiter bei der Vereinbarkeit von Arbeit und Familie, z.B. durch flexible Regelungen zur täglichen Arbeitszeit oder durch variable Regelungen zu Teil- und Vollzeitbeschäftigung.

Seit 2015 ist das Institut zertifiziert durch das audit berufundfamilie. Damit verbunden hat es Ziele einer familienbewussten Personalpolitik definiert und sich verpflichtet, entsprechende Maßnahmen in den nächsten drei Jahren umzusetzen und weiterzuentwickeln. Das audit steht unter der Schirmherrschaft der Bundesfamilienministerin und des Bundeswirtschaftsministers, nähere Informationen finden sich unter www.beruf-und-familie.de

IKZ as family-friendly employer

The institute intends to create a co-operative and open working environment for all employees. It places special emphasis on the reconcilability of job and family, offering flexible working time models as well as full or part-time employments. In 2015, the institute has been awarded the audit berufundfamilie certificate for its family-friendly human resources policy. The objectives defined in this process will be implemented in the next three years.

The certificate is issues under the auspices of the German Federal Minister for Families and the German Federal Economics Minister. More information is available under www.beruf-und-familie.de

Highlight

Steuerung der Polarität von Gruppe III-Nitriden auf Saphir

Die Gruppe III-Nitride (GaN, InN, AlN und deren Legierungen) sind heute das wichtigste Materialsystem für Anwendungen in der Optoelektronik – z.B. für blaue und grüne Leuchtdioden und Halbleiterlaser. Sie kristallisieren im Wurtzitgitter und haben in der für Bauelemente interessanten Kristallorientierung polare Oberflächen, die entweder durch Stickstoff (N-polar) oder das jeweilige Metallatom (Ga, In, Al) terminiert sind (metallpolar). Optoelektronische Bauelemente werden heute überwiegend als metallpolare heteroepitaktische Schichten auf nichtpolaren Saphirsubstraten abgeschieden. Das reproduzierbare Wachstum von Ga-polaren Schichten auf nichtpolaren Saphirsubstraten durch eine geeignete Pufferschicht gehört zu den wesentlichen Durchbrüchen auf dem Weg zu optoelektronischen Bauelementen durch Amano, Akasaki und Nakamura. Dafür wurden sie Im Jahr 2014 mit dem Nobelpreis für Physik ausgezeichnet. Neuere theoretische Arbeiten zeigen die vorteilhaften Eigenschaften von stickstoffpolaren GaN-Heterostrukturen für Hochfrequenztransistoren. Bislang ist es jedoch nicht gelungen, N-polare Schichten mit vergleichbarer struktureller Perfektion wie die metallpolaren Schichten herzustellen. Das hat das Interesse an den elementaren Mechanismen, die es erlauben die Polarität von Gruppe-III-Nitrid-Schichten zu steuern, erneuert. Jüngste Arbeiten der Arbeitsgruppe Elektronenmikroskopie am Institut konnten die elementaren Mechanismen aufklären, die empirisch gefundenen Rezepten wie der Nitridierung von Saphir und Niedertemperaturpufferschichten zugrunde liegen. Die Untersuchungen wurden im Rahmen der Doktorarbeiten von Natalia Stolyarchuk und Stefan Mohn in enger Zusammenarbeit zwischen dem Leibniz-Institut für Kristallzüchtung, dem CNRS-CRHEA in Frankreich und der North Carolina State University in den USA durchgeführt.

Um die elementaren Mechanismen, mit denen sich die Polarität epitaktischer Schichten einstellen lässt, zu bestimmen, stellten unsere Projektpartner Proben zur Verfügung, die es uns erlaubten, die Anfangsphase des Epitaxie-Prozesses Schritt für Schritt nachzuvollziehen. Naturgemäß begannen die Arbeiten mit der Analyse der AlN und GaN-Pufferschichten, von denen bekannt ist, dass sie für das kontrollierte Wachstum von metallpolaren Schichten entscheidend sind. Zusätzlich wurde die Nitridierung von Saphir untersucht, eine häufig angewandte Technik, bei der die Substratoberfläche vor dem Abscheiden der Pufferschicht unter Ammoniakfluss geätzt wird. Mit hochentwickelten elektronenmikroskopischen Techniken ist es möglich die Kristallstrukturen auf atomarer Ebene zu analysieren und zwischen Al, O und N Säulen zu unterscheiden.

Basierend auf unseren transmissionselektronenmikroskopischen Arbeiten können wir zeigen, dass es die Umwandlung der Saphiroberfläche in eine rhomboedrische Aluminium-Oxinitrid-Schicht (AlON) ist, die die anfänglich N-polare Oberfläche in eine Al polare Oberfläche konvertiert. Es ist die Vielfalt von $Al_xO_yN_z$ Phasen im pseudobinäre Al_2O_3-AlN-System und deren Toleranz gegen intrinsische Defekte, die einen kontinuierlichen Übergang vom oktaedrisch koordinierten Al im Saphir zum tetraedrisch koordinierten Al in AlN ermöglicht. Mit dem so gewonnenen Verständnis des Epitaxie-Verfahrens, sind wir in der Lage, ein schlüssiges Bild von den Prozessen zu zeichnen, die die Polarität von Gruppe-III-Nitrid-Schichten auf Saphir bestimmen.

Understanding polarity control in group-III nitrides on sapphire

Group-III nitrides (GaN, InN AlN and their alloys) are today the most important material system for optoelectronic applications (e.g. blue and green light emitting diodes (LED) or semiconductor lasers). Group-III nitrides crystallize in the wurtzite lattice. In the crystal orientation that is most relevant for applications they exhibit polar surfaces terminated either by N (N-polar) or by metal atoms (metal polar) (Ga, In, Al). The vast majority of today's group-III nitride devices are based on metal-polar heteroepitaxial layers grown on non-polar sapphire substrates. Controlling the polarity of GaN by an appropriate buffer layer was among the breakthroughs by Amano, Akasaki and Nakamura that paved the way to device grade group-III nitride materials in the past. In 2014, the Nobel Prize in Physics has been awarded for this research. Understanding polarity control has now gained renewed interest since the intrinsic scaling advantages of nitrogen-polar GaN heterostructures for high-frequency transistors have been discovered. Recent work, performed in the Electron Microscopy group at the institute unravels the elementary mechanisms behind empirically found recipes like nitridation of sapphire and low temperature buffers that have been used for decades in the field of group-III nitride epitaxy. The investigations are a part of the PhD work from Natalia Stolyarchuk and Stefan Mohn and have been performed within a joint collaboration of the Leibniz-Institute for Crystal Growth, the CNRS-CRHEA in France and the North Carolina State University in the US.

To identify the important mechanisms of polarity control, our project partners provided samples, which allowed us to follow gradually through the initial stages of the epitaxial process. Naturally our attention was focussed on the effect of AlN and GaN buffer layers as they are well known to be crucial for the growth of metal-polar layers.

Highlight

Additionally, the nitridation of sapphire, a commonly applied technique, where the substrate surface is etched in ammonia prior to the deposition of the buffer layer, proved to be essential for polarity as well.

With advanced electron microscopy techniques we were able to resolve the crystal structures on an atomic scale and distinguish between Al, O and N atomic columns. Based on our transmission electron microscopy studies we show that it is the conversion of the sapphire surface into a rhombohedral aluminum-oxynitride (AlON) layer that converts the initial N-polar surface to Al polarity. With the various $Al_xO_yN_z$ phases of the pseudobinary Al_2O_3-AlN system and their tolerance against intrinsic defects, typical for oxides, a smooth transition between the octahedrally coordinated Al in the sapphire and the tetrahedrally coordinated Al in AlN becomes feasible. With our gained understanding of the epitaxial process, we are now able to draw a conclusive picture of how polarity is controlled during the growth of group-III nitrides on sapphire.

Nitridation

The conventional idea behind nitridation of the sapphire substrate is to chemically etch the sapphire surface in ammonia and to substitute the topmost oxygen atoms by nitrogen to form a kind of natural transition layer between substrate and film during heteroepitaxy. At temperatures above 850°C the sapphire reacts with ammonia, while AlN and water is formed.

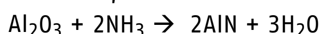

$Al_2O_3 + 2NH_3 \rightarrow 2AlN + 3H_2O$

Figure 1 shows such a nitrided sapphire surface. After 10 min of ammonia flow at around 1080 °C a 2-3 nm thick layer is present instead of a converted purely sapphire surface.

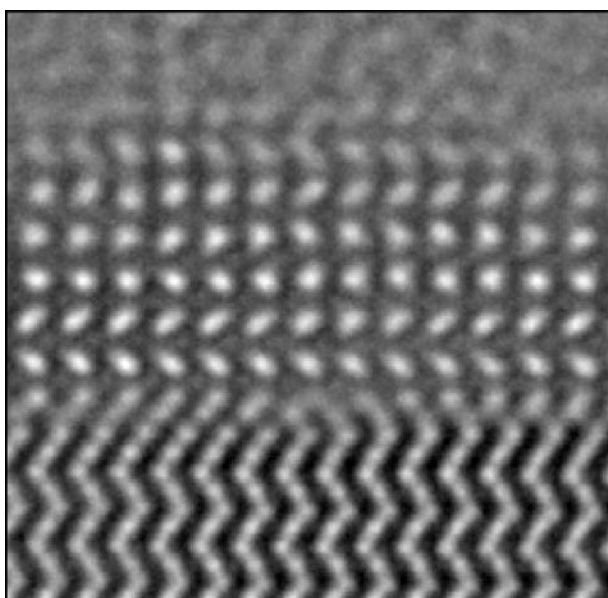

Fig. 1
A 2-3 nm nitride-layer is obtained by the chemical conversion of sapphire in ammonia at around 1080 °C.

The formation of such layers was investigated previously by x-ray photoelectron spectroscopy (XPS) [1,2]. These studies revealed, that the reaction could be described by diffusion of oxygen and nitrogen with the oxygen out diffusion being the rate limiting step. Furthermore, an incomplete substitution of O by N leads to Al-atoms, which are bonded to O as well as to N. Such materials belong to the pseudo binary AlN-Al_2O_3 system. Figure 1 allows us to study the structure of the layer more in detail. For understanding the atomic configuration at the interface, we use contrast simulations of theoretical structural models and compare them to experimental TEM images. The structure of thin AlN layers, grown under Al-rich or N-rich growth conditions on sapphire, have been calculated by density functional theory the past [3]. It was shown, that Al-rich growth conditions lead to sapphire that is terminated with a layer of Al, and causes Al-polar AlN (see Fig. 2a). N-rich growth in contrast leads to a N-terminated surface and to N-polar AlN (Fig. 2c): The comparison of the experimentally recorded interface structure with the simulated images based on the structural models is shown in Fig. 2. We can clearly confirm an N-polar interface structure and the nucleation of N-polar AlN, which is visible in the first two monolayers above the sapphire.

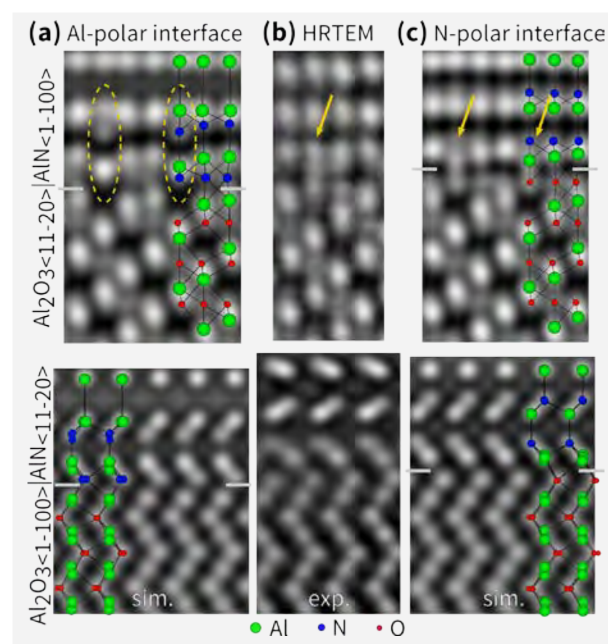

Fig. 2
Analysis of the interface structure of AlN on sapphire as shown in Fig. 1.

Highlight

Figure 3a shows a cross-sectional high resolution (HR) TEM image of the first 4 nm above the sapphire substrate. Comparing the interface structure with the film obtained by nitridation, as shown in Fig. 1, we see a similar N-polar Al_2O_3/AlN interface structure. The first AlN monolayers continue to be N-polar. After around 2 nm of N-polar AlN the polarity of the layer is switched to metal-polarity, which is marked by an inversion domain boundary (IDB). Around that IDB, we are not able to resolve the polarity of the layer anymore. In addition, the stacking sequence of the wurtzite lattice is violated at the IDB. Additional information is gained by scanning transmission electron microscopy (STEM). with a high-angle annual dark-field (HAADF) detector, where the contrast is mainly given by the mean atomic number of the column. While STEM-HAADF investigations reveal a similar picture of the layer, as shown in Fig. 3b, i.e. we see a change of polarity after around 2 nm as our TEM investigations, the IDB shows reduced HAADF intensity, which corresponds to a reduced mean atomic number in the region. For a complete understanding of the crystal structure or such IDBs, we searched for suitable chemical compounds that could explain the observed structural features. We used the various AlON phases as the natural choice. Recent studies of Asaka et al. on the AlN-Al_2O_3 pseudo-binary system gave important clues that we could use for our investigations, i.e. $Al_9O_3N_7$ [4] or $Al_7O_3N_5$ [5]. The AlN content of these are as high as 80% and are therefore close to pure AlN. They have a highly disordered structure, with interpenetrating Al- and N-polar cation sublattices that share a common anion (N,O) sublattice.

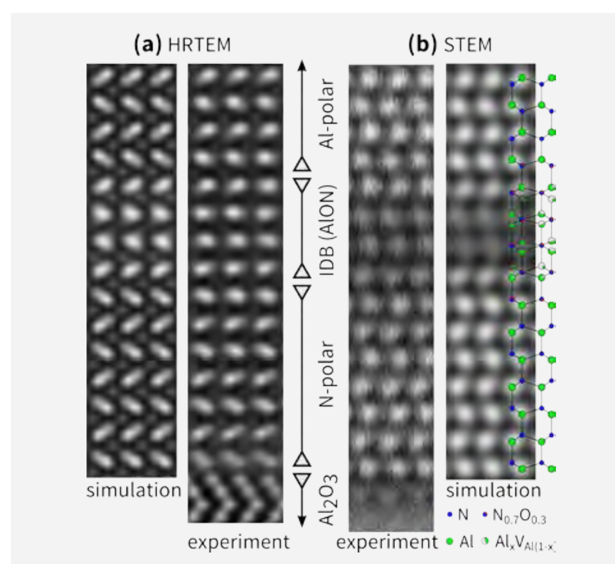

Fig. 3
HRTEM and STEM images of an AlN low temperature buffer layer

TEM-contrast simulations of such phases resembles the structure of the IDB. The HRTEM and STEM contrast simulations, as shown in Fig. 3, of an N-to-Al-polar IDB of $Al_9O_3N_7$ within a matrix of AlN reproduces the features of the recorded TEM images, like the discontinuity in the stacking sequence, the triangular shapes of the columns in HRTEM and the reduced contrast in the STEM image excellent.

The role of the low temperature buffer

With this proof that AlON mediates metal-polarity, the role of the low temperature buffre layer, that is considerd to be crucial in polarity control has to be revisited.

The use of low temperature AlN buffer layers or low temperature GaN buffer layers is the most common used approach to obtain metal polar films [6]. For analysis by STEM-HAADF Z use of GaN over AlN buffers is adavntageous since it allows easy to distinguish between the AlON nitridation layer and the buffer layer. In Fig. 4a we present HRTEM and STEM images of a low temperature GaN buffer that was grown at 560 °C on nitridated sapphire. Combining the information from HRTEM and STEM measurements, our previous results are confirmed. The AlON layer that converts the polarity from n-polar to Al-polar is seen at low intensity in STEM. The GaN, which appears bright in STEM, covers the AlON and grows metal-polar from the beginning. These results are now compared to an N-polar AlN template. Such samples are obtained, when AlN is grown directly at temperatures above 1100 °C on top of nitridated sapphire. In this layer the layer grown N-polar from the beginning. We do not reveal the characteristic features of the AlON layer neither by HRTEM nor by STEM:

As a confirmation, we present the evaluation of the lattice displacement Δc_{AlN}. Across the four monolayers of the AlON inversion domain boundary the effective cation position, which is in imaging a mixture of the "Al polar"-like and the "N-polar"-like position is shifted through the gradually shift in occupation from the N- to the Al-polar position in respect to the anion. The overall displacement along the <0001> axis that is introduced by AlON is as big as 17 % of c_{AlN}.

Highlight

To evaluate the displacement in the layers, we use the STEM-HAADF images, where the intensity is mainly given by the cation position of the lattice.

In Fig. 4c the displacement of metal-polar samples with different buffers and the N-polar AlN without buffer is shown. In both metal-polar layers, we see a strong displacement over of the mean cation position across the first monolayers, caharcteristic of AlON. In the case of the GaN buffer, the displacement increases linearly afterwards, which corresponds to the larger c-lattice parameter of GaN. For the N-polar sample no displacement in regard to pure AlN is measured.

Conclusions

During nitridation the sapphire surface is chemically converted from Al_2O_3 to aluminum-oxynitride (AlON) by the substitution of O by N. AlON converts the initially N-polar interface structure to a metal polarity surface. Upon further growth, these AlON layers prove to be unstable in high temperature epitaxial growth conditions, where they dissolve and N-polar growth results. With low temperature growth conditions AlON can be preserved and metal-polarity is promoted for the ongoing process.

This work has been published in 2016 [7].

References

[1] F. Dwikusuma and T. F. Kuech, J. Appl. Phys. 94 (2003) 5656

[2] Y. Cho, Y. Kim, E. R. Weber, S. Ruvimov, and Z. Liliental-Weber, J. Appl. Phys. 85 (1999) 7909

[3] R. Di Felice and J. Northrup, Appl. Phys. Lett. 73 (1998) 936

[4] T. Asaka, H. Banno, S. Funahashi, N. Hirosaki, and K. Fukuda, J. Solid State Chem. 204 (2013) 21

[5] T. Asaka, T. Kudo, H. Banno, S. Funahashi, N. Hirosaki, and K. Fukuda, Powder Diffr. 28 (2013) 171

[6] S. Nakamura, Jpn. J. Appl. Phys. 30 (1991) L1705

[7] S. Mohn, N. Stolyarchuk, T. Markurt, R. Kirste, M. P. Hoffmann, R. Collazo, A. Courville, R. Di Felice, Z. Sitar, P. Vennegues, M. Albrecht; Phys. Rev. Appl. 5 (2016) 5

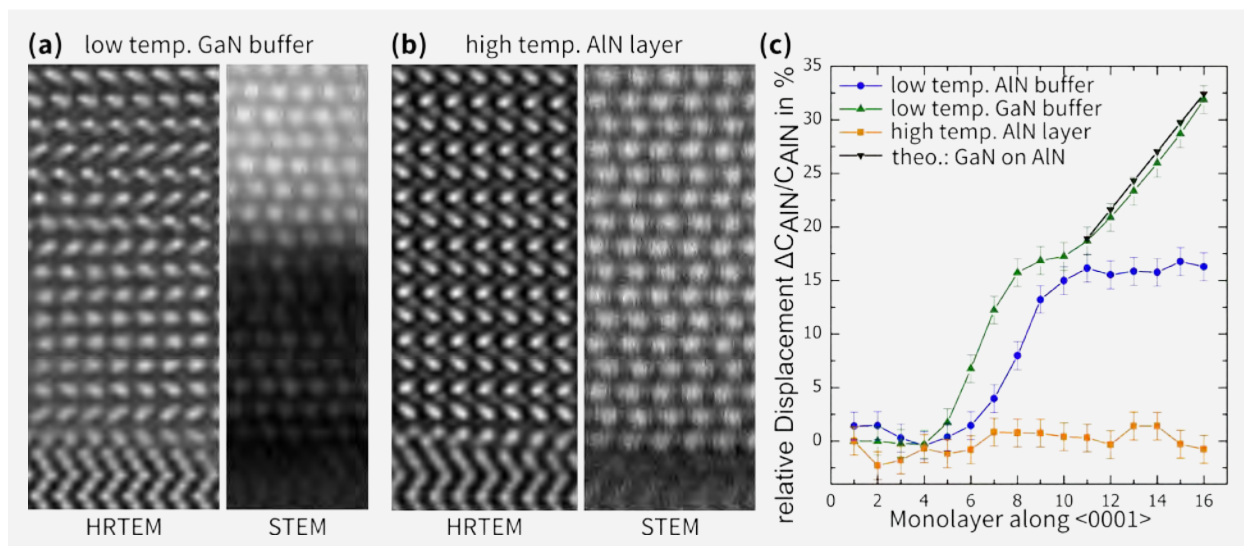

Fig. 4
HRTEM and STEM images of low temperature GaN (a) and high temperature AlN films (b). c) Relative Displacement of different layers.

Classical Semiconductors

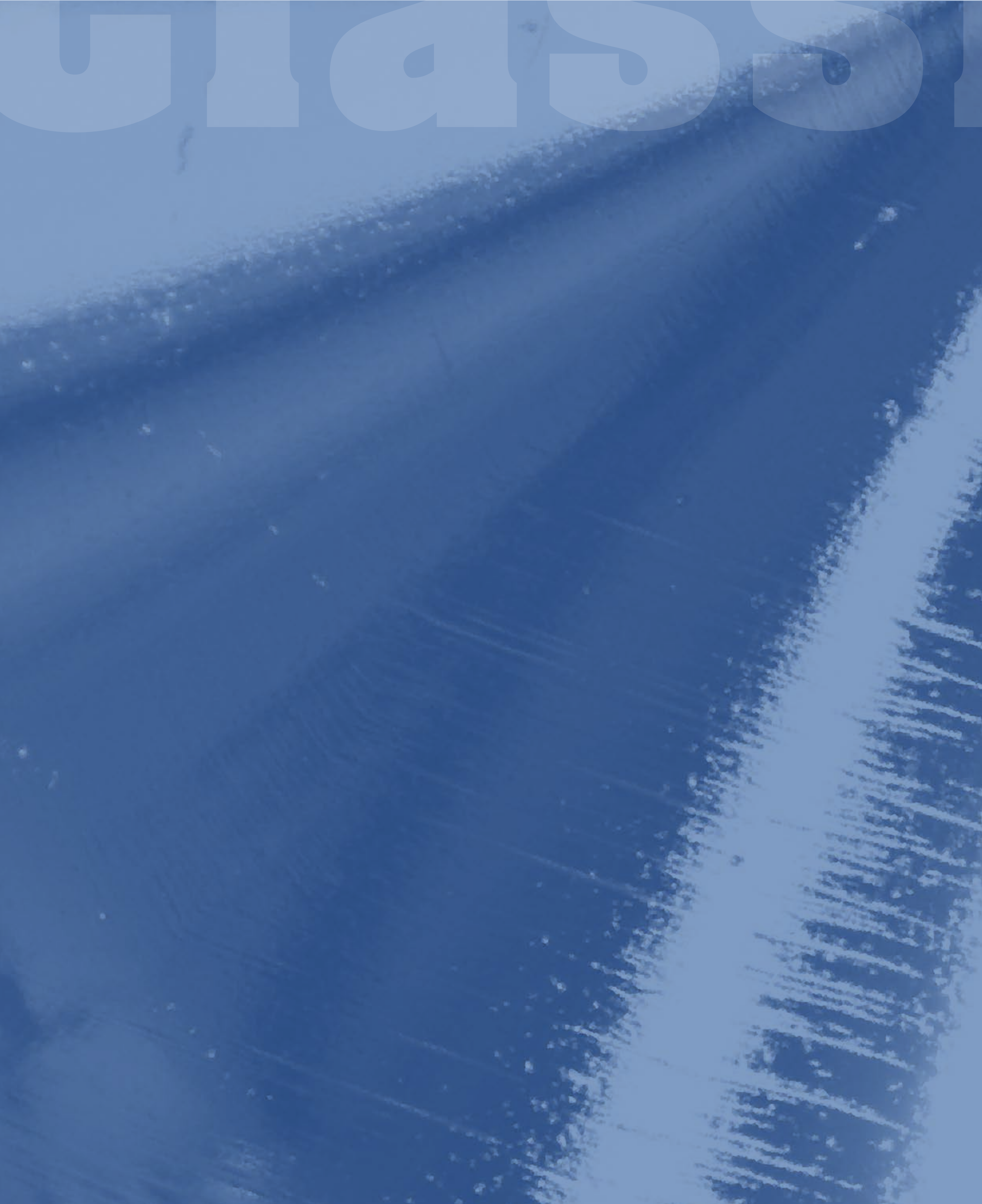

Silicon & Germanium 20

Multi-crystalline Silicon 26

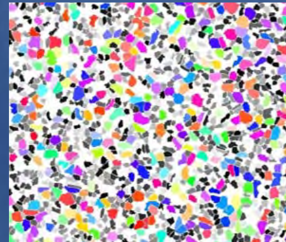

Gallium Arsenide 30

Classical Semiconductors

Acting head of department: Dr. Frank M. Kießling

Die Abteilung Klassische Halbleiter ist überwiegend durch industrienahe Forschungsaktivitäten gekennzeichnet. Als eine der Säulen des Instituts werden traditionell Drittmittel in engem Verbund mit der Industrie eingeworben. Obwohl die Mittelbeschaffung auch in diesem Jahr herausfordernd war, konnten der überwiegende Teil des wissenschaftlichen und technischen Personals der Abteilung über Drittmittel finanziert werden, u.a. auf der Basis verschiedener bilateraler Industrieprojekte. Die Abteilung sieht sich in der Verantwortung, Forschung und Entwicklung auf dem Gebiet der Massivkristallzüchtung von Silicium, Germanium, deren Mischkristallen und III-V-Halbleitern aus der Schmelze weiter voranzutreiben. Als Methoden werden im wesentlichen Float-Zone (FZ), Czochralski (Cz) und Vertical Gradient Freeze (VGF) eingesetzt. Es werden großvolumige Einkristalle und Kristalle mit definierter Gefügestruktur in Züchtungsanlagen gezüchtet, die denen in der industriellen Fertigung ähnlich sind. Der Hauptforschungsschwerpunkt ist die Züchtungsprozessentwicklung zur Reduzierung oder gezielten Einstellung gewünschter Defektkonfigurationen im vorindustriellen Volumenmaßstab. So sind grundlegende und innovative Forschungsarbeiten zu Regelungsalgorithmen für die automatische Kontrolle des Kristalldurchmessers und der Wachstumsgeschwindigkeit bei der Cz- und FZ-Züchtung thematisch angesiedelt. Die numerische Berechnung thermischer Felder in der Schmelze und den Kristallen oder die Berechnung des Einflusses magnetischer Felder auf die Konvektion der Schmelze und den damit verbundenen Effekten an der Wachstumsfront werden innerhalb der Abteilung durchgeführt. Um erfolgreich Wachstumsprozesse entwickeln zu können, werden die Kristalle zeitnah charakterisiert. Dies geschieht unter anderem in enger Zusammenarbeit mit den Themengruppe Kristallbearbeitung und Physikalische Charakterisierung, welche geeignete Proben bearbeiten und anschließend die Defektsituation in den gezüchteten Volumenkristallen charakterisieren. Die Auswertung dieser Informationen zusammen mit den numerischen Resultaten und den langjährigen Erfahrungen der Kristallzüchter erlaubt effektiv eine direkte Umsetzung auf die Entwicklung der Züchtungsprozesse. Die Züchtung nach dem Float-Zone-Verfahren, angesiedelt in der Themengruppe Silicium & Germanium, bestimmt schon seit Jahrzehnten das Weltniveau mit. Das kommt auch dadurch zum Ausdruck, dass ein millionenschwerer Sondertatbestand gewonnen werden konnte. Bei dieser anstehenden Investition handelt sich es um eine 8-Zoll FZ-Anlage, welche die Forschung an modernsten Prozessentwicklungen und damit verbundenen Themen zur Materialentwicklung erlauben soll.

Ein Alleinstellungsmerkmal bei der Forschung stellt desweiteren die Entwicklung von Züchtungsprozessen unter Nutzung der am Institut entwickelten KRISTMAG®-Technologie dar. Für alle in den Themengruppen Multikristallines Silicium und Galliumarsenid genutzten VGF und auch ausgewählten Cz-Kristallzüchtungsanlagen sind spezielle Magnet-Heizer Module im Einsatz. Durch das kontaktlose Einwirken der Magnetfeldkräfte auf die Schmelze kann die Konvektion effektiv beeinflusst und die Wachstumsbedingungen vorteilhaft kontrolliert werden.

The department Classical Semiconductors is predominantly characterized by industry-related research activities. As one backbone of the institute, third-party funding takes part traditionally in close connection with industry. Although the funding was challenging this year, the vast majority of the scientific and technical stuff of the department could be financed through external funds, among others, based on various bilateral industrial projects. The department believes that it has a responsibility for research and development in the field of bulk crystal growth of Si, Ge, their solid solutions and III-V semiconductor compounds from the melt. Basically, Float-Zone (FZ), Czochralski (Cz) and Vertical Gradient Freeze (VGF) are the methods used. Single crystals as well as crystals with a defined microstructure are grown in furnaces, which are similar to those in industrial manufacturing. The development of growth processes for reduced or controlled adjustment of desired defect configurations in pre-industrial scale is the main research focus. Innovative research on control algorithms for automatic control of crystal diameter and growth rate in the Cz- and FZ-growth are established. The numerical calculation of thermal fields in the melt and the crystals or the calculation of the influence of magnetic fields on the melt convection and the associated effects on the growth interface are carried out within the department. In order to develop successfully growth processes, the crystals are characterized promptly. This is done, inter alia, in close cooperation with the thematic groups Crystal Machining and Physical Characterization, who prepare appropriate samples and then characterize the defect situation in the bulk crystals. The analysis of this information along with the numerical results and the extensive experience of crystal growers effectively allow a direct feedback on the growth process development. For decades float-zone growth, based in the thematic group Silicon & Germanium, already codetermined the community worldwide. This is also expressed by the fact that a million dollar special dispensation was won. This upcoming investment is an 8-inch FZ-furnace, which is intended to allow research on advanced process development and related issues for materials development.

Another unique feature in research provides the development of growth processes using the KRIST*MAG*® technology developed at the Institute. All the VGF and also selected Cz crystal growth furnaces used in the thematic groups Multicrystalline Silicon and Gallium Arsenide are equipped with these heater magnet modules. Through the contactless action of the magnetic forces on the melt, convection can be effectively influenced and the growth conditions are controlled advantageously.

Classical Semiconductors: **Silicon & Germanium**

Head Dr. Nikolay Abrosimov
Team M. Czupalla, J. Fischer, B. Hallmann-Seifert, S. Kayser, L. Lehmann, Dr. A. Lüdke, Dr. R. Menzel, Dr. W. Miller, K. Reinhold, M. Renner, Dr. H. Riemann, Dr. H.-J. Rost, T. Turschner, S. Weiß

Übersicht

Forschungsschwerpunkt dieser Gruppe ist die Kristallzüchtung von Silizium hoher Reinheit einschließlich isotopenreinem ^{28}Si, Germanium und Silizium-Germanium (Si_xGe_{1-x})- Mischkristallen in Verbindung mit der wissenschaftlich-technischen Weiterentwicklung entsprechender Züchtungsverfahren. Das Floating Zone Verfahren für Silizium mit ca. 0,5- 150 mm Durchmesser ist die historisch gewachsene Kernkompetenz dieser Gruppe, weitere wesentliche Forschungsfelder sind alternative tiegelfreie sowie modifizierte Czochralski (Cz)-Techniken unter Verwendung spezieller Tiegel für kleinere isotopenangereicherte Germanium und Silizium Kristalle. Kristalldiagnoseverfahren für den Eigenbedarf werden entwickelt und finden auch externes Interesse.

Die Gruppe arbeitet im Rahmen nationaler und internationaler Projekte – wie dem „Kilogramm-Projekt“ – sowie industriell geförderter Forschungsvorhaben im EU-Rahmen. Typische Serviceleistungen sind u.a. kleinere tiegelfrei gezogene Kristalle zur Materialcharakterisierung ohne züchtungsbedingten Fremdstoffeintrag, die auf breites Interesse im In- und Ausland stoßen und z.B. von der Firma Silicon Products in Bitterfeld, der lettischen KEPP EU in Riga oder der Firma TOPSIL Semiconductors aus Dänemark in Anspruch genommen werden.

Eines der Highlights der Gruppe ist das „Kilgramm-Projekt“ unter Federführung des nationalen metrologischen Instituts Deutschlands, der Physikalisch-Technischen Bundesanstalt (PTB) in Braunschweig. Das Projekt soll eine Neubestimmung des Kilgramm-Maßstabs ermöglichen und damit den bisher verwendeten Prototypen, das Urkilogramm in Paris, ablösen. Ziel dieses Projekts ist eine wesentlich genauere Bestimmung der Avogadro-Konstante, die die Anzahl der Atome pro Masseneinheit (mol) eines bestimmten Elements angibt. Auf diese Weise kann anstelle des künstlichen Urkilogramms für die Grundeinheit Kilogramm ein sicherer und genauer Standard geschaffen werden, der auf der natürlichen Basis der Atommasse ^{28}Si beruht. Um das zu erreichen werden versetzungsfreie und hochreine Kristalle aus angereichertem ^{28}Si nach der FZ-Methode gezogen mit einem Durchmesser von knapp über 100 mm, der die Präparation einer Kugel von exakt 1kg Masse laut heute gültigem Standard erlaubt. Das Isotop ^{28}Si wurde vorher in Russland mit Ultrazentrifugen auf weit mehr als 99,999% angereichert.

Die geordnete Gitterstruktur und hohe Reinheit des Kristalls erlaubt es dann aus dem genauen Wert des Kugelvolumens die Anzahl der Si Atome in der 1kg-Kugel zu bestimmen. Diese Zahl definiert dann die Kilogramm Einheit unabänderlich. Die maximal zulässige Unsicherheit dieser Zahlbestimmung wurde 2007 im ersten Anlauf (Avogadro-Projekt) nicht befriedigend unterschritten. 2015 wurde die Prozesskette unter verbesserten Bedingungen erneut durchlaufen. Nach 6 FZ-Züchtungsdurchgängen teils im Vakuum konnten wir 2015 einen zweiten ^{28}Si- Kristall an die PTB übergeben mit höherer Isotopenanreicherung (>5,5N) und Reinheit, der z. Zt. noch vermessen wird. Nicht zuletzt um die Reproduzierbarkeit zu demonstrieren, wurde die Zusammenarbeit im November 2015 erneut verlängert, um die strengen Bedingungen für die weltweite Anerkennung des neuen Kilogramm-Standards zu erfüllen.

Die numerische Modellierung des Si-FZ-Prozesses spielt für die Kristallzüchtung bei großen Durchmessern und speziell bei <111>-Orientierung eine zunehmend große Rolle. Unser dänischer Industriepartner Topsil Semiconductor Materials gab den Anstoß zur weiteren Entwicklung unseres numerischen FZ-Modells, der auf die räumliche Simulation des elektromagnetischen Feldes, des Temperaturgradienten und der thermomechanischen Spannung während der instationären Anfangsphase des Wachstums des Kristallkonus zielte. Die numerische Simulation führte zu verbesserten Induktoren und höherer Prozess-Stabilität.

Zwei große Schritte wurden auf dem Weg zu ultrareinen Germanium Einkristallen getätigt, wie sie im Projekt GERDA (GERmanium Detector Array) benötigt werden: die Cz-Züchtung eines ersten Ge-Kristalls in reinem Wasserstoff mit reduzierter Defektdichte und die Inbetriebnahme der selbstentwickelten und im IKZ gebauten Multizonen Reinigungsanlage für das Ausgangsgermanium mit vier separaten horizontalen Booten. Voraussetzung war in beiden Fällen die Beherrschung der Wasserstofftechnik unter strengen Sicherheitsvorgaben.

Die Arbeit am BMBF- Projekt „In TerFEL“ (Time-resolved ***In****frared and* ***Ter****aherz spectroscopy of sallow donors and acceptors in semiconductors with* ***F****ree* ***E****lectron* ***L****asers) konzentriert sich auf die Kristallzüchtung und die Pobenpräparation für die Spektroskopie an flachen Störstellen in Si und Ge.*
Ge Kristalle wurden beim Wachstum aus einer Phosphinquelle mit Phosphor dotiert, hochreine Si Kristalle wurden für die Magnesium-Diffusionsdotierung präpariert sowie undotierte natürliche und von ^{76}Ge-abgereicherte Germaniumkristalle gezüchtet für die Neutronen-Transmutationsdotierung (zu Ga, As, Se).

Ge-Kristalle dotiert mit P und co-dotiert mit P und Ga wurden im Rahmen einer Kooperation mit der Fa. Photonic Sense in Eisenach gezogen. Hierbei kam die am IKZ entwickelte mini-CZ Methode mit Induktionsheizung zum Einsatz, die es gestattet, Si-Kristalle aus sehr kleinen Materialmengen zu züchten. Diese wurde hier für Germanium mit 2“ Durchmesser angepasst, um die Phosphin- Gasdotierung einer Si-FZ Anlage nutzen zu können.

An der Uni Göttingen läuft das ESA-Projekt SEMITHERM, das Messung der thermophysikalischen Eigenschaften von unterschiedlich unterkühlten Halbleiterschmelzen unter Mikrogravitation gewidmet ist. Die Züchtung von Si_xGe_{1-x}-Kristallen mit definierten Werten für x von 0,75-0,9 bei gleichzeitig hoher Bor-Dotierung sowie die Präparation von sphärischen Proben daraus stellte eine Anspruchsvolle Aufgabe dar. Die Kugeln wurden für Levitations- Schmelzversuche an Bord der ISS übergeben.

Zur Unterstützung bzw. Bewertung von Kristallzüchtungsexperimenten werden in der Gruppe die eigenentwickelten Kristall-Diagnoseverfahren Lateral Photovoltage Scanning (LPS) und Scanning Photolumineszence (SPL) gepflegt und weiterentwickelt. Sie erlauben es das Wachstumsstreifen-Muster an Mono- und Multikristallinen Schnitten abzubilden und u.a. die Form der Kristallisationsfront zu analysieren. Die physikalischen Effekte und methodische Weiterentwicklungen dieser Messverfahren sind Gegenstand einer Promotion, die 2017 abgeschlossen werden soll.

Overview

The Silicon & Germanium group focuses its research activities on Float Zone (FZ) growth of silicon with diameter of about 0.5 – 150 mm, including isotopically enriched ^{28}Si, and on Czochralski (Cz)-growth of germanium and Silicon-Germanium (Si_xGe_{1-x})-solid solution crystals. Cz-growth of silicon crystals up to 1 kg weight and 2" in diameter can be realized too. We use this technique e.g. for the growth of ^{28}Si from $^{28}SiO_2$ coated crucibles to minimize the material loss by processing of ^{28}Si for the "kilogram" project.

The work of the group includes both the participation in national (e.g. SAW) and international projects with industrial partners and research institutes and the growth of crystals as service according to customer specification. Amongst others there is the demand on the growth of small crystals for material characterisation. The crucible-free growth methods such as FZ technique allow characterisation of the material without adding impurities from the growth process. This is the topic of a cooperation with the company KEPP EU, Riga, Latvia and Topsil in Denmark. FZ crystals were grown from the core of polycrystals and polycrystals too with the purpose to enable impurity analysis in the starting material. Also small FZ crystals were grown from cores of polycrystals on demand of the German company Silicon Products Bitterfeld.

The kilogram project is one of highlights of the Silicon & Germanium group. The project managed by the Physikalisch-Technische Bundesanstalt (PTB) (the German National Metrology Institute) aims at a more precise determination of the Avogadro constant, which describes the number of atoms contained in a certain quantity of substance, i.e. in one mole. Finally, based on this precisely defined natural constant, this could lead to a new definition of the kilogram standard. In the frame of this project, FZ grown dislocation free ^{28}Si crystals of 4" in diameter are used for the preparation of silicon spheres which in turn are used for measurements to give a connection between the volume and the number of atoms in the highly ordered crystalline structure. In 2015, a ^{28}Si single crystal, as second crystal after "Avogadro"-crystal grown in year 2007, was delivered to PTB after 6 FZ-runs carried out partly in vacuum for additional purification of the polycrystalline starting material. The next crystal is under preparation. To prove the reproducibility of the results achieved, growth of more crystals are planned in frame of the subsequent project started in November 2015.

Classical Semiconductors: **Silicon & Germanium**

Numerical modelling of the FZ for Si plays an important role in the group. The current development of a new growth process for crystals with large-diameter and for crystals of <111> orientation, at the facility of our Danish industry partner Topsil Semiconductor Materials, gave another impetus for the evolution of our numerical model for FZ growth. The focus was on the simulation of the electromagnetic field in 3D, as well as the temperature gradients and thermal stress during the critical cone growth phase in the beginning of the process, where the crystal diameter increases over time and the growth conditions are unsteady. The results of the calculations led to an improved inductor design and helped to improve the process stability.

Two big steps were made in our group in developing a technology for the growth of germanium single crystals with high purity, to be used in the project GERDA - GERmanium Detector Array. One of them is the first Ge growth experiment in H_2-atmosphere by the Czochralski technique. This experiment showed the advantage of the H_2-atmosphere to improve the quality of the crystals including control of dislocation density. As second achievement in this field we started the operation of a zone refining furnace constructed and manufactured in our group. Four separate reactors for Ge purification will be used for preparation of polycrystalline high-purity germanium as starting material for Cz-growth.

Our work in the frame of BMBF-Project InTerFEL (*Time-resolved infrared and terahertz spectroscopy of carrier dynamics in semiconductors with free electron lasers*) concentrated on the crystal growth and sample preparation for time-resolved spectroscopy and Raman spectroscopy of shallow donors and acceptors in silicon and germanium. Some crystals were doped during the growth, e.g. doping of Ge with phosphorus was carried out using gas-doping with phosphine as a phosphorus source. Un-doped high purity Si crystals were grown for Mg diffusion doping and both un-doped natural and ^{76}Ge- depleted Ge samples were prepared for neutron transmutation doping (to Ga, As, Se).

Ge crystal doped with phosphorus and co-doped with phosphorus and gallium were grown also in frame of the cooperation with the German company Photonic Sense using the mini-Cz technique. This technique, developed earlier in IKZ for the growth of isotopically pure Si and Ge crystals from extremely small charges (melt volume of some milliliters) was up-scaled for the growth of Ge crystals with 2" in diameter. The peculiarity of this method is in using of equipment for Si FZ growth, namely the furnace is equipped with inductive heating of working frequency 2.7 MHz. The crystals were doped with phosphorus using gas-doping as standard in FZ growth of silicon.

Some $Si_{1-x}Ge_x$ polycrystalline crystals with x between 0.75 and 0.9 were grown by Cz technique for Göttingen University in frame of the ESA project SEMITHERM – "Investigation of thermophysical properties of liquid semiconductors in the melt and the undecooled state under micrigravity conditions". The highly boron doped samples in the spherical form prepared from the crystals grown are provided as a starting material for levitation experiments on the board of the ISS space station.

In addition, the crystal growth experiments in our group are supported by Lateral-Photovoltage-Scanning- (LPS) and Scanning-Photoluminescence (SPL) allowing us to detect the solid-liquid interface and defect structure in Si, Ge and SiGe crystals. The further development of both methods is made in the frame of a PhD thesis with the goal to explain the relation between physical parameters of samples with LPS and SPL measurement signals. Finally, since October 2015 the PhD student Xiaofang Qi from Xi'an University is staying in the group with a grant by the Chinese Scholarship Council on a project for computing the grain evolution during the solidification of silicon on a macroscopic scale. The model is implemented in the software tool WaLBErla provided by the chair of Prof. Rüde of Universität Erlangen-Nürnberg.

Results

For the growth of the requested perfect ^{28}Si single crystal in the frame of the "Kilogram"-project, only the crucible-free Floating Zone (FZ) technique is suitable to achieve the purity needed and to save isotopic enrichment. The isotopically enriched starting material has to be prepared in form of the rod and is limited in quantity. However, before crystal growth, the FZ method requires the preparation of a rod from polycrystalline starting material including a cut of the contacts and making cone on one side and a groove for the holder on the other side. Both procedures lead to losses of some material in form of fragments and this material will be missing in the final crystal.

Classical Semiconductors: **Silicon & Germanium**

Even small losses have to be avoided, because on one hand, we only have a certain amount of starting material available, and on the other hand, the crystalline volume and shape must allow the preparation of two crystalline spheres from each crystal. In addition, because the initial oxygen and carbon concentrations in the starting polycrystalline rod are too high many growth runs have to be done and every run leads to losses of original (as-deposited) material. To minimize the losses, the process from starting material to the growth of the final crystal of high perfection should be optimized.

From the very first, one should estimate (based on the oxygen and carbon concentration in poly-Si) how many growth runs would be required. C and O content were measured using FTIR both in the polycrystalline material and in the end of the crystal after the first growth run. As-deposited polycrystalline samples were annealed before the measurement over 10 hours at about 1350°C to make them transparent for IR beam [1]. Both measurements gave nearly the same result of carbon concentration $[C]=2.5\times10^{15}$ cm^{-3} while oxygen concentration measured in the FZ crystal was an order less than in the polycrystalline sample, measured as $[O]=5.2\times10^{17}$ cm^{-3}, because of oxygen evaporation during the FZ growth process. For further decrease of oxygen concentration in the crystal, two growth runs were made in vacuum and the next runs were carried out in an argon atmosphere where the low oxygen concentration was preserved by a previous long-time desorption of the water layers in vacuum.

Carbon can be reduced by the segregation effect of multiple FZ passing. The number of growth runs was estimated using the theory of zone refining for many passes [2] based on the carbon concentration in the starting material and the target concentration $< 2.0\times10^{15}$ cm^{-3} over the whole crystal length and was determined as 6 runs. Two of these runs were made in vacuum to minimize oxygen concentration. However, the freeze-off technique used in the end of each run to avoid new preparation of the grown crystal for the next run resulted in loss of some additional material. To cope with this problem, we used the procedure developed in our group [3]: all cut fragments of polycrystalline silicon were regrown by Czochralski technique to a 2″ crystal and joined to the FZ crystal just after the first run. To avoid the isotope dilution during Cz growth, the quartz crucible was coated before the growth process with a $^{28}SiO_2$ layer of about 100 µm thickness [4]. In this way, no isotope dilution was measured in the Cz crystal grown.

The final crystal of 100.3 mm in diameter was of n-type except the first 50 mm in cone having p-type and had a mass of 5.12 kg (Fig.1). <100> oriented ^{28}Si seed crystals were grown in previous steps of the project by the crucible-free pedestal technique. At the end of the growth process, the crystal was tapered down to diameter 79 mm using our automatic diameter control system to protect the cylindrical part of the crystal from back-gliding dislocations.

Fig. 1
^{28}Si dislocation free single crystal grown by FZ technique

Classical Semiconductors: **Silicon & Germanium**

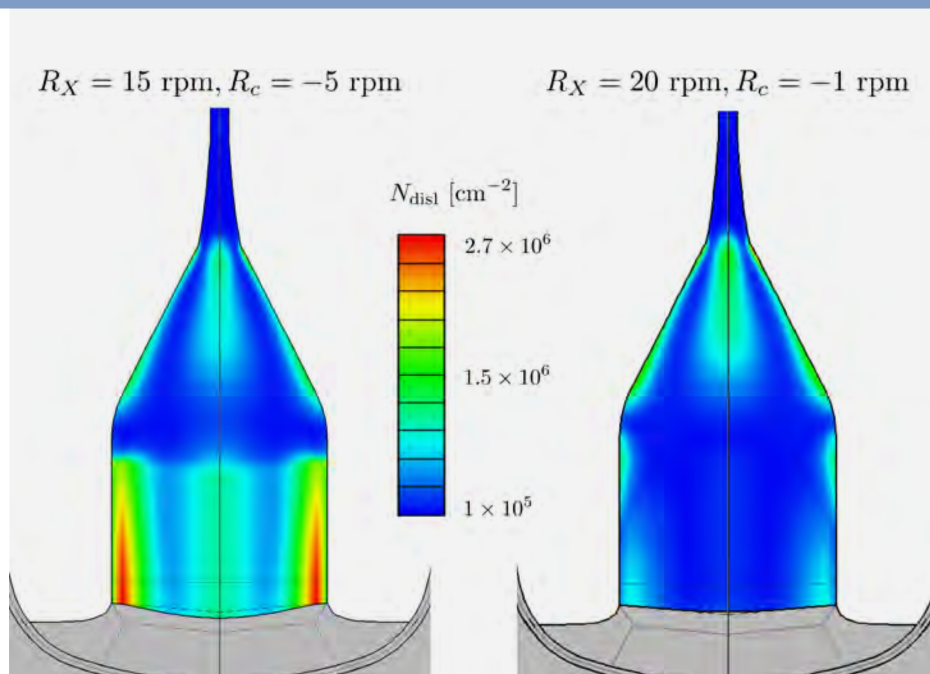

Fig. 2
Fully transient calculations of dislocation densities in the Ge crystal grown by Cz technique

Another great challenge, addressed by our group is the Czochralski growth of highly pure Ge crystals with low dislocation density (< 10^4 cm^{-2}). The experimental efforts to grow such crystals have been accompanied by axisymmetric but fully transient calculations with the software tool CGsim, which enables us to compute the dislocation densities. Because the multiplication rate of dislocations depends exponentially on the temperature, the stress in the vicinity of the melt/solid interface is critical. The simulations exhibit that a higher rotation rate of the crystal leads to a flatter interface and thus a reduced dislocation density (Fig. 2). A direct comparison with experiment was not yet possible, because experiments were performed in Ar atmosphere and in all crystals a high dislocation density was already observed in the neck and beginning of the cone. However, in the experiment with a higher crystal rotation rate we observed no further increase of the dislocation density in the cylindrical part. Additionally, in November 2015 the first Ge crystal was grown in H_2-atmosphere. Nearly no dislocations were observed in the beginning of the cone and the density in the cylindrical part was one magnitude lower than in the best case before. That means that the crystal growth of germanium in H_2-atmosphere allows for better control of dislocation density in growing crystals. In the frame of project GERDA, we will use these research findings as starting point to improve the crystalline quality as well as the purity further to meet the high requirements of this project. The project aims at the detection of the neutrinoless ββ-decay, a very rare occurrence, using germanium crystals at the same time as material for the decay and as detector.

LPS- [5, 6] and SPL-methods are important analytic methods to determine the quality of Si, Ge and SiGe crystals. The characteristic solid-liquid-interface [6] is detectable, which leads to information about the temperature field, growth direction during solidification, homogeneity of the charge carrier density and grain boundaries. The flexibility and the possibility to characterize various parameters of a semiconductor crystal after growth is outstanding for these methods, hence they are highly desired by the solar and crystal growth industry.

A focused laser beam (650nm≤λ≤1080nm, 10µm≤d≤30µm, 0.3mW≤P≤300mW) amplifies electron-hole-pairs in the SPL-setup. The resulting luminescence is detected spatially-resolved by a photodiode. In contrast the LPS-method detects the Dember-voltage [7] of excited electron-hole-pairs by a laser. This Dember-voltage is caused by inhomogeneities of the charge carrier density. Therefore, the derivation of the charge carrier density is detectable by the LPS-method.

Due to the applied laser power, the sample also heats up. Up to now, the resulting temperature field is unknown, especially for a local resolution in size of the focus diameter. A structural change of the observed crystal as a result of sample heating was not yet detected but could never be excluded completely. The information of the temperature field is essential for further simulations of the LPS- and SPL-method.

To measure the heating of the sample in the focal area, we used a multicrystalline silicon sample (800mm × 800mm × 0.18mm) and a Platinum thermometer Pt-100 (2mm × 4mm × 0.2mm), which was placed at the bottom of the sample. Due to the heat transfer in the silicon sample, the heating by a laser (λ=830nm, d=10µm, P=140mW) in continuous operation was detected.

The maximum temperature is exponentially dependent on the laser intensity, which was already described by Rainer [8]. This measurement is the basis for time-dependent simulations of the temperature field caused by a pulsed moving laser as used in the measurement setup.

Therefore, we simulated that measurement with COMSOL Multiphysics® using a finite element method, and found a match for a heat transfer coefficient h=0.13W/m^2 K. Due to different penetration depth of the laser beam in silicon (t=15.4µm) and germanium (t=0.25µm) the simulation model had to be adapted. For silicon we used a 3 dimensional heat flux in the sample in form of a Gaussian distribution with an exponential decrease due to the penetration depth. That implementation was not necessary for a germanium sample because 99,7% of the absorption of the laser beam takes place in the surface elements of the computed sample. That's why we could increase the resolution by using a 2 dimensional Gaussian model independently of the penetration depth. Recently we added a laser spot velocity (v=5mm/s) and a laser modulation frequency (f=1kHz) to represent the scanning method of LPS and SPL.

For Ge, the results of this simulations are shown in Fig.3. An oscillating behaviour of the focal temperature with respect to the modulation frequency is displayed. The accumulation of heat is visible in the v=0mm/s line with an increasing temperature. This is justified by the fact that, to decrease the computational time, we added no temperature decreasing possibility but still the accumulation of heat is a minor effect in this simulation. That's why we neglect it in our setup for a pulsed laser with moving focal point completely.

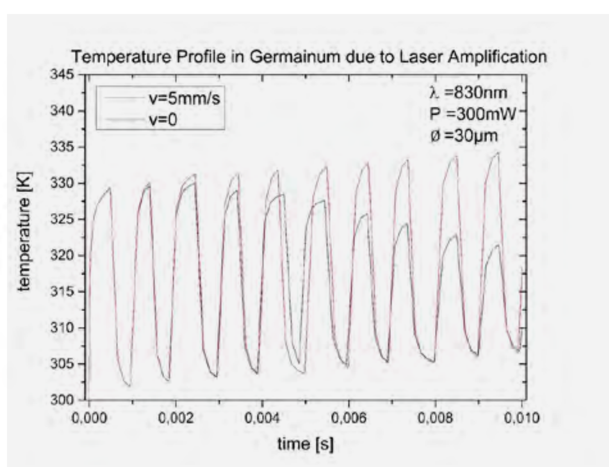

Fig. 3
imulation results: temperature profile in the laser focus for a germanium sample with respect to the time for different laser spot velocities for a modulation frequency f=1kHz

In Table 1 one can see the maximum amplitude of that oscillating temperature for different laser parameters with a moved focus. The reason for a decreased temperature while the laser power was increased is the lowered power density; hence the heating temperature is dependent of the laser power density. The higher heating temperature in Ge is also related to an increased laser power density in this case caused by the extremely short penetration depth.

λ=830nm	d=10µm, P=140mW	d=30µm, P=300mW
silicon	ΔT=11K	ΔT=10K
germanium	ΔT=35K	ΔT=29K

Tab. 1
Simulation results for different laser parameters in silicon and germanium.

Based on this simulation results we are able to estimate the impact of the local sample heating. There will be no structural change in the sample during LPS and SPL measurements. Those results are a milestone for further simulations of the measurement system. It allows implementing the crystal parameters with respect to the local sample temperature.

References

[1] L.L. Hwang, J. Bucci, J.R. McCormick; J. Electrochem. Soc. 138 (1991) 576

[2] W.G. Pfann; Zone melting, Johm Wiley&Sons (NY-London-Sydney) 1966, p.44

[3] P. Becker, H.-J. Pohl, H. Riemann, N. Abrosimov; Phys. Status Solidi A 207 (2010) 49

[4] A.V. Gusev, V.A. Gavva, E.A. Kozyrev, H. Riemann, N.V. Abrosimov; Inorg.Mater. 49 (2013) 1167

[5] A. Lüdge, H. Riemann; Inst. Phys. Conf. Ser. No 160, (1997) 145

[6] N.V. Abrosimov, A. Lüdge, H. Riemann, W. Schröder; J. Crystal Growth 239 (2002) 356

[7] H. Dember; Physikalische Zeitschrift 32 (1931) 554

[8] T. Rainer; Laserstrahlinduzierte Bildung von Silbernanopartikeln in Glas, Master's thesis, Martin-Luther-Universität Halle-Wittenberg, 2002

Classical Semiconductors:
Multi-crystalline Silicon

Head Dr. Frank M. Kießling
Team I. Buchovska, Dr. N. Dropka, Dr. T. Ervik, Dr. R. Menzel

Überblick

Die Photovoltaikindustrie ist stark technologiegetrieben und als Kennziffer gilt die Gesamtheit der Kosten, die über den Herstellungs- und kompletten Funktionszeitraum anfallen. Die Schlüsselparameter in diesem Zusammenhang sind entsprechend die Erhöhung der Solarzelleneffizienz und eine signifikante Kostenreduktion in der gesamten Wertschöpfungskette. Da das Ergebnis der Zelleffizienzen sehr stark von der Materialqualität abhängt, ist die Forschung der Ursachen für die Entstehung und Entwicklung von Defektdichten ein immerwährendes Thema. Derzeit liegt der Marktanteil des kristallinen Siliciums bei 90%, welches entweder mit dem Czochralski-Prozess oder gerichtet erstarrt (directional solidification – DS) hergestellt wird. Letztere Methode ist Gegenstand der Forschung der Gruppe Multikristallines Silicium am IKZ. Da die überwiegende Zahl der Defekte während der gerichteten Erstarrung entsteht, ist die kontinuierliche Reduzierung von Lebensdauer verringernden Defekten und deren Kontrolle während des DS-Wachstumsprozesses die Motivation zur Entwicklung verschiedener Erstarrungstechniken. Dabei werden drei wesentliche Wachstumsansätze verfolgt, um unterschiedliche Blockqualitäten zu erhalten (Fig. 1): multikristallin (mc)-Si, quasi-mono (QM)-Si, und das sogenannte high performance mc-Si (HPmc-Si).

Die Gruppe Multikristallines Silicium hat ihre Forschungsaufgaben und F&E-Aktivitäten in 2015 fortgeführt und erweitert. Alle oben erwähnten Variationen des Vertical Gradient Freeze (VGF)-Verfahren zur Erstarrung von Silicium kommen dabei zur Anwendung. Bei diesen Verfahrensentwicklungen werden Öfen für Tiegelgrößen G1 und G2 eingesetzt, die mit KRISTMAG® Heizer-Magnet-Modulen ausgerüstet sind. Diese Heizelemente erzeugen neben der üblichen Wärme Magnetfelder, um die Schmelze zu durchmischen und die Form der fest-flüssigen Grenzfläche zu kontrollieren. Die projektfinanzierte Forschung zur Optimierung der Wachstumsprozesse von QM-Si-Blöcken in der Größe G2 unter dem Einfluss von Wandermagnetfeldern wurde fortgesetzt. Die erfolgreiche Erstarrung von Silicium unter Verwendung von Keimen ist eine anspruchsvolle Züchtungstechnik. Dabei muss die Schmelze des Ausgangsmaterials präzise kontrolliert werden, um ein Auflösen der Keime am Boden zu verhindern. Der Einsatz von mehreren Keimen führt dabei typischerweise zu Defektbildungen an den Keimstößen und infolge von Fehlorientierungen aufgrund der Platzierungsungenauigkeiten.

Während der Erstarrung ist es wichtig, die Defektentwicklung an Keimstößen sowie an den Tiegelwänden zu vermeiden und zu kontrollieren. Körner und ihre Grenzen sind als Hauptquelle für die Entwicklung von unerwünschten rekombinationsaktiven Versetzungsclustern bekannt. Einige Ergebnisse sind im Folgenden dargestellt.

Im Jahre 2015 wurde der Ofen mit der Tiegelgröße G1 genutzt, um einen Züchtungsprozess für HPmc-Si-Blöcke zu entwickeln. Die entwickelten Wachstumsprozesse für mc-Si und HPmc-Si führten zu signifikanten Materialunterschieden hinsichtlich ihrer Kornstruktur und Versetzungsdichte. Zusätzlich wurde Ausgangsmaterial in verschiedenen Qualitäten verwendet und wandernde Magnetfelder für eine starke Durchmischung der Schmelze während des gesamten Erstarrungsprozesses eingesetzt. In Kooperation mit den Industriepartnern Elkem Technology und Elkem Solar wurden erfolgreich Solarzellen aus dem Material der G1-Blöcken mit ihren unterschiedlichen Materialqualitäten hergestellt. Einige Projektergebnisse sind ebenfalls unten vorgestellt. Ebenfalls begann im Jahre 2015 ein Zwei-Jahres-Projekt zur Untersuchung des Einflusses von verschiedenen Heißzonenmaterialien auf das Verunreinigungsniveau bei gerichtet erstarrtem Silicium. Die Verfahrensentwicklungen wurden vollständig von numerischen Modellierungen begleitet, insbesondere um die Einflüsse der angewandten magnetischen Kräfte auf das Temperaturprofil und die Form der fest-flüssigen Grenzfläche zu untersuchen. Traditionell findet eine intensive abteilungsübergreifende Zusammenarbeit mit den IKZ-Gruppen Kristallbearbeitung und Physikalische Charakterisierung statt.

Overview

The photovoltaic (PV) industry is heavily technology-driven and the figure of merit is total cost of ownership. In this context the enhancement of solar cell efficiencies and significant cost reduction in the whole value chain are key parameters. Since the outcome of the cell efficiencies depends largely on the material quality, studying the origin and development of defect densities is a field of ongoing investigations. Up to now, more than 90 % of the PV market share is based on crystalline silicon obtained either by Czochralski growth or directional solidification (DS), the latter of which is the scientific task of the group Multi-crystalline Silicon at IKZ.

Classical Semiconductors: **Multi-crystalline Silicon**

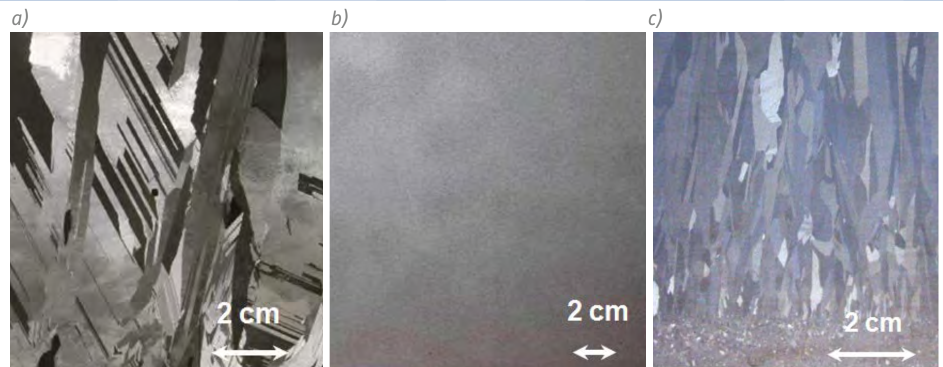

Fig. 1
Grain structure visualized on vertical cuts
a) mc-Si
b) QM-Si and
c) HPmc-Si

Since the solidification process is responsible for introducing most of the defects, the continuous reduction of lifetime limiting defects and their control during the DS growth process is the impetus to develop various solidification techniques. Three main types of growth concept are applied in order to obtain different ingot qualities (Fig. 1): multi-crystalline (mc)-Si, quasi-mono (QM)-Si, and the so-called high performance mc-Si (HPmc-Si).

The group Multi-crystalline Silicon has proceeded with its research tasks and R&D activities, and continued to develop processes for all the variations of vertical gradient freeze type solidification processes of silicon mentioned above. For these process developments, G1- and G2-sized furnaces equipped with KRIST*MAG*® heater magnet modules have been in use. These heaters are capable of producing magnetic fields in order to stir the melt and control the solid-liquid interface properties while maintaining the common function as a heat source during the solidification process.

The project-based investigation of growth process optimization of G2-sized QM-Si ingots under the influence of TMFs has been proceeded. The successful solidification of silicon using seeds is an ambitious growth technique. It requires the exact control of melting the feedstock material without dissolving the seeds on the bottom. The use of multiple seeds results typically in defect generation due to seed junctions and off-orientations by displacement. It is essential to avoid and control defects from the seed junctions as well as those formed at the crucible walls. Grains and their boundaries are known to be major sources for the development of unfavorable recombination active dislocation clusters. Some of the results are presented below.

In 2015 the G1-sized furnace was used to develop a growth process for HPmc-Si ingots. The applied mc-Si and HPmc-Si growth processes resulted in significant differences in the grain structure and dislocation densities of the material. Additionally, different feedstock qualities have been used while applying travelling magnetic fields for strong stirring of the melt during the solidification process. In cooperation with industry partners Elkem Technology and Elkem Solar, solar cells were successfully fabricated on wafers from G1-ingots characterized by their different material quality. Some of the project results are also presented below.

Additionally, a 2-year project investigating the influence of different hot-zone materials on the impurity level in directionally solidified silicon has started in 2015. All the process developments came along with simulations, especially the influences of the applied magnetic forces on temperature profiles and the shapes of the solid-liquid interface. Traditionally, a strong interdepartmental cooperation took place with the IKZ groups Crystal Machining and Physical Characterization.

Results

Quasi-mono silicon solidified with TM fields

The approach to grow quasi-mono ingots is driven by the idea that the conversion efficiency of cells for PV applications made of such material is higher compared to those of mc-Si or HPmc-Si. This may give an advantage, even though the production costs are higher and the growth technique is quite sophisticated. As one might already suppose, the challenging part of the process lies in the seeding procedure. Prearranged seeds are carefully placed at the bottom of the crucible and all the feedstock and partially the seed has to be melted slowly beginning from top to bottom. That process is followed by crystallization, which starts at the seeds in order to transfer the seed orientation onto the solidifying material. If the melting process is optimized, melt penetration does neither occur in between the seed junction nor at the seed corner and edges as it is shown on the photograph in Fig. 2. As a result, the global heat transport and the TMF driven melt flow applied in the optimized growth process resulted in symmetric seeding.

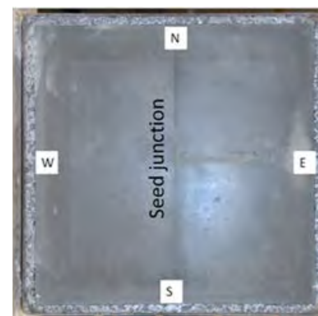

Fig. 2
Bottom view on the as-grown ingot showing the full geometry of the used seeds.

To develop successfully such an sophisticated melting and growth process, 3D simulations of the travelling magnetic fields (TMF) have been performed to study its influence on the melting and solidification conditions. TM fields have been applied with a frequency of 10 Hz and a phase shift of -90°. Melting and growth have been performed with similar velocities of 0.8 – 1.2 cm/h except the transient velocities from melting to growth. The obtained as-grown G2-sized (75 kg) silicon ingots of 38 x 38 x 23 cm^3 in volume were cut vertically and their defect structure was analyzed. Information was obtained on the curvature of the solid-liquid interface, the grains nucleated at the crucible walls and the electrical activity of dislocations. Using the Lorenz forces of the TMF in appropriate strength and direction during the growth process, a nearly flat solid-liquid interface could be kept during the growth cycle. A main focus of this investigation was on the control of dislocation formation, which can easily originate from the seed junction. Typically a dislocation cascade is observed in the middle originating from the junction between the two seeds (Fig. 3a) due to seed junctions itself and off-orientations by displacement. These recombination active defects can easily be detected by photoluminescence measurements. Applying an optimized growth process, dislocation clustering could be avoided (Fig. 3b). In both cases, the seed junction was placed in the middle. Dark areas show high recombination active zone due to mainly iron diffusion from the crucible known as "red zone". Process related the red zone at the bottom is found to be approximately 1.5 to 2 times as large as for standard mc-Si.

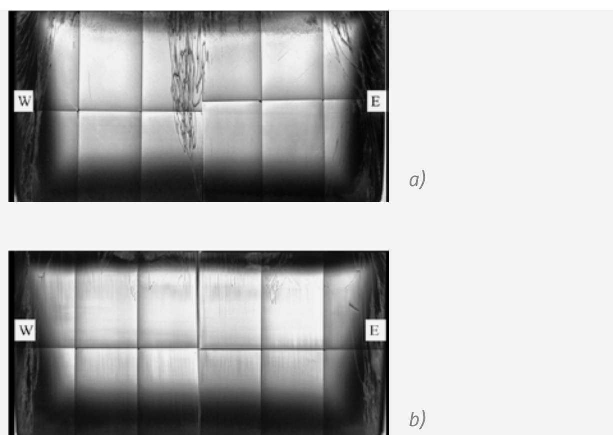

Fig. 3
a) A dislocation cascade is observed in the middle originating from the junction between the two seeds,
b) Photoluminescence measurements on a vertical cut shows no dislocation clusters.

High performance mc-Si

The implementation of HPmc-Si material has resulted in a reduction of lifetime-killing dislocation clusters and a more homogenous cell efficiency distribution over ingot height [1]. Recently, industrial mc-Si producers have shifted towards this technology where small grains with uniform size and orientation distribution are nucleated in the bottom. The initiation of small grains is controlled by an incubation layer, such as small Si-feedstock or Si-granulates. A high proportion of random angle grains boundaries are characteristic for HPmc-Si material and its grain structure leads to a situation where dislocation clusters are terminated by random angle grains boundaries and are therefore not allowed growing and filling entire grains.

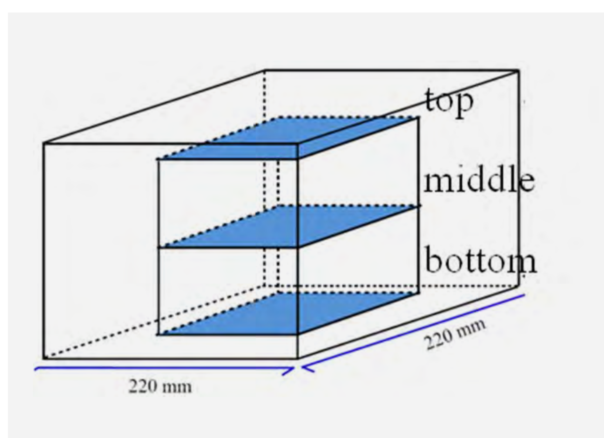

Fig. 4
Cutting sketch of an HPmc-Si ingot for characterization

The melting procedure of the complete feedstock without dissolving prearranged seeds or chip-seeds is one of the challenges in seeded ingot growth, both quasi-mono and HPmc-Si. Though the HPmc-Si seeding process is less pretentious, the remaining seed layer should be as thin as possible in order to obtain a maximum material fraction with high lifetime. To investigate the material characteristics along the growth direction after the growth experiments, an HPmc-Si ingot was cropped and sliced into 156 156 mm^2 wafers. As sketched in Fig. 4, wafers from bottom, middle and top were taken and then investigated by various characterization methods. The grain size and its distribution were measured on wafers by the circle filling method and by granulometric filtering. A Laue scanner was used to analyze grain orientations and the grain boundary character [2]. The grain orientation results were obtained by measuring 800, 400 and 200 grains of an area equivalent to a quarter wafer size from bottom, middle and top position, respectively. Since the nucleation starts from the silicon chips, this process can be aligned in all different orientations. The grain size is small and uniform in the beginning, and most grains are in the range of 1 mm^2, yet a rapid grain growth towards the top leads to average sizes of 6 mm^2 in the topmost wafer.

In addition, the uniformity of the grain size decreases. From the bottommost wafer to the middle wafer, the changes are significant. This is due to grain competition.

Figure 5 shows the grain orientation development of this ingot. The grain orientation development goes in the direction of less {100} and {110} grains, and an increase of grain orientations close to {111} and {112}. Especially the area fraction covered by orientations close to {112} is increasing towards the top. About 30% of the area fraction of the topmost wafer is covered by orientations close to {112}, and 15% is covered by orientations close to {111}. However, in this special case the number of grains having orientations close to {112} is 62, whereas 25 grains have orientations close to {111}. This means that the average grain size of the {111} grains are bigger than the {112} grains.

Since this significant grain competition in size and orientation results in changes of material properties, further investigation will be performed in order to control the grain development and hence defect densities.

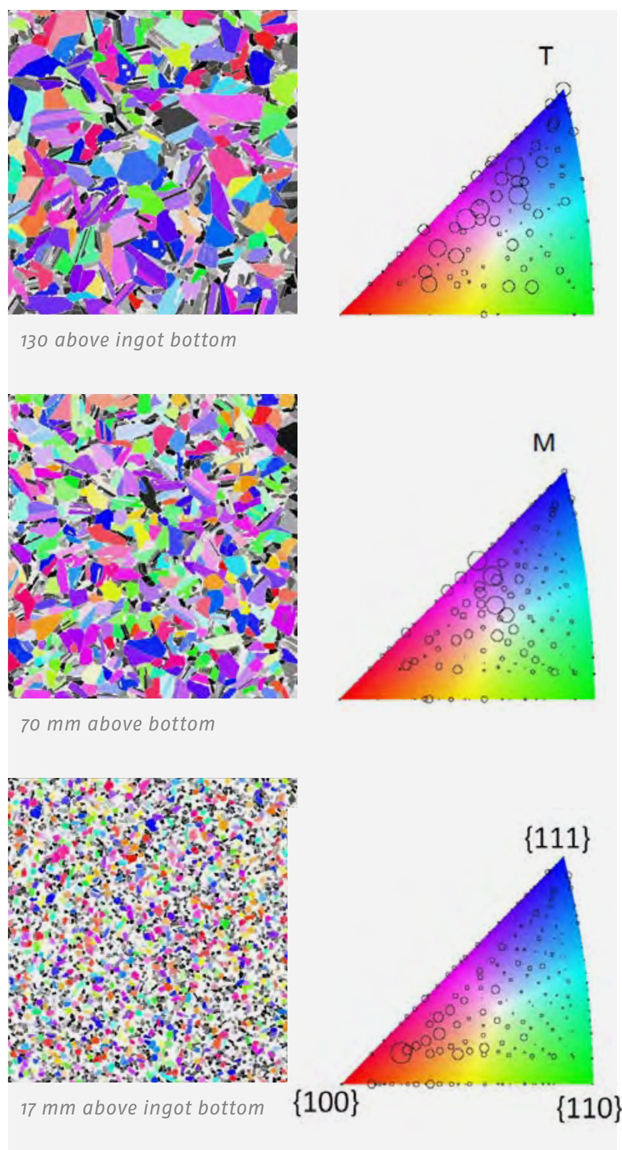

Fig. 5
The development of the dominating (main) orientations from bottom to top in an HPmc-Si ingot.

References

[1] Yang Y. M., Yu A., Hsu B., Hsu W. C., Yang A. and Lan C. W., Prog. Photovolt: Res. Appl., 23 (2015) 340

[2] Lehmann, T., Trempa, M., Meissner, E., Zschorsch, M., Reimann, C., Friedrich, J., Acta Materialia 69 (2014) 1

Classical Semiconductors: Gallium Arsenide

Head Dr. Christiane Frank-Rotsch
Team Dr. A. Glacki to 31.03.15, Dr. K. Giziewicz since 01.12.15, O. Root, Dr. R. Bertram

Überblick

Das III-V-Halbleitermaterial Galliumarsenid (GaAs) ist nach Silicium das meist entwickelte Halbleitermaterial. GaAs wird in der WLAN-Kommunikation sowie in der Mikrowellen- und in der Hochfrequenztechnologie eingesetzt. In den letzten Jahren ist der GaAs-Markt durch den rasanten Anstieg der mobilen Kommunikation stark gestiegen. Neben der stetigen Verbesserung der Kristallqualität stehen die Steigerung der Ausbeute der Kristallisationsprozesse sowie die Senkung der Prozesskosten im Fokus der Forschungsaktivitäten. Diese Zielstellungen sind nur durch eine gezielte Beeinflussung der Schmelzkonvektion während der Kristallisation möglich. Der Einsatz von externen Feldern, insbesondere von Wandermagnetfeldern, zeigt hierbei großes Potenzial.

Die KRISTMAG®*-Technologie, welche am IKZ entwickelte wurde, stellt ein leistungsstarkes Werkzeug zur Erzeugung von Wandermagnetfeldern in der Kristallzüchtung mit einer großen Parametervielfalt dar. Es wurde bereits erfolgreich für verschiedene kristalline Materialien, beispielsweise Halbleiter wie GaAs, Germanium und Silicium, eingesetzt. Gegenwärtig sind zwei VGF-Anlagen mit* KRISTMAG® *Heizer-Magnet-Modulen (HMM) zur simultanen Erzeugung von Wärme und Wandermagnetfeld (TMF) ausgerüstet. Die Forschungsaktivitäten des Themas Galliumarsenid wurden auch im Berichtszeitraum unter dem Fokus der Steigerung der Effizienz des VGF-GaAs-Züchtungsprozesses fortgeführt. Zur Lösung dieser technologischen und wissenschaftlichen Herausforderung wurden unterschiedliche Strategien verfolgt, z.B. die simultane Kristallisation in mehreren Tiegeln und die Vergrößerung der Kristalllänge (siehe hierzu auch vorhergehende Jahresberichte) sowie die Erhöhung der Kristallisationsgeschwindigkeit. Weiterhin werden auch grundlagenrelevante Aspekte zu GaAs-Wachstumsprozessen untersucht. Einen Schwerpunkt hierzu stellen insbesondere Untersuchungen zum Einfluss des Magnetfeldes auf die Mikrostruktur der Kristalle dar.*

*Weiterhin wurden die Forschungsaktivitäten im Rahmen des BMBF-Verbundprojektes TEMPO – „Toxikologische, physikalisch-chemische und gesellschaftliche Erforschung innovativer Materialien und Prozesse der Optoelektronik" – zum Lösungsverhalten von GaAs und weiteren Halbleitermaterialien unter definierten Bedingungen (z.B. in Abhängigkeit von Temperatur, Korngröße, Lösungsmittel und pH-Wert) fortgeführt. Die Projektergebnisse sollen in den toxikologischen Bewertungsprozess von GaAs im Zusammenhang mit den REACh-(***R***egistration,* ***E***valuation,* ***A***uthorisation and Restriction of* ***Ch***emicals) und CLP-Bestimmungen der EU einfließen.*

Overview

The III-V compound semiconductor gallium arsenide (GaAs) is, apart from silicon, the most widely deployed semiconductor material. Gallium arsenide is commonly used for wireless communication in microwave or high frequency technology. In the last years, strong growth of the GaAs market took place, mainly because of the rapid growth of the mobile telecommunication market. Besides the continual improvement of the GaAs single crystal quality, the enhancement of the yield of the growth process and a reduction of the process costs are the key research activities. To achieve these objectives a precise and constant control of the melt flow is of crucial importance. The use of external fields, especially traveling magnetic fields (TMF), shows great potential to enable these prospects.

The KRIST*MAG*® technology developed at IKZ provides a simple yet powerful tool to create such traveling magnetic fields within a broad parameter range. It has been successfully applied to the growth of different crystalline materials, among them semiconductors like gallium arsenide, germanium or silicon. Currently two of our VGF furnaces are equipped with a KRIST*MAG*® heater magnet module (HMM) allowing simultaneous generation of heat and traveling magnetic field. The research activities in the gallium arsenide group have been continued to further improve the efficiency of the Vertical Gradient Freeze (VGF) crystallization process. To meet this technological and scientific challenge, different strategies were applied e.g. simultaneous crystallization in multiple crucibles and enhanced crystal lengths (see former annual reports) as well as an increase of crystal growth velocity.

Further, fundamental aspects of the GaAs crystal growth process were investigated. The investigation of the influence of the magnetic field on the micro structure of VGF crystals is another focus of the group's work.

In addition, the research activities in the BMBF-funded framework "TEMPO" on the solubility of solid GaAs and other important semiconductor materials as a function of specific parameters (e.g. temperature, grain size, solvent, pH-value) were continued. Project results will be considered in the toxicological evaluation process of GaAs in connection with REACh (**R**egistration, **E**valuation, **A**uthorisation and Restriction of **Ch**emicals) and CLP (**c**lassification, **l**abelling and **p**ackaging of substances and mixtures) regulations of the EU.

Results

The enhancement of the GaAs VGF growth process by application of traveling magnetic fields has been one of the main focus areas of the group's investigations [1-3]. Key results of previous work on process optimization and intensification by using the KRIST*MAG*®-HMM are partially presented in the annual reports of the last three years. In particular, the successful simultaneous growth of single crystals in a multi-crucible HMM with the help of special designed traveling magnetic fields should be highlighted, as well as the successful growth of 4 inch GaAs single crystals with a 2.5-fold increased growth velocity under adjusted TMF parameters without loss of crystal quality.

During this reporting period, the growth of VGF-GaAs crystals in the KRIST*MAG*®HMM under the influence of TMF has been continued. Aside from this, the main focus of the investigations moved to the improvement of the GaAs crystal quality especially with regards to microhomogeneity and the stability of facets during growth. In this context crystals were grown partially with and without the influence of the magnetic field respectively. Besides the reduction of concave solid/liquid interface bending, a well-adjusted magnetic field improved the microstructure of the crystals. One proof of the impact of the magnetic fields is that the crystals grow without striations, but when the TMF is switched off striations resume markedly.

Figure 1 shows an example of the effect of the switch of TMF by means of an etched longitudinal cut. The thermal fluctuations based on buoyancy driven convection were clearly reduced in the case of growth under TMF influence.

Fig. 1
Detail of DSL-etched longitudinal cuts of Si-doped GaAs VGF crystals grown with and without TMF influence.

A further important parameter of the real structure of VGF-grown of GaAs is the existence and stability of facets in the conical segment of the crystal.

Figure 2 shows the conical segment of an <100>-orientated VGF GaAs crystal with distinct facets. The track of the facets shows an evident 4-fold symmetry corresponding to the <100>-orientation of the crystal.

Fig. 2
Image of 4 inch GaAs VGF single crystal with strong facets.

Classical Semiconductors: **Gallium Arsenide**

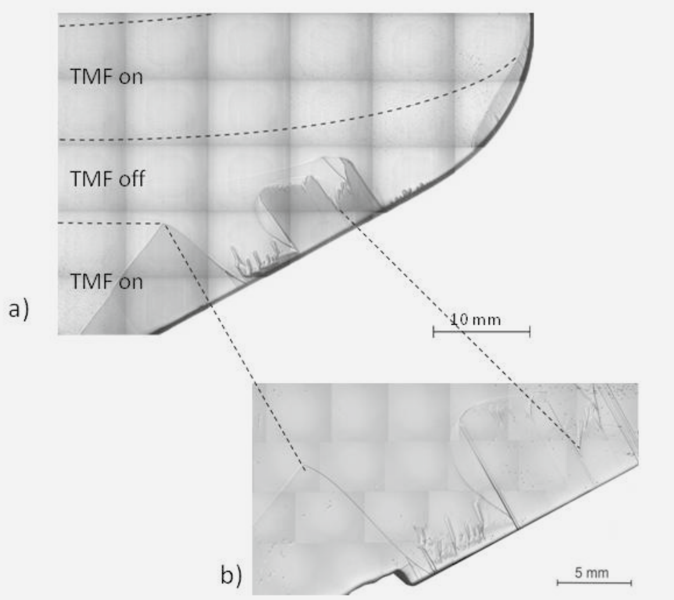

Fig. 3
Detail of a longitudinal cut in <110> orientation of a GaAs VGF crystal grown with and without TMF influence
a) Infrared topogram b) DSL etched.

Figure 3 a/b illustrates the positive impact of TMF on facet formation. In the segment of the crystal grown under the influence of TMF, we observed nearly stable facets. At the moment the traveling magnetic field was switched off, facets broke down and became unstable. A detailed Image of the critical fluctuation of facets without TMF is illustrated in Figure 3b. We found that under the influence of TMF the temperature fluctuations and correspondingly the facet fluctuations due to the change of thermal conditions could be reduced.

To stabilize the single crystal growth of compound semiconductors like GaAs the stabilization of facet growth is of great importance. It also plays a crucial role for the avoidance of twinning during single crystal growth.

Due to these promising results, the investigations of facet stabilization using an adjusted traveling magnetic field will be continued in the coming year.

Beside the enhancement of GaAs crystal growth, a second major research point was focused on the systematic continuation of solubility experiments of semiconductors within the framework "TEMPO". The abbreviation "TEMPO" stands for the German title of the BMBF funded project:"**T**oxikologische, physikalisch-chemische und gesellschaftliche **E**rforschung innovativer **M**aterialien und **P**rozesse der **O**ptoelektronik", which means "Toxicological, physical-chemical and social investigation of innovative materials and processes of the optoelectronics".

The studies started with solubility experiments of solid GaAs, and as previously reported one of the main parameters influencing the solubility is the surface area of the samples. The solubility increased significantly with larger surface area, which explained the higher values of dissolved powder compared to wafer material. While powders due to the large surface area are dissolved solid wafer material is attacked much less. To investigate the influence of further parameters we used only GaAs powder of the same quality. The results achieved were combined with those of project partners to clarify the solubility of these semiconductors.

Some selected results of solubility investigations are presented here. One important parameter of solubility of semiconductor materials is the pH-value of the solvent. We investigated solvents with pH-values in the range from pH=1.6 (HCl) to pH=13 (NaOH). Inorganic simulated body fluids are of particular importance: lung fluid – Gamble (pH=7.4) [4] and artificial lysosomal fluid (ALF) (pH=4.5) [5]. In all solvents, we observed an increase of GaAs solubility with pH-value, as shown in Figure 4.

Fig. 4
Comparison of the amount of dissolved arsenic in dependence of pH-value of the solution at T=37°C, without light and stirred as a function of time. The initial GaAs weight in each case was 50 mg GaAs.

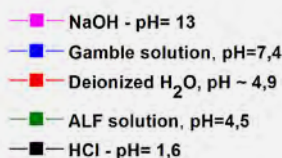

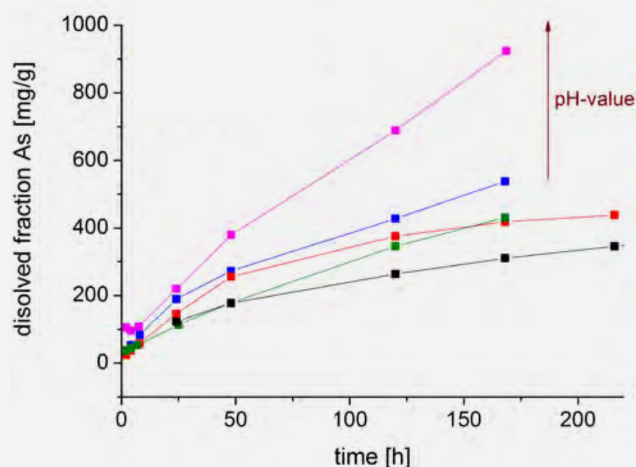

Classical Semiconductors: **Gallium Arsenide**

Furthermore, we observed higher solubility if the solvent is exposed to light. We also measured higher concentrations of As and Ga when stirring or shaking the solvent. All measurements of As- and Ga-concentrations were carried out by inductively coupled plasma optical emission spectrometry (ICP-OES). The particular solvents were also used for the utilized standards of quantitative determination of gallium and arsenide.

Figure 5 shows an example of the comparison of solubility of different semiconductor materials using artificial lysosomal fluid (ALF) with pH=4.5. Compared to gallium arsenide, gallium antimonide showed a slightly different behaviour. Regardless of the solvent, we measured for GaSb always the highest amount of dissolved material. The solubility of the lighter nitride and phosphide compounds GaN and GaP is significantly lower compared to GaAs and GaSb.

Despite the relatively low solubility we determined a comparable quantitative time dependence of the solution behaviour in ALF as shown in Figure 6. In the next year, these investigations within the TEMPO project will be continued. In addition to the inorganic simulated body fluids we will introduce experiments with human blood plasma to investigate the solubility behaviour of semiconductors in correlation to the toxicological evaluation process of these materials.

References

[1] Ch. Frank-Rotsch, N. Dropka, A. Glacki, U. Juda; J. Crystal Growth 401 (2014) 702

[2] A. Glacki, N. Dropka, Ch. Frank-Rotsch, U. Juda, M. Naumann; J. Crystal Growth 397 (2014) 6

[3] N. Dropka, A. Glacki, Ch. Frank-Rotsch; Cryst. Growth & Design 14 (2014) 5122

[4] B. Pierson, S. van Wagenen, K.W. Nebesny, Q. Fernando, N. Scott, D. E. Carter; Am. Ind. Hyg. Assoc. J. 50 (1989) 455

[5] M. R.C. Marques, R. Loebenberg, M. Almukainzi; Dissolution Technologies (August 2011) 25

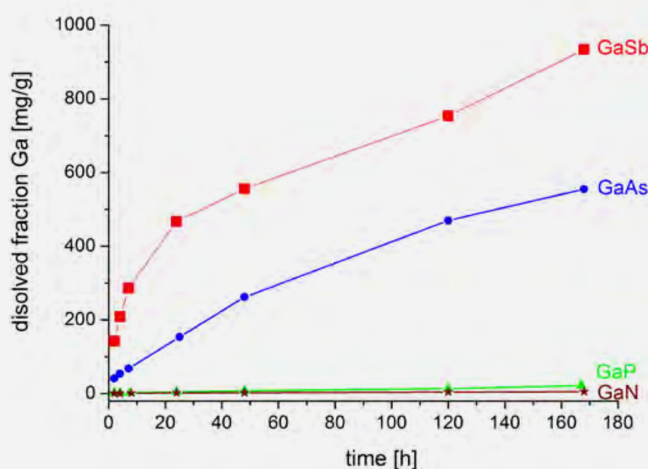

Fig. 5
Comparison of the amount of dissolved gallium of different semiconductor materials in ALF (pH=4.5) at T=37°C, without light and stirred as a function of time. The initial weight of GaSb, GaAs and GaP was 50 mg and GaN – 100 mg.

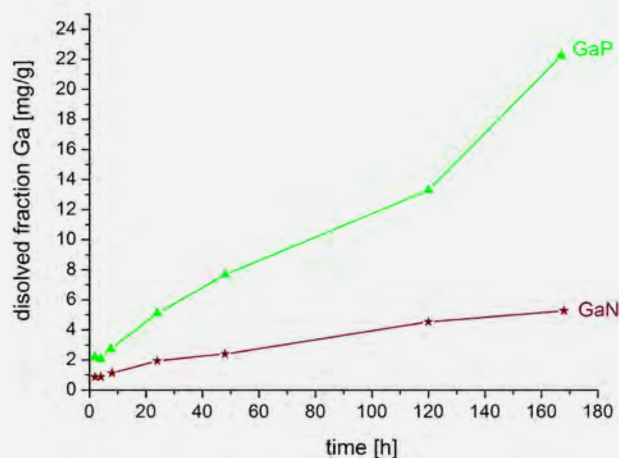

Fig. 6
Comparison of the amount of dissolved gallium of GaP and GaN in ALF (pH=4.5) at T=37°C, without light and stirred as a function of time. The initial weight of GaP was 50 mg and GaN – 100 mg.

Dielectric & Wide Bandgap Materials

Oxides/Fluorides 38

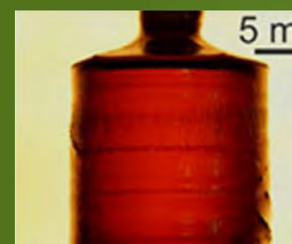

Gallium Nitride 48

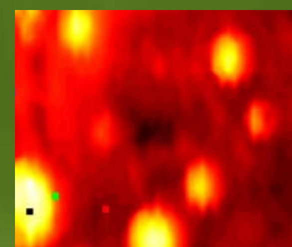

Aluminium Nitride 54

Dielectric & Wide Bandgap Materials

Head of department: Prof. Dr.-Ing. Matthias Bickermann

Die Abteilung Dielektrika und Wide-Bandgap-Materialien befasst sich mit der Volumenkristallzüchtung von Nitriden, Oxiden und Fluoriden. Die Kristalle finden Anwendung als Epitaxiesubstrate sowie in der Optik und Sensorik. Die Forschung am IKZ zielt ab auf die Herstellung einkristalliner Materialien mit bisher unerreichter struktureller Qualität, wie sie für neuartige und energieeffiziente elektronische, optoelektronische und piezoelektrische Anwendungen und Bauelemente benötigt werden. In den Themengruppen Aluminiumnitrid (AlN), Galliumnitrid (GaN) und Oxide/Fluoride arbeiteten in 2015 insgesamt 11 Wissenschaftler, 3 Doktoranden und 8 Techniker.

Die Gruppe AlN erforscht und entwickelt die Technologie der AlN-Kristallzüchtung aus der Gasphase. AlN-Substrate dienen der Herstellung von effizienten Leuchtdioden im tiefen Ultraviolett oder neuartigen Leistungsbauelementen. Die Aktivitäten am IKZ sind durch eine starke Zusammenarbeit mit Industriepartnern und anderen Forschungseinrichtungen geprägt. Seit August 2015 wird die AlN-Züchtungstechnologie im Konsortium „Advanced UV for Life“ zu einer industrietauglichen Methode weiter entwickelt. Gleichzeitig werden den Partnern hochwertige Substrate für die Bauelemententwicklung zur Verfügung gestellt. Dazu untersucht die Gruppe neue Tiegel- und Isolationsmaterialien. Auch wurde ein neues Projekt zur plasmagestützten Abscheidung von hochreinen dicken AlN-Schichten begonnen.
Die GaN-Gruppe befasst sich weiterhin mit der DFG-geförderten Herstellung von kohlenstoffdotierten GaN-Dickschichten mit der am IKZ entwickelten pseudohaliden Gasphasenepitaxie (PHVPE).

Die Aktivitäten der Gruppe Oxide/Fluoride lassen sich gliedern in die Herstellung von Substratkristallen mit Perowskit-Struktur, von Volumenkristallen transparenter halbleitender Oxide (TSO), Hochtemperatur-Piezoelektrika, optischen und Laser-Kristallen sowie von speziellen Referenzkristallen für die Materialforschung. Dabei wird vorwiegend die Schmelzzüchtung bei hohen Temperaturen im Czochralski-Verfahren angewandt. Unsere Perowskit-Kristalle und -substrate mit für die Anwendung maßgeschneiderten Gitterkonstanten werden am IKZ sowie weltweit bei der Erforschung verspannter multiferroischer Schichten eingesetzt. 2015 wurden erfolgreich Strontiumtitanat SrTiO3-Kristalle mit anwendungsrelevanten Eigenschaften aus der Schmelze mittels Formgeber (EFG-Verfahren) gezüchtet. Dazu wurden mit LaLuO3 und La(Sc,Lu)O3 neue Perowskit-Kristalle demonstriert, so dass erstmals Substrate mit Gitterkonstanten im Bereich von 4.09-4.18 Å zur Verfügung stehen. Die Palette an TSO-Materialien wird von β-Ga_2O_3 dominiert. Hier gibt es am IKZ und auch weltweit Aktivitäten, neuartige oxidische Leistungsbauelemente auf der Basis von β-Ga_2O_3-Epitaxieschichten zu entwickeln. Dazu wurden 2015 die ersten erfolgreichen Versuche durchgeführt, BaSnO3-Volumenkristalle herzustellen, als Substrat für die Oxidelektronik und für komplexe Schichtstapel mit hoher Elektronenbeweglichkeit. Schließlich hat die Gruppe hochreine Kristalle aus Wüstit FeO und Olivin $(Mg,Fe)_2SiO_4$ gezüchtet, die aufgrund der hohen strukturellen Qualität als Referenzmaterialien für geologische Untersuchungen gefragt sind.

The department Dielectric and Wide Bandgap Materials focuses on the bulk crystal growth of nitrides, oxides, and fluorides. The crystals find their applications as substrates for epitaxy and in optical and sensor devices. Our research goal is to prepare single crystal materials of unprecedented structural quality to enable novel and energy-efficient electronic, optoelectronic, and piezoelectric devices and applications. In 2015, the department consists of 11 senior scientists, 3 PhD students, and 8 technicians/engineers and is subdivided into the teams Aluminium nitride (AlN), Gallium nitride (GaN), and Oxides/Fluorides.

The AlN team researches and develops the preparation of AlN bulk single crystals by the physical vapour transport (PVT) method. These crystals are used as substrates for the preparation of efficient deep-UV optoelectronic and novel power electronic devices. Our activities are characterized by strong collaborations with companies and other research institutes. Technology development aiming at future industrial application as well as substrate supply for device development is conducted since August 2015 within the "Advanced UV for Life" consortium. Additionally, we investigate advanced crucible and insulation materials, and we have started a project for plasma-assisted deposition of thick, high-purity polycrystalline AlN films. The GaN team continued DFG-funded research to grow thick GaN layers with controlled carbon doping using our proprietary pseudo-halide vapour phase epitaxy (PHVPE) method.

The Oxides/Fluorides team's activities fall in the categories of perovskite substrate crystals, bulk transparent semiconducting oxides (TSO), crystals for high-temperature piezoelectrics, optical and laser crystals, and unique crystals for material references and benchmarks. Mainly, high temperature Czochralski melt growth techniques are used. Our perovskite crystals and substrates with tailored lattice constants are used both at IKZ and worldwide for research on strained multiferroic layers. In 2015, edge-defined film-fed melt growth (EFG) of strontium titanate $SrTiO_3$ bulk single crystals with relevant size and structural quality was successfully pursued. Also, $LaLuO_3$ and $La(Sc,Lu)O_3$ were added to the list, providing hitherto unavailable substrates in the 4.09-4.18 Å range. The TSO materials palette at the IKZ is dominated by β-Ga_2O_3, used at the IKZ and worldwide for epitaxy aiming at novel oxide semiconductors power devices. 2015 saw the first successful attempts to prepare $BaSnO_3$ bulk crystals, which are very promising for high-mobility oxide electronics and complex multiferroic layer stacks. Finally, the team has prepared wüstite FeO and olivine $(Mg,Fe)_2SiO_4$ bulk crystals of highest purity and structural quality as a benchmark for geological investigations.

Dielectric & Wide Bandgap Materials:

Oxides/Fluorides

Head Dr. Reinhard Uecker
Team M. Brützam, Dr. Z. Galazka, Dr. S. Ganschow, Dr. C. Guguschev, D. Kok, M. Rabe, I. Schulze-Jonack, Dr. D. Schulz, A. Tauchert, E. Thiede

Überblick

Seit der Institutsgründung im Jahr 1992 bearbeitet die Gruppe Oxide/Fluoride Forschungsaufgaben zur Züchtung und Charakterisierung von oxidischen und fluoridischen Einkristallen, wobei die Oxide im Fokus stehen. Als Standardzüchtungsmethode für die Volumenkristalle dient dabei die Czochralski-Methode, die am weitesten entwickelte Technik zur Herstellung von Kristallen mit hoher struktureller Perfektion. Mit dieser Methode werden bei uns Kristalldurchmesser bis zu 50 mm und -längen bis zu 150 mm erreicht. Diese Methode ist jedoch nicht für jeden Kristall anwendbar. Hinweise zur Eignung einer Züchtungsmethode kann man aus dem thermodynamischen Verhalten des jeweiligen Materials ableiten, das in enger Kooperation mit der Gruppe Chemische & Thermodynamische Analyse erforscht wird. So kommen auch andere Schmelzzüchtungsmethoden wie die EFG-Methode (edge-defined film-fed growth), die Bridgman- und die Kyropoulos-Methode zum Einsatz. Inkongruent schmelzende Verbindungen werden aus der Schmelzlösung nach dem TSSG-Verfahren hergestellt. Bei hoher Flüchtigkeit erfolgt die Züchtung über die Gasphase. Immer häufiger erfordern jedoch neue Materialien auch aufwendig angepasste neue Züchtungsbedingungen. Hierzu zählt die in der Gruppe entwickelte „Levitation-Assisted Self-Seeding Crystal Growth Method", die eigens für die Züchtung von In_2O_3-Volumenkristallen entwickelt wurde und als Patent anhängig ist. Neben der Volumenkristallzüchtung werden in der Gruppe auch Kristallfasern mittels Micro-Pulling Down-Methode (MPD) hergestellt.

Nach der Züchtung werden die Kristalle in der eigenen Gruppe einer Vorcharakterisierung unterzogen, die weitere Charakterisierung erfolgt in den Gruppen Physikalische Charakterisierung und Elektronenmikroskopie.

Das besondere Interesse der Gruppe liegt in der Entwicklung neuer Materialien. Die „Schwergewichte" haben sich dabei oft im Zuge langfristiger Kooperationen entwickelt. Die längste Zusammenarbeit besteht mit der Schweizer Firma Kistler Instrumente AG (seit 1993). Forschungsgegenstand dieser Industriekooperation ist die Entwicklung neuer, vom Langasit ($La_3Ga_5SiO_{14}$) abgeleiteter piezoelektrischer Kristalle für den Einsatz als Hochtempemperatursensoren.

Das ursprüngliche Ziel, die Überführung der 2-Zoll-Technologie, wurde bereits in der ersten Dekade realisiert. Die anschließenden Arbeiten befassten sich mit Untersuchungen zur Züchtung neuer Verbindungen mit höherer Empfindlichkeit und besserer Temperaturstabilität. Eine Reihe der in unserer Gruppe gezüchteten Verbindungen werden inzwischen kommerziell genutzt.

Seit dem Jahre 2000 sind wir eng mit der Gruppe von Prof. D. G. Schlom – zunächst Pennsylvania State University, nun Cornell University/USA – verbunden. Für seine Aktivitäten auf dem Gebiet des Strain-engineering von epitaktischen Perowskitschichten waren Substrate mit Gitterkonstanten oberhalb von 3,9 Å erforderlich. Eine gemeinsame Entwicklung von Schloms Gruppe, dem FZ Jülich und dem IKZ machte erstmals Perowskitsubstrate in diesem Gitterkonstantenbereich zugänglich: die Seltenerdscandate (3,95-4,02 Å), die bis heute ausschließlich am IKZ hergestellt werden [1]. Diese Substratkristalle ermöglichten u.a. ein strain-engineering von $SrTiO_3$- und $BaTiO_3$-Schichten, bei dem durch ein geeignetes Substrat Verspannungen in der Schicht induziert werden, die ihrerseits zu – teils gravierenden – Veränderungen der Schichteigenschaften führen. Mit derartig modifizierten Materialien lassen sich völlig neue Anwendungsgebiete z.B. in der Oxidelektronik erschließen. Inzwischen erfordern verschiedene aussichtsreiche neue Perowskite (u.a. $BaSnO_3$, $BiScO_3$, $PbZrO_3$) Substrate mit noch größeren Gitterkonstanten. Auf der Basis von Grundlagenuntersuchungen wurde das Mischkristallsystem $(LaLuO_3)_{1-x}(LaScO_3)_x$ als Substratmaterial für diese Schichten identifiziert. Mit der Züchtung dieser Kristalle konnten erstmals Perowskitsubstrate für den Gitterkonstantenbereich 4,09 – 4,18 Å verfügbar gemacht werden.

Ein Perowskitkristall von besonderer Bedeutung ist das Strontiumtitanat ($SrTiO_3$). Seit einigen Jahren erlebt dieser Kristall eine Renaissance. Er ist u.a. das bislang einzige oxidische Substratmaterial, bei dem die Bildung eines zweidimensionalen Elektronengases an der Grenzfläche zu einer anderen Oxidschicht nachgewiesen werden konnte. Voraussetzung für die Realisierung dieser und anderer moderner Anwendungen ist aber eine deutliche Verbesserung der Kristallqualität. Die Züchtung qualitativ hochwertiger $SrTiO_3$-Kristalle gelang im Rahmen eines im Rahmen des Leibniz-Wettbewerbs bis 2016 geförderten Projektes durch umfassende Untersuchungen zum Kristallisationsverhalten.

Ein 2009 gestartetes gemeinsames DFG-NSF-Projekt mit der University of California Santa Barbara (J. Speck) und dem Institut für Physik der HU Berlin (R. Manzke) begründete das inzwischen „modernste" Schwerpunktthema der Gruppe: die transparenten halbleitenden Oxide (TSO`s). Sie sind mit ihren vielversprechenden Eigenschaften aussichtsreiche Materialien für moderne Anwendungen. Zu den zunächst bearbeiteten Verbindungen ZnO [2], β-Ga_2O_3 [3], In_2O_3 [4], SnO_2 [5] und $MgGa_2O_4$ [6] kamen 2015 $BaSnO_3$ und $CuAlO_2$ (Delafossit) hinzu. Für Letzteres wurde ein DFG-Projekt bewilligt. Etliche der im IKZ gezüchteten TSO-Volumenkristalle sind ausschließlich am IKZ verfügbar. Weltweit arbeiten über 20 Institutionen mit dem IKZ auf dem Gebiet der TSO-Forschung zusammen.

Neben diesen Schwerpunktaufgaben wurden auch 2015 wieder verschiedenen Forschungsinstituten oxidische und fluoridische Einkristalle zur Verfügung gestellt.

Overview

Since the institute was formed in 1992, the Oxides/Fluorides group works in the field of growth and characterization of oxide and fluoride bulk single crystals, with a clear focus on oxides. These crystals are mainly prepared by the Czochralski method, as it is the most developed technique for growing crystals of high structural quality. The crystals grown have diameters up to 50 mm and lengths of up to 150 mm. However, this method is not applicable for all crystals. Hints for the suitability of a certain growth method are derived from the thermodynamic behavior of the respective material, which is investigated in close collaboration with the IKZ group Chemical and Thermodynamic Analysis. Thus, also other melt growth techniques such as EFG (edge-defined film-fed growth), Bridgman and Kyropoulos are pursued. Incongruently melting compounds are grown from flux by the top seeded solution growth (TSSG) method. If the volatility is high, growth from the gas phase is employed. More and more, though, novel materials require adapted or specially tailored growth conditions. One example is the "Levitation-Assisted Self-Seeding Crystal Growth Method" (LASSCGM), which was designed in particular for preparation of In_2O_3 bulk single crystals in our group, and for which a patent is pending. Apart from bulk crystal growth, crystal fibers are prepared by the micro-pulling down (MPD) method. After growth, the crystals are pre-investigated within the group, whereas in-depth characterization is performed by the IKZ groups Physical Characterization and Electron Microscopy.

The special interest of the group lies in the development of new crystalline materials. The emphases are often developed in the course of long-term cooperations. The longest cooperation exists with the Swiss company Kistler Instrumente AG (since 1993). Research topic of this industrial cooperation is the development of new piezoelectric crystals based on the langasite ($La_3Ga_5SiO_{14}$) for use as high temperature sensors. While the original goal, the technology transfer of 2-inch crystal growth, was already completed in the first decade of our collaboration, the IKZ has continued its research with the focus shifted to explore and investigate growth of new compounds with even higher sensitivity and temperature stability. Several of the compounds grown in our group so far are now used commercially.

Since 2000, we are closely connected with the group of Prof. D. G. Schlom -first Pennsylvania State University, now Cornell University / US. He required for his activities in the field of strain engineering of epitaxial perovskite thin films substrates with lattice constants above 3.9 Å. A joint development of Schloms group, the Jülich Research Centre and the IKZ made first perovskite substrates in this lattice constant range available: the rare earth scandates (3.95-4.02 Å) that are produced today exclusively at the IKZ [1]. These substrate crystals enabled the first time strain engineering of $SrTiO_3$ und $BaTiO_3$ thin films. Thereby, a suitable substrate induces strain into the film leading to –partly drastic- changes of its properties. With these modified materials new applications can be introduced, e.g., into oxide electronics. Meanwhile, several promising new perovskites (e.g., $BaSnO_3$, $BiScO_3$, $PbZrO_3$) require substrates with even larger lattice constants. On the basis of fundamental studies, the solid solution system $(LaLuO_3)_{1-x}(LaScO_3)_x$ was identified as substrate material for these layers. With the growth of these bulk crystals for the first time perovskite substrates for the lattice constant range 4.09 – 4.18 Å could be made available.

A perovskite crystal of particular importance is strontium titanate ($SrTiO_3$). For several years, this crystal is experiencing a renaissance. So far it is the only oxide substrate material which can host a two-dimensional electron gas at the interface to another oxide crystal layer. The precondition for the realization of these and other modern applications is a significant improvement in crystal quality. The growth of high-quality $SrTiO_3$ crystals succeeded within a project, funded in the frame of the Leibniz competition until 2016 by comprehensive studies on the crystallization behavior.

Dielectric & Wide Bandgap Materials: **Oxides/Fluorides**

In 2009 IKZ launched a joint DFG-NSF project with the University of California Santa Barbara (J. Speck) and the Institute for Physics of the HU Berlin (R. Manzke). It was the trigger for the latest focus of the group: the transparent semiconducting oxides (TSO`s). With their promising properties they are hopeful materials for modern applications. To the first processed compounds ZnO [2], β-Ga_2O_3 [3], In_2O_3 [4], SnO_2 [5] and $MgGa_2O_4$ [6] in 2015 $BaSnO_3$ and $CuAlO_2$ (Delafossite) were added. For the latter, a DFG project was approved. Many of the TSO volume crystals grown at IKZ are available exclusively at the IKZ. The collaboration on TSO crystals involves over 20 institutions worldwide.

In addition to these main tasks in 2015 again oxide and fluoride single crystals were provided to several research institutes.

Results

New large-lattice-constant perovskite single-crystal substrates

The pseudobinary system $LaLuO_3$-$LaScO_3$ was explored in hope of discovering new perovskite-type substrates with pseudocubic lattice parameters above 4 Å.

Over the past several decades, a broad range of oxide single crystals with cubic and pseudocubic perovskite structures has been used as substrates for the epitaxy of high quality perovskite thin films. The pseudocubic lattice parameters of the more or less commercially available oxide perovskites range from 3.67 Å ($LuAlO_3$) to 4.18 Å ($LaLuO_3$) (Fig. 1).

This broad assortment of more than 20 available perovskite substrates with finely spaced pseudocubic lattice constants has enabled the misfit strain in epilayers to be precisely targeted. Such strain engineering has been exploited to enhance of the properties of some oxides as well as to access the exceptional properties of the hidden ground state of others [1].

However, when considering the need for substrates for thin films of new promising oxides with interesting properties, there exists a serious lack of perovskite substrates with lattice parameters above four Ångstrom. For many years, $SrTiO_3$ was the perovskite-type substrate of choice with the largest lattice parameter: a = 3.905 Å. The introduction of the rare earth scandates $LnScO_3$ (Ln = Dy - La) as substrates, which was initiated about a dozen years ago by a collaboration between Pennsylvania State University, Forschungszentrum Jülich and IKZ [2,3] shifted the upper limit to 3.95 - 4.05 Å. Unfortunately, the exceptionally high melting temperature (>2200 °C) of the largest of the rare earth scandates - $CeScO_3$ and $LaScO_3$ - excludes them from growth by the Czochralski method. Therefore, $PrScO_3$ with 4.02 Å has the largest pseudocubic lattice constant achievable with $LnScO_3$ substrates. Above this value there is only one perovskite known which can be grown as a bulk single crystal: $LaLuO_3$ with a = 4.18 Å [1,4].

Fig. 1
Pseudocubic lattice parameter of perovskite and perovskite-related films and substrates. Except for $LuAlO_3$, $CeScO_3$, and $LaScO_3$, all substrate crystals are grown at the IKZ.

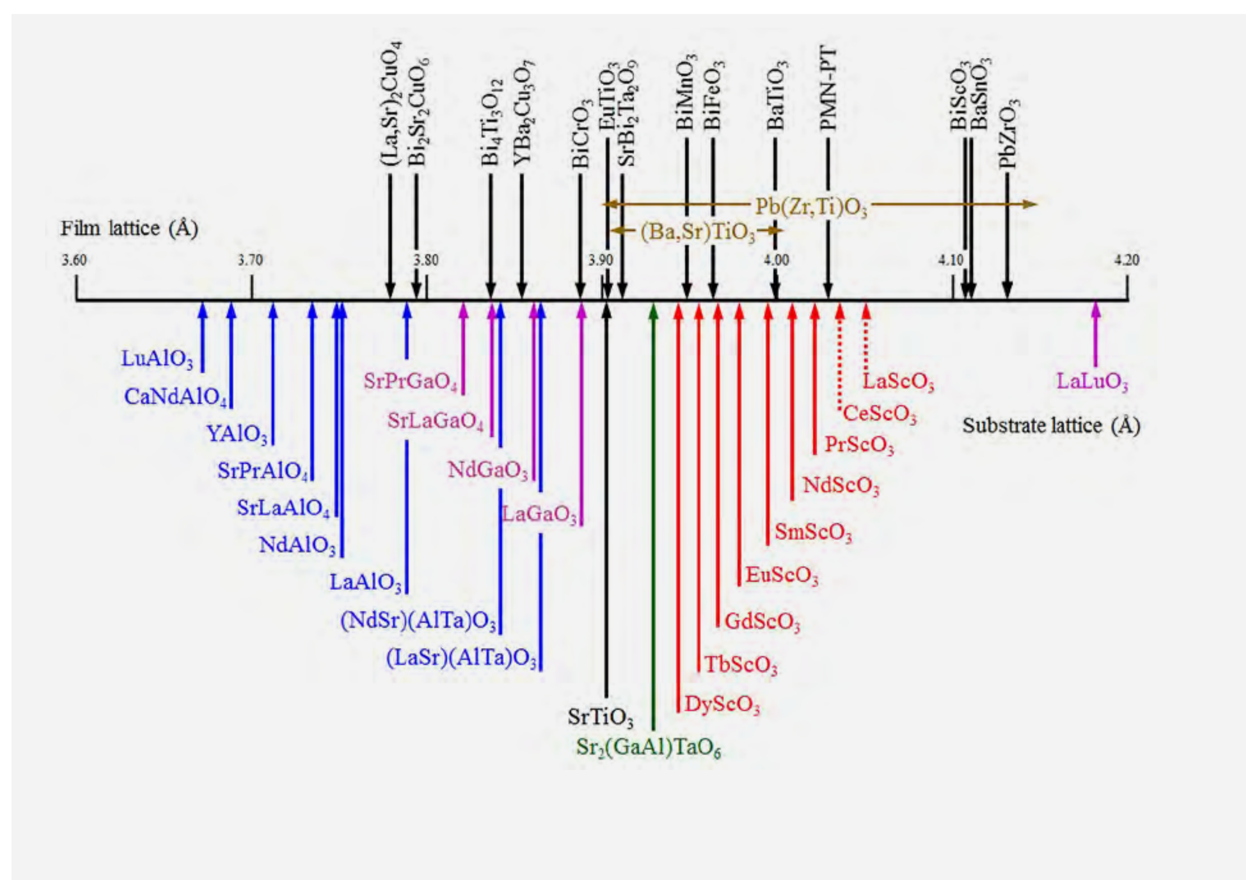

Dielectric & Wide Bandgap Materials: **Oxides/Fluorides**

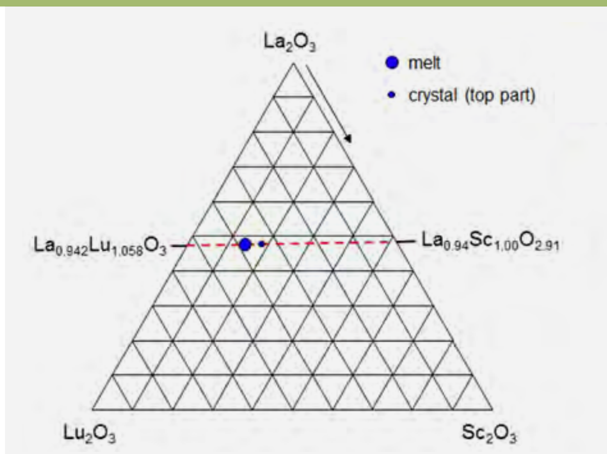

Fig. 2
Ternary phase diagram La_2O_3 – Sc_2O_3 – Lu_2O_3, with the pseudo binary crystallization section (red dashed line).

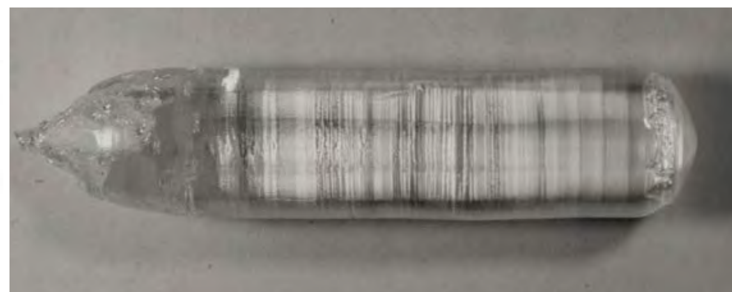

Fig. 3
Crystal grown from a melt with x = 0.276. The cylinder length is about 50 mm and the diameter 16 mm. Despite this crystal being grown from an iridium seed rod, the boule became single crystalline shortly beyond the shoulder. The whole cylinder was colorless and transparent.

As is evident from Fig. 1, a significant gap exists between two lanthanum oxide-containing compounds: $LaScO_3$ (a = 4.05 Å) and $LaLuO_3$ (a = 4.18 Å). To fill this gap, it was obvious to investigate whether these both compounds form a solid solution [5]. For this purpose, the crystallization within the pseudobinary system $LaLuO_3$-$LaScO_3$ was investigated by thermal measurements of different mixtures in the Chemical and Thermodynamic Analysis group at IKZ. The results indicate for this system a complete solid solution of the type $(LaLuO_3)_{1-x}(LaScO_3)_x$ (see the corresponding phase diagram at the report of the group). From this diagram we also derive that because of the maximum load of the iridium crucible of about 2200 °C, the highest x-value of a melt to be applied for Czochralski growth must not exceed 0.5. However, the La_2O_3 content of both end members of this solid solution system is lying a bit below 50 mol%. In the case of $LaLuO_3$, the composition analysis yielded a La_2O_3 content of 47.10 mol%. For $LaScO_3$, the La_2O_3 content was found to be 48.45 mol%. Therefore, the crystallization proceeds at the corresponding pseudo binary section of the ternary phase diagram La_2O_3 – Sc_2O_3 – Lu_2O_3, just a few percent below 50 mol% La_2O_3 (Fig. 2).

Three mixtures with x-values of about 0.50, 0.33 and 0.25 were chosen for the growth experiments. To start at relatively "low" temperature, we began the growth experiments with a small x-value-melt: 0.276 (Fig. 3).

The segregation in the $LaLuO_3$-$LaScO_3$ system was investigated by ICP-OES and XRF scanning measurements. The x-values of melts and corresponding crystals (top part) agree excellent with the calculated phase diagram. Whereas the lanthanum oxide content was found to remain unchanged at 47.50 mol% over the whole crystal length, the lutetium content increases linearly from top to bottom and the scandium content linearly decreases (Fig. 4).

Fig. 4
Segregation during crystal growth measured at four areas of the crystal.

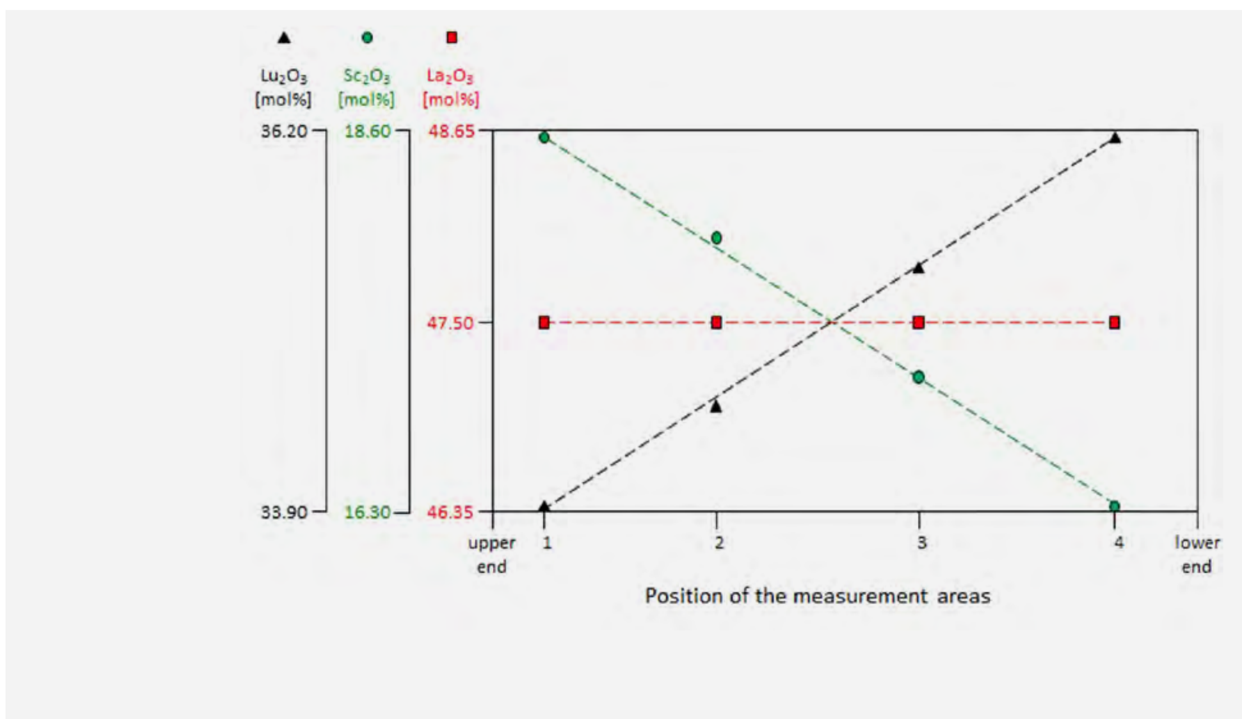

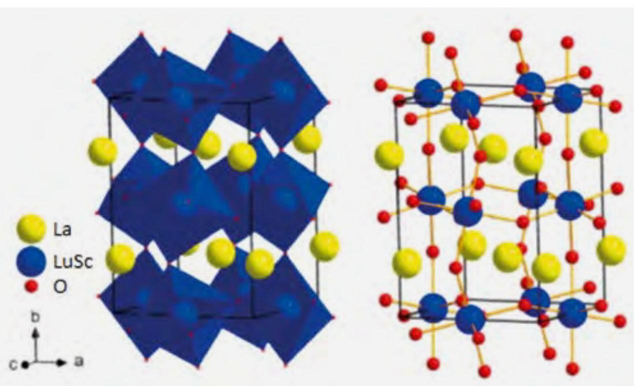

Fig. 5
Crystal structure of the $La_{1.94}Lu_{1.166}Sc_{0.894}O_6$ solid solution.

The structure of the solid solution was explored on crystalline material grown from a melt with x = 0.33. Its sum formula is $La_{1.94}Lu_{1.166}Sc_{0.894}O_6$ (x = 0.43). It is a distorted perovskite crystallizing in the orthorhombic space group Pnma (62) –the same as $LaLuO_3$ and $LaScO_3$. The cell parameters are a = 5.9199(7) Å, b = 8.2422(11) Å, c = 5.7422(8) Å and V = 280.872 Å^3 (Fig. 5). This corresponds to a pseudocubic lattice constant of 4.1224 Å –nearly halfway between those of the end members. The calculated density is 7.18 g/cm^3.

Furthermore, it was found, that about five percent of the lutetium atoms also occupy the A-position of the lanthanum atoms, i.e., lutetium drives lanthanum out of the structure. The explanation for this is that lutetium belongs to those 15 elements of the periodic table known to occupy both the large A- and the small B-position in a perovskite structure [6]. This clarifies the "lanthanum-oxide-poor" composition of this solid solution. Its resulting formula is $(La_{1.94}Lu_{0.06})(Lu_{1.106}Sc_{0.894})O_6$. This special property of lutetium also affects the end member $LaLuO_3$, resulting in a shift of the single-crystal composition to lower La_2O_3 values given by the formula $(La_{0.942}Lu_{0.058})Lu_{1.000}O_3$. For the other end member, $LaScO_3$, the lanthanum oxide deficiency is caused by a lanthanum deficiency on the A-site. This is thought to be due to a coupled substitution involving vacancies, which can be written as $^{A}*(2La^{3+}\ 3O^{2-})_{-1}$ [7].

To investigate the dependence of the lattice parameters on the composition of the $(LaLuO_3)_{1-x}(LaScO_3)_x$ solid solution, the lattice parameters of four solid-solution samples with strongly differing x-values were measured (Fig. 6).

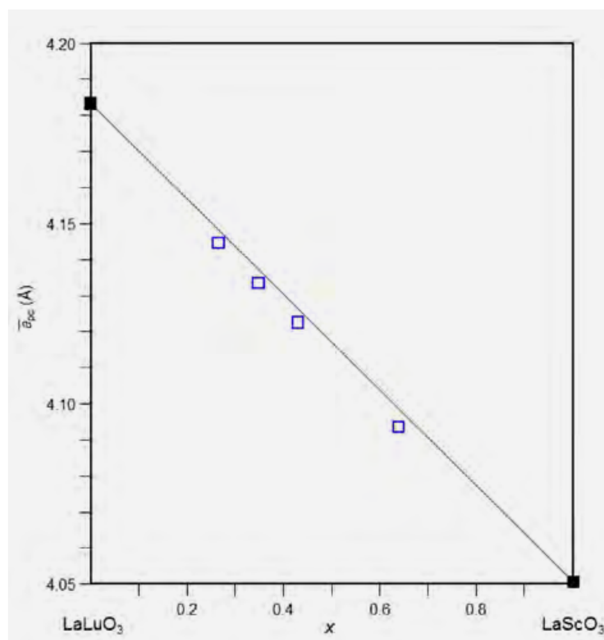

Fig. 6
Dependence of the pseudocubic lattice parameter on the composition of the $(LaLuO_3)_{1-x}(LaScO_3)_x$ solid solution.
(The size of the squares corresponds to the size of the error bars.)

It is obvious that this dependence follows Vegard's law, i.e., the lattice parameter changes linearly with the composition of the solid solution. Because of the maximum thermal load of the iridium crucible (2200 °C), the maximum x-value that can be achieved is about ~0.67. Thus, from Vegard's law it is concluded, that solid solutions with a pseudocubic lattice parameter range of 4.09 – 4.18 Å can be grown by the Czochralski method.

With the solid solution $(LaLuO_3)_{1-x}(LaScO_3)_x$ a new system for the single-crystal growth of large-lattice-parameter perovskites was discovered. Its pseudocubic lattice parameters cover the range between 4.05 and 4.18 Å (realizable as bulk single crystals: a = 4.09 - 4.18 Å), a region in which so far no large single-crystal perovskites have been grown. We anticipate that these new solid-solution single crystals will enable the epitaxial growth of high quality thin films of promising materials whose growth until now has been inhibited by the lack of suitable substrates. Examples include high-quality epitaxial films of $BaSnO_3$ (a transparent conducting oxide with the highest mobility of all known high-bandgap semiconductors [8]), $BiScO_3$ (an important constituent of a new class of high-temperature piezoelectrics [9,10]), and $PbZrO_3$ (an antiferroelectric material relevant to energy storage [11]).

Substrates made from the diamagnetic $(LaLuO_3)_{1-x}$ $(LaScO_3)_x$ solid solution are also advantageous when it comes to measuring the magnetic properties of thin films grown on them, e.g., multiferroics, as the magnetic background of these substrates will be quite low.

The still remaining lattice parameter gap between 4.02 and 4.09 Å is hoped to be closed by solid solutions of the type $LnScO_3$-$LnLuO_3$ with Ln = Pr, Nd, because $PrLuO_3$ and $NdLuO_3$ are orthorhombic perovskites with space group Pnma (62) and pseudocubic lattice parameters of 4.161 and 4.145 Å, respectively [12]. Provided that they melt congruently, it is likely that they can be grown as bulk crystals by the Czochralski method. Studying the feasibility of these solid solutions is object of a master thesis in our group. It is an avenue for future exploratory studies to identify additional needed perovskite substrates.

Growth of improved $SrTiO_3$ crystals by the edge-defined film-fed growth

The unique properties of $SrTiO_3$ (STO) along with the phase stability allow a very broad application in the field of thin film growth. STO has been used as a substrate for high temperature superconducting, thermoelectric and multiferroic applications, including sensors, transducers, ferroelectric field effect transistors, memory devices and data storage. It can be considered as a key model material for oxide electronics based on an interfacial two-dimensional electron gas (2DEL) and for metal-oxide-semiconductor field-effect transistors. So far these devices are fabricated on commercially available substrate crystals grown by the Verneuil method, but the available crystal quality hinders progress for several applications in these fields and is not expected to be improved much further. Consequently, to develop devices outperforming today's limitations, STO substrates of high perfection are needed.

During realization of our SAW project, funded by the Leibniz Association, we developed several bulk crystal growth technologies to fill that gap [13,14,15]. One of most successful methods we applied is called the edge-defined film-fed growth (EFG) method [16], in which the crystal is grown from a melt film on top of a die which is fed through a capillary. Often this method is merely considered for the growth of crystals in special shapes (e.g. tubes, ribbons or rectangular prisms), but we used this technique to grow cylindrical $SrTiO_3$ bulk single crystals with diameters of about 15 mm and lengths between 13 and 50 mm (Fig. 7) [13]. With the EFG method, a gentle, slow and very symmetric crystal diameter enlargement after seeding became possible. This was not achieved by using the Czochralski method due to the unfavorable optical and thermal properties of the material [13,15,17].

Furthermore, in contrast to the Czochralski method, the position of the growth interface is independent on the melt level by using a fixed die (Fig. 8), which allows effective and continuous cooling of the crystal periphery. This fact is very important, since only by an excellent controllability of the crystal broadening stage and by an improved interface shape stability during cylindrical growth high quality crystals can be grown.

Investigations of chemo-mechanically polished cross sections of these crystals revealed after the application of a selective etchant typical etch pit density (EPD) values between 8.2×10^4 and 2.8×10^5 cm^{-2}. Rocking curve measurements have shown very good full width half maximum (FWHM) values of the 200 reflexes, typically in the range between 28 and 41. Mosaicity values of the crystals did not exceed 155″ and large parts of the crystals were mosaicity-free. The obtained crystal quality of the bulk crystals with volumes between 2-3 and 9 cm^3 remarkably exceeds the quality of commercial Verneuil crystals: EPD values are at least one order of magnitude better, FWHM values are 2 two 14 times better and mosaicity values are 2 to 3 times better.

At the current state of the art, our technology has enormous upscaling potential to reach industrially relevant crystal sizes. A further improvement of EFG crystal quality can also be expected by using seed crystals that are prepared from self flux grown crystals which exhibit still much lower dislocation densities. These goals are targeted for the next project and would then potentially allow a transfer of our technology to a company specialized in the growth of high quality single crystals.

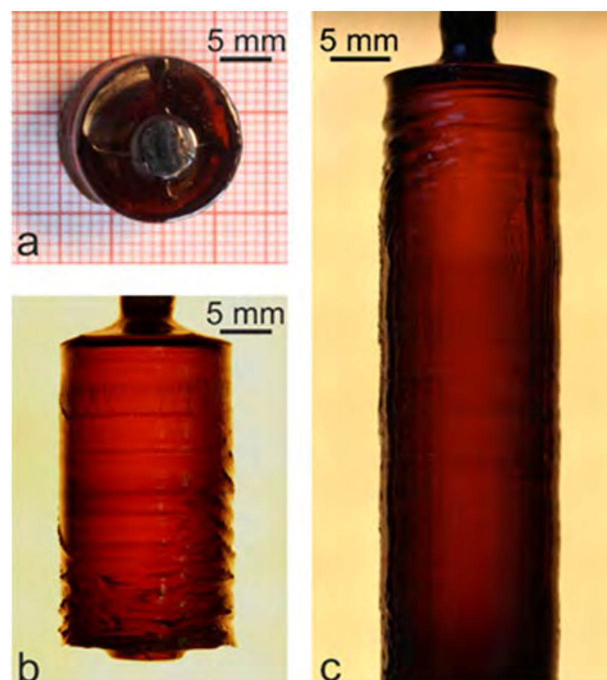

Fig. 7
$SrTiO_3$ single crystals grown by the EFG method with diameters of about 15 mm and lengths of (a) 13 mm, (b) 27 mm and (c) 50 mm [13].

Dielectric & Wide Bandgap Materials: **Oxides/Fluorides**

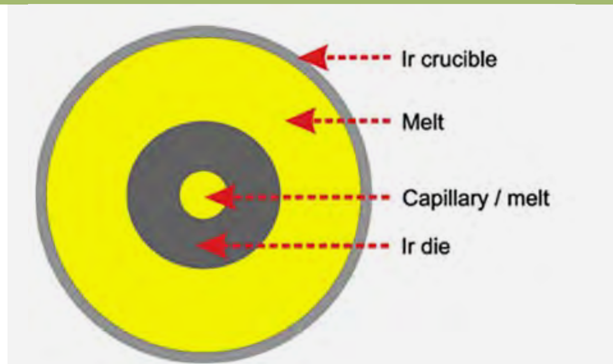

Fig. 8
Schematic configuration of the iridium based edge-defined film-fed growth setup operating at temperatures exceeding 2080°C (top view on the crucible and the fixed die) [13].

Growth of wüstite crystals by the micro-pulling-down crystal growth method

Iron(II) oxide, known under its mineral name wüstite, is one end-member of magnesiowüstite (Mg,Fe)O solid solutions and a main constituent of the Earth's lower mantle. Laboratory experiments on artificial specimen in anvil cells with conditions similar to those in depths of a few thousand kilometers are of great value for geophysical research. We have grown small wüstite crystals using the micro-pulling-down crystal growth method and analyzed those crystals using X-ray diffraction techniques. The growth atmosphere was a mixture of CO and CO_2 in Ar in an appropriate ratio to yield an oxygen fugacity fitting the predominance field of $Fe^{II}O$ over a wide temperature range. Crystals grown at very high pulling rate (50 mm/min) were single phase wüstite. The diffraction patterns of crystals grown at lower speed showed additional peaks arising from the presence of magnetite precipitations. For those crystals all wüstite peaks were split into two peaks, one of lower and the other at higher diffraction angle than the original (Fig. 9). Both features are a consequence of the eutectoid decomposition of wüstite at 560°C and do not occur if the crystals were cooled at sufficiently high rate.

Obvious occurrence of two wüstite phases of different stoichiometries clearly supports the model of a spinodal type disproportionation at the eutectoid temperature. Composition of these two metastable phases can be estimated from extrapolation of the wüstite solvus lines (Hultgren extrapolation) to temperatures below the eutectoid temperature. This was done numerically by calculating the Fe-O phase diagram as if there were no stable magnetite respectively iron phases. The computational result along with the obtained wüstite compositions is shown in the Figure 10.

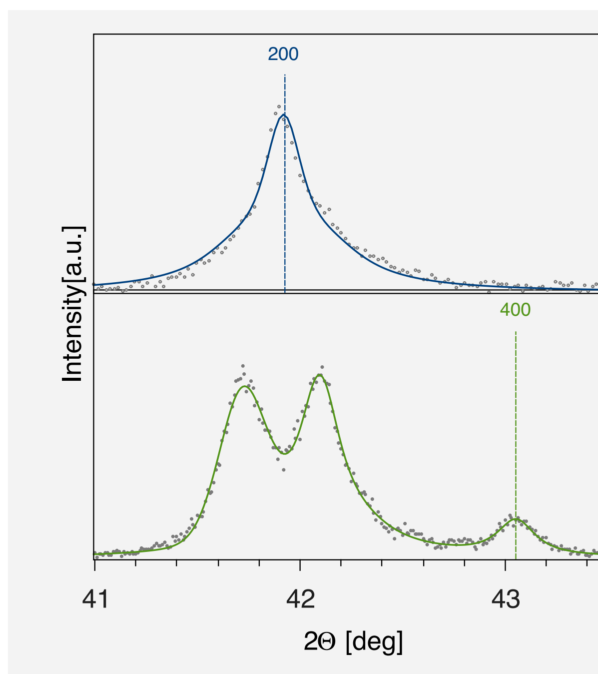

Fig. 9
Detail of the powder diffraction pattern of wüstite crystals grown at 50 mm/min (top, with wüstite reflections indexed) and 20 mm/min (bottom, with magnetite reflections).

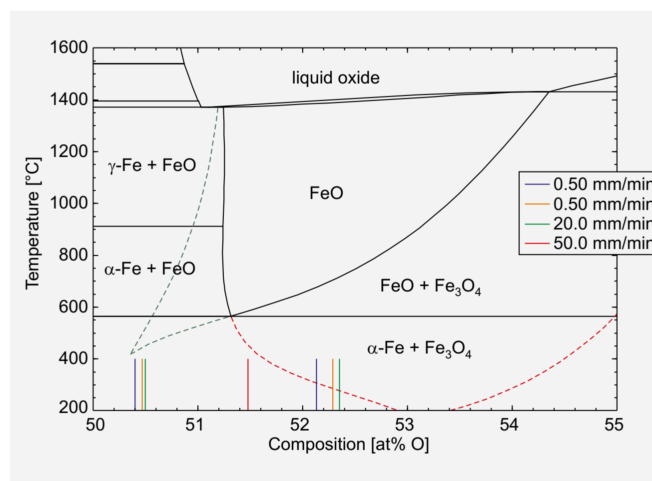

Fig. 10
Detail of the computed Fe-O equilibrium phase diagram close to the wüstite field including metastable extrapolations of the wüstite solvus lines and compositions of pulled crystals calculated from their lattice parameters.

Growth of $BaSnO_3$ bulk single crystals

Recently $BaSnO_3$ attracts much scientific attention as a transparent n-type conducting oxide with a wide energy gap of 3.1 – 4.05 eV and high electron mobility of 200 – 320 $cm^2V^{-1}s^{-1}$ for electron concentrations at the level of 10^{19} – $4x10^{20}$ cm^{-3} when doped with lanthanum [18]. It has the ideal cubic perovskite structure with space group Pmm and lattice constant a = 4.117 Å [19]. Due to very high thermal instability at high temperatures, only very small bulk crystals of maximum size 1-3 mm were grown by the flux method [18, 20, 21].

Through a series of melting experiments and thermodynamic studies we have demonstrated for the first time the feasibility of melting $BaSnO_3$ and obtaining first bulk crystals from the melt [22].

The melting experiments were performed between 1800 and 1990°C, and the melting point (MP) of $BaSnO_3$ was measured at 1855°C ± 25 K. At this temperature an intensive decomposition and non-stoichiometric evaporation takes place as the partial pressure of SnO(g) is about 90 times higher than that of BaO(g). The starting composition was prepared (i) in the stoichiometric ratio of SnO_2/BaO, (ii) with an excess of SnO_2 up to 10 mol.% to cover Sn losses at high temperatures, (iii) with La_2O_3 as an intentional dopant up to 2 mol.%, and (iv) a combination of both: an excess of SnO_2 and doping with La_2O_3. Growth experiments were performed by the direct solidification method using an inductively heated Ir crucible and oxygen partial pressure between 0.02 and 1 bar. The external pressure was either 1 or 19 bar. Examples of obtained crystals are shown in Fig. 11. The undoped crystals are typically red, but they are getting brown to dark brown when obtained at higher temperatures. On the other hand, La-doped crystals are typically black.

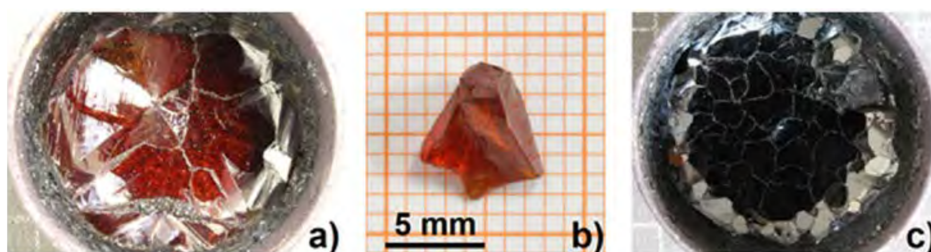

Fig. 11
Undoped $BaSnO_3$ obtained at 1858°C (a), bulk crystal (b), and La-doped $BaSnO_3$ obtained at 1915°C (c).

The chemical analysis by ICP-OES revealed a stoichiometric composition of the obtained crystals, while X-ray powder diffraction identified only the $BaSnO_3$ perovskite phase. Further, rocking curve measurements on a $BaSnO_3$ crystal sample by HR XRD showed a narrow peak with the full width at half maximum (FWHM) of 26 arcsec only, as shown in Fig. 12. Etch pit density was not exceeding 10^6 cm^{-2}, what is about five orders of magnitude lower than the dislocation density measured for thin films (4 – 8.9×10^{10} cm^{-2}) [23, 24].

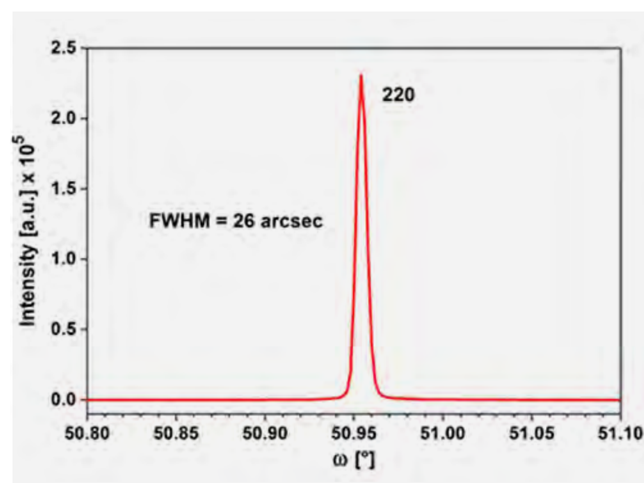

Fig. 12
Rocking curve of a $BaSnO_3$ crystal sample.

Dielectric & Wide Bandgap Materials: **Oxides/Fluorides**

The undoped, as-grown crystals showed different electrical behaviour depending on the coloration. The light brown or yellow and red coloured crystals were all electrical semi-insulators. The crystals with dark-brown coloration were semiconductors with the free electron concentration at the level of mid 10^{17} cm^{-3} and Hall mobility of about 45 $cm^2V^{-1}s^{-1}$. Annealing the as-grown crystals in an oxidizing atmosphere (air or O_2) at 1200 – 1400 °C for 10 – 40 h resulted in semi-insulating crystals independent on the coloration. On the other hand, annealing the undoped crystals in a reducing atmosphere (5% H_2+Ar) at 600 – 700°C for 10 h results in semiconducting crystals with a free electron concentration between 10^{16} – 10^{18} cm^{-3} and a Hall mobility of about 3 $cm^2V^{-1}s^{-1}$ only. Doping $BaSnO_3$ starting material with La_2O_3 at the level of 0.05 and 0.2 mol.% in the melt increased both the free electron concentration to a level above 10^{19} cm^{-3} and the electron mobility to values above 200 $cm^2V^{-1}s^{-1}$. This is consistent with the previous studies of flux-grown $BaSnO_3$ crystals showing an electron mobility of 200 – 320 $cm^2V^{-1}s^{-1}$ for electron concentrations in the range of 10^{19} – $4{\times}10^{20}$ cm^{-3} [18]. Annealing of La-doped crystals in an oxidizing atmosphere (air) at 1200°C for 10 h had no measurable effect on the electrical properties.

Fig. 13 shows the transmittance spectra of as-grown and undoped samples having different colorations and being electrical insulators, what is also manifested by no free carrier absorption in the near infrared spectrum. The cut-off wavelength of the near-edge transmittance is located at about 400 nm, wherein the red crystal sample showed much higher absorption in the visible spectrum.

Additionally, based on optical absorption measurements of melt grown $BaSnO_3$ we determined the indirect allowed energy gap of 3.00 ± 0.05 eV.

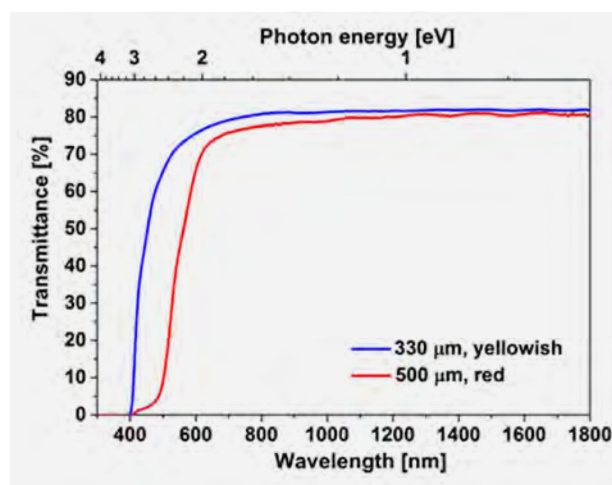

Fig. 13

Transmittance spectra of undoped $BaSnO_3$ crystal samples having different thicknesses of 500 (red line) and 330 (blue line) µm, respectively, and different colorations, red and yellowish or brownish, respectively.

References

[1] D. G. Schlom, L. Q. Chen, C. J. Fennie, V. Gopalan, D. A. Muller, X. Pan, R. Ramesh, R. Uecker; MRS Bulletin 39 No. 2 (2014) 119

[2] J. Schubert, O. Trithaveesak, A. Petraru, C. L. Jia, R. Uecker, P. Reiche, D. G. Schlom; Applied Physics Letters 82 (2003) 3460

[3] J. H. Haeni, P. Irvin, W. Chang, R. Uecker, P. Reiche, Y. L. Li, S. Choudhury, W. Tian, M. E. Hawley, B. Craigo, A. K. Tagantsev, X. Q. Pan, S. K. Streiffer, L. Q. Chen, S. W. Kirchoefer, J. Levy, D. G. Schlom; Nature 430 (2004) 758

[4] K. L. Ovanesyan, A. G. Petrosyan, G. O. Shirinyan, C. Pedrini, L. Zhang; Optical Materials 10 (1998) 291

[5] R. Uecker, R. Bertram, M. Brützam, Z. Galazka, Th. M. Gesing, C. Guguschev, D. Klimm, M. Klupsch, A. Kwasniewski, D. G. Schlom; Journal of Crystal Growth (2016), http://dx.doi.org/10.1016/j.jcrysgro.2016.03.014

[6] D. G. Schlom, L. Q. Chen, X. Q. Pan, A. Schmehl, M. A. Zurbuchen; J. Am. Ceram. Soc. 91 (2008) 2429

[7] B. Veličkov, V. Kahlenberg, R. Bertram, M. Bernhagen; Z. Kristallogr. 222 (2007) 466

[8] H. J. Kim, U. Kim, H. M. Kim, T. H. Kim, H. S. Mun, B.-G. Jeon, K. T. Hong, W.-J. Lee, C. Ju, K. H. Kim, K. Char; Appl. Phys. Express 5 (2012) 061102

[9] R. Eitel, C. A. Randall, T. R. Shrout, P. W. Rehrig, W. Hackenberger, S.-E. Park; Jpn. J. Appl. Phys., Part 1 40 (2001) 5999

[10] R. E. Eitel, C. A. Randall, T. R. Shrout, S.-E. Park; Jpn. J. Appl. Phys., Part 1 41 (2002) 2099

[11] I. Burn, D. M. Smyth; J. Mater Sci. 7 (1972) 339

[12] U. Berndt, D. Maier, C. Keller; J. Solid State Chem. 13 (1975) 131

[13] C. Guguschev, Z. Galazka, D. Kok, U. Juda, A. Kwasniewski, R. Uecker; CrystEngComm. 17 (2015) 4662

[14] C. Guguschev, D. Klimm, F. Langhans, Z. Galazka, D. Kok, U. Juda, R. Uecker; CrystEngComm. 16 (2014) 1735

[15] C. Guguschev, D.J. Kok, Z. Galazka, D. Klimm, R. Uecker, R. Bertram, M. Naumann, U. Juda, A. Kwasniewski, M. Bickermann; CrystEngComm, 17 (2015) 3199

[16] H.E. Labelle, A.I. Mlavsky, Nature, 216 (1967) 574

[17] D.J. Kok, K. Irmscher, M. Naumann, C. Guguschev, Z. Galazka, R. Uecker; Phys. Status Solidi A, 212 (2015) 1880

[18] H. J. Kim, U. Kim, H. M. Kim, T. H. Kim, H. S. Mun, B.-G. Jeon, K. T. Hong, W.-J. Lee, C. Ju, K. H. Kim, K. Char; Appl. Phys. Express 5 (2012) 061102

[19] A. J. Smith and A. J. E. Welch; Acta Crystallogr. 13 (1960) 653

[20] H. J. Kim, U. Kim, T. H. Kim, J. Kim, H. M. Kim, B.-G. Jeon, W.-J. Lee, H. S. Mun, K. T. Hong, J. Yu, K. Char, and K. H. Kim; Phys. Rev. B 86 (2012) 165205

[21] X. Luo, Y. S. Oh, A. Sirenko, P. Gao, T. A. Tyson, K. Char, S.-W. Cheong; Appl. Phys. Lett. 100 (2012) 172112

[22] Z. Galazka, R. Uecker, K. Irmscher, D. Klimm, R. Bertram, A. Kwasniewski, M. Naumann, R. Schewski, M. Pietsch, U. Juda, A. Fiedler, M. Albrecht, S. Ganschow, C. Guguschev, M. Bickermann; J. Phys. Cond. Matt. (2016) submitted

[23] H. Mun, U. Kim, H. M. Kim, C. Park, T. H. Kim, H. J. Kim, K. H. Kim, K. Char; Appl. Phys. Lett. 102 (2013) 252105

[24] U. Kim, C. Park, T. Ha, R. Kim, H. S. Mun, H. M. Kim, H. J. Kim, T. H. Kim, N. Kim, J. Yu, K. H. Kim, J. H. Kim, K. Char; APL Mat. 2 (2014) 056107

Dielectric & Wide Bandgap Materials: **Gallium Nitride**

Head apl. Prof. Dr. Dietmar Siche
Team Dr. S. Golka, Dr. K. Kachel, R. Nitschke

Übersicht

In Fortsetzung unserer im letzten Bericht geschilderten Arbeiten, haben wir das Wachstum einkristalliner, Kohlenstoff-dotierter GaN-Schichten aus der Gasphase entwickelt. Ziel war es, Proben zur Untersuchung der Eigenschaften von Kohlenstoff im GaN herzustellen und semi-isolierendes (SI) Material für die Leistungselektronik zu erhalten.

Allgemein verursachen Kompensationseffekte tiefer Niveaus den hohen Widerstand der SI-GaN-Schichten. Die n-Typ-Leitfähigkeit gezüchteter GaN-Kristalle wird auf das allgegenwärtige Silicium und den Sauerstoff zurückgeführt. Die freien Ladungsträgerkonzentrationen können bei Raumtemperatur oft 10^{18} cm^{-3} überschreiten [1]. Dotieren mit tiefen Akzeptoren, z.B. mit Übergangsmetallen wie Fe [2], ermöglichte, SI GaN-Schichten ohne starke strukturelle Störungen mit verschiedenen Methoden zu erzeugen, wie mit der Metal Organischen Chemischen Gasphasenabscheidung (MOCVD) [3] und der Haliden Gasphasenepitaxie (HVPE) [4]. Aber die Einstellung des Kompensationsniveaus hinsichtlich der Hintergrunddotierung von Si und/oder O und der Löslichkeitsgrenze des tiefen Dotanden war eine Herausforderung [5].

Aus der Literatur ist auch bekannt, dass SI-GaN-Schichten durch C-Dotierung in verschieden Epitaxiemethoden hergestellt werden können. Weil das Ersetzen von Ga durch Kohlenstoff in n-Typ-GaN eher unwahrscheinlich ist, liegt der Fokus auf C_N. Lyons et al. [6] haben dessen Rolle kürzlich revidiert. Aus Dichtefunktional-Berechnungen fanden sie, dass C_N ein tiefer Akzeptor mit einer Ionisationsenergie von ca. 0.9 eV ist. Daher sollte der Kohlenstoff restliche Donatoren in GaN effektiv kompensieren. Außerdem stabilisiert die Selbstkompensation das semi-isolierende Verhalten sogar für starke Überkompensation. Dieser augenscheinliche Vorteil stimulierte unsere weiteren Studien. Unsere Züchtungsmethode ähnelt der etablierten HVPE, aber statt Cl^- wird das Pseudo-Halogen-Ion CN^- als chemisches Ga-Transportagens benutzt.

Ein kleiner Eigenbaureaktor aus Quarz für die Pseudo-Halide Gasphasenepitaxie (PHVPE) [7] wird genutzt, um die kontrollierte C-Dotierung bei der Reaktion von GaCN mit Ammoniak zu GaN zu untersuchen. Diese Studie wird in Zusammenarbeit mit dem Institut für Festkörperphysik an der Technischen Universität Berlin, Prof. A. Hoffmann, im Rahmen des DFG-Projekts QuarzGaN durchgeführt. Dr. Kryzstof Kachel hat die vorläufigen Ergebnisse in seiner Dissertation [8] zusammengefasst und diese im März 2015 an der Humboldt-Universität erfolgreich verteidigt.
Er blieb als Postdoc in unserer Gruppe und hat seine Ergebnisse zur „FTIR-Abgasanalyse bei der Pseudo-Haliden Gasphasenepitaxie von GaN" publiziert [9].

Das Wachstum dicker InN – Schichten auf Fremdsubstraten durch Plasma-basierte Lösungszüchtung war das Ziel eines bis Juni 2015 laufenden ZIM-Projektes („Zentrales Innovationsprogramm für kleine und mittlere Unternehmen" des BMWi). Der Reaktor mit beheiztem Tiegel für die Indium-Quelle wird in ein Plasma mit hoher Elektronendichte (ca. 10^{11} cm^{-3}) bei niedrigem Druck (5 Pa) getaucht. Die Konstruktion erfolgte in Kooperation mit den Projektpartnern DTF Technologie GmbH (Dresden) und Plasmetrex GmbH (Berlin). Der Plasma-aktivierte Stickstoff überwindet die Energiebarriere für die Lösung von Stickstoff in der Indium-Schmelze. Das gelöste Indium diffundiert in einem Temperaturgradienten zum Keim, wo die Übersättigung zur Kristallisation führt. Allgemein kann Plasma einen Stickstoff-Massenfluss zu einer Oberfläche liefern und einen steuerbaren Energiefluss in eine Oberfläche durch Bombardierung mit Elektronen und Ionen. Das kann gegenüber Züchtungsmethoden, die einfach Ammoniak als Stickstoffquelle nutzen, zu einem Vorteil führen, wenn Stickstoffplasma wie in der folgend beschriebenen Methode angewandt wird. Eine der größten Herausforderungen im Projekt war es, große Temperaturgradienten von der Schmelzenoberfläche zum Keim am Boden zu erreichen, um die diffusionsbegrenzte Wachstumsrate zu erhöhen.

Overview

In continuation to our previously reported work, we developed the growth of single crystalline, carbon doped gallium nitride (GaN) layers from the gas phase. Our goal was to prepare samples for the study of carbon behavior in GaN and to achieve semi-isolating (SI) material for power electronics.

Generally, compensation effects of deep levels cause the high resistivity of SI GaN films. The n-type conductivity of as grown GaN crystals is due to ubiquitous silicon and oxygen. Free carrier concentrations may exceed 10^{18} cm^{-3} at room temperature [1]. Doping with deep acceptor impurities, e.g. transition metals as Fe [2], was able to produce SI GaN films without strong structural deterioration by various methods, like Metal Organic Chemical Vapour Deposition (MOCVD) [3] and Halide Vapour Phase Epitaxy (HVPE) [4]. But the adjustment of the compensation level regarding the background impurity concentrations of Si and/or O and the solubility limit of the deep level dopant was challenging [5].

It is also known from literature, that SI GaN layers were produced with carbon doping by epitaxial methods. Because the carbon substitution of Ga is rather unlikely in n-typ GaN, the focus is on C_N. Lyons et al. [6] recently revised its role. From hybrid functional density calculations they found C_N as a deep acceptor level with about 0.9 eV ionization energy. Therefore, carbon should effectively compensate residual donors in GaN. Additionally, self-compensation stabilises the semi-insulating behaviour even for high over-compensation. This apparent advantage stimulated our further studies.

Our growth method is very similar to the established HVPE, but instead of Cl^- the pseudo halogen CN^-ion was used as chemical transport agent of Ga. A homemade small quartz reactor for the Pseudo-Halide Vapor Phase Epitaxy (PHVPE) [7] is used to study controlled C doping during the reaction of GaCN with ammonia to GaN. This study is done in collaboration with the Institute of Solid State Physics at the Technische Universität Berlin, Prof. A. Hoffmann, in the frame of the DFG project QuartzGaN.Dr. Kryzstof Kachel has summarized the preliminary results in his thesis [8], which he successfully defended at Humboldt Universität Berlin in March 2015. He stayed in our group as a postdoc and published his results of "FTIR Exhaust Gas Analysis of GaN Pseudo-Halide Vapour Phase Growth" [9].

The growth of thick InN layers on foreign substrates by plasma based solution growth was the aim of a ZIM project (central innovation program for small and medium-sized businesses of BMWi) running until June 2015. The reactor with heated crucible for the molten In source is submerged in a plasma with high electron density (ca. 10^{11} cm^{-3}) at low pressure (5 Pa). The construction has been performed in cooperation with our project partners DTF Technology GmbH (Dresden) and Plasmetrex GmbH (Berlin). The plasma-excited nitrogen overcomes the energy barrier for nitrogen solution in indium melt. The solved nitrogen diffuses in a temperature gradient to the seed where supersaturation leads to crystallization. In general, plasma can supply a nitrogen mass flow onto a surface and a steerable energy flow into a surface by bombardment with electrons and ions. This can lead to an advantage over growth methods that simply use ammonia as a nitrogen source instead of nitrogen plasma as employed in the method described below. One of the major challenges of the project was to achieve a large temperature gradient from the melt surface to the seed at the bottom, to increase the diffusion limited growth rate.

Results

Pseudo-Halide Vapour Phase Epitaxy (PHVPE) of GaN:C layers

The effect of carbon doping on electronic properties of GaN is not fully understood yet. PHVPE may result in GaN layers with higher carbon concentrations up to 8 x 10^{19} cm^{-3} measured by Secondary Ion Mass Spectroscopy (SIMS), whereas the growth rate also depends on the carbon supply from GaCN flux. Various coalesced layers were grown (Fig. 1) by controlled methane supply for synthesis of HCN as Ga precursor. Thermodynamic studies [7] led us to the conclusion that the main growth reaction is:

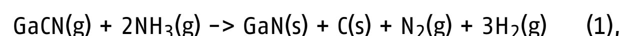

$$GaCN(g) + 2NH_3(g) \rightarrow GaN(s) + C(s) + N_2(g) + 3H_2(g) \quad (1),$$

while reaction:

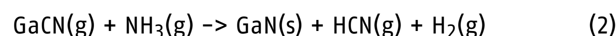

$$GaCN(g) + NH_3(g) \rightarrow GaN(s) + HCN(g) + H_2(g) \quad (2)$$

is also possible. This was confirmed by HCN detection in the waste gas line with in-situ Fourier Transform Infrared (FTIR) spectroscopy [9]. All layers were grown on 2.3 µm thick MOCVD-GaN/sapphire templates. The grown layers were characterized by Scanning Electron Microscopy (SEM), Secondary Ion Mass Spectroscopy (SIMS), Photoluminescence (PL), Micro-Raman-Spectroscopy, Hall effect measurement, and High Resolution X-Ray Diffractometry (HRXRD). The control of homogeneous C doping as well as the high level of background impurities proved to be challenging and have to be improved.

Dielectric & Wide Bandgap Materials: **Gallium Nitride**

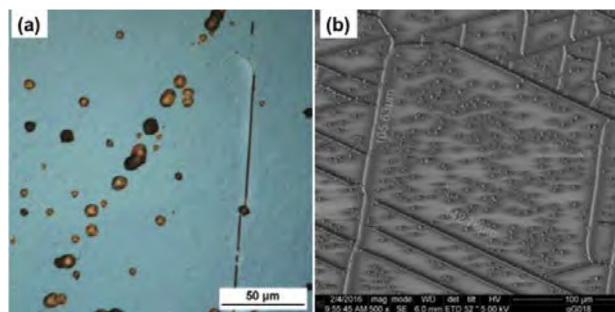

Fig. 1
a) qG016: facetted V-pits and a crack at the right side, dark contrast could arise from higher carbon incorporation on facets; higher density of smaller round depressions with central pits, possibly closed V-pits (micrograph) and
b) qG018: trenches from cracks and V-pits (SEM, sample tilted at 52°)

The pits on as grown surfaces (Fig. 1a) are V-pits as confirmed by SEM images (Fig. 1b). Their width in sample qG016 is up to 8 µm, some of them are much smaller and most of them are overgrown. They result in the higher density of smaller round depressions with flat central pits and of lower contrast. The lower brightness of facetted pits stems probably from enhanced carbon incorporation on their facets. This is a possible mechanism of inhomogeneous impurity incorporation. Some larger holes in the layer show impurities at the bottom, supporting the assumption that surface obstacles form V-pits by hindering the coalescence of 3D nuclei. EDX images of qG017 and qG018 (not shown) reveal the macroscopically homogeneous but microscopically inhomogeneous C incorporation.

SIMS also reveals the inhomogeneous impurity incorporation. Whereas the N reference signal and the metals Mg, Al, Ni, and Zn were measured with an oxygen beam, a Cs beam was used to measure the Ga reference, H, C, O, Si, Se, and Pt signals. Each sample was measured at three different points A, B, C and the layer thickness proved to be inhomogeneous. Figure 2a shows the profiles for positive ions at point B: quantitative for Mg, Mn and Zn (left axis) and qualitative for Al, Ni and Pt in counts/sec (right axis). Mn is much below 10^{16} cm^{-3}, Zn and Mg are somewhat above. Zn could stem from ZnSe windows in the FTIR gas cell, attacked by the aggressive exhaust gases. There was no search for Se, but the low signals of Se and Zn were found by EDX in qG018. The Mg signal could arise from a mass interference of carbon. Two times $^{12.01}$C gives $^{24.02}$X, which is near $^{24.32}$Mg. Al comes from the sapphire substrate, Ni is from the diaphragm between the source and growth area and Pt is the catalyst in the HCN synthesis oven.

Figure 2b shows the concentration profiles of negative ions H, C, O and Si. Hydrogen comes from ammonia, methane and HCN decomposition, silicon from the quartz reactor and oxygen as the main impurity coming from reactor leakage, Ga source, sapphire substrate and nitrogen carrier flow. Sputtering is from the left side in Fig. 2 and oxygen goes up if it reaches the layer sapphire interface and therefore gives the layer thickness. In case of sample qG016 the layer is 7-10 µm thick. The seed temperature T_{seed} was 1010°C, the growth time (flow of GaCN through the reactor) was t = 50 min, and the flow rates of NH_3, CH_4 and NH_3 through the ring shower were = 55, 45, and 100 sccm, respectively.

The growth rate related intentional in-situ carbon doping was about 3x10^{18} cm^{-3}. Considering also measuring points A and C the carbon concentration [C] varied from 10^{18} – 10^{19} cm^{-3}.

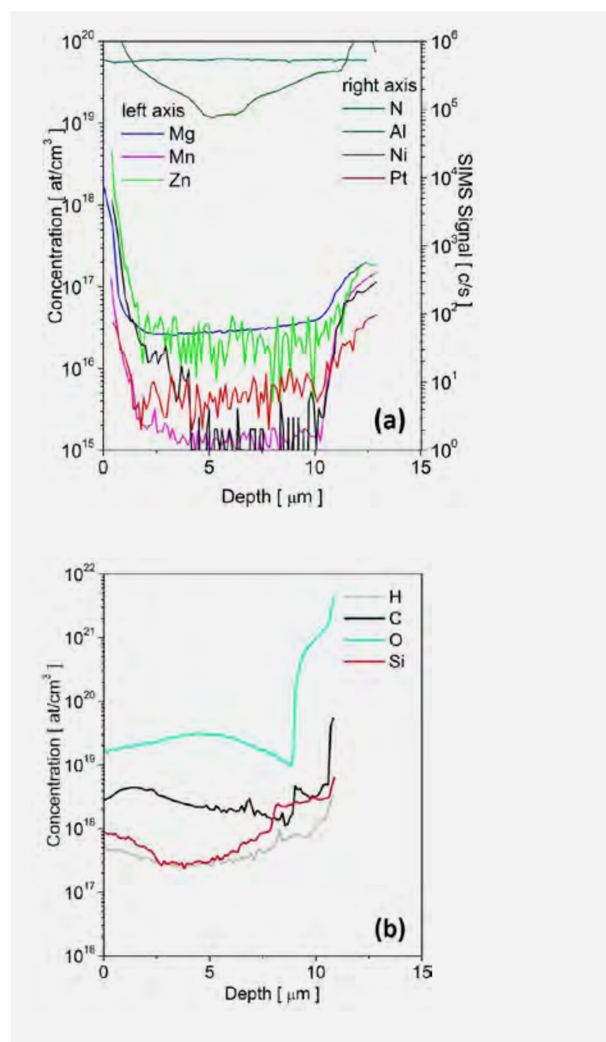

Fig. 2
SIMS profiles of qG16, thickness 7-10µm, measurement point B,
a) concentration of some metallic impurities (left scale) and signal counts (right scale);
b) concentration of some non-metallic impurities (measured by R. Jakieła, IFPAN Warszawa)

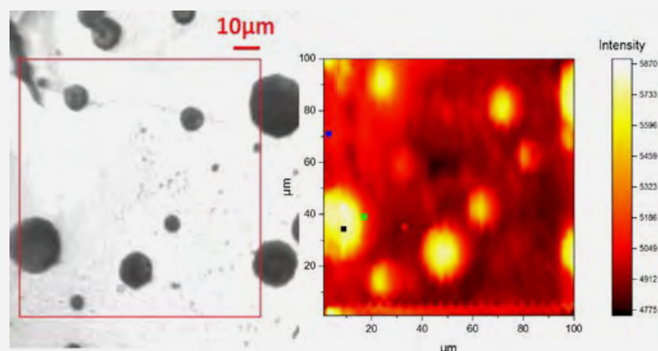

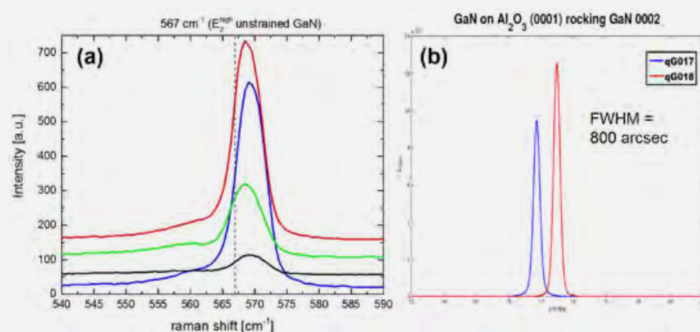

Fig. 3

Increased PL intensity in V-pit regions (measured by N. Jankowski, TU Berlin)

Fig. 4

a) Raman shift of qG106 (measured by N. Jankowski, TU Berlin) and b) comparison of XRD rocking curves of qG017 and 018 (measured by A. Kwasniewski, Physical Characterization, IKZ)

PL and µRaman studies were performed by our project partner at TU Berlin, the XRD and Hall effect measurements by the group Physical Characterization at IKZ. Figure 3 shows an increased PL intensity in V-pit regions. Comparing with studies at dislocation etched GaAs surfaces [10] this effect is partly a geometrical one. The pits facets reflect emitted photons and direct them to the sensor. Additionally, higher carbon concentration resulted in Burstein-Moss-shift of near band gap emission close to and on dark spots (not shown). In Figure 4a, the E_2^{high} intensity vs. Raman shift is shown for the measuring points in Figure 3 right. The intensity decreases and in comparison to unstrained material a shift of ~2 cm^{-1} to higher wave numbers is observed. This means there is a biaxial compressive pressure of ~ 0.64 GPa. Comparing the XRD rocking curves of qG017 and qG018 (Fig. 4b) in both samples a large FWHM of ~ 800 arcsec was found. The reason is the mosaicity from columnar growth and high density of screw and mixed dislocation from the seed-layer lattice misfit (pure edge dislocations do not contribute to broadening of 0002 reflex). There was no epitaxial lateral overgrowth nor other technique utilized to decrease the dislocation density. The peak intensity of qG017 was lower than the one of qG018 because the layer was grown for only 35 min (9 µm thick) in comparison to the qG018 growth of 130 min resulting in 20-µm thick GaN. The peak position changes slightly with different sample adjustment.

Finally, it was obvious that the e-beam in SEM could not charge the samples. This was inconsistent with SI material. Hall effect measurements revealed n- type conductivity of the as grown GaN samples. Table 1 shows that the resistivity ρ in the grown material was even lower than in the template seed layer. Therefore, the oxygen and silicon background levels have to be lowered and the carbon doping level has to be increased and homogenized. The strong dependence of carbon incorporation on surface orientation results in the need for better substrates, which can support the prevention of V-pit formation.

sample	d [µm]	ρ [Ωcm]	n [cm^{-3}]	μ_H [cm^2 $(Vs)^{-1}$]
template	2,3	0.22959	3,0E+17	89.7
qG014	30 - 40	0.0016003	7,0E+19	55.4
qG015	4 - 10	0.023479	1,1E+19	24.3
qG018a	15 - 20	0.14956	1,9E+18	21.5
qG026A	10 - 13	0.3524	7,8E+17	22.7
qG027	3 - 5	0.138	1,2E+18	38.5
qG028	30	0.02	2,2E+19	14.1

Table 1

Specific resistance ρ, free electron concentration n and Hall mobility μ_H from Hall effect measurements carried out by K. Irmscher (Physical Characterization, IKZ).

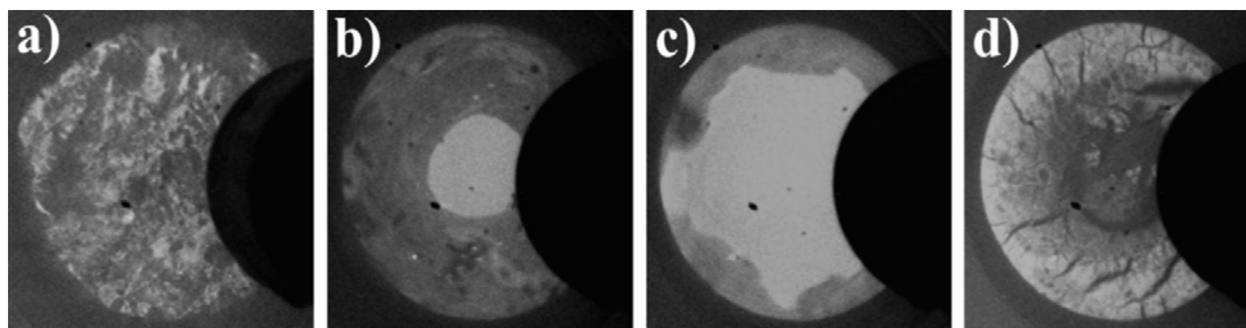

Fig. 5
Indium surface in 4 cm diameter crucible from 1 m distance, illuminated by plasma emission only.
a) Immediately after plasma ignition.
b) At the beginning and
c) at the end of H_2 purification.
d) After some seconds in pure N_2 plasma.
(camera images)

Low pressure, high-density plasma based solution growth

The final version of the reactor prototype contained a cylindrical 2 MHz inductive plasma source with ca. 17 cm inner diameter to deliver a nitrogen or hydrogen plasma or a mixture of both. The inner diameter of the tungsten crucible for the In source is 4 cm, its depth is 1 cm. The sapphire seed is fixed at the crucible bottom. The plasma irradiates the crucible from above and a sophisticated chuck, which can be set on an electrical potential, cools it from below. Such setup prevents plasma damage of the growing layer because the plasma only interacts with the melt surface. For the same reason the seed environment is near thermal equilibrium, since the gas-melt interface is sufficiently far away from the melt-layer interface.

A molybdenum coil heats the crucibles cylinder barrel. The bottom is cooled by heat conduction through solid copper. The top surface loses heat via radiation and conduction. With plasma heating, the latter has to be overcome to get the surface hotter than the seed. Temperature field simulations show that 20K temperature difference require roughly 100 W at a surface temperature of 600°C. A combination of 13.56 MHz excitation and DC current towards earth can accommodate up to 100 W without electrical arcing. With hydrogen admixture, the formation of an InN crust that would block nitrogen solution was suppressed. A typical photograph of the crucible during growth is shown in Fig. 5. The temperature of the top surface is difficult to measure with pyrometer since its emissivity depends largely on the degree of nitration.

The formation of bubbles containing molecular nitrogen as reported for GaN solution growth in the literature can be suppressed with our method in many cases. However, parasitic growth of InN still occurs, that might be suppressed by a much larger temperature gradient, requiring a stronger cooling at the crucible bottom. This was not realized during the project period. Resulting microcrystals growing on the seed are shown in Fig. 6. Adding 20 % of tin to the solution was beneficial to the growth rate. At 1000°C, deposition rates on various substrates exceed 100 nm/min.

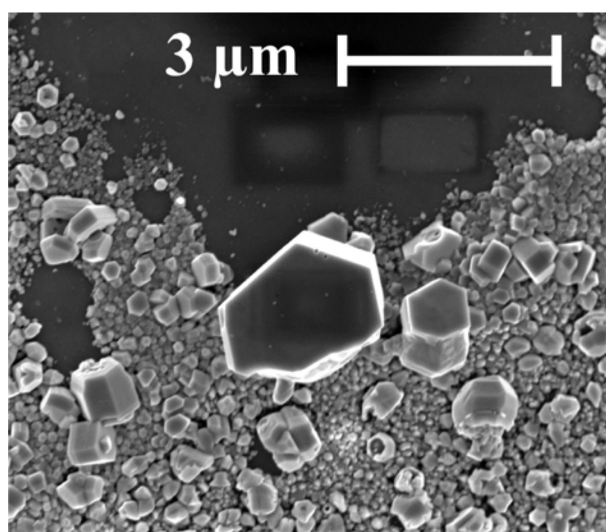

Fig. 6
InN crystallites on sapphire seed.

References

[1] D. Ehrentraut, E. Meissner, M. Bockowski (Eds.); *Technology of Gallium Nitride Crystal Growth*; Springer Verlag, Heidelberg (2010)

[2] B. Monemar, O. Lagerstedt; J. Appl. Phys. 50 (1979) 6480

[3] S. Heikman, S. Keller, S.P. DenBaars, U.K. Mishra; Appl. Phys. Lett. 81 (2002) 439

[4] R.P. Vaudo, X.P. Xu, A. Salant, J. Malcarne, G.R. Brandes; Phys. Status Solidi A 200 (2003) 18

[5] A.Y. Polyakov, N.B. Smirnov, A.V. Govorkov, S.J. Pearton; J. Vac. Sci. Technol. B 22 (2004) 120

[6] J.L. Lyons, A. Janotti, C.G. Van de Walle; Appl. Phys. Lett. 97 (2010) 152108

[7] K. Jacobs, D. Siche, D. Klimm, H.-J. Rost, D. Gogova; J. Cryst. Growth 312 (2010) 750

[8] K. Kachel, *Pseudo Halide Vapour Phase Epitaxy Growth of GaN Crystals*, PhD thesis; Humboldt-Universität zu Berlin (2015)

[9] K. Kachel, D. Siche, S. Golka, P. Sennikov, M. Bickermann; Mater. Chem. Phys. 177 (2016) 12

[10] U. Juda (IKZ); private communication

Dielectric & Wide Bandgap Materials: **Aluminium Nitride**

Head Dr. Jürgen Wollweber
Team Prof. M. Bickermann, Dr. A. Dittmar, Dr. C. Dufloux, Dr. C. Hartmann, S. Kollowa, F. Langhans, R. Nitschke, H. Oppermann, A. Wagner

Übersicht

Die Erfindung der Glühlampe durch Thomas Alva Edison im Jahr 1879 war auch der Ausgangspunkt für die Suche nach zuverlässigeren, preiswerteren und vor allem helleren Lichtquellen. In der Folge entstand eine schnell wachsende Industrie, die eine große Breite von Lampentypen mit Glühfaden oder als Leuchtstofflampe herstellte. Trotz einiger schwerwiegender Nachteile existierten diese Lampentypen für lange Zeit. Erst durch die revolutionäre Erfindung der Leuchtdiode (LED- light emitting diode) und der Laserdiode (LD- laser diode) im Jahr 1962 wurden völlig neue und hocheffiziente technologische Beleuchtungskonzepte möglich. Unabhängig von allen Unsicherheiten bei der Bestimmung des Weltmarktvolumens der LED-Beleuchtungstechnologie, ist es heute gerechtfertigt festzustellen, dass dieser Markt ein Multimilliarden-Dollar-Geschäft mit hohen Wachstumsraten ist.[1]

Gegenwärtig wird der überwiegende Teil der LED-Produktion durch Abscheidung von aktiven (AlGaIn)N-Schichten auf Saphir- oder Siliciumsubstraten hergestellt. Dabei basiert der Erfolg des (AlGaIn)N-Mischkristallmaterials auf dem Umstand, dass es sich um direkte Halbleiter mit zusammensetzungsabhängiger Breite der verbotenen Zone handelt (E_G^{InN} =1,9 eV, E_G^{GaN} =3,4 eV, E_G^{AlN} =6,2 eV), bei dem sich der adressierbare Wellenlängenbereich von Infrarot bis zu 210 nm erstreckt. Hinzukommt die relativ gute thermische Leitfähigkeit, die das GaN-AlN-InN-System auch für elektronische Hochleistungs- und Hochtemperaturbauelemente interessant macht.

Da für den langwelligen Teil des Lichtspektrums große und preiswerte Substrate für die LED-Fertigung verfügbar sind, kann in diesem Sektor ein gutes Preis/Leistungsverhältnis realisiert werden.

Am anderen Ende des spektralen Fensters ist die Situation weniger vorteilhaft, da die Gitterfehlpassung zwischen den (AlGaIn)N-Schichten und den allgemein genutzten Substraten zu hohen Defektdichten in den aktiven Schichten führt. Die Wirkungsgrade der LEDs sinken dadurch auf technisch uninteressante Werte. Wenn man über eine Lösung für dieses Problem nachdenkt, sollte im Auge behalten werden, dass die akzeptable Defektdichte, bei der es sich vor allem um Versetzungen handelt, bei maximal 10^6 cm^{-2} liegen darf. Dabei stellt dieser Wert die Summe aus bereits im Substrat vorhandenen Versetzungen und in den aktiven Schichten neu generierten Versetzungen dar.

In der Konsequenz bedeutet das eine maximal zulässige Versetzungsdichte für die Substrate von zirka 10^4 cm^2. Darum setzt die technologische Nutzung von (AlGaIn)N-Schichten in UVC-LEDs strukturell nahezu perfekte AlN-Wafer als Quasi-Eigensubstrate voraus.

Die Grundlagen für das Wachstum von AlN-Volumenkristallen als der Grundlage für AlN-Wafer wurden in den letzten Jahrzehnten entwickelt, wobei sich die Sublimations/Rekondensationstechnik (PVT) als Methode der Wahl erwiesen hat. Im IKZ ist die AlN-Gruppe seit mehr als 10 Jahren eng in diese Entwicklung eingebunden und hat in dieser Zeit für alle mit der AlN-Züchtung verbundenen Schlüsselprobleme Lösungen erarbeitet. Besondere Aufmerksamkeit ist dabei dem homoepitaktischen Wachstum mit Durchmesseraufweitung und der Optimierung der elektrischen und optischen Eigenschaften gewidmet worden.

Angesichts der Tatsache, dass weltweit nur drei Quellen für homoepitaktisch gewachsene AlN-Kristalle existieren, unter denen die AlN-Gruppe des IKZ der einzige Lieferant ohne Nutzungsbeschränkungen ist, gibt es einen breiten Bereich von Kooperationen und Anwendungen, die auf ihre Realisierung warten. Unsere gegenwärtigen Aktivitäten umfassen die technologische Entwicklung der Infrastruktur für die Züchtung, die Untersuchung der physikalischen und kristallografischen Eigenschaften des gezüchteten kristallinen AlN und anwendungsorientierte Aktivitäten. In diesem Zusammenhang haben wir Untersuchungen zur Plasma-gestützten Abscheidung von Gruppe III-Nitrid-Targets (BMWi-Verbundprojekt, ZIM-Programm) begonnen und wir arbeiten an AlN-Substraten mit definierten Eigenschaften (Konsortium "Advanced UV for Life", BMBF-Innovationsinitiative „Unternehmen Region"). Darüber hinaus entwickeln wir spezielle Tiegel- und Isolationsmaterialien (BMWi-Kooperationsprojekt, ZIM-Programm). Ein wichtiger Teil dieser Arbeiten sind zwei Promotionen, bei denen der Fokus auf Defektanalysen und dem Dotierverhalten von AlN liegt.

An dieser Stelle soll hervorgehoben werden, dass ein Großteil der physikalischen Charakterisierung in Kooperation mit internen und externen Partnern realisiert wurde. Besonderer Dank gebührt der Abteilung Simulation & Charakterisierung des IKZ, der Gruppe Halbleiterphysik des Instituts für Physik der TU Chemnitz und der Gruppe Hochtemperatur-Sensorik des Instituts für Energieforschung und Physikalische Technologien an der TU Clausthal.

Overview

The invention of the incandescent lamp by Thomas Alva Edison in 1879 was the starting point for the search for more reliable, less expensive, and above all brighter lighting sources. Subsequently, rapidly growing industries emerged to produce a great variety of lamps with filament or as fluorescent lamp. Despite some serious drawbacks, these types of lamp has been for a long time. Only through the revolutionary inventions of the light-emitting diode (LED) and of the laser diode (LD) both in 1962 entirely new and highly efficient technological concepts of lighting were possible. For all the uncertainty still surrounding the world market value of LED lighting technology, this market is a multi-billion dollar business characterized by high growth rates [1].

Today, the vast majority of the LED production is made by deposition of active (AlGaIn)N-layers on substrates from sapphire or silicon. Thereby the success of (AlGaIn)N mixed crystals is based on their direct transitions with a band gap energy variety from 1.9 eV for InN, to 3.4 eV for GaN, to 6.2 eV for AlN, which allows a wavelength range from IR to 210 nm, in combination with their fairly high thermal conductivity and the possibility to adapt physical properties by changing the composition. This makes the GaN-AlN-InN-System also interesting for high-power and high-temperature electronic applications.

Since large and cheap substrates (sapphire, SiC, Si) are available for the long-wave part of the spectrum a good price/performance ratio can be realized. Unfortunately, the situation is much less favorable at the other end of spectral window where the lattice misfit between (AlGaIn)N-layers and commonly used substrates lead to highly defected active layers by which the LED efficiencies drop down to technically uninteresting values.
When thinking about a solution for this problem one has to keep in mind that the desired defect density (mostly dislocations) must be in the order of 10^6 cm^{-2} as maximum. But this value is the sum of native dislocations from the substrate and the newly generated dislocations in the active layers. As a consequence, the dislocation density (DD) in the substrate should be in the order of 10^4 cm^{-2} or even less. Therefore, the technological use of (AlGaIn)N-layers in UVC LEDs assumes best fitting quasi-substrate as possible in the form of nearly perfect AlN wafers.

The principles for growing AlN bulk crystals as the base for AlN wafers were developed during the last decades. For this approach sublimation-recondensation (PVT) is the method of choice in any case. The IKZ-internal AlN group is closely involved in this process for more than 10 years. Solutions for all key issues in making AlN substrates ready for application have been developed in this time.

Particular attention was paid to the homoepitaxial growth with diameter enlargement and the optimization of the electrical and optical properties of the bulk AlN crystals.

In view of the fact that only three sources for homo-epitaxially grown AlN crystals exist worldwide, among them the internal AlN group acts as the only free supplier without any limitations, a whole range of potential co-operation/applications await their realization. Our current activities extend over technological development of the growth equipment, investigation of physical and crystallographic properties of the grown crystalline AlN, and application driven activities. Within this context, we started investigations on plasma-assisted deposition of high purity III-nitride targets (joint BMWi project, ZIM program) and we work on AlN substrates with defined properties ("Advanced UV for Life" consortium; BMBF Innovation Initiative "Entrepreneurial Regions"). Furthermore, we investigate advanced crucible and insulation materials (BMWi cooperation project, ZIM program). An important part of this work are two doctoral theses with focus on defect characterization and doping behavior of AlN.

It should be emphasized at this point, that a major portion of the physical characterization was realized in cooperation with internal and external partners. Special thanks are due to the IKZ department Simulation & Characterization, the group Semiconductor Physics, Institute of Physics, TU Chemnitz, and the Group Sensors for high temperature processes, Institute of Energy Research and Physical Technologies, Clausthal-Zellerfeld.

Results

According to our last publications freestanding AlN crystals with high structural quality can be grown close to the thermodynamic equilibrium by spontaneous nucleation (TDD < 10^3 cm^{-2}, rocking curve full width at half maximum values FWHM < 15 arcsec) [2,3]. The growth design limits the crystal dimensions to approximately 9x9x14 mm^3. Nevertheless, the needed N-polar seeds could prepared from these crystals for subsequent homoepitaxial growth runs. In order to reach an appropriate crystal diameter expansion, a radial temperature gradient in front of the growth interface has to be formed (i) low enough that no additional structural defects are generated by the induced thermal strain, [4,5,6] and (ii) high enough to ensure technological relevant growth rates on the {10-10} facets for the diameter enlargement [7]. The seed holder design was supported by numerical simulations (Virtual Reactor for AlN, STR GmbH) which finally lead to convex shaped thermal fields (axial temperature gradient 6 – 8K/cm) and corresponding high quality AlN single crystals grown with 130 µm/h to 200 µm/h (Fig. 1).

Dielectric & Wide Bandgap Materials: **Aluminium Nitride**

The crystal enlargement of the AlN single crystals is limited to maximum 1 – 2 mm per growth run. C-plane wafers cut from this AlN single crystals are again used for subsequent growth runs in order to obtain further gradual diameter expansion.

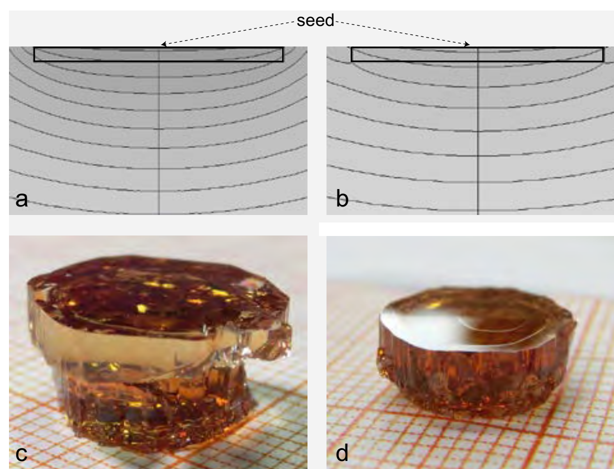

Fig. 1

Comparison of different seed holder designs; (a-b): simulation of the thermal field in front of the seed by ViR for AlN, STR GmbH (1K between isotherms; the axial gradients above the seed interfaces are $\Delta T_Y \sim 8$ K/cm (a) and $\Delta T_Y \sim 6$ K (b); (c-d): corresponding AlN single crystals, (a,c) refer to seed holder design and crystal one, (b,d) refer to seed holder design and crystal two [7].

The structural quality of the grown AlN crystals are analysed by default by x-ray measurements. 0002 and asymmetric 10-13 rocking curves are measured on as-grown N-polar facets with a 4-bounce Ge-220 monochromator attached to the source (Fig. 2). The obtained value of ~11 arcsec for the 0002 reflection corresponds to the resolution function of the instrument and confirms an exceptional good structural quality of the analyzed sample except in regions where sub-grains sometimes build the crystal edge.

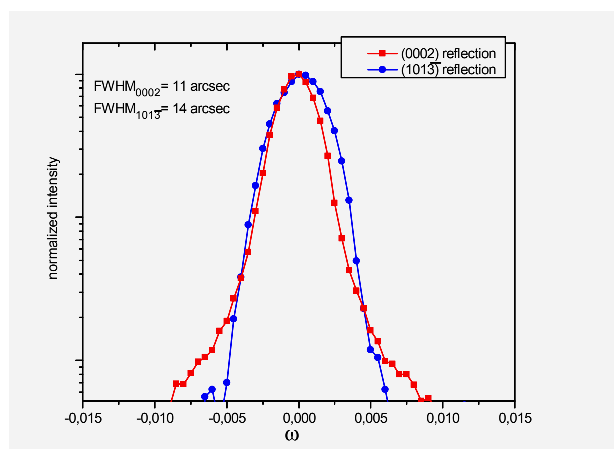

Fig. 2

Rocking curves (semi logarithmic scale) measured with 4-bounce Ge-220 monochromator and open detector aperture over the full as-grown (0001) facet area of AlN crystal two in the 0002 and 10-13 reflection [7].

The sub-grains induces strain, resulting in basal plane dislocations (BPDs) of a-type (b=1/3<1120>) around the sub-grains (characterized by 10-10 topographs). No BPDs occur in the areas distant to the sub-grains. However, threading dislocations (TDs) are observed at low densities in these regions. The square, labeled TD in Fig. 3, was used to estimate the threading dislocation density (TDD) in the wafer, which is around 2×10^3 cm^{-2} in the counting area. By analogy with the BPDs, a significant portion of the TDs disappear in the 10-10 topographs, indicating the threading dislocations are also mainly of a-type. The TDs are inhomogeneously distributed and concentrate in clusters. Large areas in the wafer center appear even free of TDs.

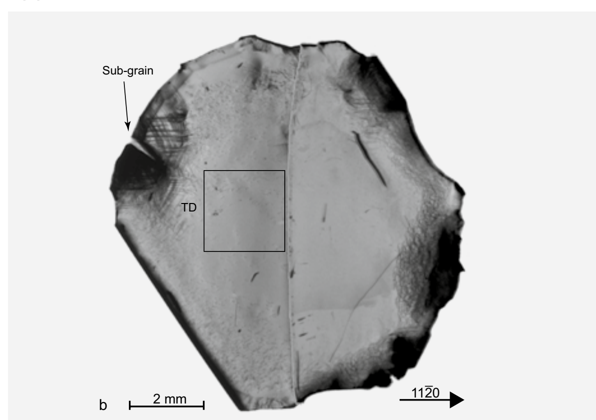

Fig. 3

11-20 transmission X-ray topographs of a c-plane AlN wafer showing sub-grains, basal plane dislocations and threading dislocations; square labeled TD exhibit a threading dislocation density of 2×10^3 cm^{-2} [7].

With a view to the use of AlN wafers as native substrates in deep UV LEDs, the absorption coefficient at the emission wavelength (250 – 280 nm) has to be as low as possible as the UV light is mostly extracted through the substrate. For technical reasons absorption coefficients of $\alpha < 30$ cm^{-1} are desirable at the respective emission wavelength since the best germicidal disinfection is expected for 265 nm.

The deep UV transparency of AlN crystals is mainly controlled by the impurities oxygen and carbon. The major amount of oxygen in the vapour phase at the growth interface is present in form of $Al_2O(g)$ originating from the oxidized fraction of AlN source. The carbon comes from graphite parts in the setup, and from a lesser extent from the TaC crucible as well.

Dielectric & Wide Bandgap Materials: **Aluminium Nitride**

The oxygen and carbon concentrations in the AlN crystals can be actively influenced by facet specific growth, by changing the growth temperature, and finally by the use of impurity getter materials. Due to the best results on the N-polar facet regarding the structural quality as well as the diameter expansion, the N-polar growth facet is fixed in our technology even though lower impurity concentrations and thus potential higher UV transparency are shown at the growth on the Al-polar facet [8]. Beside the growth facet, the growth temperature is another important parameter to increase the deep UV transparency, as it determines volatility and chemical reactivity of the impurity-containing materials. Fig. 4 shows SIMS measurements and absorption spectra at three different growth temperatures T_G.

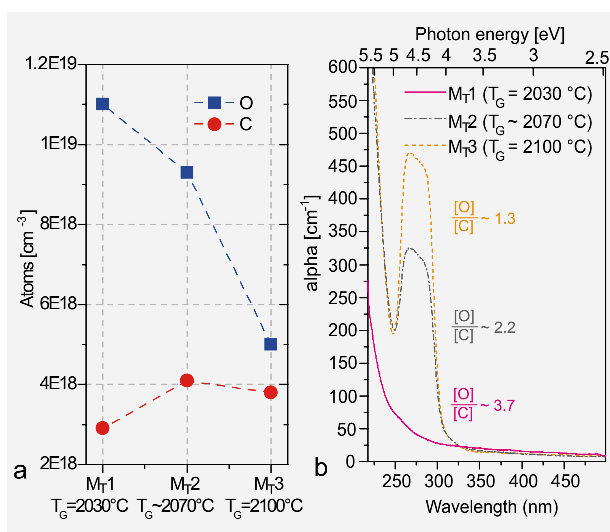

Fig. 4
Carbon and oxygen concentrations (SIMS) in AlN (m-plane cut) grown at different growth temperatures (a) and related (b) absorption spectra [7].

The carbon concentration of about of 3 – 4 x 10^{18} cm^3 is nearly unaffected by the variation of growth temperature from 2030 to 2100 °C.

In contrast, the oxygen concentration decreases from [O] = 11 x 10^{18} cm^3 at T_G = 2030 °C to [O] = 5 x 10^{18} cm^3 at T_G = 2100 °C. A strong UV absorption band at 265 nm is completely quenched at T_G = 2030 °C at [O]/[C] = 3.7. In such areas, the absorption coefficient at 265 nm can be reduced to values around $\alpha_{265\ nm} \sim 50\ cm^{-1}$. At T_G > 2070 °C, the UV absorption band appears.

As already stated above, both carbon and oxygen influence this absorption. For understanding the interrelation in detail, information about defects and their energy levels within the band gap are required. Collazo et al. attributed the broad UV absorption band at 265 nm to carbon on nitrogen site C_N [9]. Irmscher et al. identified a tri-carbon defect complex and showed that this complex contributes to the broad UV absorption band [10]. However, there is not a direct proportionality between the carbon concentration and that absorption, as can be easily identified in Fig. 4b. This behavior has its reason in the influence of oxygen which can be explained by a model, developed by the IKZ group Physical Characterization, that respect the Fermi level position in relation to the charge state transition levels of the carbon defects, which cause deep state acceptors [10]. An upward shift of the Fermi level transfers the carbon related defects into a charge state which is inactive in the UV absorption transition. Such an upward shift of the Fermi level may be accomplished by doping with donor impurities like oxygen or silicon. Oxygen doping may quench the UV absorption when the oxygen concentration exceeds the carbon concentration.

As described above the UV absorption band at 265nm can be quenched in case of [O] $\gtrsim$ 3 [C]. However, there remains absorption that decreases from the band edge to the UV range of interest. We presume that mainly oxygen related defects are responsible for this absorption and it can be decreased by reducing both the oxygen and the carbon concentration while preserving the [O] $\gtrsim$ 3 [C] condition.

The reduction of the oxygen concentration can be achieved by better pre-cleaning of the AlN source material, as $Al_2O(g)$, which evaporates from the AlN source, reveals a substantial partial pressure. Coarse-grained TaC pieces on the top of the AlN source are highly effective by converting $Al_2O(g)$ to CO(g) according the following reaction:

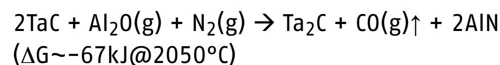
$$2TaC + Al_2O(g) + N_2(g) \rightarrow Ta_2C + CO(g)\uparrow + 2AlN$$
$(\Delta G \sim -67 kJ@2050°C)$

Carbon can be efficiently gettered by adding tungsten sheets inside the TaC crucible which reacts partially to W_2C during the growth.

Using these getter effects of TaC and W, a decrease of the oxygen and carbon concentrations is achieved (M_G1 and M_G2 in Fig. 5). The concentrations are [C] = 1.5x10^{18} cm^{-3} – 2x10^{18} cm^{-3} and [O] < 7x10^{18} cm^{-3}. Fig. 5b shows the corresponding absorption spectra. For the measurements M_T1 (without getter materials) and M_G1 (with getter materials) the [O] $\gtrsim$ 3 [C] condition is met and the 265 nm absorption band is absent. The reduction of the impurity concentrations by the getter materials at M_G1 is the reason for the drastically improved deep UV transmission ($\alpha_{265\ nm} = 14\ cm^{-1}$).

Dielectric & Wide Bandgap Materials: **Aluminium Nitride**

M_G2 shows the lowest total impurity concentration, but in spite of the low carbon concentration of [C] < $2x10^{18}$ cm^{-3}, the deep UV absorption band appear due to [O] < 3 [C], resulting in $\alpha_{265\ nm}$ > 100 cm^{-1}.

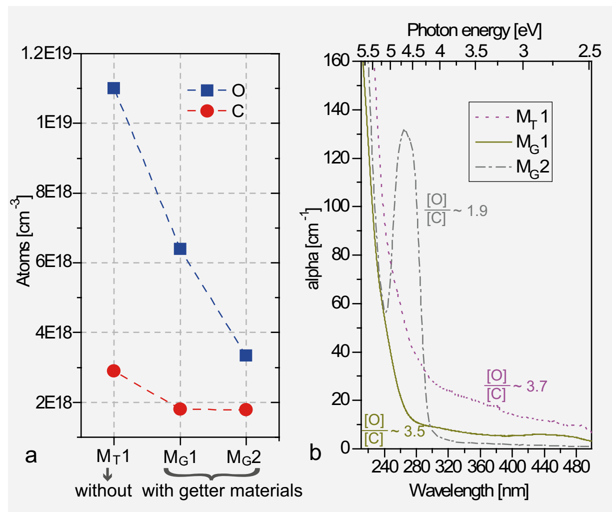

Fig. 5
(a) Carbon and oxygen concentrations (SIMS) in AlN and (b) related absorption spectra in dependence of the use of getter materials TaC and W [7].

We conclude that the requirements of the main impurity concentrations in the crystals in order to achieve a very high deep UV transparency in AlN ($\alpha_{265\ nm}$ < 15 cm^{-1}) must meet the conditions [O] $\gtrsim$ 3 [C] and [C] + [O] < 10^{19} cm^{-3} [7].

Beside the point defect-related issues, a certain kind of more or less macroscopic defect occurs when growing under impurity charged growth conditions. In this case, even observations with the naked eye show an optical phenomenon that resembles as milky diffuse nebula-like structure close to the growth interface and linear structures in the bulk volume of homoepitaxial grown AlN crystals. The latter could be attributed to precipitations decorating dislocations [11,12]. The structural analysis of the decorated dislocations with TEM and SEM revealed particles oriented along <11-20> with sizes between 50 and 400 nm and a commensurate structure. Furthermore, the lattice constants of the unknown particles could be determined via Moiré interference pattern analysis to those of tungsten hemicarbide W_2C. Additionally, WDX and TEM-EDX analysis of the precipitates were accomplished showing high concentration of tungsten and lower concentration of oxygen and carbon.

How exactly the tungsten transport works is a matter of speculation. Tungsten and tungsten carbides have low equilibrium partial pressures and are therefore stable and remain in a solid state over the whole growth process of AlN. But it is reasonable to consider the residual oxygen.

The low evaporation temperature of tungsten oxides and their relatively simple generation already at low temperatures in oxygen containing atmosphere, make them the perfect transport agent for tungsten [13].

A "before and after" investigation of used tungsten sheets of an AlN growth cycle revealed a high difference of the oxygen concentration at the tungsten plates indicating a noticeable amount of oxygen was introduced by the growth atmosphere. Furthermore, as already mentioned above, the AlN source powder and the nitrogen growth atmosphere are also contaminated with trace amounts of oxygen. From the thermochemical point of view, the facts justify the assumption that tungsten transport is realized by oxygen-assisted phases.
It is obviously, that a conflict between preconditions for UVC transparent AlN growth crystals and generation of W-based precipitates exists. When assuming a constant carbon concentration, oxygen control is the key in both cases. A low oxygen level helps to avoid W precipitates. A high oxygen level enhanced the UVC transparency.
The only way to dissolve this contradiction was the well adapted use of getter materials as described above and an upstream purification with different temperature levels to minimize the interaction of volatile oxygen compounds and growth interface. As a result, regular shaped crystals with defined properties for specific applications can be now grown with distinctly enhanced reproducibility (Fig. 6).

Fig. 6
AlN single crystal grown by sublimation/recondensation, maximum 10 mm Ø, diameter enlargement from 8 mm to 10 mm.

Epi-ready AlN wafer were provided to partners in the BMBF funded project "Zwanzig20 – Advanced UV for Life" for device technology development. First results have confirmed the great potential of AlN.

References

[1] Lighting the way perspectives on global lighting market; McKinsey & Company (2012)

[2] C. Hartmann, J. Wollweber, A. Dittmar, K. Irmscher, A. Kwasniewski, F. Langhans, T. Neugut, M. Bickermann; Jpn. J. Appl. Phys. 52 (2013) 08JA06

[3] C. Hartmann, A. Dittmar, J. Wollweber, M. Bickermann; Semicond. Sci. Technol. 29 (2014) 084002

[4] B. Raghothamachar, Y. Yang, R. Dalmau, B. Moody, S. Craft, R. Schlesser, M. Dudley, Z. Sitar; Mater. Sci. Forum 740-742 (2013) 91

[5] R. Dalmau, B. Moody, J. Xie, R. Collazo, Z. Sitar; Phys. Status Solidi A 208 (2011) 1545

[6] F. Langhans, S. Kiefer, C. Hartmann, T. Markurt, T. Schulz, C. Guguschev, M. Naumann, S. Kollowa, A. Dittmar, J. Wollweber, M. Bickermann; Cryst. Res. Technol. 51 (2016) 129 – Reproduced by permission of The Royal Society of Chemistry

[7] C. Hartmann, J. Wollweber, S. Sintonen, A. Dittmar, L. Kirste, S. Kollowa, K. Irmscher, M. Bickermann; CrystEngComm 18 (2016) 3488 – Reproduced with permission of The Royal Society of Chemistry

[8] M. Bickermann, B. M. Epelbaum, O. Filip, P. Heimann, S. Nagata, A. Winnacker; Phys. Status Solidi C 7 (2010) 21

[9] R. Collazo, J. Q. Xie, B. E. Gaddy, Z. Bryan, R. Kirste, M. Hoffmann, R. Dalmau, B. Moody, Y. Kumagai, T. Nagashima, Y. Kubota, T. Kinoshita, A. Koukitu, D. L. Irving, Z. Sitar; Appl. Phys. Lett.100 (2012) 191914

[10] K. Irmscher, C. Hartmann, C. Guguschev, M. Pietsch, J. Wollweber, M. Bickermann; J. Appl. Phys. 114 (2013) 123505

[11] F. Langhans, S. Kiefer, C. Hartmann, T. Markurt, T. Schulz, C. Guguschev, M. Naumann, S. Kollowa, A. Dittmar, J. Wollweber, M. Bickermann; Cryst. Res. Technol. 51 (2016) 129

[12] F. Langhans; *Extended defects in PVT-grown AlN*; PhD thesis; Technische Universität Berlin (2016)

[13] E. Lassner and W.-D. Schubert; Tungsten: Properties, Chemistry, Technology of the Element, Alloys, and Chemical Compounds, Springer US (1999) chap. 3

Layers & Nanostructures

Semiconducting Oxide Layers 64

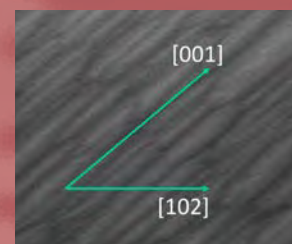

Si/Ge Nanocrystals 70

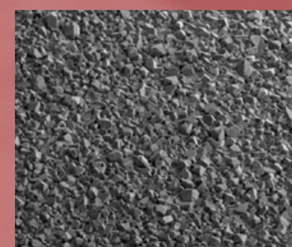

Ferroelectric Oxide Layers 74

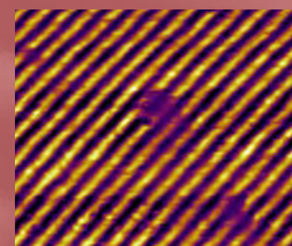

Layers & Nanostructures

Acting head of department: Dr. Günter Wagner

In der Abteilung Schichten und Nanostrukturen werden folgende Fragestellungen bearbeitet:

- *Grundlegende Untersuchungen zur Keimbildung und zu Wachstumsmechanismen*
- *Weiterentwicklung von Beschichtungstechnologien*
- *Entwicklung, Herstellung und Charakterisierung von Schichten und Mikrostrukturen für Anwendungen in der Sensorik, Mikro- und Leistungselektronik, Energiewandlung und für Speicher.*

In Zentrum der Aktivitäten steht der Anspruch, die physikalischen Eigenschaften verschiedener kristalliner Substanzen durch maßgeschneiderte Größe, Form, chemische Zusammensetzung und Verspannungszustand gezielt einzustellen, um neue Anwendungsgebiete zu erschließen.

Folgende Forschungsschwerpunkte wurden in 2015 in den drei Gruppen der Abteilung bearbeitet:

1. *Homoepitaktisches Wachstum von transparenten halbleitenden Oxidschichten: Dies beinhaltet die Entwicklung und Herstellung von β-Ga_2O_3 Schichten auf arteigenen einkristallinen Substraten mit zielgerichteter Abweichung von der (100)-Orientierung und mit (010)-Orientierung sowie Untersuchungen zur kristallinen Perfektion und den elektrischen Eigenschaften in Abhängigkeit von der Substratorientierung. Durch den Einbau von Silicium oder Zinn werden Schichten mit definierter n-Typ Leitfähigkeit und einer hohen Beweglichkeit der Ladungsträger abgeschieden.*
2. *Abscheidung von ferro-/piezoelektrischen bleifreien Oxidschichten: Hierzu zählen ferro-/piezoelektrische $K_xNa_{1-x}NbO_3$ Schichten und Übergitterstruk-turen mit variabler Zusammensetzung (x=0-1), $SrTiO_3$ Schichten, sowie leitfähiges $SrRuO_3$ und $La_{0,7}Sr_{0,3}MnO_3$ als Elektrodenschichten. Durch die Dotierung der $K_xNa_{1-x}NbO_3$ Schichten mit Cu und Sn konnte der Leckstrom in den Schichten reduziert und der piezoelektrische Koeffizient erhöht werden. Zudem erfolgt die Abscheidung auf gitterfehlangepassten Oxidsubstraten (Heteroepitaxie) zum gezielten Einbau von anisotropen Gitterverspannungen. Das Ziel dabei ist es ihren Einfluss auf die ferroelektrische Domänenbildung und das Relaxorverhalten zu untersuchen.*
3. *(1) Wachstum von polykristallinen Siliciumschichten auf Fremdsubstraten, insbesondere auf Glas, mittels selbst entwickelter Züchtungsmethoden zur Kostenreduktion in der Photovoltaik, (2) Wachstum von $Cu(In_xGa_{1-x})Se_2$ (CIGSe) Inseln für Mikrokonzentrator-Solarzellen und (3) Züchtung von Si, Ge und $Si_{1-x}Ge_x$ Nanodrähten durch Molekularstrahlepitaxie (MBE). Diese Arbeiten sind in nationale und europäische Verbundprojekte eingebunden. Schwerpunkte der EU-Förderung sind die Entwicklung neuer Konzepte von Solarzellen mit hohem Wirkungsgrad bei gleichzeitiger Einsparung kostenintensiver Materialien.*

Die Abteilung verfügt über eine sehr moderne, hochwertige Ausstattung:

Metallorganische Gasphasenepitaxie (MOVPE) sowohl für flüssige als auch für gasförmige Precursoren, Molekularstahlepitaxie (MBE), gepulste Laserabscheidung (PLD) und eine selbst entworfene Epitaxieapparatur für die Temperatur-Differenz-Methode (TDM). Zur sofortigen Charakterisierung der Schichten und Mikrostrukturen stehen u.a. folgende Methoden zur Verfügung: Atomkraftmikroskopie (AFM) mit diversen Messoptionen (u.a. Piezoresponse Force Microscopy PFM), taktile Profilometrie und spektrale Ellipsometrie.

The activities at the department „Layers and Nanostructures“ focuse on:

- fundamental investigations on nucleation and growth mechanisms
- development of deposition technologies
- development, growth and characterization of layers and microstructures for applications as sensors and memories, in microelectronics powerelectronics and photovoltaics.

By controlling chemical composition and strain of epitaxial layers as well as size, shape and position of nanostructures, it is possible to tailor the physical characteristics to open up novel applications.

The department consists of three groups, which performed the following research activities in 2015

1. Epitaxy of transparent semiconducting oxides.
   This includes deposition of β-Ga_2O_3 layers on native single crystalline substrates with an exact misorientation from (100) lattice direction and on (010) oriented substrates and the dependence of structural and electrical properties of the layers on the lattice orientation. By doping with silicon or tin, the tuning of n-type conductivity and free carrier mobility is a main task.

2. Deposition of ferro-/piezoelectric lead free oxide layers
   The research tasks focus on ferro-/piezoelectric $Na_xK_{1-x}NbO_3$ layers and superlattice structures with variable composition (x=0-1), deposition of $SrTiO_3$ layers and conductive $SrRuO_3$ and $La_{0.7}Sr_{0.3}MnO_3$ as conductive layers. Another topic is the deposition on lattice mismatched oxide substrates (heteroepitaxy) for targeted adjustment of lattice strain and investigation of the influence of the layers’ functional properties.

3. In the third group three topics are under investigation:
   (1) The growth of polycrystalline silicon layers on low cost substrates preferentially on glass by an in-house developed growth technique, (2) the deposition of indium droplets as precursors for the development of $Cu(In_xGa_{1-x})Se_2$ (CIGSe) micro-concentrator solar cells, and (3) the MBE growth of Si, Ge and $Si_{1-x}Ge_x$ compound nanowires. Joint projects funded by the European Commission promote these activities largely. These projects aim for the development of advanced photovoltaic technologies enabling higher efficiency of solar cells and a cost reduction by minimising the consumption of expensive raw materials.

The department has an excellent infrastructure for the deposition and characterization of epitaxial layers and nanostructures:

Metal-Organic Vapour Phase Epitaxy systems for both, liquid and gaseous precursors, Molecular Beam Epitaxy, Physical Vapour Deposition, Pulse Laser Deposition and in-house designed Temperature Difference Method to grow thin films. A variety of methods for the immediately characterization of the layer properties are available: Atomic Force Microscopy at two state-of-the-art AFM devices enabling a variety of measuring options (e.g. Piezoresponse Force Microscopy PFM), Contact Stylus Profilometry and spectral Ellipsometry.

Layers & Nanostructures:
Semiconducting Oxide Layers

Head Dr. Günter Wagner
Team Dr. M. Baldini, Dr. D. Gogova, R. Grüneberg, R. Schewski

Überblick

Die Materialklasse der transparenten oxidischen Halbleiter (TSO) rückt verstärkt in den Fokus einer immer größer werdenden Forschungscommunity. Diese neue Klasse von Halbleitern kombiniert die elektrischen Eigenschaften von Halbleitern mit großen Bandabstand mit der Transparenz von Oxiden. In dieser Materialklasse ist das β-Ga_2O_3 eine der interessantesten Verbindungen. Wegen des großen Bandabstandes von 4,8 eV ist diese Modifikation des Galliumoxids bis in den tiefen UV-Bereich transparent. Wegen seiner physikalischen Eigenschaften wird diesem Material ein großes Anwendungspotential für die Entwicklung von Bauelementen der Leistungselektronik vorausgesagt. Diese könnten sogar die die zurzeit verwendeten SiC- und GaN-Bauelemente in ihren Leistungsparametern übertreffen [1,2]. Der sehr große Bandabstand ist dafür verantwortlich, das die "Baliga figure of merit" für Leistungsbauelemente ein Vielfaches größer als die konventioneller Bauelementen ist und sich daraus eine extrem hohe Durchbruchsspannung von 8 MV/cm errechnet. Dies würde die Prozessierung von Leistungsbauelementen mit einer viel höheren Durchbruchsspannung (V_{br}) ermöglichen. Ein großer Vorteil von Ga_2O_3 für die Bauelementeentwicklung besteht zudem darin, dass für die Epitaxie von Funktionsschichten arteigene Substrate zur Verfügung stehen, da Ga_2O_3-Kristalle durch Standardtechniken aus der Schmelze gezüchtet werden können. SiC und GaN Substrate sind gegenwärtig nicht durch eine kosteneffektive Methode herstellbar, weder mit halbleitenden noch semi-isolierenden Eigenschaften [3,4].

Die Gruppe Halbleitende Oxidschichten im Leibniz-Institut für Kristallzüchtung ist eine von wenigen in der Welt, die die homoepitaktische Abscheidung von β-Ga_2O_3-Schichten mit dem Verfahren der metallorganischen Gasphasenepitaxie (MOVPE) als Schwerpunkt betreibt [5-7]. Bis vor einigen Jahren wurde vorwiegend die Molekularstrahl-Epitaxie (MBE) für die Abscheidung von homoepitaktischen β-Ga_2O_3-Schichten eingesetzt, die für die Prozessierung von Schotty-Dioden und Feld-Effekt-Transistoren verwendet wurden [1,8,9]. Obwohl die MOVPE ein in der Halbleitertechnologie etabliertes Verfahren zur Abscheidung von elektronisch und strukturell hochqualitativen Schichten ist, wurde dieses zur Abscheidung von Ga_2O_3-Schichten bisher selten angewendet. Da das Schichtwachstum bei der MOVPE nahe am thermodynamischen Gleichgewicht erfolgt, ist die Abscheidung von Schichten mit hoher kristalliner Perfektion möglich.

Außerdem ist dieses Epitaxieverfahren wegen des großen Durchsatzes und den flexiblen MOVPE-Systemen, welche bei moderaten Vakuumbedingungen arbeiten, sehr gut für eine Produktion im industriellen Maßstab geeignet.

2014 hat unsere Gruppe demonstriert, dass durch den Einsatz von Indium als oberflächenaktives Element in einer Trimethylgallium-basierten Gasatmosphäre die strukturelle Perfektion der gewachsenen β-Ga_2O_3-Schichten signifikant verbessert werden konnte [6]. Durch den Austausch von Trimethylgallium (TMGa) durch Triethylgallium (TEGa) wurden Ga_2O_3-Schichten mit halbleitenden Eigenschaften abgeschieden [7]. Um ein tieferes Verständnis bei der Interpretation der Ergebnisse zu bekommen und eine weitere Verbesserung der elektrischen und strukturellen Eigenschaften der Epitaxieschichten zu erreichen, konzentrierten sich die Forschungsarbeiten in 2015 auf die folgenden Schwerpunkte: i) Untersuchungen zum Kohlenstoff-Einbau während der Schichtabscheidung, ii) Abscheidung von n-Typ-Ga_2O_3-Schichten mit Silicium als Donator, iii) Untersuchung zu Bildung von Planardefekten und deren Vermeidung, iv) Verwendung von (010) orientierten β-Ga_2O_3 Substraten für die Schichtabscheidung.

Overview

Transparent Oxide Semiconductors (TSOs) are an emerging class of materials, which combine the electrical properties typical of large band gap semiconductors with the high transparency of oxides. Among TSOs, monoclinic β-Ga_2O_3 is one of the most interesting compounds due to a wide band gap (4.8 eV) that makes it transparent to deep-UV wavelengths. The most promising application field of β-Ga_2O_3 is high power device applications, where it is predicted to outperform the leading technology based on SiC and GaN [1, 2]. The ultra-wide bandgap leads to a much larger Baliga's figure of merit for power electronics and to an extremely high calculated field strength of 8 MV/cm. This will, in principle, enable the fabrication of devices with higher breakdown voltage (V_{br}) than their SiC and GaN counterparts. Another key advantage of β-Ga_2O_3 is that native substrates can be fabricated from bulk single crystals that are grown by standard techniques from the melt, while SiC and GaN substrates have to be synthesized by alternative not cost-effective methods. In our institute, high quality bulk crystals of β-Ga_2O_3 are grown by the Czochralski method with both semiconducting and semi-insulating electrical properties [3, 4].

Our group in IKZ is one of the very few in the world working on the growth of homoepitaxial β-Ga_2O_3 layers by metal organic vapour phase epitaxy (MOVPE) [5-7]. Indeed, the homoepitaxy of β-Ga_2O_3 has been performed up to now mainly by molecular beam epitaxy (MBE), leading to the fabrication of Schottky diodes and field-effect transistors [1,8,9]. Although less investigated, MOVPE is a very promising method for the growth of high quality β-Ga_2O_3 layers. By MOVPE epitaxial layers with excellent crystalline perfection are expected, due to growth conditions that are close to the thermodynamic equilibrium. Moreover, this technique is highly suitable for a future mass production, thanks to large deposition areas and more flexible deposition systems working at moderate pressures instead of ultra-high vacuum conditions.

In 2014 we demonstrated the improvement of the structural perfection of β-Ga_2O_3 layers by using indium as a surfactant in trimethylgallium (TMGa)-based growth [6] and the achievement of semiconducting layers by switching the Ga-metalorganic precursor to triethylgallium (TEGa) [7]. In order to more deeply understand the previous results and further improve the crystalline perfection and the electrical properties of β-Ga_2O_3 layers, in 2015 our research work developed through the following main points: i) investigation of C incorporation, ii) alternative n-type doping by Si, iii) study of planar defects and approaches to prevent their formation, iv) growth on (010)-oriented β-Ga_2O_3 substrates.

Investigation of C incorporation

The conductivity in layers grown with TEGa has been attributed to a lower carbon contamination of the layers due to this specific metalorganic precursor in comparison to TMGa, as already pointed out for the growth of GaAs and (In)GaN at growth temperatures similar to ours. Unfortunately, as already observed from preliminary measurements in 2014, the detection of carbon in the layers resulted to be not practicable by SIMS. More in depth experiments have been performed, but a clear signal relative to C profile was never measured, even using two different SIMS systems at RTG Mikroanalyse GmbH Berlin and at Fraunhofer IAF, Freiburg. The explanation for this result appears to be an extremely high reactivity of Ga_2O_3 surface with C, which is collected from the environment of the SIMS chamber and sticks on the surface of the samples.

Alternative n-type doping by Si

In literature, Sn [1, 9] and Si [10, 11] are the most successfully employed dopants for β-Ga_2O_3. Sn^{4+} has an ionic radius of 69 pm, very similar to that one of Ga^{3+} (62 pm), while Si^{4+} is slightly smaller (40 pm). Both dopants form shallow donor levels in β-Ga_2O_3 bandgap and have relatively low formation energy, as calculated by Varley et al. with DFT methods [12], resulting in effective n-type doping. The main difference between Sn and Si is that the first tends to substitute Ga atoms in the octahedral coordination, while Si in the tetrahedral one. From this point of view, the use of Si could be favourable for a more effective doping since it could compete with C, which also prefers the tetrahedral Ga site, decreasing the compensation ratio.

In order to dope with Si, tetraethylorthosilicate (TEOS) was employed as a precursor. By fixing the flow rate of TEGa at $6x10^{-6}$ mol/min, the flow rate of TEOS was varied between $7x10^{-11}$ and $1x10^{-7}$ mol/min in order to explore the whole doping range. Fig. 1 shows the concentration of Si atoms in the layers, obtained by SIMS, versus the TEOS flux. The incorporation of Si increases linearly, over more than three orders of magnitude, with the amount of precursor injected in the reactor, showing a constant incorporation efficiency. In comparison to what observed for Sn-doping, Si from TEOS is incorporated in β-Ga_2O_3 about 10 times less efficiently than Sn from TESn. This means that in order to incorporate in the layers a given amount of dopant, a flux of TEOS 10 times higher than that one of TESn has to be used. This behaviour can be attributed to a different efficiency in the decomposition of the precursor molecules at the growth temperature (850 °C) or to a different reactivity of the dopant atoms within β-Ga_2O_3. All the grown layers were electrically conductive, however, an unambiguous Hall effect was measurable only for Si doping concentrations higher than 2×10^{18} cm^{-3}. The resulting electron concentration *n* versus the Sn incorporation is plotted in Fig. 2. In the Sn doping range from 2×10^{18} cm^{-3} to 2×10^{20} cm^{-3} the electron concentration increased only from 1×10^{18} to 5×10^{18} cm^{-3}. This indicates a considerable compensation ratio and/or an electrically inactive incorporation of Si, namely in interstitial position or in the octahedral Ga site. A similar behaviour was observed in Sn-doping experiments, but in that case the doping could be tuned in a comparable interval width, at half order of magnitude lower carrier concentrations (5×10^{17}–2×10^{18} cm^{-3}). The electron mobility measured in the layers scattered mainly between 15 and 30 cm^2/Vs, in the same range of Sn-doping experiments.

Since the observed relatively low doping efficiency for both Si and Sn is likely mainly due to the presence of planar defects in the layers, the specific role of these crystallographic defects on the electrical properties of our samples was studied in detail.

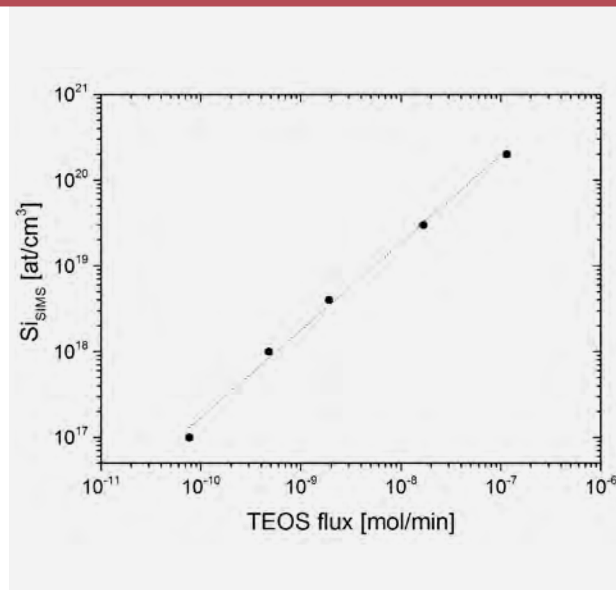

Fig. 1
Si concentration obtained by SIMS vs. TEOS flux for homoepitaxial β-Ga_2O_3 layers

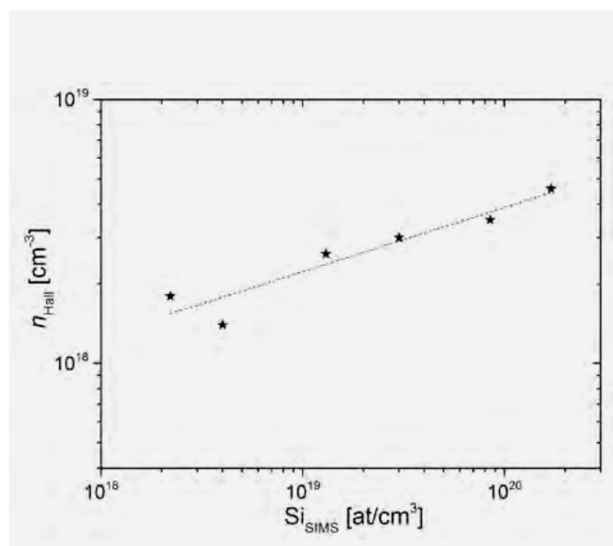

Fig. 2
Free carrier concentration obtained by Hall vs. Si concentration (SIMS)

Study of planar defects and approaches to prevent their formation

The structure of the epitaxial β-Ga_2O_3 layers was investigated by TEM. As shown in Fig. 3, the main defects were identified as stacking faults and twin lamella parallel to the (100) plane, crystallographically described by a *c*/2 glide reflection. At the intersection on the *c*-plane between the two different crystalline orientations, incoherent boundaries are present, involving the formation of dangling bonds. These are thought to act as traps and scattering centres for charge carriers, increasing the compensation ratio and decreasing the mobility of electrons through the material. A more detailed model is presented in the Physical Characterization section of this report.

The stacking defects are the result of the growth of 2D islands that form independently of each other in epitaxial and twin-related orientation relationship. This mechanism, well known in literature for the formation of twins, is named double positioning. However, double positioning per se is not the only cause of defect formation, which is primarily ascribable to a limited diffusion length of the atomic species at the growth interface that hinders a step-flow growth mode. The latter would allow an ideal growth mechanism that involves nucleation only at the kinks on the substrate surface resulting in the reproduction of the β-Ga_2O_3 lattice periodicity. A higher growth temperature could be a suitable solution to increase the diffusion length of the adatoms, but at the same time it would increase the desorption rate of adatoms from the surface, resulting in a further decrease of the growth rate. We then investigated two alternative approaches to improve the growth mechanism of β-Ga_2O_3 layers, namely the use of In as a surfactant and the growth on misoriented substrates.

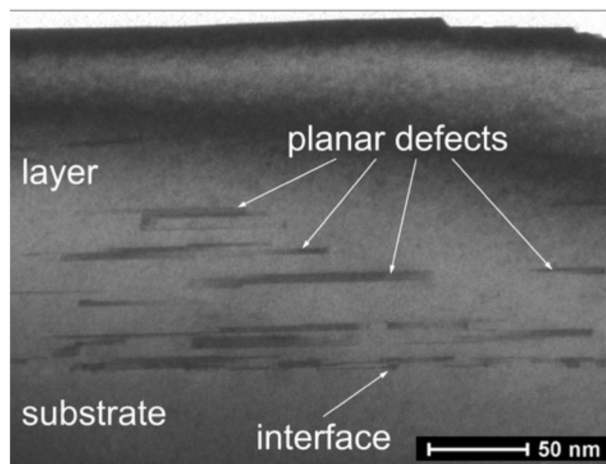

Fig. 3
Bright field TEM image showing the presence of planar defects in the layers grown by TEGa and O_2 on (100) substrates

In as a surfactant

In TMGa-based growths, the injection in the reaction chamber of TMIn, together with TMGa and H_2O, revealed to exert a beneficial effect on the growth of layers with improved crystalline perfection through the surfactant effect of a liquid In layer on the surface of the substrate [6]. We then tried the same approach in the growths with TEGa and O_2. However, the simple addition of TMIn to the best growth conditions previously identified, resulted in no layer growth at all. The same happened by changing experimental parameters as growth temperature, reactor pressure and precursor flow rates in a wide range. This issue can be explained by an extremely strong reactivity of TMIn molecules or In atoms with O_2, as already observed in the growth of mixed $(Ga_{1-x}In_x)_2O_3$ layers on sapphire by TMGa, TMIn and O_2 [13]. In this way, no oxygen atoms are anymore available for the growth of β-Ga_2O_3 layers. In order to solve this issue, different flow rates of H_2O were added to those of TEGa, TMIn and O_2. In this case, layers were properly grown, but the growth rate was halved. The surface of the layers presented similar features to those grown with TMGa, with large terraces parallel to the *b*-axis, typical of step bunching (Fig. 4a). By TEM, however, stacking defects were still observed, but with a more elongated shape along the *c*-axis, as shown in Fig. 4b. By Hall effect the layers resulted to be insulating, pointing out a possible detrimental effect of H_2O on the electrical conductivity of the layers. These results clearly demonstrate that the use of TMIn to reduce the concentration of planar defects in samples grown by TEGa is not effective. Nevertheless, in the near future it would be interesting to investigate whether the surfactant effect could be successfully exploited by using an alternative In-precursor as, for example, TEIn.

Growth on (100) misoriented β-Ga_2O_3 substrates

The use of misoriented substrates aims to improve the crystal quality of the layer not by increasing the diffusion length of the adatoms, but by reducing the terrace width of the substrate. For adatom diffusion lengths lower than the substrate terrace width the growth proceeds with the nucleation of 2D islands that through double positioning can lead to the formation of twins. By increasing the miscut angle of the substrates, on the other hand, the terrace width decreases so that the diffusion length can be long enough to trigger an optimized step-flow mechanism. If the miscut angle is too high, however, step bunching may occur and leave large terraces behind that may promote 2D island formation in turn.

For the first time, the effect of the substrate misorientation on the formation of stacking defects in layers grown by MOVPE was investigated for substrates with random miscut angles lower than 1.5°. By TEM analysis, it was observed that the defect density in the layers decreased systematically for higher off-orientation of the substrates. In the last part of the year, a second set of experiments was carried out on substrates with higher miscut angles, up to 6°, in order to identify the optimal misorientation angle for our specific growth process. The investigation of these samples is still in progress and will be completed in the first part of 2016. A comprehensive study of the influence of the substrate misorientation on the defect concentration of the layers is described in the Electron Microscopy section of this report.

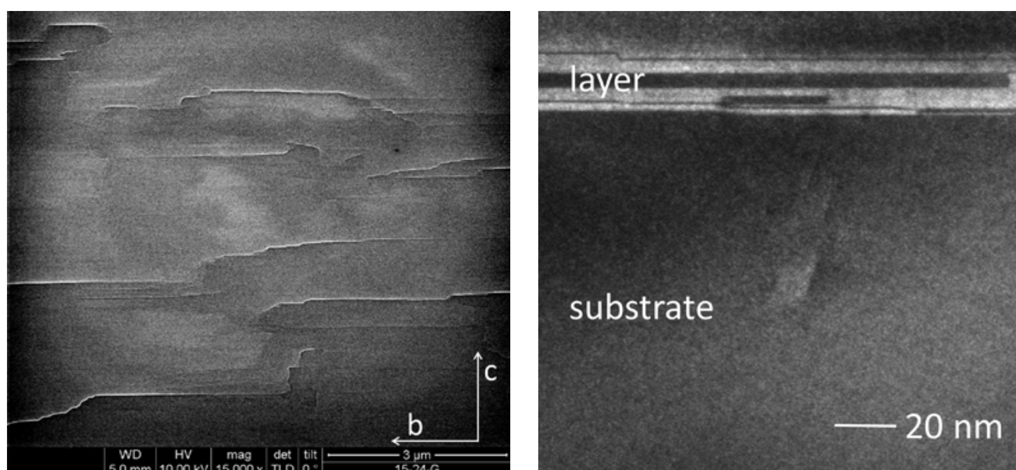

Fig. 4

a) Characteristic SEM image of the surface of layers grown with TEGa, TMIn, O2 and H2O.

b) TEM image of the sample reported in Fig.4 a. Elongated stacking defects are clearly visible.

Growth on (010)-oriented β-Ga_2O_3 substrates

Since the double positioning of Ga and O atoms only occurs on (100) β-Ga_2O_3 surfaces, the growth on alternative substrate orientations, as the (010)-one, looks promising in order to obtain defect-free layers. Moreover, the thermal conductivity along [010] direction is two times higher than along [100], making layers grown on (010)-oriented substrates more suitable for the fabrication of high power devices, where the heat management is a key aspect for high performances. On the other hand, the preparation of (010) wafers is more challenging from a technological point of view, since the (010) plane is not cleavable, contrarily to the (100) and (001) ones. The wafers have then to be cut out from the bulk crystals leading to a higher risk of material loss by undesired cleavages.

With these motivations, in the last part of 2015 a set of growth experiments on (010) β-Ga_2O_3 substrates was performed. By using the same set of experimental parameters optimized for (100)-growth, smooth monocrystalline layers, with typical RMS roughness of ~1 nm, were obtained. The surface of the layers presented a peculiar pattern with elongated islands parallel to the [001] direction, as shown in Fig. 5. The dopant (Sn) incorporation was measured by SIMS and revealed to be one order of magnitude lower than in (100)-oriented layers, showing a reduced incorporation efficiency of Sn on the (010) β-Ga_2O_3 surface (Fig. 6). From SIMS depth profiles was also extracted the film thickness, pointing out a growth rate 20% higher than on (100) substrates. This result differs significantly from what reported in the literature for MBE growths, where the growth speed on (010) was ten times higher than on (100), making the first orientation much more interesting of the second one [11]. The crystal perfection of the layers, characterized by TEM analysis, resulted to be dramatically improved a shown in Fig. 7. No planar defects were formed, because of double positioning on the (010) surface, and a perfect lattice continuity at the substrate-layer interface was observed. The effect of the improved crystal quality of the layers on their electrical properties was studied by C-V measurements, since Hall effect was not measurable due to the high conductivity of the substrates. Very preliminary data are reported in Fig. 8, where a strongly reduced compensation ratio in comparison to (100) layers is observable. As a result of these very promising results, a much more accurate investigation of layers grown on a set of semi-insulating (010) substrates is planned for the beginning of 2016.

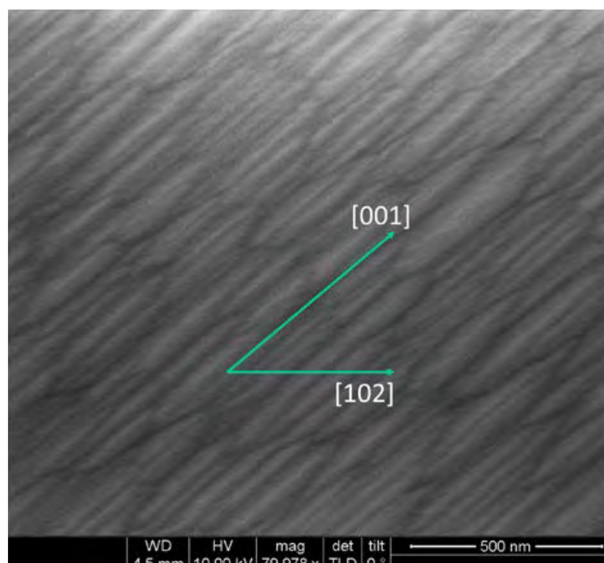

Fig. 5
Typical SEM image of homoepitaxial β-Ga_2O_3 layers grown on (010)-oriented substrates

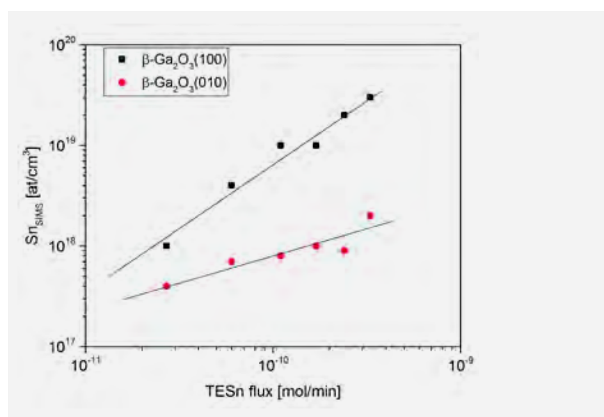

Fig. 6
Comparison between Sn incorporation (SIMS) vs. TESn flux for layers grown on (100) and (010) substrates

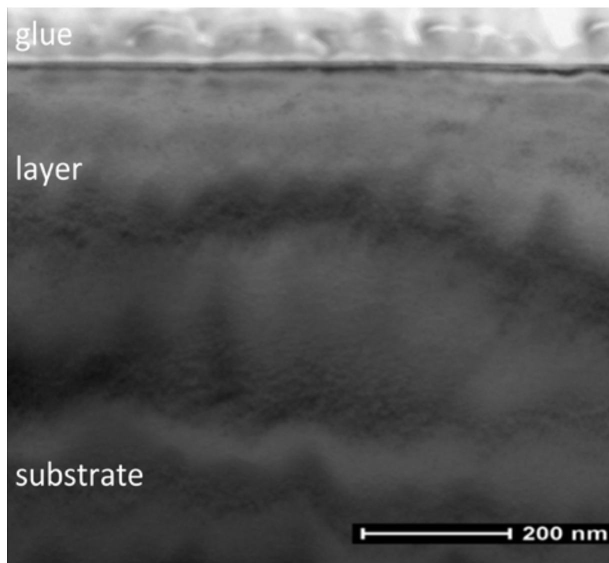

Fig. 7
Typical bright field TEM image of layers grown on (010)-oriented substrates. No planar defects are visible

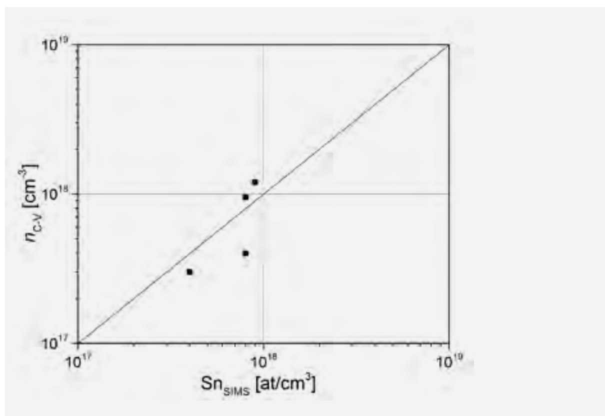

Fig. 8
Free carrier concentration obtained by C-V vs. Sn concentration (SIMS) for layers grown on (010)-oriented substrates

References

[1] M. Higashiwaki, K. Sasaki, A. Kuramata, T. Masui, S. Yamakoshi; Appl. Phys. Lett. 100 (2012) 013504

[2] M. Higashiwaki, K. Sasaki, H. Murakami, Y. Kumagai, A. Kuramata, T. Masui, S. Yamakoshi; Semicond. Sci. Technol. 31 (2016) 034001

[3] Z. Galazka, R. Uecker, K. Irmscher, M. Albrecht, D. Klimm, M. Pietsch, M. Brutzam, R. Bertram, S. Ganschow, R. Fornari; Cryst. Res. Technol. 45 (2010) 1229

[4] Z. Galazka, K. Irmscher, R. Uecker, R. Bertram, M. Pietsch, A. Kwasniewski, M. Naumann, T. Schulz, R. Schewski, D. Klimm, M. Bickermann; J. Cryst. Growth 404 (2014) 184

[5] G. Wagner, M. Baldini, D. Gogova, M. Schmidbauer, R. Schewski, M. Albrecht, Z. Galazka, D. Klimm, R. Fornari; Phys. Status Solidi A 211 (2013) 27[6] M. Baldini, M. Albrecht, D. Gogova, R. Schewski, G. Wagner; Semicond. Sci. Technol. 30 (2015) 024013

[7] M. Baldini, M. Albrecht, A. Fiedler, K. Irmscher, R. Schewski, G. Wagner; J. Mater. Sci. 51 (2016) 3650

[8] M.-Y. Tsai, O. Bierwagen, M. E. White, J. S. Speck; J. Vac. Sci. Technol. A; 28 (2010) 354

[9] K. Sasaki, M. Higashiwaki, A. Kuramata, T. Masui, S. Yamakoshi; J. Cryst. Growth 392 (2014) 30

[10] E. G. Víllora, K. Shimamura, Y. Yoshikawa, T. Ujiie, K. Aoki; Appl. Phys. Lett. 92 (2008) 202120

[11] K. Sasaki, M. Higashiwaki, A. Kuramata, T. Masui, S. Yamakoshi; Appl. Phys. Express 6 (2013) 086502

[12] J. B. Varley, J. R. Weber, A. Janotti, C. G. Van de Walle; Appl. Phys. Lett. 97 (2010) 142106

[13] M. Baldini, D. Gogova, K. Irmscher, M. Schmidbauer, G. Wagner R. Fornari; Cryst. Res. Technol. 49 (2014) 552

Layers & Nanostructures: **Si/Ge Nanocrystals**

Head Dr. Torsten Boeck
Team R. Bansen, Dr. K. Böttcher, C. Ehlers, K. Eylers, Dr. F. Ringleb, Dr. J. Schmidtbauer, H.-P. Schramm, Dr. T. Teubner

Überblick

Die Gruppe befasst sich mit drei Forschungsthemen: (1) Züchtung von polykristallinen Siliciumschichten auf kostengünstigen Substraten, insbesondere auf Glas (2) Wachstum von $Cu(In_xGa_{1-x})Se_2$ (CIGSe) Inseln für Mikrokonzentrator-Solarzellen und (3) Züchtung von Si, Ge und $Si_{1-x}Ge_x$ Nanodrähten durch Molekularstrahlepitaxie (MBE).

Die Arbeiten sind zum überwiegenden Teil projektfinanziert. Das EU-Projekt CHEETAH fördert mit zwei sogenannten Work Packages sowohl die Züchtung von polykristallinen Si-Schichten auf dünnen Folien aus reorganisiertem, porösem Silizium und auf Glas (1) als auch die Materialforschung zu CIGSe-Mikrokonzentrator-Solarzellen (2). Schwerpunkte der EU-Förderung sind die Entwicklung von Solarzellen mit hohem Wirkungsgrad und die Kostenreduktion durch Materialeinsparung. Die Gruppe ist engagiert in weiteren Arbeitspaketen des EU-Projektes, so bei der europäischen Nachwuchsförderung und beim Aufbau eines Netzwerkes zu langfristigen Kooperationsbeziehungen.

Grundlagenorientierte Forschung wird zu den Themen (1) und (2) im Rahmen der durch die Deutsche Forschungsgemeinschaft (DFG) geförderten Projekte „Lösungsmittelinduzierte Phasenumwandlung von kristallinen Siliciumschichten" und „Lokal gewachsene $Cu(In,Ga)Se_2$-Mikroinseln für Konzentratorsolarzellen" betrieben.

Abgeschlossen wurde ein Verbundprojekt zum Thema (3), MBE-Wachstum von Si, Ge- und SiGe-Nanodrähten, mit der Abteilung „Physik der Halbleiter und Mikroelektronik" der Staatlichen Universität Jerewan (YSU) und dem Paul-Drude-Institut für Festkörperelektronik (PDI), das durch das Bundesministerium für Bildung und Forschung (BMBF) gefördert wurde.

Bei allen Forschungsthemen gibt es gute nationale und internationale Kooperationsbeziehungen. Genannt seien das Fraunhofer Institut für Solare Energiesysteme Freiburg (ISE), das Helmholtz-Zentrum Berlin (HZB), die Bundesanstalt für Materialforschung und -prüfung (BAM), das Interuniversity Microelectronics Centre (IMEC), Belgien, SINTEF Energy Research, Norwegen sowie Centro Ricerche ENEA di Portici, Italien. Nachwuchswissenschaftler, Doktoranden und Studenten haben einen sehr großen Anteil an allen Forschungsergebnissen.

Im Berichtszeitraum waren zwei Postdocs, drei Doktoranden und zwei Master- bzw. Bachelor-Studenten an den Arbeiten beteiligt. Bewilligt wurde auch ein DFG-Stipendium für einen 6-monatigen Forschungsaufenthalt eines jungen Wissenschaftlers am Center for Nanoscience at Lund University in Schweden (NanoLund).

Overview

The group's work is focused on three research topics: (1) growth of polycrystalline silicon layers on low-cost substrates, particularly on glass, (2) growth of $Cu(In_xGa_{1-x})Se_2$ (CIGSe) islands for micro-concentrator solar cells, and (3) growth of Si, Ge and Si-Ge nanowires by molecular beam epitaxy (MBE).

The research is mainly financed by project funding. In two work packages, the EU project CHEETAH supports research on the growth of polycrystalline Si-layers on thin foils made of reorganized, porous silicon and on glass (1), and the material research on CIGSe micro-concentrator solar cells. Emphasis of this European project is the increase of solar cell efficiencies and cost reduction by the development of material saving cell concepts. The group is also engaged in further aspects of this project, such as the promotion of young scientists and the intensification of European networks and cooperations.
Fundamental research on the topics (1) and (2) is carried out within the framework of two projects funded by the German Research Association (DFG): "Solvent-induced phase transformation of crystalline silicon layers", and "Locally grown $Cu(In,Ga)Se_2$ micro islands for concentrator solar cells".

A joint project on topic (3), MBE growth of Si, Ge, and SiGe nanowires, has been finished in cooperation with the department of physics of semiconductor and microelectronics of Yerevan State University (YSU), and with the Paul-Drude-Institut für Festkörperelektronik (PDI). It was funded by the Federal Ministry of Education and Research (BMBF).

In all three research topics, the group is embedded in a national and international network of cooperation. This includes the Fraunhofer Institute for Solar Energy Systems (ISE), the Helmholtz-Zentrum Berlin (HZB), the Federal Institute for Materials Research and Testing (BAM), the Interuniversity Microelectronics Centre (IMEC), Belgium, SINTEF Energy Research, Norway as well as the Centro Ricerche ENEA di Portici, Italy.

Postdocs, PhD students, as well as graduate and post-graduate students contributed significantly to the scientific results. Within the report period, two post-docs, three PhD students, as well as one postgraduate and one graduate student carried out research in the group. To one of the postdocs, the DFG provided funding for a 6-month research period at the Center for Nanoscience at Lund University in Sweden (NanoLund).

Results

Silicon on glass

In this research topic we investigate the growth of polycrystalline silicon on glass at low temperatures from metallic solutions in a two-step growth process.

In the first process step, nanocrystalline Si (nc-Si) films are formed at temperatures in the range of 230 °C to 450 °C, either by direct deposition on heated substrates, or by metal-induced crystallization (see Fig. 1).

In the former case, small nanocrystallites form and expand into larger crystallites during further Si deposition. In the latter case, an in-plane movement of liquid metallic solvent droplets on an amorphous Si film is accompanied by precipitation of crystalline Si, a process we refer to as amorphous-liquid-crystalline (ALC) transition. For the direct deposition on heated substrates, characterization by TEM showed that there is no homogeneous nanocrystalline layer, but that the layer is in fact composed of individual seeds, embedded in a quasi-amorphous matrix. The ALC process has been investigated and successfully applied with tin as the solvent, after indium had been used for this purpose before. The oxidation of the seed layers prior to the second process step was found to be a major obstacle. To overcome this issue, a UV laser system has been developed and installed. First promising results show unobstructed epitaxial growth where the oxide has been removed.

In the second process step, the seed layers serve as templates for the growth of significantly larger Si crystallites by means of steady-state solution growth. In contrast to common liquid phase epitaxy, the supersaturation in front of the seed layer is established by a stationary temperature difference between a Si source and the substrate. Micrometer-sized Si crystallites with low impurity concentrations are grown by this technique.

Steady-state solution growth on ALC seed layers was found to start from a few larger seed crystals, and then cover the surrounding areas by lateral overgrowth. Although crystallites with sizes of up to 50 µm were obtained, it was not yet possible to achieve full surface coverage with a continuous layer [1]. By solution growth on nc-Si seed layers, however, it was eventually possible to achieve this goal. Continuous, polycrystalline Si layers were grown, on which all Si crystallites are interlocked (see Fig. 2). All formerly amorphous parts in the seed layer have crystallized, and the impurity concentrations stay well within the specifications for solar grade silicon. The growth experiments were accompanied by 3D simulations. Different heater configurations have been simulated, in which the top and side heater configuration produced the steadiest temperature gradients. It also produced the best experimental growth results so far (see Fig. 3). The influence of geometric variations in the growth setup has also been simulated, and changes in the solvent fill height were found to have a profound impact on both temperature and convection in the crucible.

In addition to the growth on glass substrates, the steady-state solution growth technique is also used for epitaxial thickening of thin foils of reorganized porous Si, produced from thick monocrystalline Si wafers at IMEC, Belgium within the scope of the EU CHEETAH project. The wafers are first porosified by dry etching through a hard mask, fabricated using deep ultraviolet lithography, and then annealed at temperatures around 1150 °C, which leads to a restructuring of the porous Si so that a detachable layer forms.

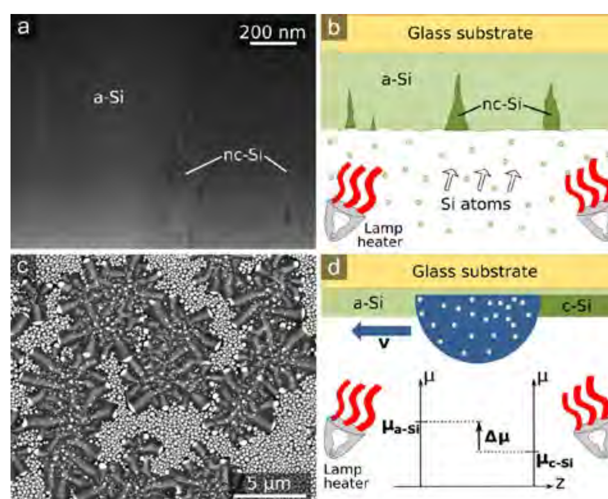

Fig. 1
(a) TEM cross-section image showing nc-Si seeds in an otherwise amorphous layer.
(b) Growth scheme for the nc-Si layers as seen in image a.
(c) SEM micrograph of the ALC process with tin.
(d) Growth scheme for the ALC layers as seen in image c.

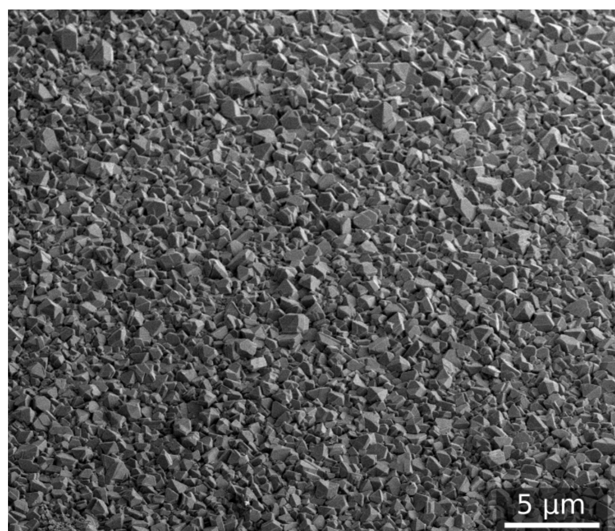

Fig. 2
Tilted view SEM micrograph of a contiguous polycrystalline Si layer on glass.

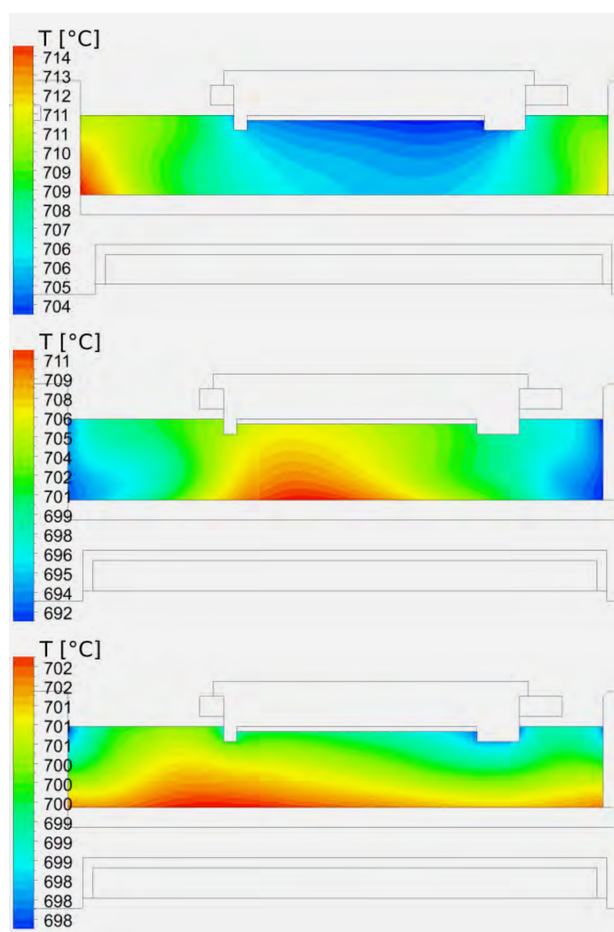

Fig. 3
3D simulation comparing different heater configurations and their influence on the growth temperature regime.
Three main configurations were simulated for an indium solution: (a) top and side heater, (b) top and bottom heater, (c) top, bottom and side heater.

CIGSe Microconcentrator Solar Cells

Cu(In,Ga)Se_2 (CIGSe) is a highly efficient direct absorber used in thin film photovoltaics (current cell efficiency record: 22.3 % [2]). Due to ongoing research on optimizing the performance, the record efficiencies for cells and modules keep continuously rising, which demonstrates, that the potential of this material is still not fully exploited. Still, to keep up and expand the current market share, pushing the efficiency further is key. Furthermore, indium, which is a constituent of this compound material, is highly demanded not only for PV, but also other applications, such as LEDs and transparent conduction oxides. These aspects motivate the groups work on a new CIGSe type of solar cell, which is based on a micro-concentrator design. Concentrator solar cells allow to increase the efficiency and save material at the same time. While macroscopic concentrators suffer from heat accumulation and therefore reduced efficiency and lifetime, micro-concentrators allow for better heat dissipation and furthermore for a compact module design. In proof-of-concept studies on CIGSe microcells prepared by lithography, an absolute efficiency enhancement of up to 5 % has been reached [3]. For saving material, however, the microcells have to be grown locally and in an ordered, well-defined fashion in a bottom-up process.

The group works on the development of such a process, which is based on the preparation of flat indium islands grown on a molybdenum-covered glass substrate by physical vapor deposition. These islands are used as precursors and can up to now be further processed to $CuInSe_2$ microabsorbers. Local substrate roughening by femtosecond laser pulses induces a strong preference of indium island nucleation at the predefined spots and allows thus to grow the islands in ordered arrays. This year's work was focused on the in-depth investigation of the optimization of the patterning morphology and spacing. It was shown that it is of importance to roughly match the pattern spacing to the intrinsic nearest neighbor distance of islands on non-patterned substrates (see Fig. 4). Furthermore, a variation of the femtosecond laser parameters showed that a moderate surface roughening was sufficient to induced the preferential island nucleation, whereas stronger surface roughening lead to undesired, irregular island morphologies. Regarding the further processing of the indium islands to microabsorbers, parameters such as the Cu-In ratio and the rapid thermal processing step in selenium vapor were greatly improved. The resulting absorbers exhibit now a high purity $CuInSe_2$ phase as shown by XRD with microcrystallites of about 2 µm size – which is common for conventional $CuInSe_2$ films as well (see Fig. 5). In addition, photoluminescence maps showed that also the electro-optical properties of the material are promising, since an emission band of about 1.03 eV, which corresponds to the band gap of $CuInSe_2$, was detected homogeneously all over the islands.

Layers & Nanostructures: **Si/Ge Nanocrystals**

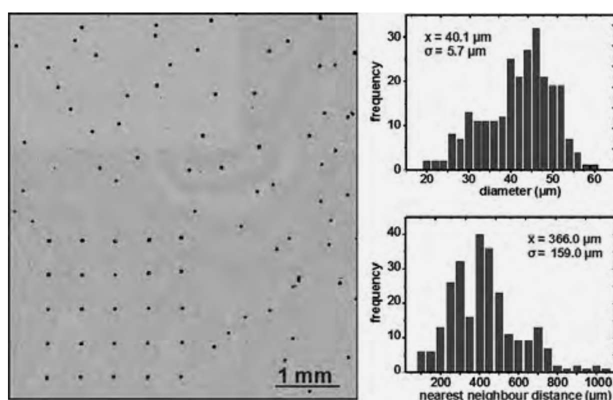

Fig. 4
Left: optical micrograph of indium island growth on partially patterned Mo/glass substrate.
Right: statistical analysis of island diameters and nearest neighbor distances on the non-patterned region of the sample.

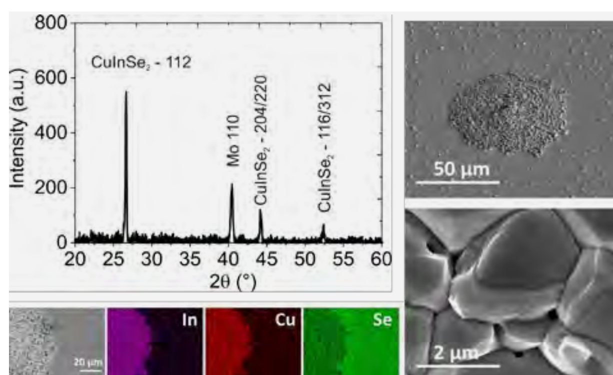

Fig. 5
Characterization of CuInSe2 microabsorber islands, which have been processed from indium precursor islands on a Mo/glass substrate.
Top left: XRD spectrum exhibiting a high-purity $CuInSe_2$ phase.
Bottom left: SEM/EDX maps.
Right: SEM images of an entire absorber island (top) and enlarged detail illustrating the microcrystalline structure.

Silicon and germanium nanowires

Investigation of the MBE growth of Si/Ge nanowires on Si substrates were focused on the suppression of parasitic epitaxial deposition of material on the substrate around the nanowires. The uniform deposition is intrinsically inherent to the applied e-beam evaporation from a solid source. Nevertheless, using oxygen together with silicon at low temperatures after the formation of gold droplets should counteract this tendency. The gold particles defining the growth location of nanowires do not interact with oxygen but selectively solve silicon. In this way, the wire grows under the gold droplet and amorphous SiO_x forms outside the wires on the substrate surface. SiO_x formation under UHV at temperatures of 360 °C requires activated oxygen at partial pressures of about 1×10^{-5} mbar.

For this purpose, an existing oxygen inlet source with thermal activation was qualified for partial pressure control. A motorized leak valve in front of the inlet has been coupled with a quadrupole mass spectrometer (QMS), measuring the mass number 32 within the MBE chamber as an indicator of the oxygen partial pressure. This concept allows precise setting of the oxygen content within the range from 6×10^{-12} mbar to 1×10^{-8} mbar (the working limit of the QMS). Control of higher oxygen contents will be realized in the future. The QMS based control of the Si evaporator has been adapted likewise. Concurrent deposition of Si and O_2 for about 30 min leads to the transition of a clean Si(111) surface to an amorphous SiO_x coverage, as is confirmed by RHEED images, which cease to show crystalline information over the course of the process time (see Fig. 6). If only Si is applied during deposition, an epitaxial Si layer is formed instead, which exhibits the same RHEED pattern as the substrate.
Funded by the German Research Foundation (DFG), a postdoc spent a period of 6 months as a visiting scientist at the center for nanoscience at Lund University in Sweden (NanoLund), where he worked on simulations of the influence of surface diffusion on the length distributions of nanowires.

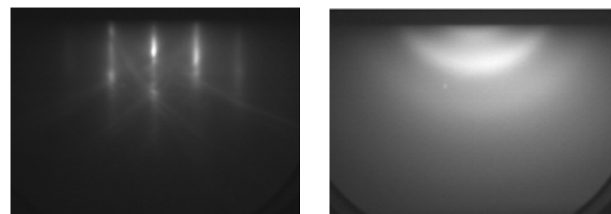

Fig. 6
RHEED images of a Si(111) surface in the MBE system before (left) and after (right) the concurrent deposition of Si and O_2 for about 30 min. An amorphous SiO_x layer forms, which suppresses the crystalline reflexes in the RHEED image.

References

[1] R. Bansen, R. Heimburger, J. Schmidtbauer, Th. Teubner, T. Markurt, C. Ehlers, T. Boeck; *Crystalline silicon on glass by steady-state solution growth using indium as solvent*; Appl. Phys. A 119(4) (2015) 1577

[2] Solar Frontier; *Solar Frontier Achieves World Record Thin-Film Solar Cell Efficiency: 22.3%;* (2015); http://www.solar-frontier.com/eng/news/2015/C051171.html

[3] M. Paire, L. Lombez, F. Donsanti, M. Jubault, S. Collin, J.-L. Pelouard, J.-F. Guillemoles, D. Lincot; *Cu(In, Ga)Se2 microcells: High efficiency and low material consumption*; , J. Renew. Sustain. Ener. 5 (2013) 011202

Layers & Nanostructures: Ferroelectric Oxide Layers

Head Dr. Jutta Schwarzkopf
Team D. Braun, C. Feldt, M. Klann, Dr. J. Sellmann

Überblick

Aufgrund ihrer exzellenten piezo-/ferroelektrischen Eigenschaften sind $K_xNa_{1-x}NbO_3$ basierte Materialien vielversprechende Kandidaten um bleihaltige Ferroelektrika zu ersetzen [1]. Dieser Umstand macht sie für potentielle technische Anwendungen wie akustische Oberflächenwellen-Filter, Mikrowellenbauelemente oder piezoelektrische Sensoren interessant. Um hochwertige $K_xNa_{1x}NbO_3$ Dünnschichten mit exzellenten di-/ferro-/piezoelektrischen Eigenschaften zu erzielen, müssen noch offene Fragen geklärt werden, die im Fokus der Forschung der Gruppe Ferroelektrische Oxidschichten stehen.

Ein Aspekt betrifft die Bildung von monoklinen Phasen, deren Existenz beim Einbau einer anisotropen Gitterverspannung in dünnen Schichten vorhergesagt werden (siehe Phasendiagramm in [2]). Diese ermöglichen außerordentlich gute piezoelektrische Eigenschaften und sind daher erstrebenswert. Der Vorteil liegt darin, dass in monoklinen Domänen die Ausrichtung des Polarisationsvektors nicht auf eine bestimmte kristallographische Achse beschränkt ist, sondern kontinuierlich mittels eines äußeren elektrischen Feldes gedreht werden kann. Infolgedessen kommt es zu einer enormen Verstärkung des piezoelektrischen Signals. Daher war es unser Ziel, eine gezielte anisotrope Gitterverspannung in $K_xNa_{1-x}NbO_3$ Dünnschichten durch geschickte Wahl von Schichtzusammensetzung und Substratmaterial einzubauen, um eben diese monoklinen ferroelektrischen Domänen zu erhalten. Anhand von zwei Beispielen soll im Folgenden die Vielfalt des Materials unter Verspannung gezeigt werden. Die Schichten wurden mit metallorganischer Gasphasendeposition (MOCVD) abgeschieden; die dafür notwendigen metallorganischen Precursor wurden von der Ruhr Universität in Bochum, AG A. Devi, geliefert.

Im zweiten Thema geht es um Fehlstellen von monovalenten Na/K Ionen in $K_xNa_{1-x}NbO_3$ Dünnfilmen, insbesondere wenn die Schichten mit gepulster Laserdeposition abgeschieden werden. Diese können beim Schichtwachstum auf Grund ihrer hohen Flüchtigkeit nicht vollständig vermieden werden. Sie stellen die Hauptursache für den hohen Leckstrom in diesen Schichten dar, der zu verschlechterten ferroelektrischen Eigenschaften führt. Die Dotierung der Schichten mit aliovalenten Ionen wie Kupfer oder Zinn stellt eine Möglichkeit dar, die elektrischen Eigenschaften zu verbessern. In diesem Zusammenhang wurde der Einfluss einer aliovalenten Dotierung auf die elektrischen und strukturellen Schichteigenschaften im Detail untersucht.

In der dritten Fragestellung wurde die Beziehung zwischen Gitterverspannung und Relaxorverhalten in $NaNbO_3$ Schichten umfassend untersucht. Nachdem gezeigt werden konnte, dass Relaxorverhalten in $NaNbO_3$ Schichten, die pseudomorph unter anisotroper Verspannung auf $NdGaO_3$ abgeschieden wurden, induziert werden kann, haben wir unsere Untersuchungen auf eine Schichtdickenserie von $NaNbO_3$ ausgedehnt. Die Ergebnisse wurden innerhalb unserer langjährigen Kooperation mit dem Forschungszentrum Jülich, AG R. Wördenweber, erzielt.

In allen Themen der Gruppe Ferroelektrische Oxidschichten sind Studenten involviert. Im Jahr 2015 wurden die Doktorarbeit von Dr. Jan Sellmann „Impact of strain and composition on structural and piezo-/ferroelectric properties of epitaxial $NaNbO_3$ and $K_xNa_{1-x}NbO_3$ thin films and superlattices grown by PLD" und die Masterarbeit von Philipp Kehne „PLD growth investigations and the influence on ferroelectric properties of $K_xNa_{1-x}NbO_3$ on $DyScO_3$" erfolgreich abgeschlossen.

Overview

$K_xNa_{1-x}NbO_3$ based materials have been shown to be a promising candidate to replace lead-based ferroelectrics due to their excellent piezo-/ferroelectric properties [1]. This make them interesting for potential technical applications like surface acoustic wave, microwave devices, ferroelectric memories or piezoelectric sensors. On the way to prepare high quality $K_xNa_{1x}NbO_3$ thin films with excellent, di-/ferro-/piezoelectric properties, some tasks still arise which are in the focus of research of the group Ferroelectric Oxide Layers.

First, by the incorporation of anisotropic strain the formation of monoclinic phases, providing giant piezoelectric properties, have been predicted (see phase diagram in [2]). In monoclinic domains, the polarization is not restricted to a distinguished crystallographic axis, rather can continuously be rotated by an external electrical field. The aim of this part was to introduce a targeted anisotropic lattice strain in $K_xNa_{1-x}NbO_3$ thin films by the appropriate choice of film composition and substrate material to achieve monoclinic ferroelectric domains. Two different examples will be presented showing the variety of the material. The films were grown by metal-organic chemical vapor deposition (MOCVD); necessary MO precursors have been delivered by Ruhr University of Bochum, WG A. Devi.

Second, due to their high volatility, vacancies of the monovalent Na/K ions cannot fully be avoided during $K_xNa_{1-x}NbO_3$ film growth, especially when films were grown by pulsed laser deposition. They represent the main reason for the high leakage current in these films leading to deteriorated ferroelectric properties. A possibility to improve electric properties is given by doping of $K_xNa_{1-x}NbO_3$ films with aliovalent ions like Cu and Sn. With regard to optimized ferroelectric film properties, influence of aliovalent doping both on electric and structural properties of the films has to be studied in detail.

In the third issue, relation between lattice strain and relaxor behavior in $NaNbO_3$ thin films is extensively investigated. After demonstrating that relaxor behavior can be induced in $NaNbO_3$ films, which were pseudomorphically grown under anisotropically compressive strain on $NdGaO_3$ substrates, we have extended now our investigations to a thickness series of $NaNbO_3$ films. These results have been achieved within our long-term cooperation with Forschungszentrum Jülich, WG R. Wördenweber.

Students have been involved in all topics of the group Ferroelectric Oxide Layers. In 2015, the PhD thesis from Dr. Jan Sellmann "Impact of strain and composition on structural and piezo-/ferroelectric properties of epitaxial $NaNbO_3$ and $K_xNa_{1-x}NbO_3$ thin films and superlattices grown by PLD" and the master thesis from Philipp Kehne "PLD growth investigations and the influence on ferroelectric properties of $K_xNa_{1-x}NbO_3$ on $DyScO_3$" has been successfully finished.

Results

Domain engineering by the application of lattice strain in $K_xNa_{1-x}NbO_3$ films grown by MOCVD

Due to the environmental risk and degradation effects in lead-based oxides, lead-free materials are of very high interest. Challenging, this material class has to prove its possibility as a real alternative in view of a huge piezoelectric response. Therefore, the question is how to adapt the familiar mechanism in order to generate similar properties like the appearance of domains with monoclinic symmetry and the abrupt change of polarization at domain walls leading to piezoelectric singularities in lead-free oxides. Theoretical and experimental studies have revealed that formation of monoclinic domains without a morphotropic phase boundary can be achieved via the application of epitaxial lattice strain, in particular when the in-plane lattice strain is anisotropic (see phase diagram in [2]). At room temperature, the system $K_xNa_{1-x}NbO_3$ exhibits orthorhombic crystal structure, which enables the incorporation of anisotropic epitaxial lattice strain. In view of ferroelectric domain arrangement consisting of monoclinic phases, for a systematic domain engineering we have estimated the elastic strain energy density for $K_xNa_{1-x}NbO_3$ thin films epitaxially grown on different rare-earth scandate substrates in dependence of the potassium content x (due to the phase symmetry of $K_xNa_{1-x}NbO_3$ compounds only x values between 0.5 and 1 have been regarded). Exemplarily, the results for $K_xNa_{1x}NbO_3$ on $NdScO_3$ and $TbScO_3$ substrates are presented in Figs. 1(a) and 1(b), respectively. Owing to the orthorhombic symmetry of both substrate and film material, we have to consider different surface and in-plane orientations of the unit cell of the film. Crucial substrate-film combinations are marked in Figs. 1(a) and (b) by arrows, where the elastic strain energy of the two possible surface orientations are equal or one strain component diminishes, respectively.

Fig. 1
(a) Elastic strain energy density e for $K_xNa_{1-x}NbO_3$ thin films on NdScO3 and

(b) in-plane lattice strain ε_{xx} and ε_{yy} for $K_xNa_{1-x}NbO_3$ thin films on $TbScO_3$, in dependence of the K concentration x.

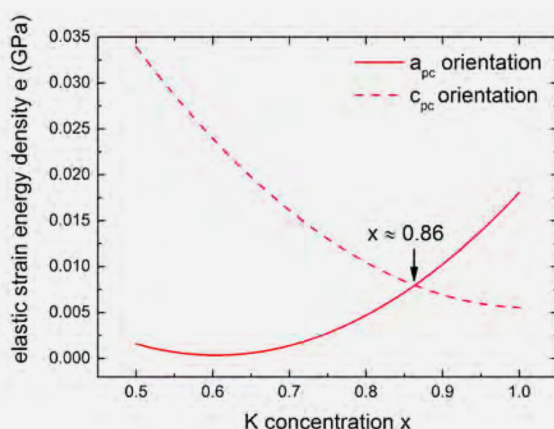

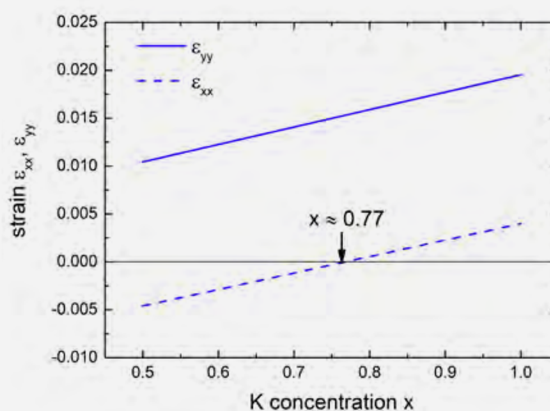

Layers & Nanostructures: **Ferroelectric Oxide Layers**

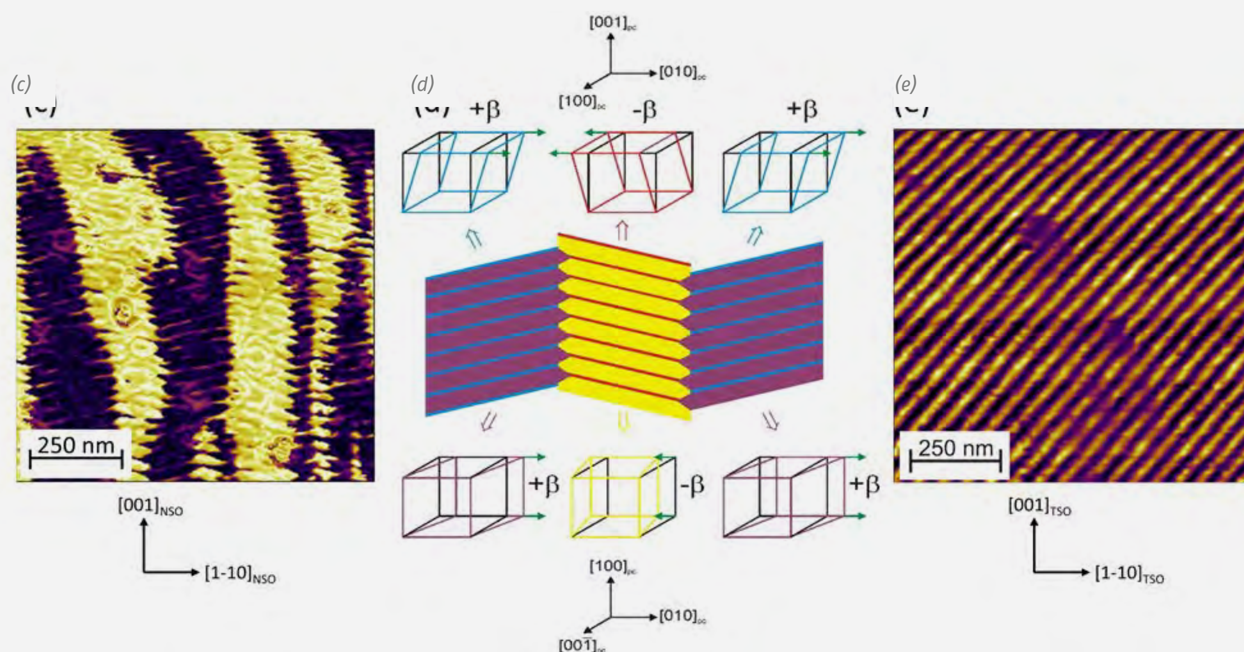

Fig. 1
(c) LPFM phase image of a 29 nm $K_{0.95}Na_{0.05}NbO_3$ thin films on $NdScO_3$
(d) domain model for the arrangement of a_1a_2/M_C domains in $K_{0.95}Na_{0.05}NbO_3$ thin films on $NdScO_3$
(e) VPFM phase image of a 29 nm thick $K_{0.75}Na_{0.25}NbO_3$ thin films on $TbScO_3$

Impacts of these two cases will be illustrated by the following examples:

1. $K_{0.95}Na_{0.05}NbO_3$ films on $NdScO_3$ (NSO): For this substrate-film combination the elastic strain energy density for $(001)_{pc}$ and $(100)_{pc}$ surface orientation is almost equal (the index "pc" denotes the pseudocubic unit cell of the $K_xNa_{1-x}NbO_3$ films). Indeed, experimental results have shown the occurrence of both film orientations. Domain patterns recorded by lateral piezoresponse force microscopy (LPFM) reveal a rather complex ferroelectric domain structure (Fig. 1c). Domains with typical lateral sizes between 50 and 200 nm are formed, which are highlighted by yellow and violet colors in Fig. 1(c). They are tentatively aligned along the $[001]_{NSO}$ direction and separated by characteristic zig-zag domain walls. On the other hand, these domain bundles exhibit a prominent substructure consisting of a highly periodic array of alternating small and large domain widths along the $[001]_{NSO}$ direction. In this direction, the lateral period amounts to about 30 nm and the domain walls are very flat. XRD measurements in combination with PFM and TEM images indicate the periodic formation of monoclinic M_C and a_1a_2 domains (Fig. 1d). Detailed structural information is given in the reports of the groups Electron Microscopy and Physical Characterization. The use of a $SrRuO_3$ bottom electrode (in cooperation with WG B. Noheda at University of Groningen) allows the determination of the piezoelectric coefficient. With d_{33} = 30 pm/V the piezoelectric coefficient is comparable to that of lead-oxide based films with similar film thickness and is attributed to the existence of monoclinic phases in the films.

2. $K_{0.75}Na_{0.25}NbO_3$ films on $TbScO_3$: For x = 0.75 the applied lattice strain in the film is quasi uniaxial, since one in-plane component (ε_{xx} in Fig. 1b) equals almost zero in this composition range. We achieved long-range ordering of well-aligned, ferroelectric stripe domains with a periodicity of a few tens of nanometers by the epitaxial growth of $K_{0.75}Na_{0.25}NbO_3$ thin films on (110) $TbScO_3$ substrates. Our experimental data prove the emergence of monoclinic M_A domains, which are characterized by strong lateral and vertical electric polarization components. This monoclinic phase is stabilized by the incorporation of high compressive lattice strain in $[1\text{-}10]_{TSO}$ in-plane direction and almost vanishing tensile strain in in $[001]_{TSO}$ in-plane direction. The domain walls in $K_{0.75}Na_{0.25}NbO_3$ thin films are almost exclusively arranged in one crystallographic direction ($[112]_{TSO}$) or $[110]_{pc}$), which is mainly attributed to the anisotropic lattice strain and the elastic anisotropy of $K_{0.75}Na_{0.25}NbO_3$ [3].

The presented results on the formation of monoclinic domains in lead-free $K_xNa_{1-x}NbO_3$ films are very promising since they open a feasible pathway towards the exploitation of ferroelectric properties in both vertical and lateral directions and the possibility to achieve enhanced piezoelectric properties similar to those of lead-containing oxide materials.

Doping of $K_{0.5}Na_{0.5}NbO_3$ thin films

Within the framework of a master thesis, PLD growth conditions have been optimized in terms of O_2 partial pressure and total pressure as well as the target-substrate distance to obtain well-ordered, smooth $K_{0.5}Na_{0.5}NbO_3$ thin films. These films have been grown on (110) $DyScO_3$ substrates, which induce compressive in-plane lattice strain to the films. The $DyScO_3$ substrates were covered with 8 nm thick $La_{0.67}Sr_{0.33}MnO_3$ films serving as a bottom electrode for electrical measurements.

Aliovalent doping with Sn and Cu has been performed by addition of small amounts of SnO_2 (nominal 1 at%) and CuO (nominal 1 at%), respectively, to the $K_{0.5}Na_{0.5}NbO_3$ target. After deposition of 25 nm thick films from undoped and doped targets, local hysteresis curves measured by PFM prove the ferroelectric nature of all films due to the circumstance of a successful poling (Figs. 2(a) – (c)). It is obvious, that the hysteresis curves of the doped samples exhibit a significantly steeper slope and larger coercive voltages given by the width of the hysteresis curve. The increase of the coercive voltages indicates a ferroelectric hardening effect. This is suggested to be caused by substituting Cu^{2+} (Sn^{4+}) ions on Nb^{5+} ion sites, since such a B site acceptor doping acts as a trap of oxygen vacancies resulting in the formation of defect complexes and domain pinning. This effect is enhanced for Cu due to its low valence state of 2+ compared to 4+ and 5+ for Sn and Nb ions, respectively.

Owing to the measurement technique in PFM mode using the tip as top electrode instead of macroscopic contacts, no resilient value for the remanence can be obtained. Therefore, for a detailed electrical characterization Ti/Au top contacts have been processed in cooperation with Ferdinand-Braun-Institut, Leibniz-Institut für Höchstfrequenztechnik, Berlin. It turned out that high leakage currents are deduced in the films, which are caused by K and Na deficiencies, impeding the measurement of macroscopic ferroelectric hysteresis curves. From I-U-measurements, we infer almost ohmic behavior for the undoped film due to the high concentration of charge carriers. Indeed, compared to the undoped sample the leakage current could significantly be reduced by Cu and Sn doping (Fig. 2d). In the positive voltage region, Cu and Sn doping results in a reduction of the leakage current by more than one order of magnitude and the slopes has become remarkably asymmetric. This behavior is tentatively explained by the formation of a Schottky barrier with blocking direction at positive voltage. The specific underlying transport mechanisms of doped and undoped films will be clarified in detail in the context of temperature dependent measurement. However, from our first experiments we conclude that aliovalent doping provides a viable way of improving electrical properties in $K_{0.5}Na_{0.5}NbO_3$ thin films.

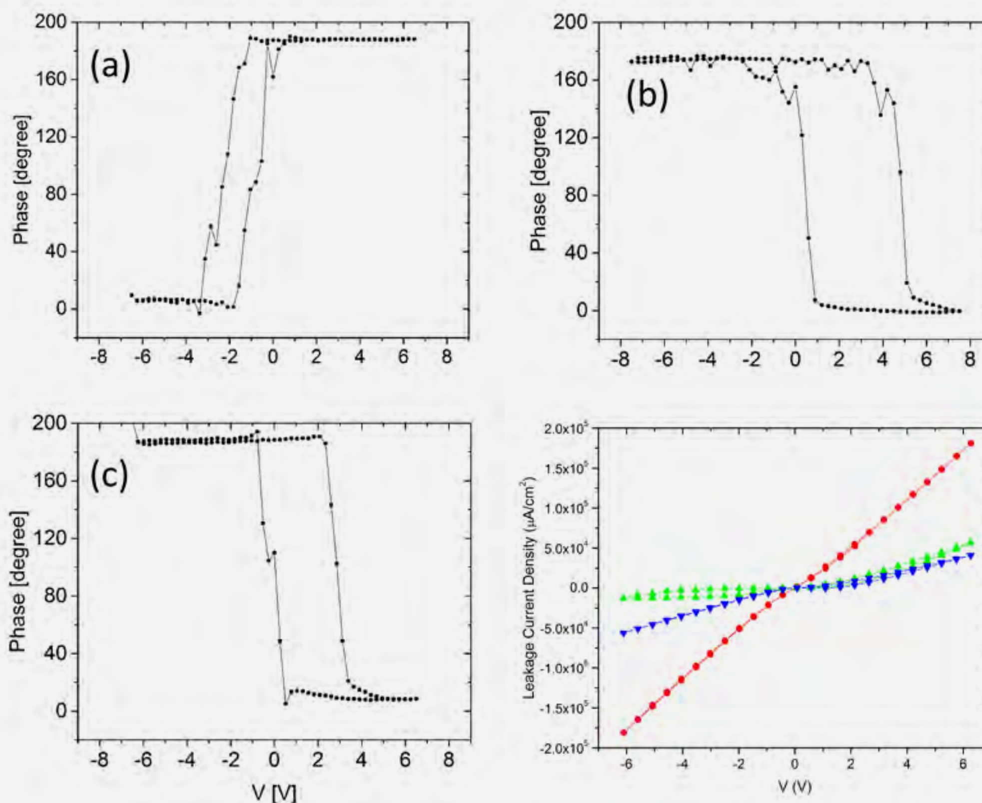

Fig. 2
Local hysteresis curves for $K_{0.5}Na_{0.5}NbO_3$ thin films grown from

(a) an undoped $K_{0.5}Na_{0.5}NbO_3$ target,

(b) a Cu doped target,

(c) a Sn doped target.

(d) I-U measurements for the undoped (red), Cu doped (green) and Sn doped (blue) films.

In-plane dielectric measurements on $NaNbO_3$/$NdGaO_3$ thickness series

Relaxor-type ferroelectrics have recently attracted considerable scientific interest. Their intriguing physics and their potentially high permittivity and tunability provide them in a number of potential applications like tunable microwave devices. In cooperation with Forschungszentrum Jülich, WG R. Wördenweber, we have demonstrated that strained $NaNbO_3$ films of different thickness, epitaxially grown on (110) $NdGaO_3$ substrates via MOCVD technique, exhibit relaxor-type behaviors, i.e. a broad and frequency-dispersion peak in the ε'-versus-T curves [4]. The compressive in-plane strain induced by the mismatch between film and substrate leads to a shift of the phase transition temperature from 628 K for unstrained bulk $NaNbO_3$ to 125 K and an enhancement of the permittivity from ε' < 500 to 1500 for fully strained films, respectively. However, both properties, transition temperature and permittivity, strongly depend on the thickness of the film. Thin films below the critical film thickness possess a larger strain, while lattice strain is reduced with increasing thickness due to the onset of plastic lattice relaxation. This leads to an increase of the transition temperature from 125 K to 140 K and a reduced permittivity at temperatures in the range of the transition peak (Fig. 3a).

Furthermore, a strong AC field dependency of the permittivity is observed (Fig. 3b) from which the size of the 'active' polar nano regions (PNRs) at the freezing temperature could be estimated. The diameter of the PNR at the freezing temperature ranges from ~5.2 nm to ~8 nm for large and small fields, respectively. This field dependence might be explained by the size reduction caused by increasing repolarization forces. Furthermore, the activation energy E_a of the PNRs has been calculated to about 10 – 20 meV at the freezing temperature. From our results we conclude that strain can not only be applied to engineer ferroelectric properties, but also be used to induce prominent relaxor properties in strained $NaNbO_3$ films which provides interesting opportunities for basic research and possible applications of this type of ferroelectrics.

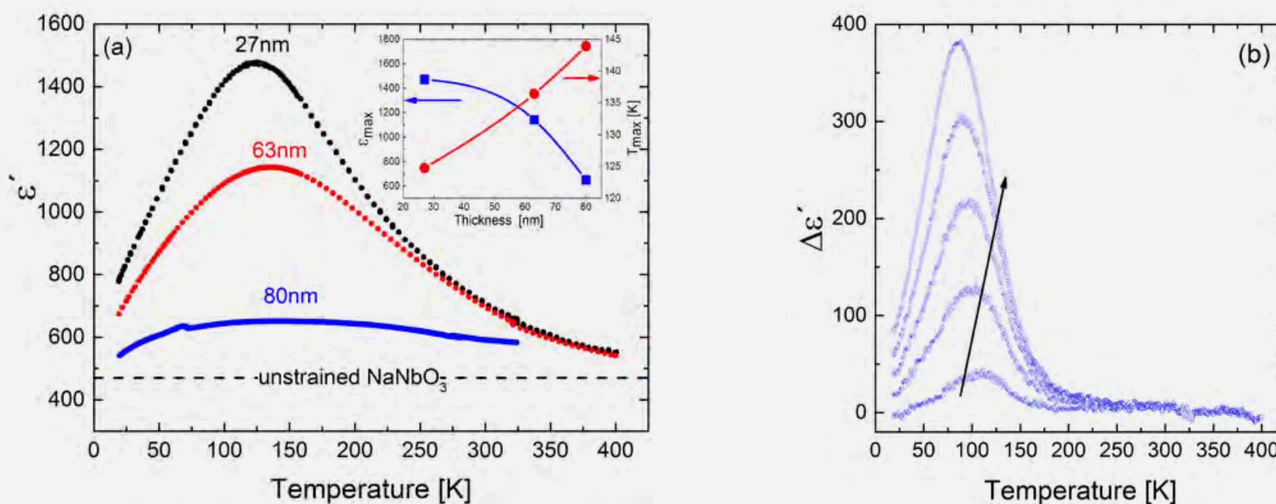

Fig. 3

(a) Temperature dependence of the permittivity of $NaNbO_3$ films with different film thickness on (110) $NdGaO_3$. The data are recorded at 1 MHz using a small AC amplitude of E_{AC} = 0.048 V/µm and zero DC-bias. The dash line represents the level of the dielectric constant of unstrained $NaNbO_3$ bulk material.
Inset: Maximum of dielectric constant ε'_{max} (blue squares) and the corresponding temperature T_{max} (red circles) as function of film thickness.

(b) Temperature dependence of the electric field induced modification of the permittivity with respect to the data shown in (a) for the 27 nm thick $NaNbO_3$ film.
Δε´ is defined as $\Delta\varepsilon' = \varepsilon'(_{EAC}, _{EDC}) - \varepsilon'(_{EAC} = 0.048 V/µm, _{EDC} = 0)$.
Along the black arrow the applied AC-field amplitude is increased in steps of 0.2 V/µm from $_{EAC}$ = 0.2 V/µm to 1 V/µm with $_{EDC}$ = 0.

Pico Switches

Within a cooperation with University of Potsdam, WG M. Bargheer, an approach to build active x-ray optical elements by optical excitation in dielectric perovskite materials is demonstrated. A switchable mirror, where the reflectivity is modulated on picosecond timescales, has been introduced. This device is called PicoSwitch. Controlled propagation of coherent acoustic phonon wave packets is utilized to modulate the lattice parameter and thus the x-ray diffraction efficiency. The PicoSwitch is built from a dielectric top layer ($LaAlO_3$) and a metallic transducer ($La_{0.7}Sr_{0.3}MnO_3$), which are both epitaxially grown on a $NdGaO_3$ substrate by PLD in IKZ. Measurements at BESSY have yielded a switching time of 5 ps and a switching contrast factor of 17. These results are rather promising characteristics for future application in third generation of synchrotron sources.

References

[1] X. Wang, J. Wu, D. Xiao, J. Zhu, X. Cheng, T. Zheng, B. Zhang, X. Lou, X. Wang; J. Am. Che. Soc. 136 (2014) 2905

[2] G. Bai and W. Ma; Physica B 405 (2010) 1901

[3] J. Schwarzkopf, D. Braun, M. Hanke, A. Kwasniewski, J. Sellmann, M. Schmidbauer; J. Appl. Cryst. 49 (2016) 375

[4] B. Cai, J. Schwarzkopf, E. Hollmann, D. Braun, M. Schmidbauer, T. Grellmann, R. Wördenweber, accepted for publication in Phys. Rev. B 93 (2016) 224107

Simulation & Characterization

Physical Characterization 84

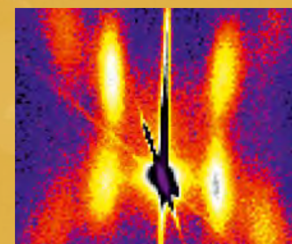

Electron Microscopy 90

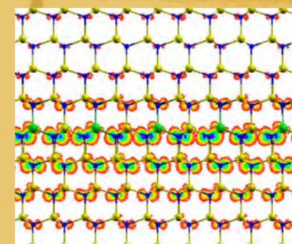

Chemical & Thermodynamic Analysis 96

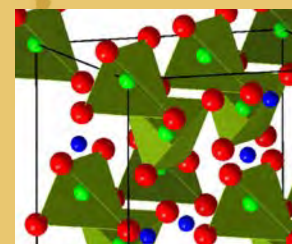

Crystal Machining 100

Simulation & Characterization

Head of the section: PD Dr. habil. Detlef Klimm

Die vier Gruppen Physikalische Charakterisierung (Röntgenbeugung, optische und elektrische Charakterisierung), Elektronenmikroskopie (REM, TEM und damit verknüpfte Analyseverfahren) Chemische & Thermodynamische Analyse (ICP-OES, DTA und simultane Techniken, Wärmetransport) sowie Kristallbearbeitung (Schneiden, Polieren einschließlich CMP, Präparation von Keimen) sind Bestandteile unserer Sektion. Ein großer Teil unserer Arbeit ist der kontinuierlichen Unterstützung der zu den anderen Abteilungen gehörenden Kristallzüchter-Gruppen gewidmet. Dazu gehören beispielsweise die Routine-Charakterisierung von Ausgangsmaterialien zur Kristallzüchtung durch verschiedene chemische und physikalische Untersuchungsverfahren; aber auch die Präparation von Keimkristallen, welche in der Regel die kristallographische Orientierung durch Röntgenbeugung sowie anschließendes Schneiden und Oberflächenbearbeitung erfordert. Die breite Palette der am IKZ bearbeiteten Materialien erfordert oftmals spezifische Präparationstechnologien, die erst entwickelt werden müssen.

Seit einigen Jahren gewannen einige Metalloxide als aktive Materialien hohe internationale Aufmerksamkeit. Beispiele sind verschiedene ferroelektrische Titanate sowie β-Ga_2O_3 als aussichtsreiches Material für elektronische Komponenten, die hohen Feldstärken bis 8 MV/cm widerstehen können. Unser Institut befindet sich in der günstigen Situation, dass solche Materialien sowohl als Volumenkristalle (für entsprechende Substrate, siehe den Beitrag der Oxide/Fluoride-Gruppe) als auch als Epitaxieschichten (für die beabsichtigte Herstellung von Bauteilen, siehe die entsprechenden Beiträge der Abteilung Schichten & Nanostrukturen) hergestellt werden können. Auch die Gruppen unserer Abteilung sind stark in diese Aktivitäten involviert. Der Beitrag der Gruppe Physikalische Charakterisierung zeigt, dass nur ein geringer Anteil der Dotierungsatome Sn und Si zur elektrischen Leitung von β-Ga_2O_3-Schichten beiträgt, die auf (100) Homosubstraten gewachsen wurden. Der Beitrag der Gruppe Elektronenmikroskopie erklärt atomistisch, warum das so ist: Die geringe Beweglichkeit von Atomen, die sich auf den breiten (100)-Wachstumsterrassen anlagern, führt zur Bildung inkohärenter 2-dimensionaler Defekte mit ungesättigten Bindungen. Vergleichsweise einfach kann dieses Problem durch Benutzung von Substraten gelöst werden, die einige Grad aus (100) heraus gekippt sind. Allerdings stellt die Präparation solcher Substrate derzeit noch ein großes Problem dar, weil β-Ga_2O_3 sehr spröde ist und zu unkontrolliertem Spalten neigt.

The four groups Physical Characterization (x-ray diffraction, optical and electrical characterization), Electron Microscopy (REM, TEM and related techniques), Chemical & Thermodynamic Analysis (ICP-OES, DTA and related techniques, thermal transport), and Crystal Machining (cutting, polishing including CMP, seed preparation) belong to our department. A major part of our efforts is devoted to the continuous support of crystal growth groups from the other IKZ departments. This includes routine inspection of starting materials by different chemical and physical methods, and the preparation of seed crystals which includes typically crystallographic orientation by x-ray diffraction as well as cutting and surface preparation. The broad palette of different materials that is investigated at IKZ requires often very specific handling and preparation technologies, which are partially not immediately available, and have to be developed.

Several functional oxides recently gained significant attention in the scientific community, such as different titanates that show strong ferroelectric effects, and β-Ga_2O_3 which is a prospective material for electronic devices because it is expected to be capable of working under high electric fields in the order of 8 MV/cm. Our institute is in the beneficial situation that these materials can be grown here in the bulk (for the substrates, see the contribution of the Oxides/Fluorides group) and as layers (for intended device application, see the corresponding reports of the Layers & Nanostructures department). Also the groups of our department are deeply involved in these activities. From the contribution of the Physical Characterization group to this report the reader can learn that only a minor fraction of group IV dopant atoms (Sn, Si) contributes to the electric conductivity of β-Ga_2O_3 layers that are grown on (100) homosubstrates. The reasons for this severe drawback is explained on an atomistic level in the contribution of the Electron Microscopy group: The insufficient mobility of adatoms on the wide (100) growth terraces leads in the end to incoherent 2D defects with dangling bonds. The usage of off-oriented substrates with narrower terraces can straightforward solve these problems. It should be noted, however, that the preparation of such miscut substrates is still a severe challenge because β-Ga_2O_3 is very brittle and tend to uncontrolled cleavage.

Simulation & Characterization: **Physical Characterization**

Head Dr. Klaus Irmscher
Team K. Banse, A. Fiedler, A. Kwasniewski, M. Naumann, M. Pietsch, Dr. M. Schmidbauer

Überblick

Die Gruppe Physikalische Charakterisierung beschäftigt sich hauptsächlich mit der Untersuchung der im IKZ gezüchteten Volumenkristalle und epitaktischen Schichten mittels Röntgenbeugung, optischer Spektroskopie und Bildgebung, elektrischer Messungen sowie verwandter Techniken. Einerseits liefern die Ergebnisse dieser Messungen die erforderliche Rückinformation an die Kristallzüchter, um die Züchtungsprozesse zu optimieren. Andererseits können interessante physikalische Effekte, die von grundlegendem oder anwendungsspezifischem Interesse sind, nachgewiesen werden. Viele wichtige Resultate werden in den Einzelberichten der entsprechenden Züchtungsgruppen beschrieben. Hier konzentrieren wir uns auf drei ausgewählte Themen unserer Arbeit: (i) eine Röntgenbeugungsuntersuchung monokliner ferroelektrischer Domänen in $K_{0.95}Na_{0.05}NbO_3$ *Schichten auf (110)* $NdScO_3$ *Substraten, (ii) eine Erklärung, wie inkohärente Zwillingsgrenzen die elektrischen Eigenschaften von homoepitaktischen* β-Ga_2O_3 *Schichten beeinflussen und (iii) ein Bericht über die Ausdehnung der Streulichttomographie auf den kurzwelligen Infrarotbereich.*

Overview

The group Physical Characterization is mainly concerned with investigations of bulk crystals and epitaxial layers grown at IKZ using x-ray diffraction, optical spectroscopy and imaging, electrical measurements, and related techniques. On one hand the results of these measurements provide necessary feedback to the crystal growers for optimizing the growth processes. On the other hand, interesting physical effects in these crystals may be revealed being of basic as well as application specific interest. Many important results are communicated in the individual reports of the respective crystal growth groups. Here we focus on three selected topics of our work: (i) an x-ray diffraction study of monoclinic ferroelectric domains in $K_{0.95}Na_{0.05}NbO_3$ thin films grown on (110) $NdScO_3$ substrates, (ii) an explanation how incoherent twin boundaries influence the electrical properties of homoepitaxial β-Ga_2O_3 layers, and (iii) a report on the extension of laser scattering tomography to the short wave infrared range.

Results

X-ray diffraction from monoclinic ferroelectric domains in $K_{0.95}Na_{0.05}NbO_3$ thin films grown on (110) $NdScO_3$ substrates by MOCVD

$KNbO_3$ and $K_xNa_{1-x}NbO_3$ have been shown to be promising candidates to replace lead-based ferroelectrics due to their excellent piezoelectric properties [1,2]. At room temperature, the system $K_xNa_{1-x}NbO_3$ exhibits orthorhombic structure, which enables the incorporation of anisotropic epitaxial lattice strain favoring the formation of monoclinic ferroelectric phases [3]. Here the electrical polarization vector is not confined to highly symmetric crystallographic directions but can continuously rotate within the mirror plane of the monoclinic unit cell leading to excellent piezo- and ferroelectric properties suitable for technological applications.

Recently, we have shown that domain symmetry as well as domain wall arrangement and density can be controlled by the targeted incorporation of anisotropic lattice strain. In this way, monoclinic M_A domains with $(001)_{pc}$ orientation and a_1a_2 domains with $(100)_{pc}$ orientation of the pseudocubic (pc) unit cell have been induced for compressively strained $K_{0.75}Na_{0.25}NbO_3$ films [4] and tensely strained $NaNbO_3$ films [5] on $TbScO_3$ orthorhombic substrates, respectively.

Here, we report on the targeted manipulation of the ferroelectric domain pattern in $K_xNa_{1x}NbO_3$ films by appropriate choice of the potassium content x and substrate material. Calculations show that for $K_{0.95}Na_{0.05}NbO_3$ films on (110) $NdScO_3$ (NSO) substrate the elastic strain energy densities for $(100)_{pc}$-orientation and for $(001)_{pc}$-orientation of the epitaxial film are almost identical (see also Fig. 1a in report Ferroelectric Oxide Layers). For $(100)_{pc}$-orientation the pseudocubic unit cell is compressively strained and exhibits an in-plane monoclinic distortion, while for $(001)_{pc}$-orientation it experiences tensile strain and an out-of-plane monoclinic distortion. The coexistence of both orientations is thus an attractive pathway for efficient strain compensation in this material system.

Simulation & Characterization: **Physical Characterization**

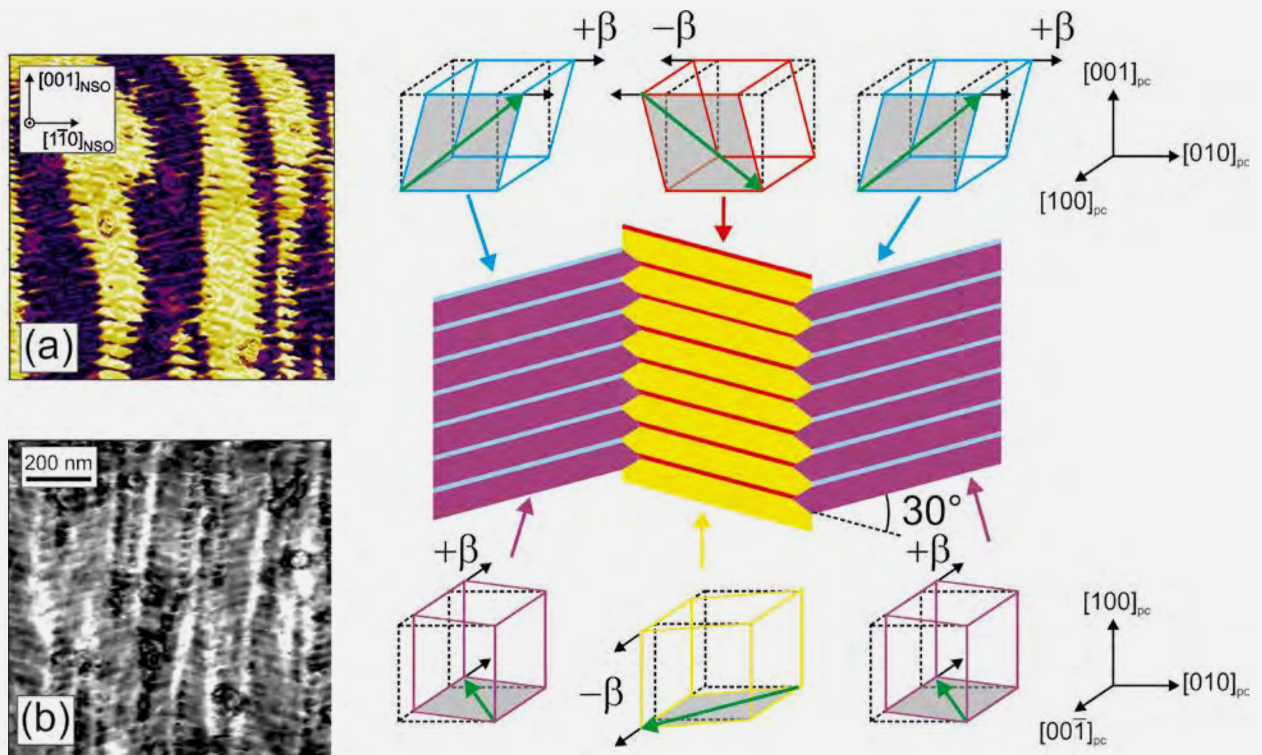

The coexistence of both surface orientations results in a complex superdomain pattern with a_1a_2/M_C symmetry, which is in strong analogy to the prominent a/c symmetry observed in lead-based tetragonal material systems. For a 28 nm $K_{0.95}Na_{0.05}NbO_3$ film grown on (110) $NdScO_3$ substrate by metal-organic chemical vapor deposition (MOCVD) this can be visualized by piezoresponse force micrographs (PFM). On one hand comparatively large irregular domain bundles with typical lateral sizes between 50 and 200 nm along $[1\text{-}10]_{NSO}$ are observed. On the other hand, a prominent subdomain structure consisting of a highly periodic array with alternating narrow and broad domain widths along the $[001]_{NSO}$ direction is observed (Fig. 1a, b). In this direction the lateral period amounts to about 30 nm while the domain walls are very flat and tilted off by about ±15° with respect to $[110]_{NSO}$. A closer look on the vertical amplitude image (Fig. 1b) reveals that the narrow subdomains manifest enlarged piezoelectric response within a matrix of low-responding domains. Coincidently, the related lateral PFM image (Fig. 1a) shows a complementarily inverted signal in that the narrow subdomains exhibit a strongly suppressed lateral response while the matrix of 30 nm domains shows a huge lateral piezoelectric amplitude. This result is a first indication of the coexistence of both $(100)_{pc}$-orientation and $(001)_{pc}$-orientation with different electrical polarization.

Fig. 1
(a) Lateral and
(b) vertical piezoresponse force micrographs
of a 28 nm $K_{0.95}Na_{0.05}NbO_3$ epitaxial film grown on (110) $NdScO_3$ substrate.
(c) Schematic view of domain pattern with corresponding orientations of the $K_{0.95}Na_{0.05}NbO_3$ pseudocubic unit cell (with monoclinic shearing angles ± β). The a_1a_2 domains with $(100)_{pc}$-orientation are given in yellow and violet colors, the M_c domains with $(001)_{pc}$-orientation in bright blue and red colors. The green arrows indicate the direction of the electrical polarization vector.

Simulation & Characterization: **Physical Characterization**

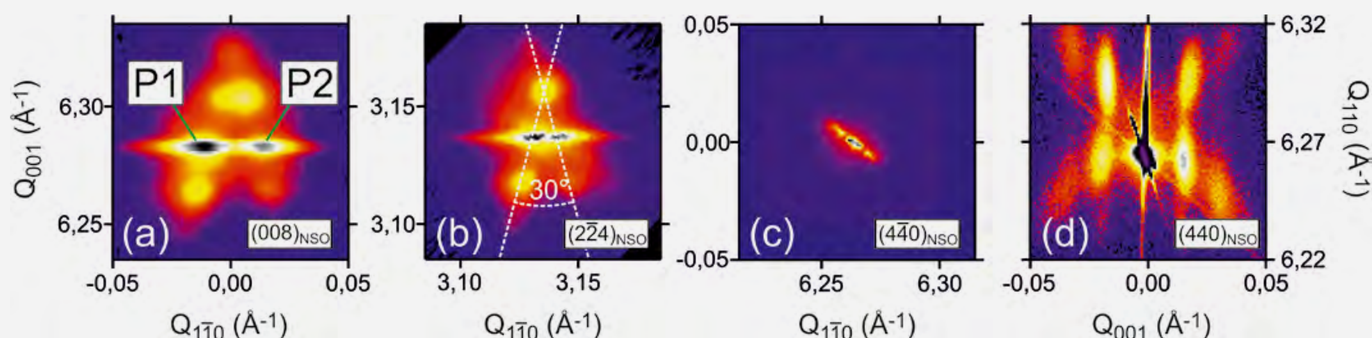

Fig. 2
In-plane reciprocal space maps in the vicinity of the $(008)_{NSO}$ (a), $(2\text{-}24)_{NSO}$ (b) and $(440)_{NSO}$ (c) substrate Bragg reflections. (d) Out-of-plane intensity distribution in the vicinity of the $(440)_{NSO}$ substrate Bragg reflection.

Grazing incidence in-plane x-ray diffraction has been performed at the European Synchrotron Radiation Facility (ESRF). A characteristic film peak splitting (P1, P2) can be observed In the vicinity of the $(008)_{NSO}$ and $(2\text{-}24)_{NSO}$ reciprocal lattice points of the $NdScO_3$ substrate (Fig. 2a and 2b, respectively), while the intensity distribution in the vicinity of $(440)_{NSO}$ shows a single peak only (Fig. 2c). Moreover, the peaks P1 and P2 are accompanied by a prominent satellite structure which is caused by the domain wall orientation and the periodic arrangement of the domains. A careful analysis reveals that the 'violet' and 'yellow' domains (in Fig. 1a) exhibit $(100)_{pc}$-orientation with alternate in-plane lattice shearing of the monoclinic unit cell of $\beta = \pm 0.12°$.

Furthermore, a complementary TEM investigation (see report 'Electron Microscopy') proves $(001)_{pc}$ unit cell orientation in the narrow subdomains. This orientation could not be directly established in our x-ray data. The intensity fraction of direct scattering is presumably too small as to lead to a detectable scattering signal. However, the existence of regions with slightly different out-of-plane lattice parameters can be indirectly proven through the appearance of satellite peaks around the out-of-plane $(440)_{NSO}$ Bragg reflection (Fig. 2d).

Our data can be consistently interpreted by the model schematically displayed in Fig. 1c. The large yellow and violet domain bundles exhibit $(100)_{pc}$-orientation. For this type of domains the pseudocubic unit cell exhibits an in-plane monoclinic distortion (Fig. 1c bottom) leading to in-plane electrical polarization. In adjacent domain bundles the polarization vector orientation differs by 90°. These domains are assigned as a_1a_2 domains. On the other hand, the narrow subdomains (sketched in bright blue and red colors in Fig. 1c) periodically interrupting the large domains exhibit $(001)_{pc}$-orientation. This monoclinic unit cell orientation is obtained by a 90° rotation of the yellow/violet unit cells around the $[010]_{pc}$ axis (Fig. 1c top) leading to a corresponding 90° rotation of the electrical polarization vector which exhibits now a strong vertical component. These domains correspond to the so-called M_C phase [6]. Both domain variants are monoclinic phases of the same symmetry while the orientation of the electrical polarization vector is controlled by the shearing direction of the monoclinic unit cell. The present results may open a feasible pathway towards the exploitation of ferroelectric properties in both vertical and lateral directions and the possibility to achieve enhanced piezoelectric properties in lead-free material caused by singularities at the domains walls.

The present results have been achieved in close collaboration with the groups Ferroelectric Oxide Layers and Electron Microscopy. We are grateful to H. Renevier for assistance with the x-ray diffraction experiment at ESRF (MA-2233).

Influence of incoherent twin boundaries on the electrical properties of homoepitaxial β-Ga_2O_3 layers grown by metal organic vapor phase epitaxy

Among the transparent semiconducting oxides, β-Ga_2O_3 is one of the most promising for optoelectronics and power electronics due to its large band gap of about 4.8 eV and the resultant high break down field of 8 MV/cm. This is the reason that several groups worldwide have intensified their research activities on this material. In our institute, we contribute to these vigorous studies by the growth and characterization of β-Ga_2O_3 bulk crystals and layers. Bulk single crystals are grown by the Czochralski method in the group Oxides/Fluorides and serve as substrates for the homoepitaxial growth of β-Ga_2O_3 layers by metal organic vapor phase epitaxy (MOVPE) in the group Semiconducting Oxide Layers (see present annual report and [7]). The resulting layers are structurally and electrically characterized in the groups Electron Microscopy and Physical Characterization, respectively.

The electrical characterization of β-Ga_2O_3 layers doped with the shallow donors Sn or Si reveals an abnormal behavior in the Hall carrier mobility as a function of the free charge carrier concentration. The Hall effect is not measurable below a "threshold" electron concentration of 1×10^{18} cm^{-3} due to a collapse of mobility. Moreover, the electron concentration is one order of magnitude lower than the dopant concentration. Additionally, the mobility of the layers grown by MOVPE is up to one order of magnitude lower than the mobility of bulk crystals. A model which explains this electrical behavior is outlined in the following.

The structural investigation by transmission electron microscopy (TEM) reveals that a high density of planar defects, i.e. of twin lamellas, is present in these layers (see Fig. 3 of the contribution by the Electron Microscopy group in the present annual report). In the case regarded here, homoepitaxial growth proceeds on (100) oriented β-Ga_2O_3 substrates. This orientation facilitates twin formation by possible double positioning of the gallium atom on the (100) plane (*a*-plane) resulting in two different orientations of the monoclinic unit cell. The arrangement of two neighboring twins is schematically shown in Fig. 3. The *a*-plane is the twin generating mirror plane and twin boundaries parallel to the *a*-plane are coherent (all bonds are preserved). The *c*-planes of the two twins are inclined by about 28°. Therefore, twin boundaries out of the *a*-plane are incoherent, and it is reasonable to assume that dangling-bond-like defects are present.

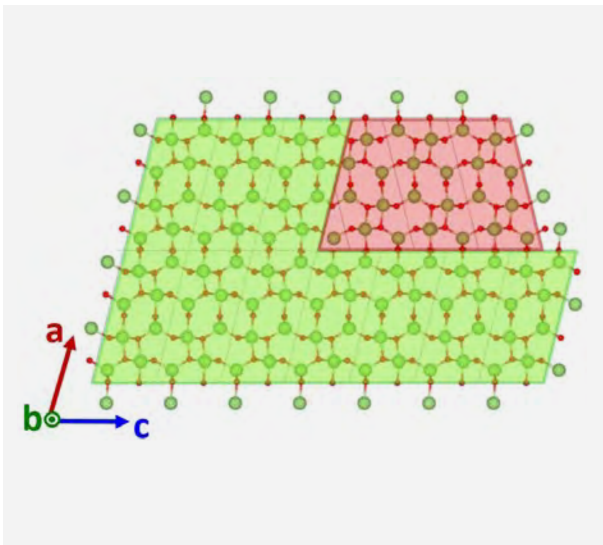

Fig. 3
Twin boundary model

We assume one dangling bond per unit cell and further, acceptor-like behavior of the dangling bond states. Therefore, the charge neutrality equation, that must be solved to obtain the electron concentration n, has to be adjusted to

$$n = (N_d^+ - N_a^-) - \frac{N_{itb}}{d} \quad (1)$$

where d is the distance between two broken bonds (for our assumption equal to the b lattice constant), N_{itb} is the concentration of incoherent twin boundaries per cross section and $(N_d^+ - N_a^-)$ is the net concentration of ionized donors and acceptors [8]. The twin boundaries along c-planes form electrically active, charged walls in the layer. To describe the transport in such layers the Read model for charged barriers can be applied [9]. A depletion zone forms around every incoherent twin boundary and can be approximated by depleted cylinders of radius

$$R = \sqrt{\frac{1}{\pi d(N_d^+ - N_a^-)}}$$

Thus, the extension of the depletion zone is indirectly proportional to the square root of the net doping concentration and gains increasing influence for small doping concentrations. The resulting potential has a minimum at the midpoint between every two charged barriers. This minimum is pivotal for the electrical transport and is given by

$$V\left(\frac{D}{2}\right) = \frac{4e^2(N_d^+ - N_a^-)R^3}{3\,\varepsilon_0\varepsilon D} - \frac{e^2}{2c\pi\varepsilon_0\varepsilon} ln(2)\,, \quad (2)$$

where D is the mean distance between two charged barriers and $\varepsilon_0\varepsilon$ is the dielectric constant [8]. The thermally activated mobility due to the presence of potential barriers can then be expressed by

$$\mu_{itb} = \frac{eL}{\sqrt{8k_B T\pi m^*}} exp\left(-\frac{V\left(\frac{D}{2}\right)}{k_B T}\right), \quad (3)$$

where L is the mean grain size of a twin lamella and m^* is the effective electron mass. Following Matthiessen's rule, the total mobility results from

$$\frac{1}{\mu_{tot}} = \frac{1}{\mu_{bulk}} + \frac{1}{\mu_{itb}}\,. \quad (4)$$

The bulk mobility μ_{bulk} ,due to normal scattering processes in β-Ga_2O_3, is calculated after Ref. [10]. From the TEM images we extract the density and average dimensions of the twin lamellas in the layers ($N_{itb}=5\times10^9 cm^{-2}$, c=0.304nm, L=50nm, D=65nm) and calculate the mobility as a function of the electron concentration as shown in Fig. 4.

The model of depletion zones around charged incoherent twin boundaries explains the "threshold" in the Hall mobility over charge carrier density. By adjusting the charge neutrality equation, the model also describes the compensation of charge carriers. All in all, the electrical properties are fully explainable by the structural defects. Thus, point defects play a minor role at this stage. The electrical properties can be tuned by reducing the density of twin lamella, which can be done by suppressing the double positioning of gallium atoms. This has been done by growing on 6° off-oriented (100) substrates and by growing on (010) oriented substrates. Reports on this will be published.

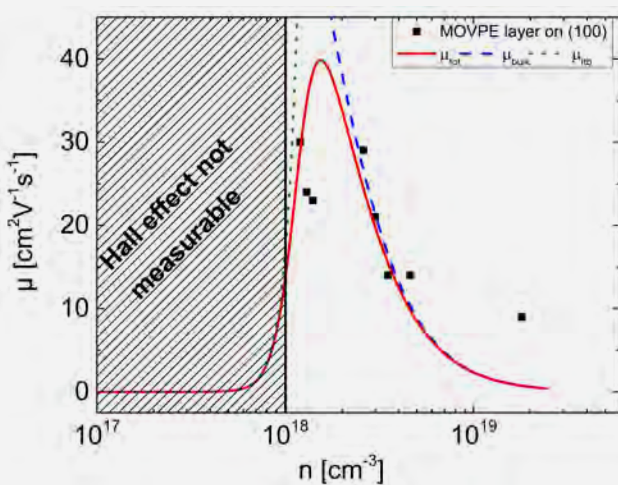

Fig. 4

Electron mobility as a function of the electron concentration at 300 K for a β-Ga_2O_3 layer homoepitaxially grown by MOVPE on (100) oriented substrates (black squares). The Hall effect is not measurable below a "threshold" charge carrier concentration of $1{\times}10^{18}$ cm^{-3} due to a collapse of mobility. The red line is the overall calculated mobility, the blue dashed line is the bulk mobility and the green dotted line is the mobility in the presence of charged incoherent twin boundaries.

Laser scattering tomography in the short wave infrared range

Laser scattering tomography (LST) images the light that is elastically scattered from inhomogeneities having a refractive index different from that of the medium in which they are embedded. We use LST to investigate submicroscopic precipitates and patterns of decorated defects in bulk single crystals. In recent years we have extended the LST method, for example, by supplement of our experimental setup by laser sources of different wavelengths and by refinements of data analysis [11,12]. In particular, the usage of light of different wavelengths for the illumination of the samples widens the range of materials that can be investigated by LST since the materials must be transparent to that light. With other words, the wavelength must be longer than that of the onset of fundamental absorption, which is determined by the bandgap energy of the material under investigation. Hence, for medium to wide bandgap crystals (bandgap energies above 1 eV) one can use light sources with wavelengths below about 1.2 µm such as Nd:YAG and argon ion lasers. For these wavelengths silicon based pixel detectors, e.g. a charge coupled device (CCD) camera, have optimal detectivity (typically in the range 300–1100 nm). However, for narrow bandgap crystals (bandgap energies below 1 eV) one needs light sources in the infrared region (above 1.2 µm) and, more stringent, pixel detectors of high sensitivity in this range. The non-availability of suitable pixel detectors or cameras had been the bottleneck in the past for an extension of LST into the infrared range. Only recently, we could get access to an InGaAs camera of sufficiently high sensitivity for our purposes in the wavelength range from 1200 nm to 2200 nm. It was provided by Photonic Science Ltd (UK) as an extended wavelength version of a so-called short wave infrared (SWIR) InGaAs camera (320×256 pixels, each of 30×30 μm^2 size). Our efforts to extent LST into the near infrared (or SWIR) region have been especially driven by the need to explore germanium crystals. They are grown as bulk single crystals in the group Silicon & Germanium, presently with focus on high-purity Ge crystals intended for a detector array for the search of neutrinoless double beta decay in ^{76}Ge (project within the GERDA collaboration). A proper light source for Ge must have a wavelength above 1.8 µm (bandgap energy 0.67 eV at room temperature). We have chosen a thulium fiber laser (TLR-5, IPG Photonics Corporation, USA) that emits at a wavelength of 1.907 µm and features enough intensity for LST.

Both laser and camera were integrated into the LST setup and linked to the in-house developed LST control and acquisition software via appropriate interfaces. In particular due to the high dark current and response non-uniformity of the InGaAs sensor, several correction schemes had to be added to the acquisition software, and one cannot expect equally high performance like in the shorter wavelength range using a silicon CCD camera. Nevertheless, we could record meaningful LST images in our preliminary experiments as shown in Fig. 5. The first image (Fig. 5(a)) exemplifies the detection of randomly distributed scattering centers in a Ge crystal grown in an Ar:H_2(5%) atmosphere. The second image (Fig. 5(b), taken under same exposure conditions) is a comparison to a Ge crystal grown in a pure hydrogen atmosphere. It shows no scattering centers except one bright spot resulting from light scattered at a surface defect. Although this improvement in structural perfection needs further confirmation, it makes hopeful to comply the stringent requirements on Ge detectors for the GERDA project.

We are sure that the application of LST to germanium and other narrow bandgap crystals will contribute to clarify their real structure and will give hints to crystal growth improvements in the near future.

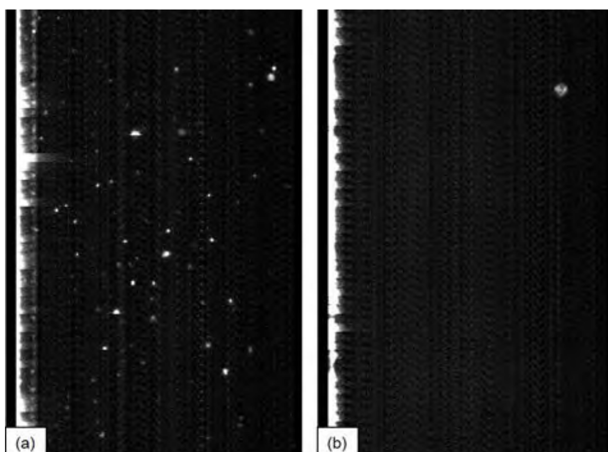

Fig. 5
LST images of two Ge crystals grown by the Czochralski technique within the GERDA project:
(a) growth in an Ar:H_2(5%) atmosphere results in randomly distributed scattering centers of still unknown nature, while
(b) growth in a pure H_2 atmosphere seems to completely suppress the formation of such scattering centers (the single spot is due to a surface defect). The images have a width corresponding to 3.5 mm object width and represent integration over 200 µm in viewing direction. (The bright lines at the left-hand sides of the images mark the sample surface where the laser beam penetrates into the crystal and undergoes scattering at an imperfect sample edge.)

References

[1] Y. Saito, H. Takao, T. Tani, T. Nonoyama, K. Takatori, T. Homma, T. Nagaya, M. Nakamura; Nature 432 (2004) 84

[2] X. Wang, J. Wu, D. Xiao, J. Zhu, X. Cheng, T. Zheng, B. Zhang, X. Lou, X. Wang; J. Am. Chem. Society 136 (2014) 2905

[3] G. Bai, W. Ma; Physica B 405 (2010) 1901

[4] J. Schwarzkopf, D. Braun, M. Hanke, A.Kwasniewski, J. Sellmann, M. Schmidbauer; J. Appl. Cryst. 49 (2016) 375

[5] A. Duk, M. Schmidbauer, J. Schwarzkopf; Appl. Phys. Lett. 102 (2013) 091903

[6] D. Vanderbilt, M. H. Cohen; Phys. Rev. B 63 (2001) 094108

[7] M. Baldini, M. Albrecht, A. Fiedler, K. Irmscher, D. Klimm, R. Schewski, G. Wagner; J. Mater. Sci. 51 (2016) 3650

[8] S. E. Krasavin; Semiconductors 46 (2012) 598

[9] W. T. Read Jr.; Lond.Edinb.Dubl.Phil.Mag. 45 (1954) 1119

[10] A. Parisini, R. Fornari; Semicond. Sci. Technol. 31 (2016) 035023

[11] J. Donecker, M. Naumann; Cryst. Res. Technol. 37 (2002) 147

[12] M. Albrecht, M. Naumann; J. Crystal Growth 310 (2008) 4031

Simulation & Characterization: Electron Microscopy

Head Dr. Martin Albrecht
Team M. Anikeeva, K. Banse, Dr. T. Markurt, S. Mohn, J. Moneta, M. Naumann, T. Remmele, N. Stolyarchuk, R. Schewski, Dr. T. Schulz

Überblick

Die Arbeitsgruppe Elektronenmikroskopie charakterisiert kristalline Materialien mit elektronenmikroskopischen Methoden sowohl im Rahmen des wissenschaftlichen Service als auch im Bereich der Grundlagenforschung. Thematischer Schwerpunkt ist der Zusammenhang zwischen physikalischen Eigenschaften und Struktur von Hableitern. Die Methoden reichen von der Rasterelektronenmikroskopie (energie- und wellenlängendispersive Röntgenspektroskopie, Elektronenrückstreubeugung (EBSD), Kathodolumineszenz) über die Ionenstrahlbearbeitung bis zur Transmissionselektronenmikroskopie (aberrationskorrigierte Transmissionselektronen-mikroskopie und Rastertransmissionselektronenmikroskopie mit atomarer Auflösung). Die Gruppe arbeitet eng mit den Gruppen des Kristallwachstums, der ab-initio Modellierung und der Simulation zusammen.

Sie trägt wesentlich zur Qualifizierung des wissenschaftlichen Nachwuchses bei. Innerhalb der Gruppe arbeiteten 2015 drei Doktoranden und eine Doktorandin, die gemeinsam mit dem Centre national de la recherche scientifique CNRS in Frankreich ausgebildet wird, sowie ein Gastwissenschaftler aus Finnland. Doktoranden und Doktorandinnen, Master- und Bachelorstudierende anderer Arbeitsgruppen des Institutes werden in elektronenmikroskopische Verfahren eingewiesen oder gemeinsam betreut. Neben der Standardcharakterisierung von Oberflächen und Zusammensetzung, Phasenanalyse und Analyse von Einschlüssen werden insbesondere grundlegende Arbeiten zu Wachstums- und Relaxationsprozessen epitaktischer Schichten sowie zu Kristalldefekten durchgeführt. Um bildgebende Verfahren zu verbessern und sie auf die spezifischen Probleme und die laufenden Arbeiten am Institut anzupassen werden eigenständige methodische Arbeiten durchgeführt. Die Gruppe arbeitet in nationalen und internationalen Forschungsprojekten und Forschungsverbünden.

2015 verteidigte Herr Dr. Toni Markurt seine Dissertation mit dem Titel "Transmission electron microscopy investigation of growth and strain relaxation mechanisms in GaN (0001) films grown on silicon (111) substrates" erfolgreich an der Humboldt Universität zu Berlin.

Da einige der Ergebnisse der Elektronenmikroskopie in den Berichten der Arbeitsgruppen der Kristallzüchtung vertreten sind, sollen im Folgenden drei ausgewählte Themen unserer derzeitigen Arbeit dargestellt werden. Dabei handelt es sich um Arbeiten (i) zu Rekombinationsmechanismen in kurzperiodischen (In,Ga)N/GaN Übergittern, die in Kooperation mit der polnischen Firma TopGaN, dem Paul-Drude Institut und dem Institut für Hochdruckphysik der polnische Akademie der Wissenschaften im Rahmen des Projekts SPRInG ("Short Period Superlattices for Rational (In,Ga)N") durchgeführt werden, (ii) zu grundlegenden Untersuchungen des homoepitaktischen Wachstums von Ga_2O_3, die zusammen mit der Arbeitsgruppe Halbleitende Oxidschichten durchgeführt werden und (iii) zur Analyse von ferroelektrischen Domänen, die zusammen mit der Arbeitsgruppe Ferroelektrische Oxidschichten durchgeführt wurden.

Overview

The electron microscopy group performs scientific service and basic research in the field of characterization of crystalline material by means of electron microscopy. Focus is the relation between physical properties and structure. The methods cover the whole field ranging from scanning electron microscopy, i.e. energy and wavelength dispersive spectroscopy, electron backscatter diffraction, cathodoluminescence through transmission electron microscopy, i.e. aberration corrected transmission electron microscopy and scanning transmission electron microscopy with atomic resolution. The team works in close collaboration with groups performing crystal growth and ab-initio modelling and simulation. In 2015, four PhD students have been working in our group, one of them is educated in a joint cooperation with the National Center for Scientific Research CNRS in France. In addition, a guest scientist from Finland is staying in our group. PhD students, master and bachelor of other groups in the institute are introduced into electron microscopy techniques and are commonly supervised.

We perform standard characterization of surfaces and composition, phase analysis and analysis of inclusions as well as basic analyses of growth and relaxation mechanisms and of defects. To improve electron optical imaging techniques and to adopt them to the specific problems at the institute we perform methodological work. The group is partner in collaborative national and international research projects.

In 2015, Dr. Toni Markurt defended his thesis on "Transmission electron microscopy investigation of growth and strain relaxation mechanisms in GaN (0001) films grown on silicon (111) substrates" successfully at Humboldt Universität zu Berlin.

Some of our results are already contained in the individual reports of the groups working in crystal growth. We will therefore highlight three selected topics of our current work. These are (i) the recombination mechanism in short period (In,Ga)N/GaN superlattices, performed in cooperation with the Polish company TopGaN, the Paul-Drude-Institut in Berlin, and the Institute for High Pressure Physics of the Polish Academy of Sciences in the frame of the European project SPRInG ("Short Period Superlattices for Rational (In,Ga)N"), (ii) fundamental studies on homoepitaxial growth of Ga_2O_3 performed together with the group Semiconducting Oxide Layers at IKZ and (iii) the analysis of ferroelectric domains performed together with the group Ferroelectric Oxide Layers at IKZ.

Results

Optical properties and recombination processes of (In,Ga)N/GaN short period superlattices

Band gap engineering in semiconductors is based on tuning composition, strain and thickness of a quantum structure to achieve a desired band gap for a particular application (e.g. a light emitting diode). In case of polar InGaN quantum wells there are a number of peculiarities that strongly limit the use of this approach. These are the high lattice mismatch between InN and GaN, the quantum confined Stark effect (QCSE) due to the presence of piezoelectric fields and alloy fluctuations and the presence of phase separation at high In contents. With increasing In concentrations required for light emitters in the green and yellow part of the spectrum these phenomena gain importance with strong negative impact on the efficiency of devices based on these alloys. In terms of optical properties they become evident by an S-shape of the PL peak position in temperature dependent photoluminescence measurements [1] and a strong blueshift of the PL peak with increasing excitation power [2].

Short period superlattices (SPSL), composed of few monolayers of InN and GaN barriers are considered a way to meet the challenges that come along with high In contents of the quantum wells. They have recently attracted interest as a substitution for conventional pseudobinary (In,Ga)N quantum wells or thick InGaN layers for use in photovoltaics [3]. The basic idea of using short period superlattices for bandgap engineering is to overcome the drawbacks of alloy fluctuations and quantum confined Stark effect present in pseudobinary alloys by using ultrathin layers of its binary components (eg. InN and GaN). Bandgaps are then tuned by changing quantum well and barrier thickness appropriately. The advantages of such digital alloying is the reduction of piezoelectric field to its minimum and complete avoidance of alloy fluctuations. Here we will discuss optical properties of InGaN/GaN short period superlattices grown by Molecular Beam Epitaxy (MBE) as dependent on the barrier thickness.

In the framework of the European project SPRInG that is performed in collaboration with the Paul-Drude-Institut in Berlin, the Polish company TopGaN and the Institute for High Pressure Physics of the Polish Academy of Sciences we study the relation between optical and structural properties of such structures as dependent on the thickness of the barrier. Therefore a series of samples, consisting of 10 periods of nominally 2-Monolayers (ML) InGaN QWs but each with different GaN barrier thciknesses of 6 ML, 11ML, 22ML and 44 MLs respectively. Composition and structural data of the samples were measured by aberration corrected transmission electron microscopy and high-resolution x-ray diffraction.

Fig. 1 shows photoluminescence spectra of the series at 20 K. According to HRTEM and x-ray the In content of the quantum well was in average 25 % with a measured thickness of the well of 1 monolayer. More detailed analysis showed that (In,Ga)N monolayers had a fractional structure consisting of ordered patches with higher In-incorporation up to 30 %. The peak position remains stable when the barrier thicknesses decrease from 44 ML to 11 ML. A pronounced redshift of about 100 meV is observed for a barrier thickness of 6 ML. While this is expected, the most striking feature of the spectra, however, is the change in the absolute and relative intensities of the quantum well luminescence and of the barrier with changing barrier thickness. When decreasing barrier thickness of the barrier from 44 monolayers to 22 monolayers the quantum well luminescence reduces. With decreasing barrier thickness this tendency increases and for the barrier thickness of six monolayers becomes dramatically low.

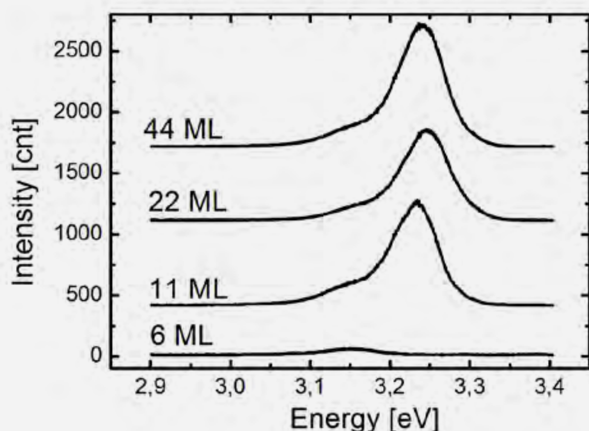

Fig. 1
Photoluminescence emission of SPSLs for different barrier thicknesses of 44 ML, 22 ML, 11 ML and 6 ML.

To explain the intensity decrease of the quantum well, DFT calculations were performed for the electron and hole distribution within $In_xGa_{1-x}N$ SPSLs. The compositions and periods of the supercells were chosen according to our experiments, though barrier thicknesses beyond 7 monolayers could not be tackled, because of the high computational effort. All supercells discussed here are strained to the in-plane lattice constant of GaN and periodic in all directions. The supercell shown in Fig. 2 consists of a single monolayer of $In_xGa_{1-x}N$ with an indium content of x=0.33 (the highest predicted value) and 7 MLs thick GaN barriers. The charge density distribution of electrons (left) and holes (right) is plotted within the supercell.

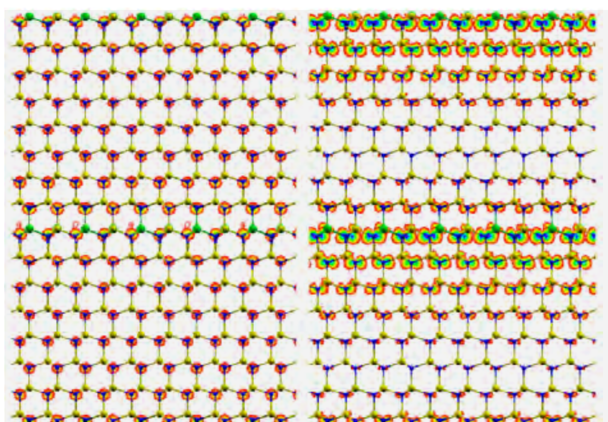

Fig. 2
Calculated charge density of electrons (left) and holes.

It is evident that the electron wave function is widely distributed within the entire supercell, while their localization effects near the Indium atoms are rather weak. In contrast, the holes are localized close to the indium atoms in the monoatomic wells although still substantial parts of the wave function penetrate into the GaN barrier.

The band offset at the achievable In concentrations is too small to significantly confine electrons within the $In0_{.33}Ga0_{.67}N$ well for the given thickness of the barriers. When further reducing the barrier thickness down to 5 and 3 monolayers the penetration of the hole-wave function into the barrier increases, while the electrons remain delocalized. This explains the decreasing PL luminescence of the quantum wells with decreasing barrier thickness. It is an effect of the strong difference in the extension of the electron and hole wave functions in III-Nitrides.

Influence of the miscut on stacking fault densities in homoepitaxial β-G_2O_3 layer grown on (100) plane

β-G_2O_3 is a transparent wide band gap (E_G = 4.8 eV) semiconductor with a predicted electrical break down field strength of 8 $MVcm^{-1}$ which makes it interesting for applications in power electronics. In contrast to other wide bandgap materials like GaN or AlN, large diameter single crystalline substrates are available. While the (100) surface of the monoclinic crystal is a natural growth surface that can be easily prepared, homoepitaxial growth experiments by MOVPE at our institute showed the presence of a high density of planar defects in these layers [4,5]. Dedicated high resolution transmission electron microscopy experiments (e.g. Fig. 3) reveals that these defects are twins or twin lamella: they can be described by a c/2 glide reflection of the lattice. While all bonds in the coherent twin boundary lying in the a-plane are fully coordinated the incoherent boundary lying in the c-plane introduces dangling bonds, which act as acceptors. These compensate n-type doping, reduce the carrier mobility and lead to complete mobility collapse below a critical doping limit. Understanding stacking formation therefore is crucial to improve electrical properties of these layers.

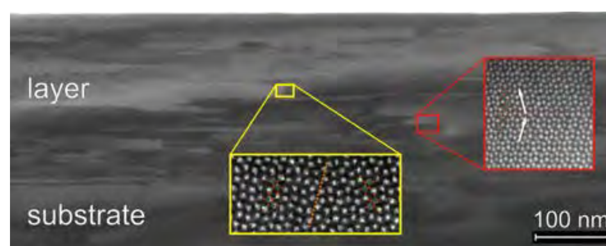

Fig. 3
Twin lamella in Ga_2O_3. The substrate is free of twin lamella. The layer shows a high density of defects that appear as dark parallel lines or lamella. Cross-sectional bright-field image along the [010] projection. The insets show high-resolution scanning transmission electron micrographs of the coherent (red frame) and incoherent (yellow frame) twin boundaries; Ga atoms appear as bright dots. Stick and ball models are introduced as a guide for the eye (octahedral bound Ga: dark green, tetrahedral bound Ga light green, oxygen: red balls).

Simulation & Characterization: **Electron Microscopy**

Twin lamella may form either through double positioning during growth or through plastic processes, i.e. splitting of perfect dislocations into partials under the action of an external shear force. Since we are dealing with homoepitaxial growth in our case, we may exclude the latter. In an early work Matthews and Allinson developed the model of double positioning to explain formation of twins and stacking faults in face centered cubic metals. It has later been adopted to other material systems ([6], [7]) . Double positioning takes place on a surface that corresponds to a mirror plane of a lattice. If the layer grows in form of two-dimensional islands these may nucleate either in the epitaxial or in the twinned orientation. Layer growth proceeds via nucleation of two-dimensional islands if surface diffusion is not sufficiently high for ad-atoms to reach step-edges (Fig. 4). If two dimensional island nucleation or incorporation at step-edges prevails depends on growth conditions (e.g. step width on the surface, substrate temperature, the flux of incoming adatoms) and materials constants (e.g. the diffusion coefficients of adatoms on the surface). If the latter is known, growth conditions can be tuned appropriately to promote step flow growth.

In the framework of an ongoing PhD thesis we studied stacking fault formation as dependend on miscut to obtain experimental access to the diffusion coefficients of adatoms. The basic idea is as follows: Assuming that stacking faults form by double positioning, we may evaluate the stacking fault density as dependent on miscut from transmission electron microscopy studies.

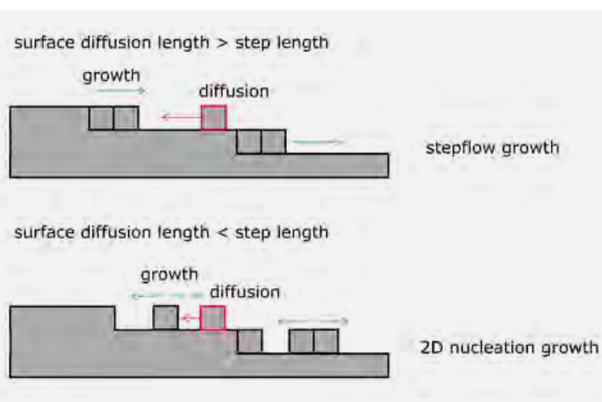

Fig. 4
Schematic of growth at a vicinal surface. Adatoms diffuse to the surface steps or form two-dimensional islands on terraces between the steps.

Fig. 5 displays the stacking fault density vs. the terrace width for the growth temperature of 850°C. The curve resembles that for island nucleation processes on vicinal surfaces. By adopting nucleation theory in the mean field approximation [8] we are able to fit our stacking fault density (inserted in Fig. 5). Knowing the incoming flux of atoms we are able to estimate the diffusion constant D for the growth of β-G_2O_3 at the growth temperature of 850°C. According to our fit it corresponds to D=$2.5 \times 10^{-9} cm^2 s^{-1}$, which is about two order of magnitude lower than recently published data on adatom diffusion in GaAs. In the framework of the Leibniz ScienceCampus GraFOx – Growth and fundamentals of oxides for electronic applications – these data will be starting point for further theoretical work by ab-initio based kinetical Monte Carlo calculations. Based on the present work we could show that under the growth conditions applied and for miscuts higher than 4°, the stacking fault density could be reduced to an minimum. This results on the one hand in mobilities of charge carriers that are similar or higher than the best values reported in literature and allowed on the other to expand the range of free carrier concentrations from 10^{17} cm^{-3} to 10^{19} cm^{-3}.

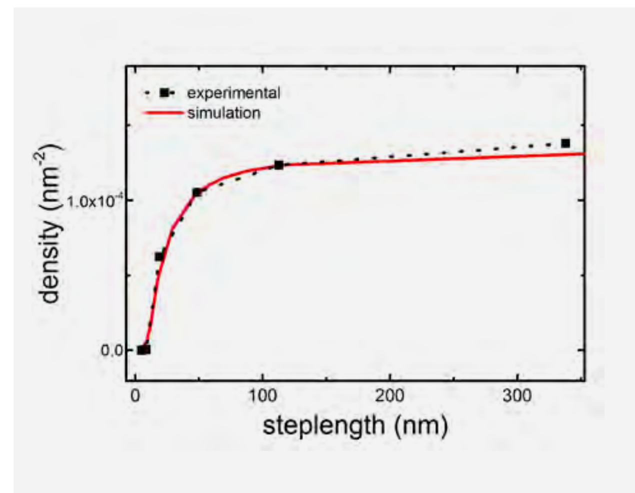

Fig. 5
Stacking fault density as dependent on terrace width. The dots are experimentally measured curves. The line is fitted by a model that assumes two dimensional nucleation on vicinal surface Bales [8]. Fitting parameter is the surface diffusion coefficient.

Study of ferroelectric domains by transmission electron microscopy

The search for an alternative lead-free piezoelectric material to replace $PbZr_{1-x}Ti_xO_3$ (PZT) has been a hot topic in research in the past years. A promising candidate is $K_xNa_{1-x}NbO_3$. High piezoelectric coefficients in perovskite solid solutions like $PbZr_{1-x}Ti_xO_3$ are attributed to the presence of the monoclinic phase at the morphotropic phase boundary[10]. This is due to the fact that the polar axis can rotate free within the monoclinic mirror plane. Recent work by the group Ferroelectric Oxide Layers at IKZ has shown that anisotropic epitaxial strain can stabilize monoclinic phases in ferroelectric perovskite thin films [11]. By tuning the strain through appropriate choice of substrate and film composition, the arrangement and size of domains and in turn piezo- and ferroelectric material properties can be tailored. An example of a piezo force microscopy image of such a structure (a 26 nm thin film of $K_{0.95}Na_{0.05}NbO_3$, epitaxially grown on top of a $NdScO_3$ (110) substrate) is shown in Fig. 6. The sample is characterized by well defined super domain structures consisting of periodic ferroelectric domains, where adjacent domain bundles (corresponding to the yellow and violet bundles in the PFM image Fig. 6a) differ by the orientation of the in-plane monoclinic distortion. The in plane monoclinic distortion of the domains is shown in Fig 6b.

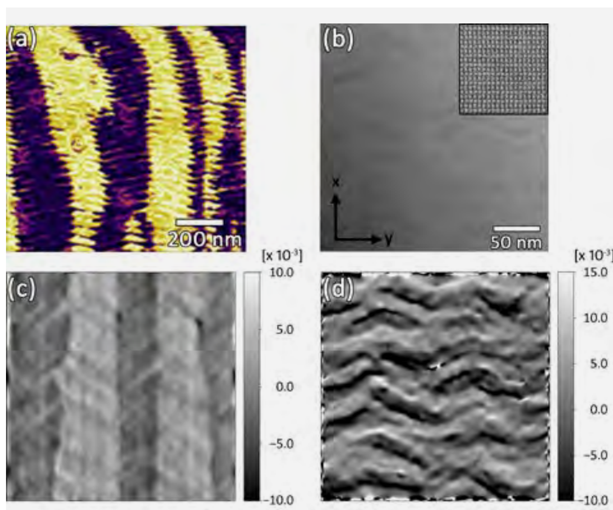

Fig. 6

(a) Lateral piezoresponse force micrograph (phase signal) of a 26 nm thick strained $K_{0.95}Na_{0.05}NbO_3$ film epitaxially grown on a (110) $NdScO_3$ substrate.

(b) Plane-view high resolution STEM ADF image of the sample. The inset in the upper right corner is a magnified view with white intensity maxima corresponding to Nb atomic columns. Indicated x- and y-axis correspond to [001] $_{NdScO3}$ and [1-10] $_{NdScO3}$ crystallographic directions.

(c) In-plane shear angle ε_{xy} map and (d) in-plane axial strain ε_{xx} map obtained from a geometric phase analysis of (b).

For a basic understanding of the materials properties, the knowledge of the local strain state of the ferroelectric film, its crystallographic phase and the domain structure is mandatory. Transmission electron microscopy now is able to provide crystallographic parameter at the unit cell scale with ultimate precision. However, when it comes to the monoclinic domains there is one major challenge. In order to preserve the as-grown strain state of the epitaxial film and thus its original domain structure plan-view TEM samples with a thick substrate layer are necessary.

Since TEM is a projective method it images typically the projected potential averaged along the beam direction including both film and substrate for a plan-view observation geometry. In our group, we have developed a method to overcome this challenge by choosing appropriate imaging conditions using high-resolution scanning TEM (STEM) annular dark field (ADF) imaging. The basic idea behind is to focus the scanning probe into the strained layer and thereby to obtain local information mainly from the ferroelectric perovskite film, while the substrate gives only rise to a uniform background intensity in the STEM ADF image.

Fig. 7a shows the principle of our approach based on image simulations by the frozen phonon approach. We performed simulations for a supercell that is very close to our experimental sample geometry, i.e. consists of a 26 nm thin $K_{0.95}Na_{0.05}NbO_3$ film on a 150 nm thick rigid $NdScO_3$ substrate (this is the minimum thickness to keep the layer strained). The layer contains two domains with a difference of the in-plane monoclinic distortion of taken from x-ray diffraction and piezo force microscopy data respectively. The evolution of the electron probe inside the supercell (Fig. 7c) shows that the high-resolution pattern is generated through channeling in the first 20-30 nm of the transmitted material. After this thickness, the wave function of the electron beam is widely dispersed, irrespectively of the initial position of the scanning electron probe. Thus the subsequent part of the TEM specimen mainly contributes to a uniform background intensity in the final ADF image. If the sample is introduced into the microscope such that the incident electron probe hits the film first and then proceeds through the substrate, the main scattered intensity is generated in the ferroelectric film. Our simulation shows that the resulting STEM ADF image pattern then directly corresponds to that of the ferroelectric domain structure. Especially the shear angle, evaluated from the simulated ADF image agrees quantitatively extremely with the lattice distortion in the $K_{0.95}Na_{0.05}NbO_3$ film in the supercell (Fig. 7b).

Simulation & Characterization: **Electron Microscopy**

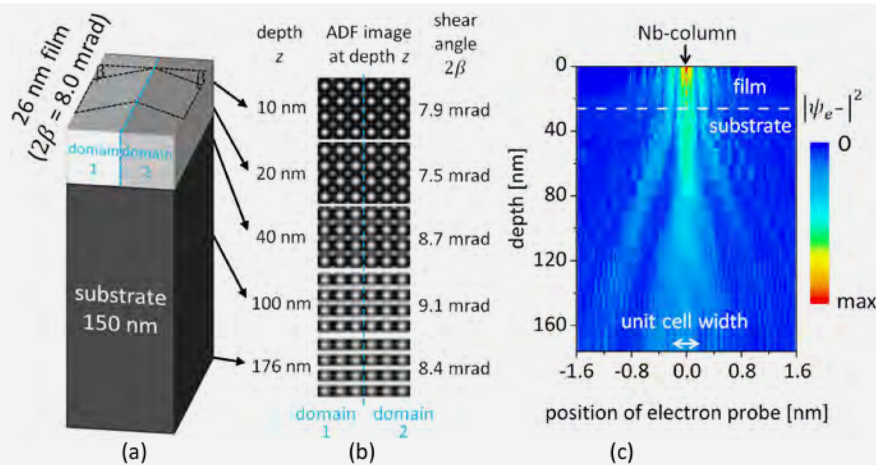

An experimental example for the plan-view high resolution STEM ADF analysis of a ferroelectric domain structure of $K_{0.95}Na_{0.05}NbO_3/NdScO_3$ is shown in Fig. 6 b-d. Fig. 6b shows the evaluation of experimental high resolution plan-view STEM ADF image patterns (Fig. 6b) by geometric phase analysis. It reveals three important results: (i) Adjacent domain bundles in the $K_{0.95}Na_{0.05}NbO_3$ film aligned approximately along the $[001]_{NdScO3}$ direction (corresponding to yellow and violet bundles in the PFM image Fig. 6a) differ by their in-plane shear component ε_{xy} corresponding to an alternate in-plane monoclinic distortion in neighboring domain bundles (see Fig. 6c). (ii) Within the domain bundles a zig-zag sub-structure of thinner stripes is visible in the in-plane shear component ε_{xy} map (Fig. 6c) as well as in the in-plane axial strain component ε_{xx} map (Fig. 6d).

This sub-domain structure appears with a pattern of alternately orientated thin stripes in adjacent domain bundles. (iii) In regions of the thin sub-domains the magnitude of the in-plane shear angle ε_{xy} is strongly reduced compared to that of the matrix domain bundle. More interestingly, the thin sub-domains exhibit an approximately 1.0% smaller in-plane lattice parameter along the $[001]_{NdScO3}$ direction. Our TEM results are in full agreement with the x-ray data, also on a quantitative level and suggest that the complex ferroelectric domain pattern of the $K_{0.95}Na_{0.05}NbO_3$ film can be explained by the coexistence of domains with monoclinic a_1a_2 and M_c symmetry (see contribution of Physical Characterization group).

Fig. 7
Frozen phonon simulation of a 26 nm thin $K_{0.95}Na_{0.05}NbO_3$ film containing two domains on top of a 150 nm thick $NdScO_3$ substrate layer.
(a) Supercell geometry with indicated in-plane monoclinic distortion (shear angle β) of the film domains.
(b) Simulated STEM ADF images at indicated depths from the supercell with evaluated difference of the in-plane shear angle 2β between the two domains.
(c) Depth dependent evolution of the electron probe initially positioned on a Nb atomic column of the $K_{0.95}Na_{0.05}NbO_3$ film.

References

[1] V. K. Dixit et al; J. Phys. D: Appl. Phys. 47 (2014) 065103

[2] T. Takeuchi et al; Jpn. J. Appl. Phys. 36 (1997) L382

[3] A. Yoshikawa et al; Appl. Phys. Lett. 90 (2007) 073101

[4] G. Wagner, M. Baldini, D. Gogova, M. Schmidbauer, R. Schewski, M. Albrecht, Z. Galazka, D. Klimm, R. Fornari; Phys. Status Solidi 211 (2014) 27

[5] M. Baldini, M. Albrecht, D. Gogova, R. Schewski, G. Wagner; Semicond. Sci. Technol. 30 (2015) 024013

[6] J. W. Matthews and D. L. Allinson; Philos. Mag. 8 (1963) 1283

[7] J.A. Venables; Philos. Mag. 27 (1973) 697

[8] G.S. Bales; Surf. Sci. 356 (1996) L439

[10] X. Wang et al.; J. Am. Chem. Soc. 136 (2014) 2905

[11] B. Noheda et al.; Appl. Phys. Lett. 74 (1999) 2059; R. Guo et al.; Phys. Rev. Lett. 84 (2000) 5423

[12] J. Schwarzkopf et al.; J. Appl. Cryst. 49 (2016) 375

Simulation & Characterization:

Chemical & Thermodynamic Analysis

Head PD Dr. habil. Detlef Klimm
Team Dr. R. Bertram, M. Klupsch, L. Schwarz, O. Reetz

Überblick

Wie bereits in den vergangenen Jahren widmete sich die Arbeit unserer Gruppe überwiegend der wissenschaftlichen Unterstützung der Züchtergruppen unseres Instituts. Dies betraf insbesondere die Abteilung Dielektrika & Wide Bandgap Materialien, und dabei vor allem die Gruppe Oxide/Fluoride wegen des behandelten breiten Substanzspektrums. Die Untersuchung von Ausgangsmaterialien und gezüchteten Kristallen durch thermische und chemische Analyse, aber auch die Untersuchung von Phasendiagrammen sind oft unumgänglich für die Züchtung neuer kristalliner Materialien. In Unterstützung der Aluminiumnitrid-Gruppe erfolgten Arbeiten zur Dotierung von AlN mit Schwefel oder Scandium.

In den Abschnitt „Resultate" fließen die Arbeitsergebnisse zweier Studenten der Humboldt-Universität zu Berlin mit ein, die in unserer Gruppe ihre Bachelor-Arbeiten durchführten. Beide Arbeiten wurden inzwischen erfolgreich verteidigt. Ein dritter Student, Oliver Reetz, arbeitet derzeit am Master-Abschluss an der Brandenburgischen Technischen Universität Cottbus-Senftenberg. Seine Arbeiten zum thermodynamic assessment, d.h. zur Bestimmung der thermodynamischen Eigenschaften des Systems $Al_2O_3 - Cu_2O - CuO$ werden zur Züchtung von Delafossit- ($CuAlO_2$) Kristallen benötigt. Die thermodynamische Beschreibung dieses Systems erweist sich unter anderem deshalb als besonders schwierig, weil kupferoxidhaltige Schmelzen sogar das Tiegelmaterial Platin angreifen. Dieses Metall muss folglich in die thermodynamische Beschreibung des Gesamtsystems mit einbezogen werden. Die Züchtung p-leitender und optisch transparenter $CuAlO_2$-Kristalle wird im Rahmen eines DFG-Projektes angestrebt, das unsere Gruppe gemeinsam mit der Gruppe Oxide/Fluoride eingeworben hat.

Für verschiedene, hauptsächlich geowissenschaftlich orientierte, Partner züchtete das IKZ $(Mg,Fe)_2SiO_4$ (Olivin)-Kristalle verschiedener Eisenkonzentration während der vergangenen Jahre. Die Stabilisierung von Fe^{2+} in der Schmelze und im wachsenden Kristall ist eine wichtige Voraussetzung für den Wachstumsprozess. In Zusammenarbeit mit der Oxide/Fluoride-Gruppe entwickelten hierfür wir reaktive Atmosphären mit CO_2 und CO als aktiven Komponenten. Olivin-Kristalle mit unterschiedlichem Fe-Gehalt können inzwischen gezüchtet werden. SIMS (Secondary Ion Mass Spectrometry) Messungen am Deutschen Geoforschungszentrum Potsdam zeigten eine exzellente Homogenität der Kristalle sowohl in chemischer Hinsicht, als auch den Isotopen-Gehalt betreffend. Sie sind damit natürlichen Olivinen bei weitem überlegen und können beispielsweise als Standards zur Geochronologie eingesetzt werden. Derzeit wird ein gemeinsamer Projektantrag für die DFG erarbeitet. Im Rahmen des geplanten Projektes sollen entsprechende Olivine gezüchtet und die Segregation von Isotopen bei der Erstarrung aus der Schmelze untersucht werden.

Overview

Like in the past, a significant share of our group's efforts is devoted to the scientific support of the crystal growth groups of our institute. This includes especially the Oxides/Fluorides group in the department Dielectric & Wide Bandgap Materials, due to the wide range of substances. The analysis of starting materials and grown crystals by thermal methods and by chemical analysis, as well as the investigation of phase diagrams that are necessary for the growth of new crystalline materials are typical tasks for our group. Other activities were performed in cooperation with the Aluminum Nitride group, e.g. in support of their attempts to reach sulfur or scandium doping of AlN.

In the "Results" section the work of two students from Humboldt University of Berlin will be presented who performed their Bachelor work in our group. Both Bachelor theses were successfully defended meanwhile. A third student, Oliver Reetz, works on his master thesis for Brandenburg University of Technology Cottbus-Senftenberg. He performs a thermodynamic assessment of the system $Al_2O_3 - Cu_2O - CuO$, as precondition for the growth of delafossite ($CuAlO_2$) crystals. This work is a real challenge, as the cuprous oxide melt attacks even the crucible metal platinum which must hence be included in the thermodynamic description of the system. The growth of the p-type *transparent conducting oxide* (TCO) $CuAlO_2$ crystals is the aim of a DFG project that runs now as collaborative effort between the oxide/fluoride and our groups.

For several external partners, mainly with geological background, IKZ grew $(Mg,Fe)_2SiO_4$ (olivine) crystals with different iron concentration during the last years. The stabilization of Fe^{2+} in the melt and in the growing crystal is a crucial issue for the growth process. For this purpose reactive atmospheres with the active components CO_2 and CO were developed in collaboration with the Oxides/Fluorides group, and olivine crystals with different Fe concentration can be grown meanwhile. SIMS (Secondary Ion Mass Spectrometry) measurements at Deutsches Geoforschungszentrum Potsdam demonstrated an excellent chemical, and especially isotopic, homogeneity of the IKZ olivines, compared to the natural mineral. Hence, such crystals could be used as standard reference samples for geochronology. A joint DFG project application is being prepared where different olivine crystals for reference purposes shall be grown, and isotope segregation during solidification from the melt will be studied.

Results

Over the last decade, the Leibniz Institute for Crystal Growth developed bulk growth technologies for dozens single crystalline materials that are used as lattice-matched substrates for epitaxy of perovskite-type functional layers. Very often these layers are ferroelectrics or multiferroics, where the properties can be manipulated by suitable substrate/layer combinations through "strain engineering" [1]. Amongst the substrate materials, rare earth scandates $REScO_3$ play a major role [2], because the choice of a suitable RE element allows tuning of the pseudocubic lattice constant from 3.95 Å for $HoScO_3$ up to 4.02 Å for $PrScO_3$. The larger RE^{3+} ions Ce^{3+} and La^{3+} cannot be used because the extremely high melting points of their scandates are beyond the stability limit of iridium crucibles.

For that reason, and for further fine-tuning of lattice parameters between the single RE based perovskite substrates, several pseudobinary systems are under investigation with the aim to identify alternative useful compositions where new mixed crystals can be grown from the melt. Usually the growth of mixed crystals in the bulk is difficult, because the different position of the liquidus and solidus lines, x_{liq} and x_{sol}, at a given temperature T, results in a separation of components during growth ("segregation"), that is proportional to $x_{liq}-x_{sol}$. Recently we showed that for some almost neighboring RE elements $x_{liq}-x_{sol}$ is so small that segregation almost not occurs, and as an example, the radioactive RE element promethium can be replaced by a mixture of its neighbors samarium and neodymium. Mixed crystals could be growth at IKZ meanwhile [3].

In his BSc thesis, Michael Klupsch (HU Berlin) investigated if a solid solution between $LaScO_3$ (distorted perovskite, space group *Pnma*, pseudocubic lattice constant 4.0504 Å) and $LaLuO_3$ (distorted perovskite, space group *Pnma*, pseudocubic lattice constant 4.1835 Å) does exist. For this purpose he performed differential thermal analysis (DTA) measurements with our STA 429CD (NETZSCH) in the temperature range from 2000°C to ca. 2300°C. Here lanthanum lutetate is the component with the (congruent) lowest melting point. After calibration with pure Al_2O_3 (T_f = 2054°C) a melting point of 2120 ±5 °C was found for $LaLuO_3$. Figure 1 shows heating curves (15 K/min, lidded tungsten crucibles in He atmosphere) for three samples ranging from pure $LaLuO_3$ to a mixture of $LaLuO_3$ with 16% $LaScO_3$ added and it is remarkable, that the begin of melting ("onset") is almost constant in this concentration range. Compositions up to 59% scandate were measured in this study, and there the onset was found at 2222°C (estimated error 15 K).

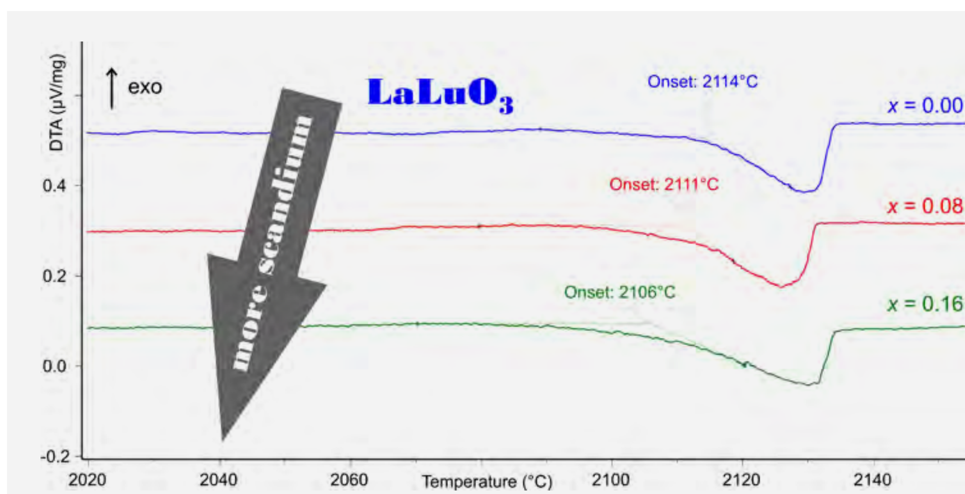

Fig. 1
The DTA heating curves for 3 samples starting from pure $LaLuO_3$ (top, x = 0.00) to a mixed crystal x $LaScO_3$ – (1–x) $LaLuO_3$ with 16 mol% $LaScO_3$ change only slightly. (Raw data without smoothing and temperature calibration).

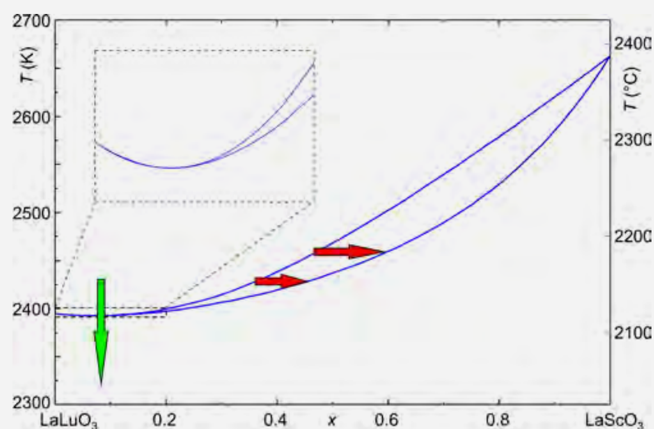

Fig. 2
The pseudobinary system $LuScO_3$–$LaLuO_3$ allows the growth of mixed crystals over a wide concentration range, especially on the $LaLuO_3$ side. For high $LaScO_3$ concentrations (ca. >50%) segregation becomes pronounced, and the temperature exceeds the load limit for iridium crucibles (ca. 2250°C).

The experimental data, together with T_f = 2390°C for pure $LaScO_3$ reported by Badie [5], allowed the construction of the pseudobinary phase diagram that is shown in Figure 2. For $LaScO_3$ concentrations below ca. 20% liquidus and solidus are almost coincident, preventing chemical segregation during cooling. Nevertheless, also from melts closer to the middle of the binary diagram (horizontal arrows in Figure 2) mixed crystals could be grown. The segregation of these mixed crystals was found to be described well by the phase diagram. In a solid solution with x = 0.43 a very high pseudocubic lattice constant 4.1224 Å was measured meanwhile [6]. This is a remarkable extension of the accessible lattice constant range, compared to the limit of 4.02 Å (for $PrScO_3$) given above.

The second BSc student of our group, Linda Schwarz (HU Berlin), continued the research on $MgGa_2O_4$ spinel that was already reported in the previous annual report. For this system, near 1000°C a shift of differential scanning calorimetry (DSC) heating curves to the endothermal direction was reported, if the corresponding sample was held prior to DSC at lower T = 800°C sufficiently long, that means typically several hours. This shift is a result of the entropy gain upon heating of the spinel structure AB_2O_4, where cation ordering changes from "largely inverse" at low temperature to "random" at high T. Cation ordering can be measured by the inversion degree x, which is the fraction of tetrahedral sites occupied by B ions. For normal spinels – such as the archetype $MgAl_2O_4$ – one has $x \approx 0$, because Mg^{2+} occupies all tetrahedral sites (green in Figure 3). $MgGa_2O_4$, in contrast, belongs to the group of largely inverse spinels where at low T the tetrahedra are preferably occupied by Ga^{3+}, and consequently octahedra by almost equal fractions of Ga^{3+} and Mg^{2+}. During heating, the cation distribution of all spinels becomes increasingly random, which corresponds to x = 2/3. This state is maximum disordered and has the highest entropy S. It is interesting to note that with, $G = H - T \cdot S$, the Gibbs free energy of the spinel phase is reduced in this high entropy state, and it becomes more stable.

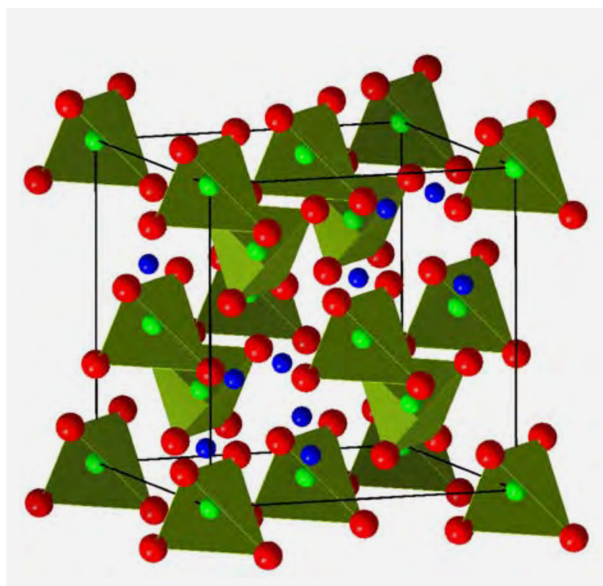

Fig. 3
The spinel structure is based on a cubic close oxygen packing (red spheres) where tetrahedral sites (green) and octahedral sites (blue spheres) are occupied by the cations.

L. Schwarz [7] performed measurements of the thermal conductivity λ in the high temperature range with our laser flash apparatus LFA 427 (NETZSCH). For most solids λ(T) drops from a maximum near the Debye temperature following a T^{-1} law as the result of increased phonon scattering [8]. Surprisingly, she observed a local maximum of λ(T) almost at that point, where the endothermal shift of the DSC curve h observed before. Actually, the inflection point of the DSC curves was observed at 1000°C, and the inflection point of λ(T) in Figure 4 is near 1030°C. A quantitative microscopic interpretation of this effect is still missing; nevertheless it is obvious that the thermally activated exchange jumps of Mg^{2+} and Ga^{3+} ions which are responsible for the DSC effect are also the origin of increased thermal conductivity. With other words: heat can be transported in solids not only by phonons and electrons, but in the spinel structure also by moving ions. These results also have been published in Crystal Research & Technology [9].

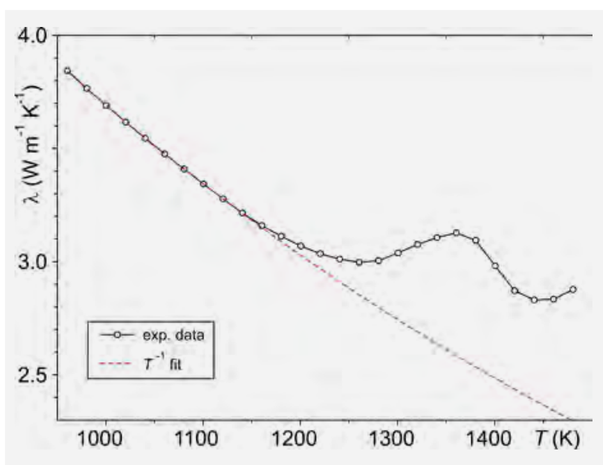

Fig. 4
Experimental data for the thermal conductivity of $MgGa_2O_4$ and a T^{-1} fit for values below 1150 K (red dashed line) [7].

References

[1] J.H. Haeni, P. Irvin, W. Chang, R. Uecker, P. Reiche, Y.L. Li, S. Choudhury, W. Tian, M. E. Hawley, B. Craigo, A. K. Tagantsev, X. Q. Pan, S. K. Streiffer, L. Q. Chen, S. W. Kirchoefer, J. Levy, D. G. Schlom; Nature 430 (2004) 758

[2] R. Uecker, B. Velickov, D. Klimm, R. Bertram, M. Bernhagen, M. Rabe, M. Albrecht, R. Fornari, D.G. Schlom; J. Cryst. Growth 310 (2008) 2649

[3] R. Uecker, D. Klimm, R. Bertram, M. Bernhagen, I. Schulze-Jonack, M. Brützam, A. Kwasniewski, Th. M. Gesing, D.G. Schlom; Acta Phys. Pol. A 124 (2013) 295

[4] M. Klupsch; *Untersuchungen zur Phasenbildung von Perowskiten im System La_2O_3-Lu_2O_3-Sc_2O_3*; BSc-Arbeit, Humboldt-Universität zu Berlin (2015)

[5] J.M. Badie; *Phases et Transitions de Phases À Haute Température Dans Les Systèmes Sc_2O_3-Ln_2O_3 (Ln = Lanthanide et Yttrium)*; Rev. Int. Hautes Temp. Réfract, Fr. 15 (1978) 183

[6] R. Uecker, R. Bertram, M. Brützam, Z. Galazka, T.M. Gesing, C. Guguschev, D. Klimm, M. Klupsch, A. Kwasniewski, D.G. Schlom; *Large-lattice-parameter perovskite single-crystal substrates*, J. Cryst. Growth (2016, in print) doi:10.1016/j.jcrysgro.2016.03.014

[7] N.L. Schwarz; *Thermische Eigenschaften des Spinells $MgGa_2O_4$ und deren möglicher Zusammenhang mit dem Inversionsgrad*; BSc-Arbeit, Humboldt-Universität zu Berlin (2016)

[8] A.M. Hofmeister; Phys. Chem. Miner. 33 (2006) 45

[9] L. Schwarz, Z. Galazka, T. M. Gesing, D. Klimm; Cryst. Res.Technol. 50 (2015) 961

Simulation & Characterization:
Crystal Machining

Head Dr. Uta Juda
Team M. Imming-Friedland, V. Lange, Th. Wurche

Überblick

Zu den Hauptaufgaben der Themengruppe Kristallbearbeitung gehören
- *die Probenpräparation für die Routinediagnostik der im Haus gezüchteten Kristalle,*
- *die Bereitstellung kristallographisch orientierter Keime und Substrate für die Kristallzüchtung,*
- *die Entwicklung von Präparationstechnologien für den Wafer-Herstellungsprozess (Trennen und Polieren) speziell für neue am Institut gezüchtete Materialien und*
- *Übernahme von Serviceaufgaben bzw. Sonderanfertigungen für Universitäten, für die Industrie und Forschungseinrichtungen.*

Die enge personelle und gerätetechnische Vernetzung mit der Themengruppe Physikalische Charakterisierung ermöglicht einen schnellen Zugriff auf Methoden der Oberflächencharakterisierung und erlaubt neben den täglichen Routineaufgaben auch die Betrachtung von wissenschaftlichen Aspekten der Probenpräparation.

Die Bearbeitung von Halbleitermaterialien und Kristallen für optische Anwendungen, für die Charakterisierung oder die Herstellung von Substraten für die Epitaxie erfordert meist eine hohe Präzision und damit eine entsprechende Anlagentechnik. Unabhängig von Material oder Verwendungszweck durchläuft jede Probe bzw. jeder Wafer bis zur Fertigstellung verschiedene Arbeitsschritte. Diese beinhalten Formatieren und Trennen des Kristalls in Wafer und anschließende Oberflächenpräparation mittels verschiedener Schleif-, Läpp- und Polierprozesse. Die bei uns zur Verfügung stehenden Methoden umfassen:

- *röntgenografisches Orientieren von Kristallen*
- *Trennschleifen von Kristallen und Wafern mit verschiedenen Verfahren – Diamantdraht-, Multidiamantdraht- und Diamant-Innentrennsägen*
- *Flachschleifen mit Diamantwerkzeugen*
- *Läppen und Polieren mit verschiedenen Abrasiven (Aluminiumoxid, Ceroxid, Siliciumcarbid, Borcarbid, Diamant unterschiedlichster Korngrößen) und Suspensionen*
- *mechanisches und chemo-mechanisches Polieren mit Präzisionspoliermaschinen*
- *Oberflächencharakterisierung mittels Lichtmikroskopie, Konfokalmikroskopie (CFM), Atomkraftmikroskopie (AFM), Rasterelektronenmikroskopie (REM) und diversen röntgenografischen Methoden*
- *Bestimmung von geometrischen Oberflächenparametern wie Durchbiegung, Ebenheit, Parallelität und Oberflächenrauigkeit mittels Weißlicht-Sensor kombiniert mit einem Konfokalmikroskop.*

Die entsprechende anlagentechnische Ausstattung und fachliche Kompetenz aller Mitarbeiter macht es möglich, anspruchsvolle Service- und Forschungsaufgaben für die Industrie, für Hochschulen und außeruniversitäre Forschungseinrichtungen zu übernehmen, die von der Präparation spezieller Proben bis zur Entwicklung von Bearbeitungstechnologien inklusive der Erstellung zugehöriger Dokumentationen reichen. Daneben können auch Sonderanfertigungen mit speziellen Anforderungen an Geometrie und Oberflächenqualität kurzfristig und in hoher Qualität hergestellt werden.

Overview

Main tasks of the work of the crystal machining group are

- sample preparation for routine characterization of the in-house grown crystals,
- preparation of seed crystals and substrates with a very precise orientation for use in crystal growth,
- development of preparation processes for wafering (sawing and polishing) of crystalline materials mainly for new materials grown at the institute and
- Service for universities, industrial customers and research institutions.

The intensive cooperation with the characterization group by a personal- and device-related network enables us to check the surface quality and contributes to a more scientific approach to crystal machining.

The preparation of crystals for semiconductor and optical applications, for diagnostics or as substrates for epitaxial processes requires high-precision machining. Whatever the application or material, each sample or wafer undergoes several stages during manufacture, which include formatting, slicing the wafer from the crystal and preparing the surface using different grinding, lapping and polishing techniques. The methods used in our group include

- crystal orientation using x-ray techniques,
- crystal cutting and wafering by different methods – single and multi diamond wire and inner diameter diamond sawing,
- wafer grinding with diamond tools,
- wafer lapping and polishing with various abrasives (aluminum oxide, cerium oxide, silicon carbide, boron carbide, diamond) in different particle sizes and suspensions,
- mechanical and chemo-mechanical polishing with high precision polishing machines,
- surface characterization by light microscopy, confocal microscopy (CFM), atomic force microscopy (AFM), scanning electron microscopy (REM) and x-ray techniques,
- determination of standard wafer geometry and surface parameters like bow, evenness, parallelism and roughness using a white light interferometer probe combined with a confocal microscope.

The available equipment and the experience and proficiency of all staff members enable us to supply custom-made samples and to accomplish ambitious service and research orders from industry, universities and other research institutions, ranging from the fabrication of machined samples to the development of technologies and related documentations. Special demands on geometry and surface quality of various samples could be fulfilled in short time and with high quality.

Results

As in the last years the major tasks had been to develop preparation technologies for new materials grown at our institute, with main focus on aluminum nitride (AlN) and some oxides. The aim of this work is to prepare epi-ready surfaces for epitaxial growth using a suitable chemo-mechanical polishing (CMP) method including a high quality mechanical pre-polishing. In 2015 the experiments on the polishing of varied orientated AlN surfaces have already been successful. As a result of our CMP, scratch-free c- and m-plane AlN surfaces of high quality with a roughness value of 0.05 nm (root mean square, RMS) over large areas could be prepared. In addition, we found that a basic requirement for successful CMP is also a high-quality mechanical pre-polish which differs on surfaces with similar orientation.

In order to proof whether the surface has epi-ready quality these samples were used as substrates for homo-epitaxial layer deposition. In the last time a good layer quality has been obtained which suggests an excellent CMP. Based on these results and depending on the availability of samples, the mechanical (and also chemo-mechanical) polishing of AlN surfaces will be optimized with respect to quality and preparation time.

Another ambitious challenge has been the development of a preparation technology for Ga_2O_3 again to achieve an epi-ready state. Different experiments on chemo-mechanical polishing were performed with different polishing fluids and varying process parameters like pressure, velocity of plate- and carrier rotation, polishing time, mixture and pH-value of polishing fluid, flow rate of the slurry and the type of polishing pad. First results show surfaces without scratches and no significant edge roll off.

On the other hand we found that cutting and mechanical polishing proves to be particularly challenging because of the strong cleavage property of the surface to be polished. These preparation steps will be investigated more intensive.

Appendix

104 Publications

106 Talks and Posters

112 Patents

114 Teaching and Education

116 Membership in Committees

117 Guest Scientists

118 Colloquia

119 External Funding

Appendix: **Publications**

Articles in books

M. Bickermann; *Growth and Properties of Bulk AlN Substrates*; in: M. Kneissl and J. Rass (eds.), III-Nitride Ultraviolet Emitters – Technology & Applications, Springer Series in Material Science 227 (2015), Chapter 2, 27-46

Articles in international peer reviewed journals

H. Ch. Alt, H. E. Wagner, A. Glacki, Ch. Frank-Rotsch, V. Häublein; *Isotopic study of mid-infrared vibrational modes in GaAs related to carbon and nitrogen impurities;* Phys. Status Solidi B **252** (2015) 1827-1831

A. V. Andrianov, A. O. Zakhar'in, R. Kh. Zhukavin, V. N. Shastin, N. V. Abosimov, A. V. Bobylev; *Terahertz intracenter photoluminescence of silicon with lithium at interband excitation;* JETP Letters, Optics and Laser Physics **100** (2015) 771-775

M. Baldini, M. Albrecht, D. Gogova, R. Schewski, G. Wagner; *Effect of indium as a surfactant in $(Ga_{1-x}In_x)_2O_3$ epitaxial growth on β-Ga_2O_3 by metal organic vapour phase epitaxy;* Semicond. Sci. Technol. **30** (2015) 024013

R. Bansen, R. Heimburger, J. Schmidtbauer, T. Teubner, T. Markurt, C. Ehlers, T. Boeck; *Crystalline silicon on glass by steady-state solution growth using indium as solvent;* Appl. Phys. A; **119** (2015) 1577-1586

S. Bin Anooz, P. Petrik, M. Schmidbauer, T. Remmele, J. Schwarzkopf; *Refractive index and interband transitions in strain modified $NaNbO_3$ thin films grown by MOCVD;* J. Phys. D: Appl. Phys. **48** (2015) 385303

G. Callsen, Gerald M. O. Pahn, S. Kalinowski, C. Kindel, J. Settke, J. Brunnmeier, C. Nenstiel, T. Kure, F. Nippert, A. Schliwa, A. Hoffmann, T. Markurt, T. Schulz, M. Albrecht, S. Kako, M. Arita, Y. Arakawa; *Analysis of the exciton–LO-phonon coupling in single wurtzite GaN quantum dots;* Phys. Rev. B; **92** (2015) 235439

S. Dadgostar, E. H. Hussein, J. Schmidtbauer, T. Boeck, F. Hatami, W. T. Masselink; *Structural properties of AlGaP films on GaP grown by gas-source molecular-beam epitaxy;* J. Cryst. Growth **425** (2015) 94-98

N. Deßmann, S.G. Pavlov, A. Pohl, N.V. Abrosimov, S. Winnerl, M. Mittendorff, R.Kh. Zhukavin, V.V. Tsyplenkov, D.V. Shengurov, V.N. Shastin, H.-W. Hübers; *Lifetime-limited, subnanosecond terahertz germanium photoconductive detectors;* Appl. Phys. Lett. **106** (2015) 171109

N. Dropka, Ch. Frank-Rotsch; *Enhanced VGF growth of single- and multi-crystalline semiconductors using pulsed TMF;* Magnetohydrodynamics **51** (2015) 149-156

Z. Galazka, D. Klimm, K. Irmscher, R. Uecker, M. Pietsch, R. Bertram, M. Naumann, M. Albrecht, A. Kwasniewski, R. Schewski, M. Bickermann; *$MgGa_2O_4$ as a new wide bandgap transparent semiconducting oxide: Growth and properties of bulk single crystals;* Phys. Status Solidi A **212** (2015) 1455-1460

D. Gogova, M. Schmidbauer, A. Kwasniewski; *Homo- and heteroepitaxial growth of Sn-doped β-Ga_2O_3 layers by MOVPE;* CrystEngComm **17** (2015) 6744-6752

S. Gu, Y. Lu, J. Kaiser, M. Albrecht, M. Ballauff; *Kinetic analysis of the reduction of 4-nitrophenol catalyzed by Au/Pd nanoalloys immobilized in spherical polyelectrolyte brushes;* Phys. Chem. Chem. Phys. **17** (2015) 28137-28143

C. Guguschev, Z. Galazka , D. J. Kok , U. Juda , A. Kwasniewski, R. Uecker ; *Growth of $SrTiO_3$ bulk single crystals using edge-defined film-fed growth and the Czochralski methods;* CrystEngComm **17** (2015) 4662-4668

C. Guguschev, D. J. Kok, Z. Galazka, D. Klimm, R. Uecker, R. Bertram, M. Naumann , U. Juda, A. Kwasniewski, M. Bickermann; *Influence of oxygen partial pressure on $SrTiO_3$ bulk crystal growth from non-stoichiometric melts;* CrystEngComm **17** (2015) 3224-3234

C. Guguschev, R. Tagle, U. Juda, A. Kwasniewski; *Microstructural investigations of $SrTiO_3$ single crystals and polysilicon using a powerful new X-ray diffraction surface mapping technique;* J. Appl. Cryst. **48** (2015) 1883-1888

M. Handwerg, R. Mitdank, Z. Galazka, S. F. Fischer; *Temperature-dependent thermal conductivity in Mg-doped and undoped β-Ga_2O_3 bulk-crystals;* Semicond. Sci. Technol. **30** (2015) 024006

S. Höfer, R. Uecker, A. Kwasniewski, J. Popp, T.G. Mayerhöfer; *Dispersion analysis of arbitrarily cut uniaxial crystals;* Vib. Spectrosc **78** (2015) 23-33

S. Höfer, R. Uecker, A. Kwasniewski, J. Popp, T.G. Mayerhöfer; *Complete dispersion analysis of single crystal neodymium gallate;* Vib. Spectrosc **78** (2015) 17-22

D. Kojda, R. Mitdank, M. Handwerg, A. Mogilatenko, M. Albrecht, Z. Wang, J. Ruhhammer, M. Kroener, P. Woias, S. F. Fischer; *Temperature-dependent thermoelectric properties of individual silver nanowires;* Phys. Rev. B **91** (2015) 024302

D. J. Kok, K. Irmscher, M. Naumann, C. Guguschev, Z. Galazka, R. Uecker; *Temperature-dependent optical absorption of $SrTiO_3$;* Phys. Status Solidi A **212** (2015) 1880-1887

E. Korhonen, F. Tuomisto, D. Gogova, G. Wagner, M. Baldini, Z. Galazka, R. Schewski, M. Albrecht; *Electrical compensation by Ga vacancies in Ga_2O_3 thin films*; Appl. Phys. Lett. **106** (2015) 242103

Appendix: **Publications**

E. Korhonen, V. Prozheeva, F. Tuomisto, O. Bierwagen, J. S. Speck, M. E. White, Z. Galazka, H. Liu, N. Izyumskaya, V. Avrutin, Ü. Özgür, H. Morkoç; *Cation vacancies and electrical compensation in Sb-doped thin-film SnO_2 and ZnO;* Semicond. Sci. Technol. **30** (2015) 024011

K.A. Kovalevsky, N.V. Abrosimov, R.Kh. Zhukavin, S.G. Pavlov, H.-W. Hübers, V.V. Tsyplenkov, V.N. Shastin; *Terahertz lasers based on intracentre transitions of group V donors in uniaxially deformed silicon;* Quantum Electronics **45** (2015) 113-120

P. W. Metz, D.-T. Marzahl, C. Guguschev, R. Bertram, C. Kränkel, G. Huber; *Growth and diode-pumped laser operation of Pr^{3+}:β-($Y_{0.5}$,$Gd_{0.5}$)F_3 at various transitions;* Opt. Lett. **40** (2015) 2699-2702

F. Meurer, M. Neubert, N. Werner; *Nonlinear state estimation for the Czochralski process based on the weighing signal using an extended Kalman filter;* J. Cryst. Growth **419** (2015) 57-63

R. Lo Nardo, G. Wolfowicz, S. Simmons, A.M. Tyryshkin, H. Riemann, N.V. Abrosimov, P. Becker, H.-J. Pohl, M. Steger, S.A. Lyon, M.L.W. Thewalt, J.J.L. Morton; *Spin relaxation and donor-acceptor recombination of Se^+ in 28-silicon;* Phys. Rev. B **92** (2015) 165201

A. Navarro-Quezada, Z. Galazka, S. Alamé, D. Skuridina, P. Vogt, N. Esser; *Surface properties of annealed semiconducting β-Ga_2O_3 (100) single crystals for epitaxy;* Appl. Surf. Sci. **349** (2015) 368-373

A. Navarro-Quezada, S. Alamé, N. Esser, J. Furthmüller, F. Bechstedt, Z. Galazka, D. Skuridina, P. Vogt; *Near valence-band electronic structure of semiconducting β-Ga_2O_3 (100) single crystals;* Phys. Rev. B **92** (2015) 195306

A. Papadogianni, M. E. White, J. S. Speck, Z. Galazka, O. Bierwagen; *Hall and Seebeck measurements estimate the thickness of a (buried) carrier system: Identifying interface electrons in In-doped SnO_2 films*; Appl. Phys. Lett. **107** (2015) 252105

K. Saeedi, M. Szech, P. Dluhy, J.Z. Salvail, K.J. Morse, H. Riemann, N.V. Abrosimov, N. Nötzel, K.L. Litvinenko, B.N. Murdin, M.L.W. Thewalt; *Optical pumping and readout of bismuth hyperfine states in silicon for atomic clock applications;* Sci. Rep. **5** (2015) 10493

J. Z. Salvail, P. Dluhy, K. J. Morse, M. Szech, K. Saeedi, J. Huber, H. Riemann, N. V. Abrosimov, P. Becker, H.-J. Pohl, M. L. W. Thewalt; *Optically enabled magnetic resonance study of ^{75}As and ^{121}Sb in ^{28}Si;* Phys. Rev. B **92** (2015) 195203-1 – 195203-11

M. Sawicka, C. Chèze, H. Turski, J. Smalc-Koziorowska, M. Kryśko, S. Kret, T. Remmele, M. Albrecht, G. Cywiński, I. Grzegory, C. Skierbiszewskia; *Growth mechanisms in semipolar (20(2)over-bar1) and nonpolar m plane (10(1)over-bar0) AlGaN/GaN structures grown by PAMBE under N-rich conditions;* J. Cryst. Growth **415** (2015) 176

R. Schewski, G. Wagner, M. Baldini, D. Gogova, Z. Galazka, T. Schulz, T. Remmele, T. Markurt, H. von Wenckstern, M. Grundmann, O. Bierwagen, P. Vogt, M. Albrecht; *Epitaxial stabilization of pseudomorphic α-Ga_2O_3 on sapphire (0001);* Appl. Phys. Express **8** (2015) 011101

G. Scholz, M. Dreger, R. Bertram, E. Kemnitz; *Nanoscopic yttrium oxide fluorides: non-aqueous fluorolytic sol-gel synthesis and structural insights by 19F and 89Y NMR;* Dalton Transactions **44** (2015) 13522-13529

L. Schwarz, Z. Galazka, T. M. Gesing, D. Klimm; *On the influence of inversion on thermal properties of magnesium gallium spinel*; Cryst. Res. Technol. **12** (2015) 961–966

P. G. Sennikov, R. A. Kornev, N. V. Abrosimov; *Production of stable silicon and germanium isotopes via their enriched volatile compounds;* J. Radioanal. Nucl. Chem. **306** (2015) 21-30

G. Wang, M. Amman, H. Mei, D. Mei, K. Irmscher, Y. Guan, G. Yang; *Crystal growth and detector performance of large size high-purity Ge crystals;* Mater. Sci. Semicond. Process. **39** (2015) 54-60

F. Willems, C. Smeenk, N. Zhavoronkov, O. Kornilov, I. Radu, M. Schmidbauer, M. Hanke, C. von Korff Schmising, M.J.J. Vrakking, S. Eisebitt; *Probing Ultrafast Spin Dynamics with High-Harmonic Magnetic Circular Dichroism Spectroscopy;* Phys. Rev. B **92** (2015) 220405

R. Kh. Zhukavin, K.A. Kovalevsky, M.L. Orlov, V.V. Tsyplenkov, N.A. Bekin, A.N. Yablonskiy, P.A. Yunin, S.G. Pavlov, N.V. Abrosimov, H.-W. Hübers, H.H. Radamson, V.N. Shastin; *Terahertz-range spontaneous emission under the optical excitation of donors in uniaxially stressed bulk silicon and SiGe/Si heterostructures;* Semiconductors **49** (2015) 13-18

Articles in conference proceedings

N. Dropka, T. Ervik, F.M. Kiessling; *Scale-up of DS-silicon growth process under TMF*; Proceedings of 8th Intern. conference on electro-magnetic processing of materials (EPM 2015) Cannes, France (2015) 129 -132

S.G. Pavlov, N. Deßmann, A. Pohl, N.V. Abrosimov, M. Mittendorff, S.Winnerl, R.Kh. Zhukavin, V.V. Tsyplenkov, D.V. Shengurov, V.N. Shastin, H.-W. Hübers; *Towards a life-time-limited 8-octave-infrared photoconductive germanium detector;* J. Phys: Conf. **647** (2015) 012070

Other publications

R. Bertram; Analyse von Kristallen mit ETV-ICP OES; TM – Technisches Messen 82 (2015) 339-344

Appendix: **Talks and Posters**

Invited talks at national and international conferences

N.V. Abrosimov; *Preparation of structually perfect Silicon and Germanium crystals with high chemical and isotopical purity;* XVth Russian conference: High purity substances and materials: Preparation, Analysis, Application; Nizhny Novgorod, Russia; May 2015

N.V. Abrosimov; *Crystal growth and application of isotopically enriched Silicon and Germanium;* 5th Sino-German Symposium: The Silicon age: Silicon and related IV group Semiconductor Materials; Hangzhou, People's Republic of China; August/September 2015

M. Albrecht (Keynote lecture); Polarity control in III-Nitrides – New insights into an old problem: M. Albrecht, S. Mohn, N. Stolyarchuk, T. Markurt, R. Kirste, M. P. Hoffmann, R. Collazo, P. Vennegues, R. Di Felice, Z. Sitar; International Symposium on Growth of Nitride Semiconductors (ISGN-6); Hamamatsu, Japan; November 2015

M. Albrecht; *Radiative and non-radiative recombination at threading dislocations in group III-Nitrides:* M. Albrecht, L. Lymperakis, J. Neugebauer; MRS Spring Meeting; San Francisco, USA; April 2015

M. Albrecht; *Structural and optical properties of dislocations in III-nitrides:* M. Albrecht, L. Lymperakis, J. Neugebauer, J. Weyher, I Grzegory, S. Porowski; 28th International Conference on Defects of Semiconductors (ICDS 2015); Helsinki, Finland; July 2015

M. Bickermann; *Deep UV transparent AlN substrates with high crystalline perfection for optoelectronic devices:* M. Bickermann, C. Hartmann, J. Wollweber, S. Kollowa, A. Dittmar, T. Schulz, A. Kwasniewski, F. Langhans, U. Juda, K. Irmscher, M. Albrecht; 6th International Symposium on the Growth of Nitrides (ISGN-6); Hamamatsu, Japan; November 2015

M. Bickermann; *Bulk Aluminium Nitride Substrates Tailored for Electronic Applications:* M. Bickermann, C. Hartmann, A. Dittmar, F. Langhans, S. Kollowa, T. Schulz, M. Naumann, A. Kwasniewski, K. Irmscher, J. Wollweber; E-MRS 2015 Fall Meeting; Warsaw, Poland; September 2015

M. Bickermann; *Tailoring electrical and optical properties of AlN during seeded AlN bulk growth:* M. Bickermann, C. Hartmann, A. Dittmar, F. Langhans, S. Kollowa, M. Naumann, K. Irmscher, J. Wollweber; 9th International Workshop on Bulk Nitride Semiconductors (IWBNS IX); Wonju, South Korea; November 2015

M. Bickermann; *Preparation and properties of bulk aluminum nitride (AlN) crystals and substrates;* 39th International Conference and Exposition on Advanced Ceramics and Composites (ICACC 15); Daytona Beach, Florida, USA; January 2015

N. Dropka; *Scale up of DS- and Cz-silicon growth processes under TMF:* N. Dropka, T. Ervik, M. Czupalla, F. M. Kiessling; 20th American Conference on Crystal Growth and Epitaxy (ACCGE-20) and 17th U.S. Biennial Workshop on Organometallic Vapor Phase Epitaxy (OMVPE-17); Big Sky, Montana, USA; August 2015

Z. Galazka; *Bulk crystal growth and properties of transparent semiconducting sesquioxides: β-Ga_2O_3 and In_2O_3;* DKT 2015, Deutsche Kristallzüchtertagung; Frankfurt/Main, Germany; March 2015

Z. Galazka; *Bulk growth and properties of high quality β-Ga_2O_3, In_2O_3 and SnO_2 single crystals:* Z. Galazka; K. Irmscher, R. Uecker, D. Klimm, M. Pietsch, M. Albrecht, M. Naumann, A. Kwasniewski, T. Schulz, R. Schewski, M. Bickermann; International Workshop on Gallium Oxide and Related Materials (IWGO 2015); Kyoto, Japan; November 2015

C. Guguschev; *$SrTiO_3$ bulk crystal growth from melt $SrTiO_3$ bulk crystal growth:* C. Guguschev, R. Uecker, Z. Galazka, D. J. Kok, D. Klimm, R. Bertram, M. Naumann, U. Juda, A. Kwasniewski, M. Bickermann; 20th American Conference on Crystal Growth and Epitaxy (ACCGE-20) and 17th U.S. Biennial Workshop on Organometallic Vapor Phase Epitaxy (OMVPE-17) and The Second 2D Electronic Materials Symposium; Big Sky, Montana, USA; August 2015

C. Guguschev; *Influence of oxygen partial pressure on $SrTiO_3$ crystal growth from non-stoichiometric melt:* C. Guguschev, D. Kok, Z. Galazka, A. Kwasniewski, U. Juda, R. Uecker; 39th International Conference and Exposition on Advanced Ceramics and Composites (ICACC 15); Daytona Beach, Florida, USA; January 2015

D. Klimm; *Thermodynamics and Phase Diagrams in Crystal Growth;* European School on Crystal Growth (ESCG 5); Bologna, Italy; September 2015

D. Klimm; *Gasphasengleichgewichte in der Kristallzüchtung;* DGKK-AK: Industrielle Kristallzüchtung; Freiberg, Germany; November 2015

D. Klimm; *Reactive atmospheres for oxide crystal growth;* 39th International Conference and Exposition on Advanced Ceramics and Composites (ICACC 15); Daytona Beach, Florida, USA; January 2015

D. Klimm; *A Suitable Tool for Understanding Gas-Phase Equilibria in Crystal Growth;* 6th Coupling Days on Hyphenated Techniques (SKT 2015), Selber Kopplungstage; Selb, Germany; April 2015

Appendix: **Talks and Posters**

W. Miller; *Epitaxial Growth of oxide layers - contributions of DFT and KMC calculations for understanding the kinetic;* SimGrow 2015, Schloss Rauischholzhausen, Germany; November 2015

W. Miller; R*outine and Challenges in Modeling Bulk Crystal Growth;* 8th International Workshop on Modeling in Crystal Growth (IWMCG-8); Spa, Belgium; November 2015

T. Schulz; *Intra-plane ordering in (In,Ga)N monolayers:* T. Schulz, M. Anikeeva, T. Markurt, M. Albrecht, C. Freysoldt, L. Lymperakis, J. Neugebauer, X.T. Zheng, D.Y. Ma, X.Q. Wang; International Conference on Nitride Semiconductors (ICNS-11), Beijing, Japan; August/ September 2015

R. Uecker (Keynote lecture); A new large-lattice-constant perovskite substrate crystal: R. Uecker, D. Klimm, R. Bertram, C. Guguschev, M. Brützam, A. Kwasniewski, M. Klupsch, T. M. Gesing, D. G. Schlom; Fifth European Conference on Crystal Growth (ECCG-5); Bologna, Italy; September 2015

Invited seminars at national and international institutions

R. Bertram; *ETV-ICP OES - eine kritische Bilanz;* 5. Anwenderseminar - Direkte Feststofftechniken; Freiberg, Germany; September 2015

Z. Galazka; Transparent semiconducting oxides – bulk single crystals and properties of β-Ga_2O_3, In_2O_3, SnO_2 and $MgGa_2O_4$; Seminar at Air Force Research Lab (AFRL); Dayton, USA; May 2015

C. Guguschev; *Growth of high perfection bulk $SrTiO_3$ single crystals by Czochralski, EFG and TSSG methods:* C. Guguschev, R. Uecker, Z. Galazka, D.J. Kok, D. Klimm, R. Bertram, M. Naumann, U. Juda, A. Kwasniewski, M. Bickermann; Max-Planck-Institut für Festkörperforschung; Stuttgart, July 2015

C. Guguschev; *Growth of high perfection bulk $SrTiO_3$ single crystals by Czochralski, EFG and TSSG methods:* C. Guguschev, R. Uecker, Z. Galazka, D. J. Kok, D. Klimm, R. Bertram, M. Naumann, U. Juda, A. Kwasniewski, M. Bickermann; Universität Hamburg, Institut für Laser-Physik; April 2015

G. Wagner; *Ga_2O_3 layers grown by metal organic vapour phase epitaxy;* Otto-von-Guericke Universität Magdeburg, Institut für experimentelle Physik, November 2015

Oral contributions at national and international conferences and workshops

M. Albrecht; *Aspects of heteroepitaxial growth and strain relaxation of Group III-Nitrides;* Tutorial Lectures SPRInG Meeting; Berlin, Germany; March 2015

M. Baldini; *Semiconducting Sn-doped Ga_2O_3 layers grown by Metal Organic Vapor Phase Epitaxy*: M. Baldini, K. Irmscher, A. Fiedler, R. Schewski, G. Wagner; International Workshop on Gallium Oxide and Related Materials (IWGO 2015); Kyoto, Japan; November 2015

M. Baldini; *Ga_2O_3 layers grown by metal organic vapor phase epitaxy with two different Ga and O precursors*: M. Baldini, G. Wagner, D. Gogova; MRS Spring Meeting; San Francisco, California, USA; April 2015

M. Bickermann; *Theorie und Praxis der Züchtung von AlN-Einkristallen bei Temperaturen über 2000°C;* Technischen Universität Berlin, Chemie, AC-Fachkolloquium; Germany; January 2015

M. Bickermann; *Preparation and properties of bulk aluminum nitride (AlN) crystals and substrates;* North Carolina State University (NCSU), Department Materials Science & Engineering; USA; January 2015

M. Bickermann; *Preparation of Oxide, Dielectric, and Laser Crystals at the Leibniz-Institute for Crystal Growth (IKZ) Berlin;* 4th French-German Workshop on Oxide, Dielectrics and Laser Crystals; Saint-Louis, France; September 2015

M. Bickermann; *Bulk AlN Substrates for Deep-UV Optoelectronic Applications:* M. Bickermann, C. Hartmann, A. Dittmar, F. Langhans, S. Kollowa, M. Naumann, K. Irmscher, J. Wollweber; DGKK-Arbeitskreis "Epitaxie von III-V-Halbleitern"; Göttingen, Germany; December 2015

T. Boeck; *CIGSe Microconcentrator and Crystalline Si Solar Cells on Low Cost Substrates:* T. Boeck, F. Ringleb, R. Bansen, C. Ehlers, T. Teubner; EU-Projekt CHEETAH, General Assembly; Chambery, France; January 2015

D. Braun; *Domain structure in anisotropically strained $K_{0.75}Na_{0.25}NbO_3$ thin films on $TbScO_3$*: D. Braun, J. Schwarzkopf, A. Kwasniewski, P. Müller, M. Schmidbauer; DPG-Frühjahrstagung; Berlin, Germany; March 2015

D. Braun; *Formation and switching behavior of monoclinic domains in strained $K_{0.90}Na_{0.10}NbO_3$ epitaxial thin films on $NdScO_3$*: D. Braun, M. Schmidbauer, A. Kwasniewski, P. Müller, J. Sellmann, M. Hanke, H. Renevier, J. Schwarzkopf; 13th European Meeting on Ferroelectricity (EMF); Porto, Portugal; June/July 2015

Appendix: **Talks and Posters**

D. Braun (lecturer M. Schmidbauer; *Complex domain structure in anisotropically strained $K_{0.90}Na_{0.10}NbO_3$ thin films on $NdScO_3$*: D. Braun, M. Schmidbauer, A. Kwasniewski, P. Müller, J. Sellmann, M. Hanke, H. Renevier, J. Schwarzkopf; EMRS Spring Meeting, European Materials Research Society; Lille, France; May 2015

C. Ehlers; *Growth and Properties of Crystalline Silicon deposited on Glass by Steady-State Solution Growth*: C. Ehlers, R. Bansen, J. Schmidtbauer, F. Ringleb, T. Teubner, T. Boeck; DPG-Frühjahrstagung, Sektion Kondensierte Materie (SKM); Berlin, Germany; March 2015

C. Ehlers; *Growth and Properties of Crystalline Silicon deposited on Glass, Silicon and Porous Silicon by Steady-State Solution Growth:* C. Ehlers, R. Bansen, T. Teubner, T. Boeck; EU-Projektt CHEETAH; Trondheim, Norway; July 2015

N. Dropka; *Scale-up of DS-silicon growth process under TMF:* N. Dropka, T. Ervik, F.M. Kiessling; 8th International Conference on Electromagnetic Processing of Materials (EPM 2015); Cannes, France; October 2015

N. Dropka; *Travelling magnetic fields in directional solidification of silicon: from lab-scale tests to commercial size equipment:* N. Dropka, T. Ervik, F.M. Kiessling; DGKK-Workshop „Herstellung und Charakterisierung von massiven Halbleiterkristallen"; Berlin, Germany; October 2015

N. Dropka; *Enhanced homogeneity of Sb doped VGF-Ge crystals using mechanical vibrations and traveling magnetic fields*: N. Dropka, Ch. Frank-Rotsch; The 8th International Workshop on Modeling in Crystal Growth (IWMCG-8); Spa, Belgium; November 2015

A. Fiedler; *Electrical and optical characterization of homoepitaxial β-Ga_2O_3layers grown by metal organic vapor phase epitaxy:* A. Fiedler, K. Irmscher, R. Schewski, M. Albrecht, M. Baldini, G. Wagner; Graduate Student Workshop on Transparent Conducting Oxide Semiconductors; Humboldt-Universität zu Berlin, Germany; November 2015

Ch. Frank-Rotsch; *Enhancement of GaAs VGF process using a heater magnet module*: Ch. Frank-Rotsch, N. Dropka, A. Glacki, U.Juda; 20th American Conference on Crystal Growth and Epitaxy (ACCGE-20) and 17th U.S. Biennial Workshop on Organometallic Vapor Phase Epitaxy (OMVPE-17); Big Sky, Montana, USA; August 2015

Z. Galazka; *Bulk single crystals and properties of transparent semiconducting oxides: β-Ga_2O_3, In_2O_3, SnO_2 and $MgGa_2O_4$*: Z. Galazka, R. Uecker, K. Irmscher, D. Klimm, M. Pietsch, M. Albrecht, A. Kwasniewski, M. Naumann, R. Schewski, M. Bickermann; 20th American Conference on Crystal Growth and Epitaxy (ACCGE-20); Big Sky, Montana, USA; August 2015

C. Hartmann; *Growth and characterization of bulk AlN crystals with optimized optical and electrical properties:* C. Hartmann, A. Dittmar, S. Kollowa, K. Irmscher, M. Naumann, F. Langhans, J. Wollweber, M. Bickermann; Deutsche Kristallzüchtungstagung (DKT 2015); Frankfurt/Main, Germany; March 2015

K. Eylers; *Photoluminescence Spectroscopy for CIGSe Microislands Characterization:* K. Eylers, F. Ringleb, T. Teubner, T. Boeck; HZB, BAM, IKZ Workshop; Berlin, Germany; October 2015

S. Kayser; *Novel Study of Lateral Photovoltage Scanning- (LPS) and Scanning Photoluminescence (SPL) Method:* S. Kayser, A. Lüdge; Deutsche Kristallzüchtungstagung (DKT 2015); Frankfurt/Main, Germany; March 2015

D.J. Kok; *Temperature dependent absorption of strontium titanate:* D.J. Kok, K. Irmscher, M. Naumann, C. Guguschev, Z. Galazka, R. Uecker; Deutsche Kristallzüchtungstagung (DKT 2015); Frankfurt/Main, Germany; March 2015

S. Kollowa; *Silicon doped AlN bulk crystals:* S. Kollowa, A. Dittmar, C. Hartmann, K. Irmscher, F. Langhans, M. Pietsch, J. Wollweber, M. Bickermann; Deutsche Kristallzüchtungstagung (DKT 2015); Frankfurt/Main, Germany; March 2015

S. Kollowa; *Silicon doped AlN bulk crystals:* S. Kollowa, A. Dittmar, C. Hartmann, K. Irmscher, F. Langhans, M. Pietsch, J. Wollweber, M. Bickermann; Technische Universität Berlin, AG Kneissl; Berlin, Germany; February 2015

F. Langhans; *Dislocation processes in AlN bulk crystals analyzed by laser scattering tomography*: F. Langhans, M. Naumann, C. Hartmann, T. Markurt, J. Wollweber, L. Kirste, A. Dittmar, S. Kollowa, M. Bickermann, M. Albrecht; Deutsche Kristallzüchtungstagung (DKT 2015); Frankfurt/Main, Germany; March 2015

T. Markurt; *Investigation of dislocations in GaN by Transmission electron microscopy and laser scattering tomography;* GaN Characterization Workshop; Weigmannsdorf, Germany; July 2015

R. Menzel; *Experimental investigations for an alternative crucible-free growth method for Si single crystals:* R. Menzel, H.-J. Rost, J. Fischer, M. Renner; 8th International Workshop on Crystalline Silicon for Solar Cells (CSSC-8); Bamberg, Germany; May 2015

R. Menzel; *Simulation of fluid flow during Si single crystal growth from melt in a Si granular bed*: R. Menzel, H. Riemann, N. Abrosimov; 8th International Conference on Electromagnetic Processing of Materials (EPM 2015); Cannes, France; October 2015

Appendix: **Talks and Posters**

W. Miller; *Evolution of grains during solidification of silicon – attempts of numerical simulations for an understanding:* W. Miller, A. Popescu; 5th European Conference on Crystal Growth (ECCG-5); Bologna, Italy; September 2015

S. Mohn; *The role of oxygen for polarity inversion of III-nitrides on sapphire investigated by HR-TEM and STEM:* S. Mohn, T. Markurt, R. Kirste, M. Hoffmann, R. Collazo, Z. Sitar, M. Albrecht; International Conference on Nitride Semiconductors (ICNS-11); Beijing, China; August/September 2015

F. Ringleb; *Indium island growth on glass at micro-roughened spots created by femtosecond laser pulses:* F. Ringleb, K. Eylers, T. Teubner, P. Schramm, T. Boeck; EU-Projekttreffen CHEETAH; Berlin, Germany, March 2015

M. Schmidbauer (lecturer M. Albrecht); *Superdomain Formation in Anisotropically Strained (K,Na)NbO_3 Thin Films on (110) $NdScO_3$ Grown by MOCVD:* M. Schmidbauer, D. Braun, A. Kwasniewski, M. Hanke, J. Sellmann, M. Albrecht, J. Schwarzkopf; MRS Spring Meeting; San Francisco, USA; April 2015

M. Schmidbauer; *Ferroelectric domains in strained (K,Na)NbO_3 epitaxial thin films on (110) $TbScO_3$*: M. Schmidbauer, A. Kwasniewski, D. Braun, J. Sellmann, M. Hanke, J. Schwarzkopf; Denver X-ray Conference; Westminster, Colorado, USA; August 2015

M. Schmidbauer; *Complex domain structure in anisotropically strained $K_{0.90}Na_{0.10}NbO_3$ thin films on $NdScO_3$:* M. Schmidbauer, D. Braun, A. Kwasniewski, P. Müller, J. Sellmann, M. Hanke, H. Renevier, J. Schwarzkopf; E-MRS Spring Meeting; Lille, France; May 2015

T. Schulz; *Preparation of epi-ready, highly UV transparent bulk AlN substrates for epitaxy of efficient UV-C emitters*: T. Schulz, C. Hartmann, A. Dittmar, K. Irmscher, U. Juda, J. Wollweber, M. Albrecht, M. Bickermann; International Conference on Nitride Semiconductors (ICNS-11); Beijing, China; August/ September 2015

J. Sellmann; *Ferroelectric Domains of partially relaxed $NaNbO_3$ films under tensile strain:* J. Sellmann, D. Braun, A. Kwasniewski, M. Schmidbauer, J. Schwarzkopf; DPG-Frühjahrstagung; Berlin, Germany; March 2015

J. Sellmann; *Ferroelectric Domains of partially relaxed $NaNbO_3$ films under tensile strain*: J. Sellmann, D. Braun, A. Kwasniewski, M. Schmidbauer, J. Schwarzkopf; EMRS Spring Meeting, European Materials Research Society; Lille, France; May 2015

R. Uecker; *A new large-lattice-constant perovskite substrate crystal*: R. Uecker, D. Klimm, R. Bertram, C. Guguschev, M. Brützam, A. Kwasniewski, M. Klupsch, Th.M. Gesing, D.G. Schlom; 5th European Conference on Crystal Growth (ECCG-5); Bologna, Italy; September 2015

G. Wagner; *Homoepitaxial Growth of beta-Ga_2O_3 Layers on (100) and (010) oriented Substrates by using MOVPE:* G. Wagner, M. Baldini, K. Irmscher, A. Fiedler, R. Schewski, M. Albrecht, M. Schmidbauer, Z. Galazka; International Workshop on Gallium Oxide and Related Materials (IWGO 2015); Kyoto, Japan; November 2015

G. Wagner; *Homoepitaxial growth of semiconducting b-Ga_2O_3 thin layers by MOVPE*: G. Wagner, M. Baldini, K. Irmscher, A. Fiedler, M. Albrecht, R. Schewski; 20th American Conference on Crystal Growth and Epitaxy (ACCGE-20) and 17th U.S. Biennial Workshop on Organometallic Vapor Phase Epitaxy (OMVPE-17); Big Sky, Montana, USA; August 2015

Contribution as co-authors

H. Ch. Alt; *Oxygen-isotope doping of GaAs bulk crystals and identification of a carbon-related defect:* H. Ch. Alt, H. E. Wagner, V. Häublein, Ch. Frank-Rotsch, A. Glacki, O. Root; DGKK-Arbeitskreis „Herstellung und Charakterisierung von massive Halbleiterkristallen“; Berlin, Germany; October 2015

S. Brandon; *On Modeling Interface attachment kinetics in melt and solution growth Systems:* S. Brandon, O. Weinstein, O. Bass, A. Virozub, A. Zeckel, W. Miller, J. J. Derby; Fifth European Conference on Crystal Growth (ECCG 5); Bologna, Italy; September 2015

B. Cai; *Ferroelectric properties of anisotropically strained epitaxial $NaNbO_3$ films grown on $NdGaO_3$:* B. Cai, J. Schwarzkopf, E. Hollmann, D. Braun, M. Schmidbauer, R. Wördenweber DPG-Frühjahrs-tagung; Berlin, Germany; March 2015

Q.M. Pillaca; *Modified Bridgman technique for grow-ing Sb-based binary compounds alloys:* Q.M. Pillaca, W. Miller, V. Cocivera, T. Maletin, P. Gille;5th European Conference on Crystal Growth (ECCG-5); Bologna, Italy; September 2015

D.G. Schlom; *World Record Tunable Microwave Dielec-trics:* D.G. Schlom, C.H. Lee, N.D. Orloff, T. Birol, Y. Zhu, Y. Nie, V. Goian, E. Rocas, R. Haislmaier, E. Vlahos, J.A. Mundy, M.D. Biegalski, D.J. Baek, S. Sung, J. Zhang, M. Bernhagen, N.A. Benedek, Y. Kim, J.D. Brock, J. Junquera, P. Ghosez, R. Uecker, X. X. Xi, V. Gopalan, D. Nuzhnyy, S. Kamba, L.F. Kourkoutis, K.M. Shen, D.A. Muller, I. Takeuchi, J.C. Booth, C.J. Fennie; AVS 62nd International Symposium & Exhibition; San Jose, California, USA; October 2015

Appendix: **Talks and Posters**

T. Wernicke; *UV Laser Diodes:* T. Wernicke, M. Martens, C. Kuhn, F. Mehnke, C. Reich, J. Jeschke, J. Rass, J. Enslin, M. Lapeyrade, U. Zeimer, A. Mogilatenko, S. Einfeldt, C. Hartmann, M. Bickermann, M. Weyers, M. Kneissl; VI Workshop on Physics and Technology of Semiconductor Lasers; Kraków, Poland; October 2015

T. Wernicke; *Challenges for AlGaN Based UV Lasers Diodes:* M. Martens, C. Kuhn, C. Reich, F. Mehnke, J. Jeschke , M. Feneberg, J. Rass, J. Enslin, M. Lapeyrade, U. Zeimer, A. Mogilatenko, S. Einfeldt, V. Kueller, S. Hagedorn, A. Knauer, C. Hartmann, J. Wollweber, R. Goldhahn, M. Bickermann, M. Weyers, M. Kneissl; Solid-State and Organic Lighting 2015 (SOLED); Suzhou, China; November 2015

R. Wördenweber; *Impact of Anisotropic Biaxial Compressive and Tensile Strain on the Properties of Epitaxial Ferroelectric Films:* R. Wördenweber, J. Schwarzkopf, B. Cai, Y. Dai, D. Braun, J. Schubert, E. Hollmann; Advances in Functional Materials; Stony Brook University; NY State, USA; June/July 2015

Poster presentations at national and international conferences

R. Bansen, C. Ehlers, J. Schmidtbauer, F. Ringleb, Th. Teubner, T. Boeck; *Crystalline Silicon on Glass by Steady-State Solution Growth;* DPG-Frühjahrstagung der Sektion Kondensierte Materie (SKM); Berlin, Germany; March 2015

I. Buchovska, O. Liaskovskiy, T. Vlasenko, S. Beringov; *High-performance silicon multicrystalline ingots and wafers produced from different feedstock and with different seeding approach;* 8th International Workshop on Crystalline Silicon for Solar Cells (CSSC-8); Bamberg, Germany; May 2015

A. Dittmar, C. Hartmann, J. Wollweber, S. Kollowa, K. Irmscher, F. Langhans, A. Kwasniewski, M. Bickermann; *Growth and point defect characterisation of bulk AlN crystals;* 5th European Conference on Crystal Growth (ECCG-5); Bologna, Italy; September 2015

A. Dittmar, C. Hartmann, S. Kollowa, F. Langhans, J. Wollweber, M. Bickermann; *Homoepitaktisches Wachstm von AlN-Volumenkristallen nach dem Ziegler-Verfahren;* Deutsche Kristallzüchtungstagung (DKT 2015); Frankfurt/Main, Germany; March 2015

C. Ehlers, R. Bansen, J. Schmidtbauer, F. Ringleb, Th. Teubner, T. Boeck; *Properties of Crystalline Silicon Layers for Photovoltaic Application grown on Glass by Steady-State Solution Growth;* 5th European Conference on Crystal Growth (ECCG-5); Bologna, Italy; September 2015

K. Eylers, F. Ringleb, B. Heidmann, C. Symietz, J. Bonse, M. Schmid, J. Krüger, Th. Teubner, P. Schramm, T. Boeck, M. Lux-Steiner; *Precursors for CIGSe Micro-Concentrator Solar Cells;* 5th European Conference on Crystal Growth (ECCG-5); Bologna, Italy; September 2015

Ch. Frank-Rotsch, A. Glacki, H. Ch. Alt, H.- E. Wagner; *VGF growth of GaAs doped with ^{12}C, ^{16}O, and ^{18}O for the study of mid-infrared vibrational modes;* 5th European Conference on Crystal Growth (ECCG-5); Bologna, Italy; 2015

A. Glacki, Ch. Frank-Rotsch, H. Ch. Alt, H. E. Wagner ; *VGF growth of GaAs doped with ^{12}C, ^{16}O, and ^{18}O for the study of mid-infrared vibrational modes;* Deutsche Kristallzüchtungstagung (DKT 2015); Frankfurt/Main, Germany; March 2015

C. Hartmann, S. Kollowa, A. Dittmar, F. Langhans, T. Schulz, M. Naumann, K. Irmscher, J. Wollweber, Yu. Suhak, H. Fritze, M. Bickermann; *Preparation of semi-insulating and weak n-type conducting AlN substrates;* 6th International Symposium of the Growth of Nitrides (ISGN-6); Hamamatsu, Japan; November 2015

S. Kayser, A. Lüdge; *Novel Study of Lateral Photovoltage Scanning- (LPS) and Scanning Photoluminescence- (SPL) Method;* Deutsche Kristallzüchtungstagung (DKT 2015); Frankfurt/Main, Germany; March 2015

S. Kayser, A. Lüdge; *Novel Study of Lateral Photovoltage Scanning- (LPS) and Scanning Photoluminescence- (SPL) Method;* 28th International Conference on Defects in Semiconductors (ICDS 2015); Helsinki, Finland; July 2015

F. M. Kiessling, N. Dropka, Ch. Frank-Rotsch, T. Ervik, D. Linke, R. Menzel, T. Richter, L. Sylla; *Characterization of G2-sized quasi-mono Si directionally solidified in TMF;* 5th European Conference on Crystal Growth (ECCG-5); Bologna, Italy; September 2015

D.J. Kok, K. Irmscher, M. Naumann, C. Guguschev, Z. Galazka, R. Uecker; *Temperature dependent optical properties in $SrTiO_3$;* 5th European Conference on Crystal Growth (ECCG-5); Bologna, Italy; September 2015

T. Markurt, T. Schulz, X.Q. Wang, X.T. Zheng, D.Y. Ma, T. Suski, I. Gorczyca, A. Svane, N. Christensen, M. Albrecht; *InN/GaN Superlattices – Resolving the Discrepancies between Theory and Experiment;* Microscopy of Semiconducting Materials (MSM-XIX 2015); Cambridge, United Kingdom; March/April 2015

W. Miller, M. Czupalla, N. Abrosimov, U. Juda; *Dislocation multiplication during Czochralski growth of germanium: Numerical studies and experimental results;* 5th European Conference on Crystal Growth (ECCG-5); Bologna, Italy; September 2015

Appendix: **Talks and Posters**

S. Mohn, N. Stolyarchuk, R. Kirste, M. P. Hoffmann, R. Di Felice, R. Collazo, A. Courville, P. Vennéguès, Z. Sitar, M. Albrecht; *Interface structure of AlN on sapphire investigated by aberration corrected TEM;* 11th International Conference on Nitride Semiconductors (ICNS 11); Beijing, China; August/September 2015

S. Mohn, N. Stolyarchuk, R. Kirste, M. P. Hoffmann, R. Collazo, A. Courville, P. Vennéguès, Z. Sitar, M. Albrecht; *Polarity control of III-nitrides on sapphire investigated by transmission electron microscopy;* Adlershofer Forschungsforum (AFF); Berlin, Germany; November 2015

F. Ringleb, B. Heidmann, C. Symietz, J. Bonse, S. Andree, Th. Teubner, T. Boeck, J. Krüger, M. Schmid, M. Lux-Steiner; *Indium Precursors for CIGS Micro-Concentrator Solar Cells;* DPG-Frühjahrstagung der Sektion Kondensierte Materie (SKM); Berlin, Germany; March 2015

F. Ringleb, B. Heidmann, M. Schmid, Ch. Symietz, J. Bonse, J. Krüger, M. Ch. Lux-Steiner, T. Boeck; *Preparation of Copper-Indium-Diselenide Absorber Islands for Micro-Concentrator Applications*; 11th International Conference on Concentrator Photovoltaic Systems (CPV-11); Aix-les-Bains, France; April 2015

M. Schmidbauer, J. Schwarzkopf, C. Feldt, A, Kwasniewski, D. Braun, M. Hanke; *Grazing Incidence X-Ray Diffraction from Ferroelectric Domains in MOCVD grown (K,Na)NbO_3 Epitaxial Layers;* HZB User Meeting; Berlin, Germany; December 2015

J. Schwarzkopf, D. Braun, M. Hanke, P. Müller, A. Kwasniewski, M. Schmidbauer; *Evolution of monoclinic domains in strained (K,Na)NbO_3 thin films on $NdScO_3$ substrates grown by MOCV;* Workshop on Oxide Electronics 22 (WOE-22); Paris, France; October 2015

J. Schwarzkopf, M. Schmidbauer, D. Braun, A. Kwasniewski, J. Sellmann, M. Hanke; *Superdomains in $K_{0.9}Na_{0.1}NbO_3$ thin films on $NdScO_3$ Substrates;* DPG-Frühjahrstagung; Berlin, Germany; March 2015

J. Sellmann, D. Braun, A. Kwasniewski, M. Schmidbauer, T. Markurt, J. Schwarzkopf; *Local ferroelectric hysteresis loops of compressively strained $NaNbO_3$ films grown by PLD;* 13th European Meeting on Ferroelectricity (EMF 2015); Porto, Portugal; June/July 2015

Appendix: **Patents**

Granted

H. Riemann, H.-J. Rost
Vorrichtung zum tiegelfreien Zonenschmelzen von Halbleitermaterialstäben
DE 196 10 650.8

S. Ganschow, R. Bertram, D. Klimm, P. Reiche, R. Uecker
Verfahren und Anordnung zur Herstellung von ZnO-Einkristallen
DE 10 2004 003 596.2

Ch. Frank-Rotsch, P. Rudolph, R.-P. Lange, O. Klein, B. Nacke
Vorrichtung und Verfahren zur Herstellung von Kristallen aus elektrisch leitenden Schmelzen
DE 10 2007 028 548.7
08784553.3 (DK, ES, FR, NO)
KRIST*MAG*®

R.-P. Lange, M. Ziem, D. Jockel, P. Rudolph, F. Kießling, Ch. Frank-Rotsch, M. Czupalla, B. Nacke, H. Kasjanow
Vorrichtung zur Herstellung von Kristallen aus elektrisch leitenden Schmelzen
DE 10 2007 028 547.9
08784554.1 (DK, ES, FR, NO)
KRIST*MAG*®

Ch. Frank-Rotsch, P. Rudolph, R.-P. Lange, D. Jockel
Vorrichtung und Verfahren zur Herstellung von Kristallen aus elektrisch leitenden Schmelzen
DE 10 2007 046 409.8
KRIST*MAG*®

P. Rudolph, M. Ziem, R.-P. Lange
Vorrichtung zum Züchten von Einkristallen aus elektrisch leitfähigen Schmelzen
DE 10 2007 020 239.5
KRIST*MAG*®

R. Fornari, S. Ganschow, D. Klimm, M. Neubert, D. Schulz
Verfahren und Vorrichtung zur Herstellung von Zinkoxid-Einkristallen aus einer Schmelze
DE 10 2007 006 731.5

P. Rudolph, M. Ziem, R.-P. Lange, D. Jockel
Vorrichtung zur Herstellung von Kristallen aus elektrisch leitenden Schmelzen
DE 10 2008 035 439.2

F. Büllesfeld, U. Sahr, W. Miller, P. Rudolph, U. Rehse, N. Dropka
Verfahren zum Erstarren einer Nichtmetall-Schmelze
DE 10 2008 059 521.7
09 749 132.8 (DK, ES, IT, NO, R, GB)

R. Fornari
Vorrichtung und Verfahren zur Züchtung von III-Nitrid-Volumenkristallen
08 161 254.1 (DE, PL, FR, GB, SE)

P. Rudolph, R.-P. Lange, M. Ziem
Vorrichtung zur Herstellung von Sililziumblöcken
DE 10 2009 045 680.5

N. Dropka, P. Rudolph, U. Rehse
Verfahren und Anordnung zur Herstelllung von Kristallblöcken von hoher Reinheit und dazugehörige Kristallisationsanlage
DE 10 2010 028 173.5

H. Riemann, N. Abrosimov, J. Fischer, M. Renner
Verfahren und Vorrichtung zur Herstellung von Einkristallen aus Halbleitermaterial
EP 2 504 470 (NO, ES, NL, FR, DK, GB, BE, IT)

N. Dropka, Ch. Frank-Rotsch, M. Ziem, P. Lange
Verfahren und Vorrichtung zur gerichteten Kristallisation von Kristallen aus elektrisch leitenden Schmelzen
DE 10 2012 204 313.6

N. Dropka, Ch. Frank-Rotsch, P. Rudolph, R.-P. Lange, U. Rehse
Kristallisationsanlage und Kristallisationsverfahren zur Herstellung eines Blocks aus einem Material, dessen Schmelze elektrisch leitend ist
DE 10 2010 041 061.6

O. Klein, F. Kießling, M. Czupalla, P. Rudolph, R.-P. Lange, B. Lux, W. Miller, M. Ziem, F. Kirscht
Verfahren und Vorrichtung zur Züchtung von Kristallen aus elektrisch leitenden Schmelzen, die in der Diamant- oder Zinkblendestruktur kristallisieren
DE 10 2009 027 436.7

Appendix: **Patents**

Pending

U. Rehse, P. Rudolph, W. Miller, N. Dropka,
F. Büllesfeld, U. Sahr
Method for the solidification of a non-metal melt
WO0002012060802A3 (CN, US, TW)

R. Fornari, F. Kießling, P. Rudolph, V. Trautmann
Kristallisationsanlage und Kristallisationsverfahren
DE 10 2009 046 845.5

H. Riemann, N. Abrosimov, J. Fischer, M. Renner
Verfahren und Vorrichtung zur Herstellung von Einkristallen aus Halbleitermaterial
DE 10 2010 052 522.7
10801372.3 (EP), 13/511,751 (US), 2012-540285 (JP)

T. Boeck, R. Fornari, R. Heimburger, G. Schadow,
J. Schmidtbauer, H.-P. Schramm, T. Teubner
Kristallisationsverfahren zur Erzeugung kristalliner Halbleiterschichten
DE 10 2010 044 014.0

F. Kießling, Ch. Frank-Rotsch, N. Dropka, P. Rudolph
Verfahren zur gerichteten Kristallisation von Ingots
DE 10 2011 076 860.2

Z. Galazka, R. Uecker, R. Fornari
Method and apparatus for growing indium oxide (In2O3) single crystals and indium oxide (In2O3) single crystal
PCT/EP2012/057447

M. Wünscher, H. Riemann
Vorrichtung für das tiegelfreie Zonenziehen von Kristallstäben
DE 10 2012 022 958.8
PCT/DE2013/000627

N. Dropka, Ch. Frank-Rotsch, P. Lange, P. Krause
Kristallisationsanlage und Kristallisationsverfahren zur Kristallisation aus elektrisch leitenden Schmelzen sowie über das Verfahren erhältliche Ingots
DE 10 2013 211 769.8
PCT/EP2014/059684

A. Dittmar, C. Hartmann, J. Wollweber, U. Degenhardt,
F. Stegner
Keimhalter einer Einkristallzüchtungsvorrichtung, Einkristallzüchtungsvorrichtung und Kompositwerkstoff
DE 10 2014 017 021.7

Z. Galazka, R. Uecker, D. Klimm, M. Bickermann
Method for growing beta phase of gallium oxide (ß-Ga2O3) single crystals from the melt contained within a metal crucible
EP 15150582.3, PCT/EP2015/079938

A. Dittmar, C. Hartmann, J. Wollweber, M. Bickermann
(Sc, Y): Einkristalle für Gitter-angepasste AlGaN Systeme
DE 10 2015 116 068.4

Registered Trademark

KRIST*MAG*®

Appendix: **Teaching and Education**

Prof. Dr. Matthias Bickermann

- *Kristallzüchtung II: Methoden und Anwendungen;* Technische Universität Berlin, Institut für Chemie WS 2014/15 und WS 2015/16
- *Kristallzüchtung I: Grundlagen und Methoden;* Technische Universität Berlin, Institut für Chemie SS 2015
- Art.06 Kunst und Wissenschaft *Chemie/Alchemie/Kunst;* Prof. Bürkle, Prof. Grohmann, Prof. Lerch, Prof. Bickermann Technische Universität Berlin, WS 2014/15
- Forschungspraktikum: Betreuung von Studierenden am IKZ Technische Universität Berlin, Institut für Chemie

PD Dr. habil. Detlef Klimm

- *Phasendiagramme*; Humboldt-Universität zu Berlin, Institut für Chemie, WS 2014/15 und WS 2015/16
- Versuch „*Phasendiagramme*" im Fortgeschrittenen-Praktikum Physik; Humboldt-Universität zu Berlin, WS 2014/15, SS 2015, WS 2015/16

Dr. habil. Martin Schmidbauer

- *Röntgenstreuung: Grundlagen und Anwendungen in der Materialwissenschaft;* Humboldt-Universität zu Berlin, Institut für Physik, WS 2014/15, SS 2015 und WS 2015/16

apl. Prof. Dr. Dietmar Siche

- *Kristallzüchtung*; Brandenburgische Technische Universität Cottbus-Senftenberg, Blockseminar SS 2015

Doctoral theses (ongoing)

Mariia Anikeeva
Transmission electron microscopy of Short Period Superlattices for Rational (In,Ga)N

Roman Bansen
Herstellung und Charakterisierung von polykristallinem Silicium auf Glas

Dorothee Braun
Ferro- und piezoelektrische Charaktersierungen von bleifreien Perowskitschichten

Christian Ehlers
Wachstum und Charakterisierung von Silizium aus Zinn Lösungen für die Photovoltaik

Katharina Eylers
Wachstum und Charakterisierung von $Cu(In,Ga)Se_2$ Absorbern für Mikrokonzentratorsolarzellen

Andreas Fiedler
Electrical and optical characterization of the transparent semiconducting oxide beta-Ga_2O_3

Stefan Kayser
Charakterisierung mono- und multikristalliner Halbleiter wie SiGe, Si, Ge_{1-x} und GaAs mit LPS- und SPL-Methoden

Dirk Kok
Einfluss der Züchtungsbedingungen auf die Realstruktur von $SrTiO_3$

Sandro Kollowa
Dotierung und Kompensation bei der Sublimationszüchtung von AlN-Volumenkristallen

Frank Langhans
Untersuchung zur Wachstumskinetik und Oberflächenmorphologie bei der Sublimationszüchtung von AlN-Volumenkristallen

Stefan Mohn
Elektronenmikroskopische Charakterisierung von heteropolaren Nitrid-Nitrid und Nitrid-Oxid Grenzflächen

Joanna Moneta
Transmission electron microdcopy of Short Period Superlattices for Rational (In, Ga)N

Robert Schewski
Wachstum und Relaxation von Gruppe III Sesquioxiden

Natalia Stolyarchuk
Investigation of III-Nitride/Oxide Interfaces of Atomic Scale

Appendix: **Teaching and Education**

Doctoral theses (completed)

Krzysztof Kachel
Pseudo Halide Vapor Phase Epitaxy- Growth of GaN Crystals
Humboldt-Universität zu Berlin, Institut für Physik

Jan Sellmann
Impact of strain and composition on structural and piezo-/ferroelectric properties of epitaxial $NaNbO_3$ and $K_xNa_{1-x}NbO_3$ thin films and superlattices grown by PLD
Technische Universität Berlin, Institut für Chemie

Toni Markurt
Transmission electron microscopy of growth and strain relaxation mechanisms in GaN (0001) films grown on Si (111) substrates
Humboldt-Universität zu Berlin, Institut für Physik

Steffen Ganschow
Melt growth of oxide single crystals in controlled oxygen fugacity atmosphere
Technische Universität Berlin, Institut für Chemie

Diploma, Master and bachelor theses (completed)

Michael Klupsch, Bachelor
Untersuchung zur Phasenbildung von Perowskiten im System La_2O_3-Lu_2O_3-Sc_2O_3
Humboldt Universität zu Berlin, Institut für Physik

Philipp Kehne, Master
PLD growth investigations and the influence on ferroelectric properties of $K_xNa_{1-x}NbO_3$ on $DyScO_3$
Technische Universität Berlin, Institut für Chemie

Lena Schmidt, Master
Temperversuche zur Silizium-Diffusion in AlN-Kristallen
Technische Universität Berlin, Institut für Chemie

Franz Kamutzki, Master
The influence of oxygen partial pressure in the growth atmosphere on the coloration of $SrTiO_3$ single crystal fibers
Freie Universität Berlin, FB Geowissenschaften

Appendix: **Membership in Committees**

Committees

Dr. Rainer Bertram
- DIN – Deutsches Institut für Normung e.V. – NA 062 – Normenausschuss Materialprüfung (NMP), member

Prof. Dr. Matthias Bickermann
- IGAFA e.V. – Initiativgemeinschaft Außeruniversitärer Forschungseinrichtungen in Adlershof e.V., member of the board

Dr. Christiane Frank-Rotsch
- Deutsche Gesellschaft für Kristallzüchtung und Kristallwachstum (DGKK), secretary
- International Organization for Crystal Growth (IOCG), member of the council
- European Network of Crystal Growth (ENCG), member of the council

PD Dr. habil. Detlef Klimm
- Commission on Crystal Growth and Characterization of Materials (IUCr), member

Dr. Wolfram Miller
- Deutsche Gesellschaft für Kristallzüchtung und Kristallwachstum (DGKK), vice-chairman
- European Network of Crystal Growth (ENCG), coordinator

Editorial committees

Prof. Dr. Matthias Bickermann
- Progress in Crystal Growth and Characterization of Materials, Elsevier B.V., associate editor

PD Dr. habil. Detlef Klimm
- Crystal Research and Technology 1'2015 (incl. Editors' Preface), guest editor

Conference committees

Prof. Dr. Matthias Bickermann
- 11th International Conference on Ceramic Materials and Components for Energy and Environmental Applications (CMCEE), June 2015, Vancouver, Canada, symposium co-organizer
- Tagung des DGKK-Arbeitskreises „Massive Halbleiterkristalle“, October 2015, workshop organizer
- 9th International Workshop on Bulk Nitride Semiconductors (IWBNS), November 2015, Wonju, South Korea, member of the program and advisory committee
- 6th International Symposium of the Growth of Nitrides (ISGN-6), November 2015, Hamamatsu, Japan, member of program-committee

Dr. Christiane Frank-Rotsch
- Fifth European Conference on Crystal Growth (ECCG-5), September 2015, Bologna, Italy, member of the international advisory Board and session chair
- 18th International Conference on Crystal Growth and Epitaxy (ICCGE-18), August 2016, Nagoya, Japan, member of international advisory board

Dr. Wolfram Miller
- Deutsche Kristallzüchtungstagung (DKT 2015), March 2015, Frankfurt/Main, Germany, member of advisory comittee
- Fifth European Conference on Crystal Growth (ECCG-5), September 2015, Bologna, Italy, member of advisory committee
- International Workshop on Modeling in Crystal Growth (IWMCG-8), November 2015, Spa, Belgium, member of advisory committee

Appendix: **Guest Scientists at the IKZ**

01.01.2015 – 31.12.2015

Prof. Dr. Karen Gambaryan
10.07. – 09.09.2015
Yerevan State University, Department of Physics,
Yerevan, Armenia

Dr. Lyudmyla Khirunenko
25.09. – 30.09.2015
Institute of Physics,
National Academy of Sciences of Ukraine

Maria Ines Lopes Caupers
03.08. – 25.09.2015
Faculdade de Ciências e Tecnologias
da Universidade Nova de Lisboa,
Portugal

Xiofang Qi
01.10. 2015 – 31.12.2015
School of Energy and Power Engineering,
Xi'an, Shaanxi, People's Republic of China

Dr. Tobias Schulz
01.01. – 31.12.2015
Humboldt Universität zu Berlin

Prof. Dr. Petr G. Sennikov
01.01. – 16.01.2015
19.04. – 22.04.2015
16.07. – 31.08.2015
RAS – Institute of Applied Physics,
Russia

Sakari Sintonen
01.02.2015 – 31.12.2015
Aalto University,
Department of Micro- and Nanosciences,
Finland

Appendix: Colloquia at the IKZ

Dr. Paul Sass
Scientific Instruments Dresden GmbH
"Optical Floating Zone crystal growth under high-pressure atmospheres – advantages and applications", February 2015

Dr. Christian Kränkel
Universität Hamburg, Institut für Laser-Physik
"Kristallzüchtung und Laserexperimente mit Seltenerd-dotierten Oxiden und Fluoriden am ILP", February 2015

Prof. Dr. Beatriz Noheda
University of Groningen, Zernike Institute for Advanced Materials, Netherlands
"Control of ferroelastic domains in epitaxial oxide films", March 2015

Dr. Daniel Lehmann
Technische Universität Chemnitz, Institut für Physik, EXIST-Forschungstransfer „Corant"
"Organic electronics: small molecule crystals for transistors, light emitting diodes, and solar cells", April 2015

Dipl.-Phys. Gleb Lukin
Technische Universität Bergakademie Freiberg, Institut für Nichteisen-Metallurgie und Reinststoffe
"GaN-Züchtung mittels Hochtemperatur-Gasphasenzüchtung", April 2015

Dr. Lutz Kirste
Fraunhofer-Institut für Angewandte Festkörperphysik, Freiburg
"X-Ray metrology for thin film group-III-nitride devices", April 2015

Prof. Dr. Christoph Koch
Universität Ulm, Institut für Experimentelle Physik
"Multiple scattering assisted electron crystallography", May 2015

Prof. Dr. Peter Gaal
Universität Hamburg, Institut für Nanostruktur- und Festkörperphysik
"Synchrotron-based ultrafast X-ray diffraction: first experiments at the new XPP-KMC3-Beamline at BESSY II", May 2015

Dr. Jari Jarvinen
Silicom Ltd, Helsinki, Finland
"The Software tool Elmer in crystal growth simulations", May 2015

Prof. Dr. Andreas Erb
Technische Universität München, Faculty of Physics, Crystal and Material Laboratory;
Walther-Meißner-Institut, Bayerische Akademie der Wissenschaften, Garching/München
"Single crystal growth of various oxide materials for basic research and applications", June 2015

Dr. Frank Habel
Freiberger Compound Materials GmbH, Research and Development / GaN
"HVPE growth of high quality bulk GaN", July 2015

Prof. Dr. Peter Rudolph
Crystal Technology Consulting, Schönefeld
IKZ-Summer Course "Defect formation during crystal growth from melt and selected epitaxial processes", July 13-16, 2015

Dr. Zuzanna Liliental-Weber
Lawrence Berkeley National Laboratory, Materials Science Devision, CA, USA
"TEM studies of defects in GaN; MOCVD layers and high pressure grown crystals", August 2015

Prof. Dr. Bruce Parkinson
University of Wyoming, USA
"Photoinduced electron transfer to semiconductor electrodes from adsorbed dyes and quantum dots", August 2015

Dr. Yasunori Furukawa
Oxide Corporation, Japan
"Introduction of OXIDE's crystal business for variety of optical application", October 2015

Dr. habil. Vladimir Shvartsman
Universität Duisburg-Essen, Institut für Materialwissenschaften
"Investigation of uniaxial relaxor ferroelectrics by piezoresponse force microscopy (PFM)", October 2015

Dr. Alessio Morelli
Queen's University Belfast, Centre for Nanostructured Media, UK
"Ferroelectric domain imaging and manipulation in multiferroic nanoislands", October 2015

Prof. Dr. Andrew J. Bell
University of Leeds, Institute for Materials Research, UK "A classical mechanics approach to understanding electromechanical coupling in solids", November 2015

Dr. Oliver Bierwagen
Paul-Drude Institut für Festkörperelektronik (PDI), Leibniz-Institut im Forschungsverbund Berlin e.V.
"Transparent semiconducting oxides: Fundamentals of the MBE growth, transport, and gas sensor application", December 2015

Appendix: **External Funding**

International programs

Cost-reduction through material optimisation and Higher EnErgy output of solAr pHotovolatics modules - joining Europe's Research and Development efforts in support of ist PV industry; EU, 2014–2017

Short Period Superlattices for Rational (In,Ga)N (SPRInG); EU, 2015–2018

Programs of Federal Ministry of Education and Research (BMBF) and Federal Ministry of Economics and Technology (BMWi)

Erforschung des human- und ökotoxikologisch relevanten Löslichkeits- und Reaktionsverhalens von GaAs sowie verwandter Arsenide und Phosphide im Verbundprojekt TEMPO: Toxikologische, physikalisch-chemische und gesellschaftliche Erforschung innovativer Materialien und Prozesse der Optoelektronik; BMBF, 2013–2016

Induktiv gekoppelter Niederdruck-Plasmareaktor zur Nitrid-Einkristallzüchtung; BMWi (Zentrales Innovationsprogramm Mittelstand ZIM) 2013–2015

InTerFEL: Zeitaufgelöste und nichtlineare Infrarot- und Terahertz-Spektroskopie mit einem FEL; BMBF, 2014–2017

Entwicklung einer Nitrid-Schaumkeramik als Graphitersatz; BMWi (Zentrales Innovationsprogramm Mittelstand ZIM), 2014–2016

Plasmaabscheidung von GaN-Bauelementen PlanB - Elektronenmikroskopische Analyse und Modellierung der Wachstums- und Relaxationsprozesse von PSD InAlGaN-Schichten auf Saphir und Silizium Substraten; BMBF, 2014–2017

ENOWA II: Entwicklung hoch- und kosteneffizienter PV-Si Wafer; BMBF 2015–2016

Entwicklung von graphitfreien keramischen Halbzeugen für die Silizium-Kristallzüchtung (CleanSi); BMWi (Zentrales Innovationsprogramm Mittelstand ZIM), 2015–2017

Entwicklung einer Plasmafackel für die Abscheidung von halbleiterreinem AlN zur Herstellung von Sputtertargets (PlasNiTar2.0); BMWi (Zentrales Innovationsprogramm Mittelstand ZIM), 2015–2017

Advanced UV for Life – Verbundvorhaben: AlN-Substrate; BMBF, 2015–2017

KrisNet: Entwicklung, Umsetzung und Professionalisierung eines Verwertungskonzepts am Leibniz-Institut für Kristallzüchtung; BMBF, 2015–2018

EXIST-Gründerstipendium: Innovativer Beschichtungs-Prozess-Service mit induktivem Plasma; BMWi, 2015–2016

Leibniz Competition

Homo- and heteroepitaxy of transparent semiconducting oxide layers of the Ga_2O_3-In_2O_3-Al_2O_3 ternary system on beta-Ga_2O_3 and In_2O_3-Substrates; 2012–2015

Growth of high perfection bulk $SrTiO_3$ single crystals; 2013–2016

DFG

Lösungsmittelgenerierte Phasenumwandlung zur Erzeugung kristalliner Si-Schichten; 2011–2014

Science of polar homo- and heterointerfaces; 2012–2015

Entwicklung einer Züchtungstechnologie für semi-isolierende GaN-Substrate und Untersuchung der in-situ Kohlenstoffdotierung; 2014–2017

Lokal gewachsene $Cu(In,Ga)Se_2$-Mikroinseln für Konzentratorsolarzellen; 2015–2018

Funding by partners from industry and other institutions

Growth and characterization of new oxide single crystals; CrysTec GmbH, Berlin; 2005–2015

Growth and characterization of new oxide crystals for piezoelectric sensors; Kistler Instrumente AG, Winterthur, CH; 2005–2019

KILOGRAMM-2; Physikalisch-Technische Bundesanstalt, Braunschweig; 2011–2015

KILOGRAMM-3; Physikalisch-Technische Bundesanstalt, Braunschweig; 2015–2019

Germanium-Kristalle für das GERDA-Experiment; Max-Planck-Institut für Physik, München; 2013–2016

Züchtung von 6 Kristallen (6° bis 15° off-orientiert [111] Si-GaAs-VGF) im Heizer-Magnet-Modul; Freiberger Compound Materials GmbH; 2014–2015

Züchtung von Einkristallen aus Germanium mit unterschiedlichen Dotierstoffen; Photonic Sense GmbH, 2014–2015

Leibniz-Institut für Kristallzüchtung (IKZ)
Acting Director: Prof. Dr. Günther Tränkle
Max-Born-Straße 2
12489 Berlin
Germany

Phone +49 (0)30 6392 3001
Fax +49 (0)30 6392 3003
Email cryst@ikz-berlin.de
Online www.ikz-berlin.de

Annual Report 2015

Editor: Dr. Maike Schröder
Layout & typesetting: www.typoly.de
Cover photo: Moritz Thau
Photo p.2: © Katja Bilo

All rights reserved.
Reproduction requires the permission
of the director of the institute.

© Leibniz-Institut für Kristallzüchtung
im Forschungsverbund Berlin e.V.

Berlin, September 2016

Leibniz-Institut für Kristallzüchtung (IKZ)

Max-Born-Straße 2
12489 Berlin
Germany

Phone +49 (0)30 6392 3001
Fax +49 (0)30 6392 3003
Email cryst@ikz-berlin.de

www.ikz-berlin.de